Novel nanoparticle-based drug delivery system for neural stem cell targeting and differentiation

Dario Carradori

UNIVERSITE BRETAGNE LOIRE

Thèse de Doctorat

Dario CARRADORI

Thesis presented for the obtainment of
Doctor Degree from the Université d'Angers (UA) and from Université catholique de Louvain (UCL)
Under the label of Université Bretagne Loire

Doctoral school : *Biology-Health*

Discipline : *Biomolecules, Drug delivery, Nanomedicine, Neurodegenerative diseases, Pharmacology*
Speciality : *Neuroscience*
Unité de recherche : *Micro et Nanomédecines Biomimétiques*

Presented in public : *21.09.2017*

Novel nanoparticle-based drug delivery system for neural stem cell targeting and differentiation

JURY

Reviewers:

Patrick COUVREUR, Professor, Institut Galien Paris-Sud, Faculté Pharmacie Paris-Sud, Châtenay-Malabry, France
Lino FERREIRA, Professor, UC Biotech, Parque Tecnológico de Cantanhede, Cantanhede, Portugal

Examinators:
Véronique PREAT, Professor, Louvain Drug Research Institut, Université catholique de Louvain, Brussels, Belgium
Patrick SAULNIER, Professor, Micro et Nanomédecines Biomimétiques, Université d'Angers, Angers, France

Thesis directors:
Joël EYER, Statutory Researcher, Micro et Nanomédecines Biomimétiques, Université d'Angers, Angers, France
Anne DES RIEUX, Professor, Louvain Drug Research Institut, Université catholique de Louvain, Brussels, Belgium

President:
Françoise VAN BAMBEKE, Professor, Louvain Drug Research Institut, Université catholique de Louvain, Brussels, Belgium

Foreword

Neural stem cells (NSCs) are located in restricted neurogenic areas of the central nervous system, called niches, where they can undergo self-renewal and differentiate into specialized neuronal cells (astrocytes, oligodendrocytes and neurons). NSC differentiation plays a crucial role in the neurogenesis process, both during the development and the maintenance of the mammalian central nervous system (CNS). Several studies have demonstrated that neurogenesis stimulation resulted in the partial recovery of injured neuronal networks and in increased behavioral performances (e.g., learning and memory). Consequently, due to their impact on neurogenesis, NSCs are a potential tool to treat CNS diseases characterized by progressive lesion of neuronal tissue and deterioration of neurological functions.

NSCs have been investigated to replace injured cells and to restore neurological functions by their differentiation into specialized neuronal cells. Different strategies have been developed which are mostly based on NSC transplantation after *in vitro* manipulation of exogenous NSCs (isolated from their niches or induced from other somatic cells). Thirty-seven NSC-based clinical trials are currently on going for gliomas, ischemic stroke, amyotrophic lateral sclerosis, spinal cord injury and Parkinson's disease, but none have reached phase III yet. The limited translation is probably due to transplantation-associated issues such as access to cell source and post-grafting cell survival.

In situ differentiation of endogenous NSCs is a promising strategy to avoid transplantation-associated issues. Nevertheless, no work based on *in situ* differentiation of endogenous NSCs has reached the clinical phase yet and the lack of NSC-targeting systems mostly promoted the development of non-selective therapies.

Endogenous NSC targeting would increase the efficacy and the safety of *in situ* NSC differentiation treatments by enhancing drug bioavailability at the targeted site and limiting drug counter effects. Thus, the development of drug delivery systems that selectively reach NSC niches and induce NSC differentiation *in situ* would greatly improve the current NSC-based therapies.

AIM AND SCOPE OF THE WORK

The aim of this work was to contribute to the development of NSC-based therapies by providing a drug delivery system able both to target endogenous NSCs and to induce their differentiation *in situ* by bioactive molecule stimulation.

The goals of this project were i) to develop and characterize a drug delivery system targeting NSCs ii) to investigate the mechanisms behind the selective interaction NSCs-drug delivery system and iii) to induce endogenous NSC differentiation *in situ* by delivering a bioactive molecule.

ORGANIZATION OF THE MANUSCRIPT

Chapter 1 – Introduction establishes the context of NSC differentiation, from the general field of NSC biology to the current NSC-based therapies aiming at the treatment of CNS diseases. Secondly, it explores the contribution of nanomedicine to improve NSC-based therapies with a particular emphasis on the potential role of the lipid nanocapsules.

Chapter 2 – NFL-lipid nanocapsules for brain neural stem cell targeting in vitro and in vivo shows the study we made to produce a NSC-targeting drug delivery system by adsorbing the peptide NFL-TBS.40-63 (NFL) on the surface of lipid nanocapsules (LNCs). NFL-LNCs were physicochemically characterized and their NSC-targeting efficiency was evaluated *in vitro* and *in vivo* on NSCs of both brain and spinal cord. NFL-LNCs selectively interact with NSCs of the brain while they do not with NSCs of the spinal cord.

Chapter 3 – The characteristics of neural stem cell plasma membrane affect their interaction with NFL-lipid nanocapsules shows the study we made to investigate the reasons behind the selective interactions between NFL-LNCs and NSCs of the brain. We characterized the plasma membrane lipid compositions of NSCs from the brain and from the spinal cord highlighting significant differences between the two types of cells. The lipid composition modulates plasma membrane properties, such as fluidity and permeability, which are involved in the interactions nanoparticle-cell. Consequently, we measured their variation before and after NSC incubation with NFL, LNCs and NFL-LNCs. We finally identified some of the factors modulating NFL-LNC preferential interaction by comparing the results between NSCs from the brain and from the spinal cord.

Chapter 4 – Retinoic acid-loaded NFL-lipid nanocapsules induce neural stem cell differentiation towards the oligodendrocyte lineage shows the study we made to induce the differentiation of NSCs from the brain *via* bioactive molecule stimulation. Retinoic acid (RA) was selected among several drugs for its neurogenic potential as well as compatibility with LNCs. We encapsulated RA into NFL-LNCs and we evaluate the NSC differentiation efficacy *in vitro* and *in vivo*. *In vitro*, the incubation with RA-loaded NFL-LNCs induces a significant NSC differentiation in oligodendrocytes, while *in vivo*, focal demyelinated rats have been treated with RA-loaded NFL-LNCs but the evaluation of the therapeutic effect is ongoing.

Chapter 5 – Discussion highlights the main achievements of the thesis, describes the implications of the new findings and explores the possible improvements which can be made. NFL-LNC represents a great novelty in the field of NSC-based therapy due to the versatility of the LNCs (e.g. encapsulation of different types of bioactive molecules) which makes NFL-LNC potentially suitable for many therapeutic applications, even though a few points remain to be improved (e.g., the way of administration).

LIST OF ABBREVIATIONS

AD	*Alzheimer's disease*
ALS	*Amyotrophic Lateral Sclerosis*
bFGF	*Basic Fibroblast Growth Factor*
CC	*Central Canal*
CC-NSCs	*Central Canal Neural Stem Cells*
Chol	*Cholesterol*
CNP	*2',3'-Cyclic-Nucleotide 3'-Phosphodiesterase*
CNS	*Central Nervous System*
CPPs	*Cell-Penetrating Peptides*
DCX	*Doubleortin*
DiD	*DiIC18(5) solid (1,1'-Dioctadecyl-3,3,3',3'-Tetramethylindodicarbocyanine, 4-Chlorobenzenesulfonate Salt)*
EGF	*Epidermal Growth Factor*
ELFEFs	*Extremely Low-Frequency Electromagnetic Fields*
eSM	*egg SphingoMyelin*
Endo	*Endogenous*
Exo	*Exogenous*
FD	*Fluorescent Dextran*
FDA	*Food and Drug Administration*
GalC	*GalactoCerebroside*
GFAP	*Glial Fibrillary Acid Protein*
GP	*Generalized Polarization*
IS	*Ischemic Stroke*
LNCs	*Lipid NanoCapsules*
MAP2	*Microtubule-Associated Protein 2*
MBP	*Myelin Basic Protein*
MIRB	*Molday ION Rhodamine B*
Msi1	*Musashi-1*
n.b.	*new-born*
NeuroD	*Neurogenetic Differentiation*
NeuN	*Neuronal nuclear epitope*
NFs	*NeuroFilaments*

NFL	*NFL-TBS.40-63*
NFL-LNCs	*NFL-TBS.40-63 functionalized Lipid NanoCapsules*
NG2	*Chondroitin sulfate proteoglycan neuron/glia antigen 2*
NSCs	*Neural Stem Cells*
NSE	*Neuron-Specific Enolase*
Pax6	*Paired box gene 6*
PCL	*PolyCaproLactone*
PD	*Parkinson's disease*
PDI	*PolyDispersity Index*
PIT	*Phase Inversion Temperature*
PLA	*PolyLactic Acid*
PLGA	*Poly(Lactic-co-Glycolic Acid)*
POPC	*1-Palmitoyl-2-Oleoyl-sn-glycero-3-PhosphoCholine*
PSA-NCAM	*PolySiAlylated-Neural Cell Adhesion Molecule*
RA	*Retinoic Acid*
SCI	*Spinal Cord Injury*
SGZ	*SubGranular Zone*
SPION	*SuperParamagnetic Iron Oxide Nanoparticles*
Sox2	*SRY-related HMG-box gene*
SVZ	*SubVentricular Zone*
SVZ-NSCs	*SubVentricular Zone Neural Stem Cells*
TH	*Thyrosine-Hydroxylase*
USPION	*Ultrasmall SuperParamagnetic Iron Oxide Nanoparticles*

Remerciements

Mes remerciements vont à toutes ces personnes qui m'ont permis de commencer ce doctorat, de le continuer et, enfin, de voir sa fin! J'ai eu beaucoup de chance de travailler avec des gens comme vous, extrêmement compétents et efficaces.

Merci à Angers, où j'ai passé la première année et demie de mon doctorat, à la douceur angevine, au vin et aux châteaux!

J'aimerais remercier le directeur de ma thèse, le Dr. Joël Eyer, pour m'avoir donné l'opportunité de travailler au sein de son laboratoire, et mon superviseur, le Pr. Patrick Saulnier, pour m'avoir transmis son enthousiasme et sa positivité.

Merci au Dr. Claire Lepinoux-Chambaud, pour m'avoir aidé au début de mon doctorat, et à Kristell Barreau, pour avoir partagé avec moi ce début de doctorat. Merci au Dr. Franck Letournel, au Dr. Catherine Fressinaud, au Dr. Guillaume Bastiat et au Dr. Jean-Christophe Gimel pour leurs conseils et leur professionnalité. Merci à Aurélien Contini, Saikrishna Kandalam, Lisa Terranova, Emilie André, Marion Toucheteau et toute la famille NanoFar à Angers. Merci à Nolwenn Lautram, Maryne Jaffré et Edith Greleau pour leur disponibilité et leur aide. Merci à Hélène Malhaire, Marion Pitorre, Carl Simonsson et tous les membres du MiNT.

Un merci spécial au Dr. Edward Milbank (il migliore), au Dr. Giovanna Lollo (la delizia al limone), au Dr. Carmelina Angotti (papà castoro) et au Dr. Gabriela Ullio (mariiiia) pour leur amitié, leur soutien, nos litiges, nos voyages ensemble, la Sicile et les "Divanetti".

Merci à Bruxelles, où j'ai passé les dernières deux années et demie de ma thèse, au chocolat, à la bière et aux frites.

Un grand merci à tous les membres de l'ADDB avec qui ça a été un plaisir et un honneur de travailler.

Je remercie mon co-directeur de thèse, le Pr. Anne des Rieux, pour son exubérance et son énergie, ainsi que mon co-superviseur, le Pr. Véronique Préat, pour sa diplomatie et son pragmatisme.

TABLE OF CONTENTS

CHAPTER 1 – INTRODUCTION

CHAPTER 2 – NFL-LIPID NANOCAPSULES FOR BRAIN NEURAL STEM CELL TARGETING IN VITRO AND IN VIVO

CHAPTER 3 – THE CHARACTERISTICS OF NEURAL STEM CELL PLASMA MEMBRANE AFFECT THEIR INTERACTION WITH NFL-LIPID NANOCAPSULES

CHAPTER 4 – RETINOIC ACID-LOADED NFL-LIPID NANOCAPSULES INDUCE NEURAL STEM CELL DIFFERENTIATION TOWARDS THE OLIGODENDROCYTE LINEAGE

CHAPTER 5 – DISCUSSION

ANNEX

CHAPTER 1

INTRODUCTION*

TABLE OF CONTENTS

1. PREFACE

The dogma of a static brain was destroyed when Smart and Leblond showed for the first time that glial cells are dividing throughout the mouse brain parenchyma [1]. A few years later, Altman and Das reported the migration of postnatally born neuroblasts from the subventricular zone to the olfactory bulb, providing the first strong evidence of neurogenesis in the adult brain [2]. Important discoveries were made in the following decades, such as the presence of adult-born neurons in the dentate gyrus of rats [3] and in the vocal control nucleus of birds [4], but the perception of neurogenesis has drastically changed only since the 1990s. One of the most important discoveries was the observation that the proliferation of progenitor cells, and the subsequent number of newborn neurons, was dynamic. Several factors such as hormonal stress [5], age [6], or alcohol [7] could modulate this process. The improvement of immunohistological techniques represented another step forward in the description of neurogenesis by providing more sensitive analyses [8,9]. Moreover, the ability to isolate, cultivate, and differentiate neural precursor cells *in vitro* provided crucial data on the cellular and biomolecular mechanisms involved in adult neurogenesis [10,11].

Meanwhile, the discovery of adult neurogenesis also showed the limits of this physiologic process. Indeed, neurogenesis is restricted to small neurogenic areas of the central nervous system and its impact on the adult organism is very limited. Neural cells can migrate, from the neurogenic regions to the injured areas of the brain, and differentiate into the damaged cell phenotype but a very little percentage (around 0.2%) is functionally replaced [12,13].

The identification of neural stem cells and their important role in adult neurogenesis motivated researchers to explore the regenerative potential of these cells.

2. NEURAL STEM CELLS

2.1 Definition

Neural stem cells (NSCs) are defined as "*stem cell derived from any part of the nervous system and which primarily make cells expressing neural markers (those of astrocytes, oligodendrocytes and neurons) in in vitro culture*" [14]. This definition is based on retrospective *in vitro* studies [11,15,16] which highlighted NSC peculiar biological properties: self-renewal and differentiation into specialized neural cells (neurons, astrocytes and oligodendrocytes) [17,18].

2.2 Biological functions

NSCs are located in restricted areas of the central nervous system (CNS), called niches, such as the central canal (CC), in the spinal cord, and the subventricular zone (SVZ) and the subgranular zone (SGZ), in the brain (Figure 1). Here, NSCs play a crucial role in the neurogenesis process both in the development and in the adulthood of the organism by generating, maintaining and regenerating the CNS *via* their differentiation into specialized neural cells.
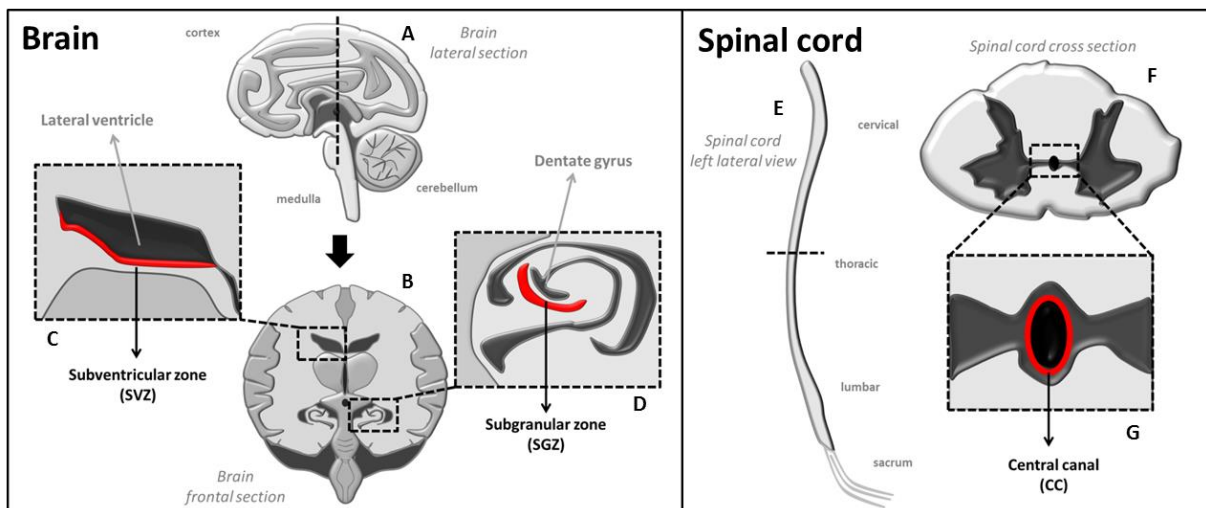
Figure 1. NSC niches in the CNS. Brain. Localization of the subgranular (SGZ) and subventricular (SVZ) zones in adult human brain. A, lateral section of the brain. B, frontal section of the brain. C, subventricular zone, highlighted in red. D, subgranular zone, highlighted in red. Spinal cord. Localization of central canal (CC) in spinal cord. E, spinal cord left lateral view. F, spinal cord cross section. G, central canal, highlighted in red.

Direct and indirect mechanisms were described to regulate the behavior of NSCs [19]. Extrinsic signals can bind to NSC plasma membrane receptors or penetrate *via* specific channels and trigger intracellular cascades inducing modifications in gene expression. The secretions of the choroid plexus such as insulin-like growth factor 1 (IGF1) [20,21] or ions such as calcium [22] are examples of extrinsic signals that can modulate NSC differentiation by their interaction with IGF1 receptor and Ca^{+2} channels, respectively. Intrinsic regulatory processes can also direct gene expression in NSCs by affecting transcriptional factors. Sonic hedgehog is the major activating ligand to initiate Hedgehog signalling in the brain and has been shown to play an important role in NSC proliferation and differentiation [23]. Both the extrinsic and intrinsic pathways are interconnected. Consequently, the identification of the origin of the niche signals is challenging.

Although NSCs are multipotent *in vitro*, recent genetic fate-mapping and clonal lineage-tracing of NSCs have highlighted the lack of similarities between NSC differentiation *in vitro* and *in vivo* [24]. The niche environment seems to limit adult NSC differentiation. In the adult SGZ, NSCs can generate dentate gyrus granular cells while in the adult SVZ, NSCs produce neuroblasts which migrate to the olfactory bulb where they differentiate into interneurons [25]. Moreover, localization in the niches would determine the type of cells derived from NSCs. In the SVZ, ventral NSCs mostly develop into calbindin-expressing cells, whereas dorsal NSCs develop into tyrosine-hydroxylase-expressing cells [26] (long-axon and dopaminergic neuron markers, respectively). In the SGZ, the adult NSC population reacts differently to environmental stimuli depending on their lineage [27]. Learning and memory processes are strictly related to adult neurogenesis in the SVZ [28-30], while SGZ-NSC-derived granule cells of the dentate gyrus have been implicated in long-term spatial memory and pattern separation [31,32]. Transplanted NSCs are also able to release immunomodulatory and neurotrophic factors (bystander effect) such as nerve growth factor, brain-derived growth factor, and leukemia inhibiting factor [33].

2.3 Neurogenesis

Adult neurogenesis was described both in the SGZ and in the SVZ (Figure 2) of the brain while it does not occur in adult spinal cord [34]. Neurogenesis consists of several developmental stages (proliferation, migration, differentiation and integration) that are characterized by distinct cell phenotypes. SGZ and SVZ do not have the same precursors;

consequently, there is not a unique nomenclature to identify cells involved in the adult neurogenesis [27,35,36].
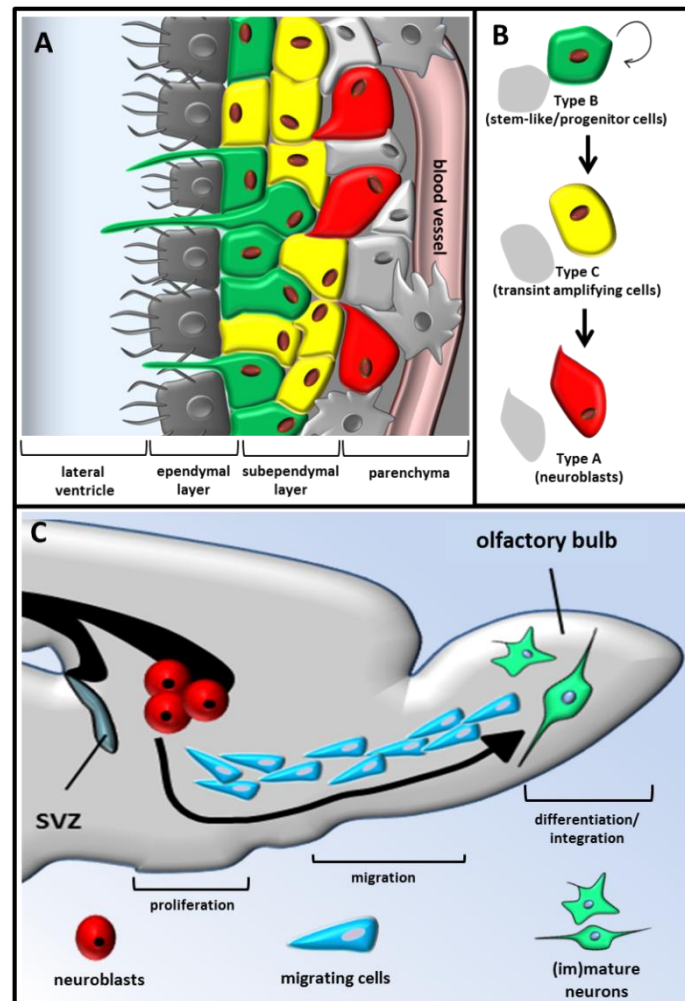
Figure 2. Neurogenesis in the SVZ. A, Cellular organization of the SVZ: lateral ventricle, ependymal layer (composed by type E cells or ependymal cells), subependymal layer (composed by type B, type C and type A cells) and brain parenchyma (composed by astrocytes, oligodendrocytes and blood vessels). B, NSC differentiation in the SVZ: type B cells undergo self-renewal or differentiate in type C cells which become type A cells. C, neurogenesis steps in the SVZ: neuroblasts proliferate in the SVZ and then migrate to the olfactory bulb where they differentiate in neurons and integrate with the existing cellular network.

Nevertheless, several markers are used to detect the different cell phenotypes involved in the neurogenic process [37,38] (Table 1). Nestin was the first marker described to identify stem-like/precursor cells and is the most widely used [39]. Nestin is a specific class of intermediate filament proteins that are expressed in non-differentiated cells. Class III β tubulin (Tuj1) [40], a protein expressed in post-mitotic neuron cytoskeleton, doublecortin (DCX) [41], which encodes a microtubule-associated protein present in migrating neuroblasts, and the polysialylated-neural cell adhesion molecule (PSA-NCAM), which is a product of post-translational modification of NCAM, are the most accepted markers for early neurons [42].

Mature neurons are identified by the microtubule-associated protein (MAP-2), the neuron-specific enolase (NSE) and the neural-specific nuclear protein (NeuN) [43,44]. Some non-neural cells can also be positive for the markers mentioned above. To avoid ambiguous interpretation of the results, it is recommended to perform multiple staining including non-neural markers such as glial fibrillary acidic protein (GFAP) [45] or calcium binding proteins (S100 and S100b) [46] for astrocytes, and 2',3'-cyclic-nucleotide 3'-phosphodiesterase (CNP) or myelin basic protein (MBP) for oligodendrocytes [47].

Table 1. Markers for adult neurogenesis.

Type of cells	Markers
Neural stem cells/Progenitors	Nestin [39]
	SRY-related HMG-box gene (Sox2) [48]
	Musashi-1 (Msi1) [49]
	Paired box gene 6 (Pax6) [50]
	Prominin (CD133) [51]
	Glial fibrillary acid protein (GFAP) [45]
NG2-glia positive cells	Chondroitin sulfate proteoglycan neuron/glia antigen 2 (NG2) [52]
Neuronal lineage (early)	III β tubulin (TUJ1) [40]
	Doublecortin (DCX, C-18) [41]
	Polysialylated-neural cell adhesion molecule (PSA-NCAM) [42]
	Neurogenetic Differentiation (NeuroD) [42]
Neuronal lineage (mature)	Neuronal nuclear epitope (NeuN) [44]
	Microtubule-associated protein 2 (MAP2) [43]
	Neuron-specific enolase (NSE) [43]
	Calbindin [53]
	Thyrosine-hydroxylase (TH) [54]
	Calretinin [53]
	Neurofilaments (NF) [53]
Astrocytic lineage	Glial fibrillary acid protein (GFAP) [45]
	Calcium binding proteins (S100/S100b) [46]
	Glutammate-aspartate transporter (EAAT1) [55]
Glial lineage	Galactocerebroside (GalC) [56]
	2',3'-cyclic-nucleotide 3'-phosphodiesterase (CNP) [47]
	Myelin basic protein (MBP) [47]

2.4 Therapeutic significance in CNS diseases

The therapeutic relevance of NSCs was investigated after several studies clearly demonstrated that the inhibition of neurogenesis decreased neurological functions [57,58], while its stimulation resulted in behavioural performance recovery (e.g., learning and memory tasks) [59,60]. Consequently, adult neurogenesis modulation could have a positive impact on the patients affected by CNS diseases, which are mostly characterized by neurological function deterioration, such as Alzheimer's (memory impairment) and Parkinson's (motor impairment) diseases. In this regard, strategies that are effectively able to restore distinct aspects of adult

neurogenesis are of specific interest for future treatments. Although the differentiation of NSCs is regulated by many physiological stimuli, these cells are considered to be key determinants in neurogenesis. Consequently, NSCs have been investigated to replace injured cells and to restore neurological functions by their differentiation into specialized neural cells.

The discovery of adult neurogenesis had a significant impact on regenerative medicine by overturning the long-held dogma that mammalian CNS cannot regenerate and renew itself. The stimulation of the neurogenesis process can result in the partial recovery of injured neural networks and in the enhancement of behavioural performances. The identification of NSCs and their role in adult neurogenesis motivated researchers to explore the regenerative potential of these cells for the treatment of the CNS diseases characterized by progressive lesion/loss of neural tissue and deterioration of neurological functions.

3. NEURAL STEM CELL DIFFERENTIATION

3.1 Exogenous and endogenous NSC-based strategies

In the last 20 years, several protocols have been developed to cultivate and differentiate NSCs *in vitro* after their isolation from CNS niches (isolated NSCs) or after derivation from pluripotent restored adult somatic cells (induced pluripotent stem cell-derived NSCs, iPSC-derived NSCs) [61]. However, the development of standard procedures to induce NSC differentiation *in vivo* or *in situ* has not yet been established. CNS repair *via* NSC differentiation can be achieved by following different strategies, which essentially depend on whether NSCs are exogenous or endogenous (Figure 3). iPSC-derived and isolated NSCs are considered exogenous NSCs when stimulated *in vitro* and transplanted *in vivo*. NSCs are considered endogenous when their differentiation is stimulated *in situ*.
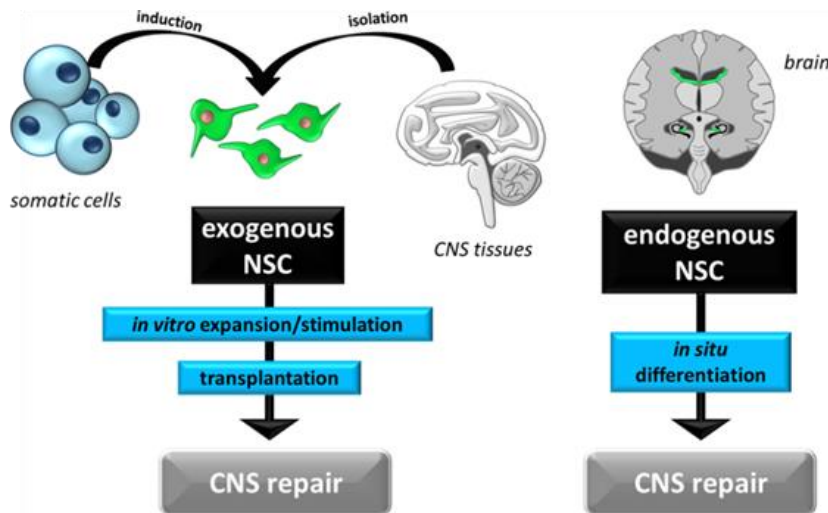
Figure 3. NSC differentiation for CNS repair. Strategies developed to achieve CNS repair with the use of exogenous or endogenous NSCs (in green). Left, exogenous NSCs can be obtained by the induction of other somatic cells (e.g., fibroblasts) or by isolation from neurogenic niches (e.g., the SVZ and SGZ). Exogenous NSCs are cultivated *in vitro* for *in vivo* transplantation and their differentiation can be designed to occur during cell cultivation or after cell transplantation. Right, endogenous NSCs are stimulated directly in the neurogenic niches and their differentiation can occur exclusively *in situ*.

3.2 Stimulation of NSC differentiation

Several methods have been developed to induce NSC differentiation *in vitro*, *in vivo* and *in situ* (Table 2).

iPSC-derived and isolated NSCs can preserve their multipotent profile in the presence of repressor-type bHLH genes [62,63], hypoxia [64], serum-free media [65], and media enriched with growth factors. Epidermal growth factor (EGF) and basic fibroblast growth factor (bFGF) are the most used growth factors to maintain NSCs in an undifferentiated state [66]. Exposure to specific compounds and conditions can induce NSC differentiation (Table 2). Recent evidences suggest that a combination of extracellular signals and niche environmental conditions, hardly reproducible *in vitro*, affect NSC behaviour in the organism [67]. Consequently, most of the strategies which provided promising results *in vitro* did not fully translated *in vivo* and *in situ* (or *vice versa*).

Numerous mechanisms controlling the behavior of NSCs were elucidated by deciphering the role of intrinsic and extrinsic signals in NSC circuits. Consequently, some of the strategies to induce NSC differentiation were based on the targeted modulation of these signals. Experimental evidence has highlighted the importance of the regulatory feedback loop between micro RNA (miR) and transcription factors, which can differentially influence NSC

behaviour [68]. miR upregulation *via* miR-9 transfection [69] or miR-195 downregulation *via* MBD1 gene-expressing lentivirus [70] can increase embryonic mouse NSC differentiation into neurons and astrocytes. The signals from cell-cell contact were also identified as modulators of NSC differentiation: co-cultures of NSCs and protoplasmic astrocytes or amniotic cells promote embryonic rat NSC differentiation into neurons [71]. The alteration of epigenetic marks is an important NSC lineage modulator as well. The overexpression of activator-type bHLH genes such as Mash1, neurogenin2, and NeuroD promotes neuronal-specific gene expression while it inhibits glia-specific gene expression [63]. Deciphering cell circuits and their regulatory signal network provides crucial information for NSC differentiation strategies [72].

In addition to endogenous modulators, pharmacological agents were found to impact NSC behaviour. Incubation with 4-aminothiazoles (e.g., neuropathiazol) or oleanoic acid led to TuJ1 (neuronal marker) expression in 90% of cells in treated primary neural progenitor cells isolated from adult rat hippocampus and NSCs isolated from the embryonic striatum of mice respectively [73]. Valproic acid [74,75] stimulates NSC differentiation by the inhibition of histone deacetylase and its combination with other active molecules (e.g., retinoids) significantly increased the percentage of MAP-2 (neuronal marker) positive cells *in vitro* [76]. The impact of addictive drugs on NSC differentiation and neurogenesis was also demonstrated [77]. Morphine promotes astrocyte differentiation [78] while D-amphetamine [79] and opioid peptides [80] increase neuron differentiation *in vitro* and *in situ*, in the hippocampus of adult mice.

NSC differentiation can also be stimulated by extremely low-frequency electromagnetic fields (ELFEFs) which affect several biological parameters such as the intracellular calcium level. ELFEFs upregulate the Ca^{2+} channels and increase the Ca^{2+} influx which induces the signalling cascade associated with the promoter of specific bHLH that control NSC differentiation [22,81]. NSCs isolated from the brain cortex of new-born mice and exposed to ELFEFs showed more cells positive for neuronal markers (+11.8% of MAP-2 and +11.9% of beta III tubulin) compared to the controls [82].

Strategies aiming at *in situ* differentiation of endogenous NSCs would bypass issues related to exogenous NSC transplantation, such as supply of exogenous NSCs (e.g., ethical concerns), immune response against allogeneic transplantation and post-grafting cell viability. Consequently, the administration of active compounds that would stimulate NSC

differentiation *in situ* is the current most common approach (instead of NSC transplantation) to enhance neurological function in neurodegenerative disease animal models (Table 2).

Table 2. NSC differentiation *in vitro* and *in vivo* (from exogenous or endogenous NSCs)

Study design	Molecule/Condition	Type of cells/area	Outcomes	Year
in vitro	neuropathiazol	primary neural progenitor cells isolated from adult rat hippocampus	+ neurons	2006 [74]
	ELFEFs	NSCs isolated from the brain cortex of nb mice	+ neurons	2008 [82]
	NSC co-culture with astrocytes or amniotic cells	NSCs isolated from embryonic rates	+ neurons	2012 [71]
	miR-9 transfection	NSCs isolated from embryonic mice	+ neurons + astrocytes	2013 [69]
	MBD1-expressing lentivirus	NSCs isolated from embryonic mice	+ neurons + astrocytes	2013 [70]
	BDNF	NSCs isolated from the forebrain cortex of nb mice	+ neurons + oligodendrocytes	2013 [100]
	oleanolic acid	NSCs isolated from the embryonic mouse striatum	+ neurons	2015 [73]
	valproic acid	NSCs isolated from embryonic rat forebrains	+ neurons	2015 [76]; 2008 [75]
	all-trans-retinoic acid	NSCs isolated from embryonic rat forebrains	+ neurons	2015 [76]; 1998 [92]
	1,25-Dihydroxyvitamin D3	NSCs isolated from adult mouse brain	+ oligodendrocytes	2015 [79]
	opioid peptides	NSCs isolated from embryonic rat striatum	+ neurons	2015 [80]
	NSC transplantation	human NSCs	prevention of further cognitive deterioration	2015 [101]
Exo NSCs	growth factor-overexpressing NSC transplantation	NSCs isolated from transgenic nb mouse hippocampus	AD deficit and synaptic density recovery	2016 [102]
Endo NSCs	morphine	adult mouse hippocampus	+ astrocytes	2015 [78]
	D-amphetamine	adult mouse hippocampus	+ neurons	2013 [79]
	ELFEFs	adult mouse hippocampus	+ neurons	2010 [98]
	retroviral Zfp488	adult mouse corpus callosum	motor function restoration	2011 [84]
	perfluorooctane sulfonate	cortical tissues of neonatal mice	+ neurons + oligodendrocytes	2013 [85]
	PCDHIIx shRNA/siRNA	lateral ventricle of mice	+ neurons	2014 [103]
	simvastatin	injured areas of adult rat brain	neurological function enanchement	2015 [83]
	ketamine	nb rat SVZ	+ neurons	2015 [104]
	nicotine	adult rat hippocampus	+ neurons	2015 [105]
	long noncoding RNA Pnky	embryonic and postnatal mouse brain	+ neurons	2015 [106]
	oxygen supply modulation	developing cerebral cortex of mice	+ radial glia	2016 [97]

ELFEFs, extremely low-frequency electromagnetic fields; Exo, exogenous; endo, endogenous; nb, new-born; SVZ, subventricular zone.

Simvastatin increased the percentage of MAP-2 (neuronal marker) and GFAP (astrocytic marker) positive cells in a rat traumatic brain injury model [83]. Its administration enhanced neurological functions such as sensory functions, motor functions, beam balance performance, and reflexes. The corpus callosum in mice exhibiting cuprizone-induced demyelination showed a significant increase in Olig2 (oligodendrocytic marker) positive cells after treatment with retroviral Zfp488 [84]. The overexpression of Zfp488 protein (activator of oligodendrocyte differentiation) induced a significant motor function restoration in demyelination-injured mice.

Perfluorooctane sulfonate induced neuronal and oligodendrocytic NSC differentiation in healthy mice, probably *via* PPARγ nuclear receptor activation, a pathway also involved in the retinoid-induced cascade for NSC differentiation [85].

Retinoic acid (RA) has an important role in neurogenesis by inducing neurite outgrowth and neural differentiation from various cell sources such as embryonic stem cells [86,87] and mesenchymal stem cells [88,89]. Several studies demonstrated that RA increases the expression of neural markers after its incubation with NSCs [76, 90]. RA signalling is transduced by two families of nuclear receptors, the retinoic acid receptors (RARs) and the retinoid X receptors (RXRs) [91,92]. RAR and RXR work as the heterodimer complex RAR/RXR and have 3 different isotypes (α, β and γ). While RARs are activated by all-trans and 9-cis RA, RXR is activated only by 9-cis RA. Unbound retinoid receptors repress transcription through the recruitment of corepressors such as NCoR and SMRT [91]. Those corepressors recruit in turn histone deacetylase protein complexes and Polycomb repressive complex 2, resulting in chromatin condensation and gene silencing. The interaction between RA and RAR/RXR induces receptor conformational changes which cause the dissociation of the corepressors and recruitment of transcriptional coactivators such as SRC/p160 family, p300/CBP and CARM-1 [92]. Coactivators induce histone acetylation and recruitment of ATP-dependent remodelling complexes which leads to the displacement of impeding nucleosomes within the proximal promoter region. The displacement facilitates the access to the general transcription machinery by promoters including RNA polymerase II [91,92]. Since RXR is able to form heterodimers with other nuclear receptors, including other peroxisome proliferator-activated receptors (PPARs), cross-talk with other signalling pathways mediated by PPAR can also occur. Additionally, ROS can induce NSC differentiation in a RA-independent way by RARα stabilization.

In vitro, the dissolution in aqueous solutions (e.g., cell media) increases RA susceptibility to the oxidative damage of light, air, and temperature (>90°C). Moreover, retinoids are adsorbed by many of the glass and plastic wares commonly used in cell culture, impacting control of the administrated doses and reproducibility of the experiments [94]. *In vivo*, chronic administration of RA showed progressive decline of its plasmatic concentrations (probably due to a progressive impairment of gastrointestinal uptake) as well as poor bioavailability (associated with acquired mutations either of RAR or CRABP) and stability (pH sensitivity) [95]. One successful strategy to overcome these issues is to incorporate RA into nanoparticles. For instance, RA encapsulation into nanovectors showed an enhanced therapeutic effect in the treatment of cancer or ischemia compared to its free form, highlighting the interest of RA-based systems [96].
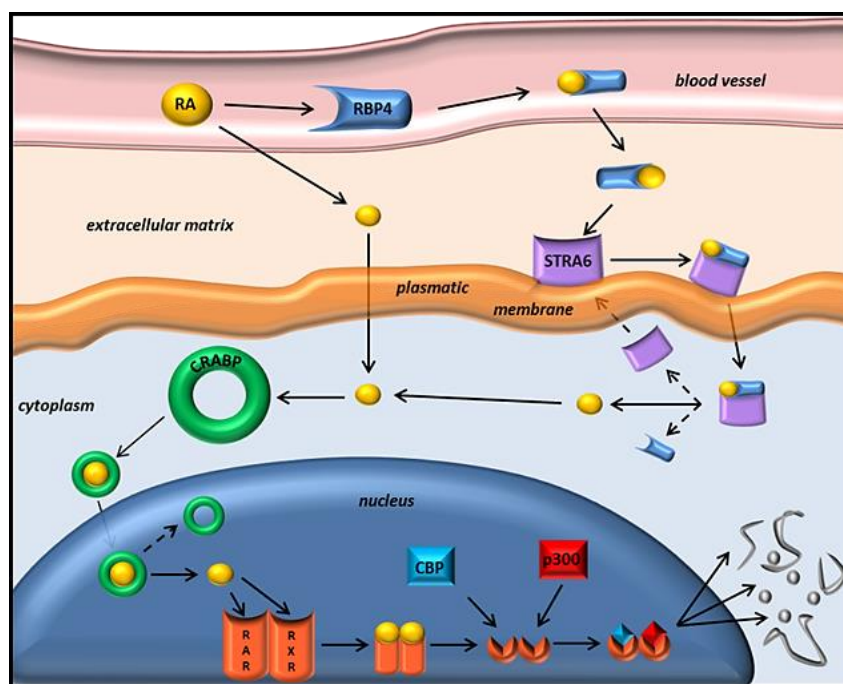
Figure 4. Cell regulation *via* retinoic acid (RA).
More than 95% of circulating retinoic acid is bound to the retinoid bounding protein 4 (RBP4) which allows the penetration into the cell *via* the transmembrane protein stimulated by retinoic acid 6 (STRA6). The complex RA-RBP4-STRA6 dissociates in the cytoplasm and RA binds to the cellular retinoic acid-binding protein (CRABP) which carry RA into the nucleus. However, free retinoic acid can cross the phospholipid bilayer of the plasmatic membrane and of the nucleus also without any transporter. Once in the nucleus, RA binds to heterodimer complex of retinoic acid receptor–retinoic x receptor (RAR/RXR) and recruits the transcriptional co-activators cAMP-response-element-binding protein (CBP) and protein 300 (p300). RAR/RXR in combination with CBP and p300 act with other factors to regulate signal transduction pathways and cell-differentiation.

Another approach to induce NSC differentiation is the oxygen supply modulation at the site of neurogenic niches. It was recently showed by Lange *et al*. that angiogenesis is linked to neurogenesis during cortical development [97]. They demonstrated that selective perturbation

of brain angiogenesis in embryos increased NSC expansion by hypoxia while exposure to increased oxygen levels stimulated NSC differentiation.

The *in vivo* application of ELFEFs on C57b1/6 mice promoted proliferation and differentiation of hippocampal NSCs [98]. NSC differentiated into neurons, which were functionally integrated in the dentate gyrus network 30 days after the ELFEF treatment. Spatial learning and memory were enhanced, highlighting the important therapeutic implications of ELFEFs for the treatment of neurodegenerative diseases. Moreover, it was demonstrated that ELFEFs increased the survival of hippocampal newborn cells [99].

Altogether, there is concurrent information demonstrating that NSC differentiation is a valid approach to enhance neurological functions during neurodegenerative diseases. The therapeutic effect achieved in neurologically compromised animal models (e.g., restoration of cognitive functions), together with the stimulation of the neurogenic process and neuroprotection in healthy animal models *via* NSC differentiation, provide precious insight for the clinical translation of NSC-based therapeutic strategy.

3.3 Clinical trials

Depending on the results obtained during pre-clinical studies, NSC differentiation-based therapies have been recently translated into the clinic [107]. Thirty-seven NSC-based clinical trials are currently on going, involving patients affected by gliomas, ischemic stroke (IS), amyotrophic lateral sclerosis (ALS), spinal cord injury (SCI) and Parkinson's disease (PD) [108]. Surprisingly, most of these therapies aimed at *in vivo* differentiation of transplanted exogenous NSCs (Table 3), while most of the pre-clinical studies focused on *in situ* differentiation of endogenous NSCs (Table 2). In the clinical trial NCT02117635, CTX0E03 cells (a human neuronal stem cell line) were stereotaxically injected by in the striatum of IS patients (site of lesion) (Phase I). The treatment promoted a partial recovery of neurologic functions [109] but no anatomical modifications. This would suggest that NSCs do not directly differentiate into neurons but rather act as cellular mediators by secreting paracrine factors.

The aim of the clinical trial NCT01640067 (Phase I) was to assess the safety of NSCs and their efficacy. The transplantation of foetal NSCs in the spinal cord of ALS patients stopped the progression of the disease for up to 18 months and did not cause side effect [110]. No mechanistic study was performed *in vivo* to explain this result, but the preservation of NSC

multipotency was demonstrated *in vitro* after the recovery of remaining NSCs in the syringe used for the injection, and culture of transplanted NSCs.

Transplantation of genetically modified NSCs has also been used for the treatment of gliomas and is being evaluated in clinical trials [111]. The strategies consisted by using genetically modified NSCs as vehicles to target tumor cells without harming healthy brain tissue. Very promising pre-clinical studies showed that NSC-based oncolytic virus delivery [112] and iPSC-derived NSCs engineered with therapeutic/diagnostic transgenes [113] were able to suppress tumour growth and to significantly extend the survival of glioblastoma-bearing mice. In another study (NCT01172964), *E.Coli* cytosine deaminase-expressing NSCs were co-injected with 5-fluorocytosine (5-FU) intra-cerebrally. The objective was to facilitate the conversion of 5-FU into its active form (fluorouracil) directly in the tumor. Another approach was to perform an intracranial injection at the tumor site of carboxylesterase-expressing NSCs to increase glioblastoma cell sensitivity to irinotecan hydrochloride, an anti-cancer drug (Camptosar) (NCT02192359).

Unfortunately, more detailed information regarding the results and efficiency of these clinical trials are not available. It seems that none of the described clinical treatments caused severe adverse events. To the extent of our knowledge, no NSC-based therapy aiming at treating neurodegenerative diseases reached phase III yet. Focusing on strategies based on *in situ* stimulation of endogenous NSC differentiation could provide promising alternatives that might be easier to translate into therapy for the treatment of neurodegenerative diseases.

Table 3. NSC-based clinical trials

Targeted disease	Cell type	Approach	Identification	Phase
ALS	exo NSC	transplantation	NCT01640067	I (finished 2015)
SCI	exo NSC	transplantation	NCT02326662	I/II (ongoing 2017)
SCI	exo NSC	transplantation	NCT01772810	I (recruiting 2017)
IS	exo NSC	transplantation	NCT02117635	II (ongoing 2017)
PD	exo NSC	transplantation	NCT02452723	I (recruiting 2017)
ALS	endo NSC	*in situ* stimulation	NCT00397423	II (completed 2007)
gliomas	g. m. NSC	transplantation	NCT01172964	I (completed 2015)
gliomas	g. m. NSC	transplantation	NCT02192359	I (recruiting 2017)

ALS, amyotrophic lateral sclerosis; SCI, spinal cord injury; IS, ischemic stroke; PD, Parkinson's disease; exo, exogenous; endo, endogenous; g. m., genetically modified. Resource: https://clinicaltrials.gov.

3.4 Challenges

Despite important and encouraging progress, the intrinsic complexity of the CNS still precludes the potential of many NSC-based therapeutic approaches. The structural fragility of the CNS limits invasive approaches whereas the stage, the area, and the type of the pathology strongly influence the impact and the effect of the treatments [114,115].

One limiting factor is the lack of correlation between *in vitro* and *in vivo* NSC behavior. The ability of NSCs to differentiate into specialized cellular lineages depends on their microenvironment. Understanding the chemical and physical signals as well as the cell-cell interactions represents the most important challenge to dynamically modulate NSC differentiation *in vivo* [67].

Another challenge is the control of the biological activity of these cells following their transplantation or stimulation. In many clinical trials involving NSCs, little is known about the mechanisms, the location, and the extent of the modulation of neurogenesis. The development of methods able both to induce NSC differentiation and to track NSC differentiating progeny would represent a promising strategy to understand NSC behavior and to design the most appropriate NSC-based therapy.

Additional problems are associated to exogenous NSC therapies, which are based on *in vitro* NSC cultivation followed by *in vivo* NSC transplantation. The incidence of tumors is one of the most important concerns in NSC transplantation. Tumor development has been rarely reported in the majority of the described stem cell-transplantation-based clinical trials [116] but it is not unheard of [117]. Moreover, the strict procedures of the cell culture (e.g., xeno-free environment) and the risk of adaptive genetic changes during the passages [118], *in vitro*, together with cell survival, graft rejection and cell source issues [119], *in vivo*, make the clinical translation more difficult.

The current inability of medical science and fundamental research to provide information and solutions to these problems represents a significant risk for the patients, and thus impairs the clinical translation of NSC research.

At the same time, under the pressure of the public and the media, the population has overestimated expectations about the ability of NSC transplantation to cure neurodegenerative diseases. Patients have been exposed to severe risks due to clinical trials with incomplete scientific knowledge, e.g., in 2013 with the "Caso Stamina" [120]. Cattaneo and Bonfanti

highlighted the importance of a constructive dialogue between science and society, which should bypass the media [121].

3.5 Conclusion

NSC differentiation, and consequently neurogenesis, can be stimulated either by endogenous modulators or pharmacological agents. Several methods have been developed to induce NSC differentiation which resulted in therapeutic effects in the treatment of CNS diseases and, some of them were included in clinical trials. Despite the rapid clinical translation, several issues are still challenging with this therapeutic approach. The intrinsic complexity of the CNS, the lack of *in vitro-in vivo* correlation, transplantation-associated issues, and the biological activity control remain difficult obstacles to overcome by conventional medicine. Considering those issues, nanomedicines provide promising solutions to solve some of these problems.

4. NANOMEDICINE FOR NSC DIFFERENTIATION

4.1 Definition of nanomedicine

Nanomedicine is the medical and pharmaceutical application of nanotechnology and its main objective is the improvement of conventional therapies by providing new skills and/or overcoming the limitations associated with conventional pharmaceutical forms.

While several regulatory authorities and medical agencies worldwide (e.g., European Medicines Agency [122] and European Science Foundation [123]) converge on this definition of nanomedicine, the term "nanotechnology" is still a matter of discussion. One of the main reasons of the disagreement is that "*the term "nano" is, however, somewhat confusing since it does not designate the same reality for the physicist, the chemist and the biologist*" [124].

The National Science and Technology Council defines nanotechnology as the "*science, engineering, and technology conducted at the nanoscale, which is about 1 to 100 nanometers.*" [125] while the European Commission defines it as the "*study of phenomena and fine-tuning of materials at atomic, molecular and macromolecular scales, where properties differ significantly from those at a larger scale*" [126].

According to our bibliographic research and scientific experience, the term "nanotechnology" would define those areas of science and engineering where both particular phenomena (e.g., plasmon resonance) and specific properties (e.g., high surface area) are present when materials, structures and devices are at nanometre scale dimensions exclusively (generally smaller than 500 nm).

4.2 Classification of the nanomedicines

Nanomedicine can use either miniaturized medical devices for imaging/clinical evaluation, called nanodevices [127], or nanoscale systems for therapy/theranostic, called nanomedicines. The classification of the nanomedicines (Figure 5) depends on whether they are biological carriers, such as virus and bacteria [128,129], or they are made of nanomaterials. While a nanocrystalline material produces nanoscale crystals [130] which are entirely composed by the drug, nanostructured materials are engineered polymeric or non-polymeric compounds that provide drug nanocarriers [131] with specific shapes and functionalities.
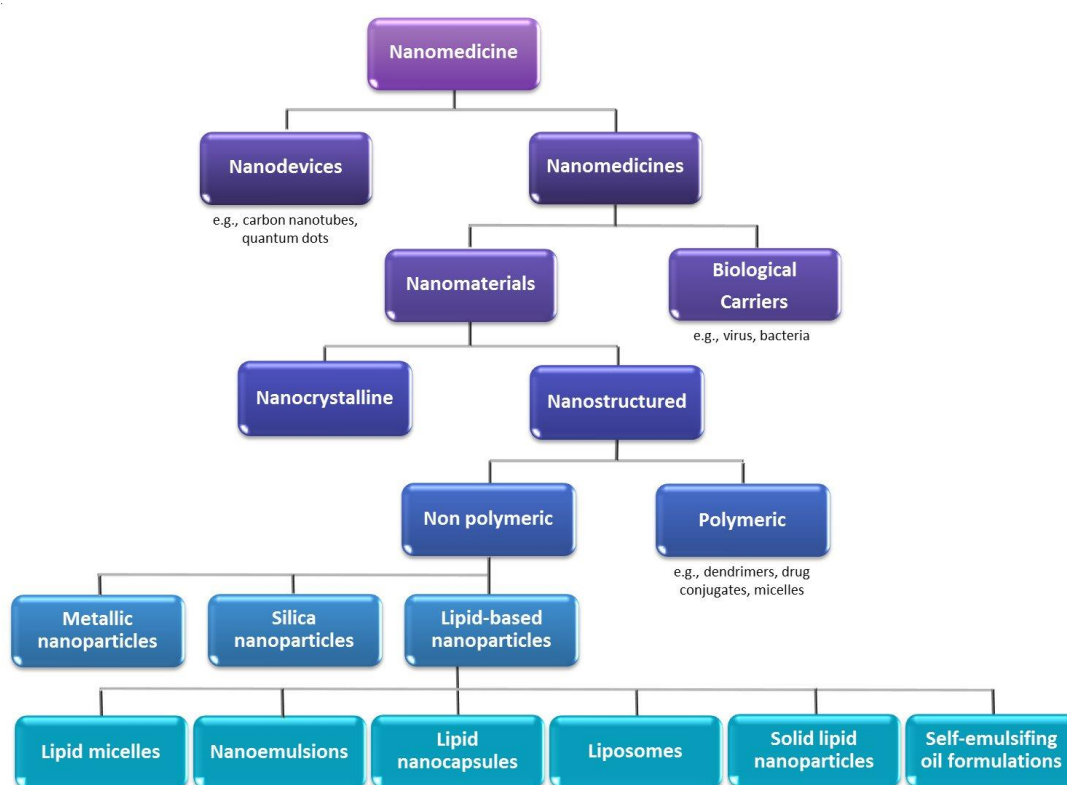

Figure 5. Different types of nanomedicines.

Among those nanostructured carriers, the lipid-based nanoparticles have attracted increasing interest due to their high degree of biocompatibility and versatility [132]. In fact, most of the excipients used to produce lipid-based nanoparticles are phospholipids, triglycerides and cholesterol which are already used in FDA-approved therapeutics. Moreover, the presence of both oily and aqueous compartments made those nanoparticles suitable for hydrophilic, lipophilic and amphiphilic drug delivery.

Lipid micelles, nanoemulsions, liposomes, solid lipid nanoparticles and lipid nanocapsules (LNCs) are some of the most studied lipid-based nanoparticles for therapeutic applications. They are produced by different methods and show different properties (Table 4).

Table 4. Main advantages/disadvantages of lipid-based nanoparticles

Type	Method of production	Advantages	Disadvantages
Nanoemulsions	♦high pressure homogenization ♦low energy emulsification method at constant temperature ♦phase inversion temperature method	spontaneous solvent free	Ostwald ripening risks of erythrocyte lysis
Micelles	♦concentration of surfactant above the critical micelle concentration	spontaneous solvent free small size	low stability low drug-loading
Liposomes	♦Bengham's method (dry film hydration with aqueous media) ♦dry film hydration with organic solvent	highly biomimetic semi-spontaneous	solvents low stability big size short half-life
Solid-lipid nanoparticles	♦high pressure homogenization ♦microemulsion ♦double emulsification	easy to scale-up highly stable solvent free controlled release	not for fragile drugs multi-steps
LNCs	♦phase inversion temperature method	solvent free highly stable easy to scale-up	multi-steps high temperatures

Liposomes [133] are the first nanomedicine successfully translated to clinic applications [134]. They are 50 nm-5 μm vesicles which can be composed by one (monolamellar) or more (multilamellar) aqueous compartments delimited by a phospholipid bilayer. Due to their highly biomimetic composition and structure, liposomes are also used in cellular membrane-modelling to study the interactions between compounds and cells [135].

Micelles [136] are colloidal solutions consisting in a mixture of water, oil and surfactant. Depending on whether the dispersant phase is aqueous or oily, micelles can be classic or

reverse, respectively. The most important characteristic of these formulations is that lipid micelles form spontaneously when the surfactant reaches the critic micellar concentration. Moreover, there is a dynamic equilibrium with a constant exchange of monomers between dispersant phase and lipid micelles.

Nanoemulsions [137] are 50-200 nm globular droplets either of oil in water (O/W) or of water in oil (W/O). Nanoemulsions have been included into different pharmaceutical forms, such as spray, creams and foams which have been administered by different routes as well (e.g., oral, intravenous and pulmonary) [138].

Both nanoemulsions and liposomes can form semi-spontaneously by mixing the components at specific ratios and by defining the final size with one or more additional steps (e.g., sonication or extrusion).

Solid-lipid nanoparticles [139] are 50 nm-1 μm colloidal carriers composed by lipids that are in a solid state both at body and room temperatures, making these nanoparticles very stable as well as suitable for lyophilisation. Moreover, solid lipids allow a better control of drug release because the diffusion of a molecule through a solid instead of liquid phase should be considerably lower.

Lipid nanocapsules (LNCs) [140] are 20 to 200 nm negatively charged nanocarriers presenting a hybrid structure between polymeric nanoparticles and liposomes. LNCs typically have an oily core composed of Labrafac® WL 1349 (a triglyceride mixture of capric and caprylic acids, liquid at room and body temperatures), surrounded by a surfactant shell of Solutol HS® (a PEG derivative mixture of PEG 660 and PEG 660 hydroxystearate) and, by Lipoid® S75-3 (a lecithin composed of 70% phosphatidylcholine soya bean lecithin and 30% stearic, oleic, linoleic and linolenic acids). LNC composition and structure are extremely versatile and they can be modified according to their application without affecting the main properties of the system. Depending on whether the drug to be encapsulated and delivered has a low solubility in Labrafac® or is hydrophilic, LNCs' core can be produced by using different triglyceride mixtures (e.g., Captex 8000® [141]) or replaced by an aqueous core (e.g., *via* polyurea bidimensional network [142] or micelles encapsulation [143]), respectively. LNCs are also suitable for shell functionalization and modification. The utilisation of longer chain of PEG (e.g., PEG_{1500} [144]) significantly increases LNC stealth properties and blood half-life while the insertion of lipopolysaccharides [145] shifts the surface charge from negative to positive values. LNCs' ligand functionalization (e.g., *via* peptide adsorption [146] or grafting [147]) enhances

LNC-cells interactions and provides targeting properties to the system. Those nanoparticles have been used to encapsulate several type of bioactive molecules (e.g., cytotoxic [148], nucleic acids [149], food complements [150]) as well as tracking compounds (e.g., fluorescent dyes [151] and radioactive molecules [152]). These nanocarriers have been administered in animal models and showed different biodistributions depending on the route of administration (e.g., intravenous [152], intracranial [146], oral [153]) and on their shell structure.

LNCs are produced by a solvent-free method named the phase inversion temperature (PIT) method (Figure 6). The PIT is a range of temperature, affected by the saline concentration of the aqueous solution, in which the surfactant of the emulsion shows the hydrophilic lipophilic balance (HLB)in equilibrium. Solutol HS® solubility changes with the temperature: at high temperatures (>80°C) it is lipophilic (dehydration of the polyoxyethylene chains) while at low temperatures (<60°C), Solutol HS® is hydrophilic. A fast cooling and dilution of the initial mixture of Labrafac®, Solutol HS® and Lipoid® during the PIT results in a final nanoscale carrier formulation which is kinetically more stable than the initial emulsion.
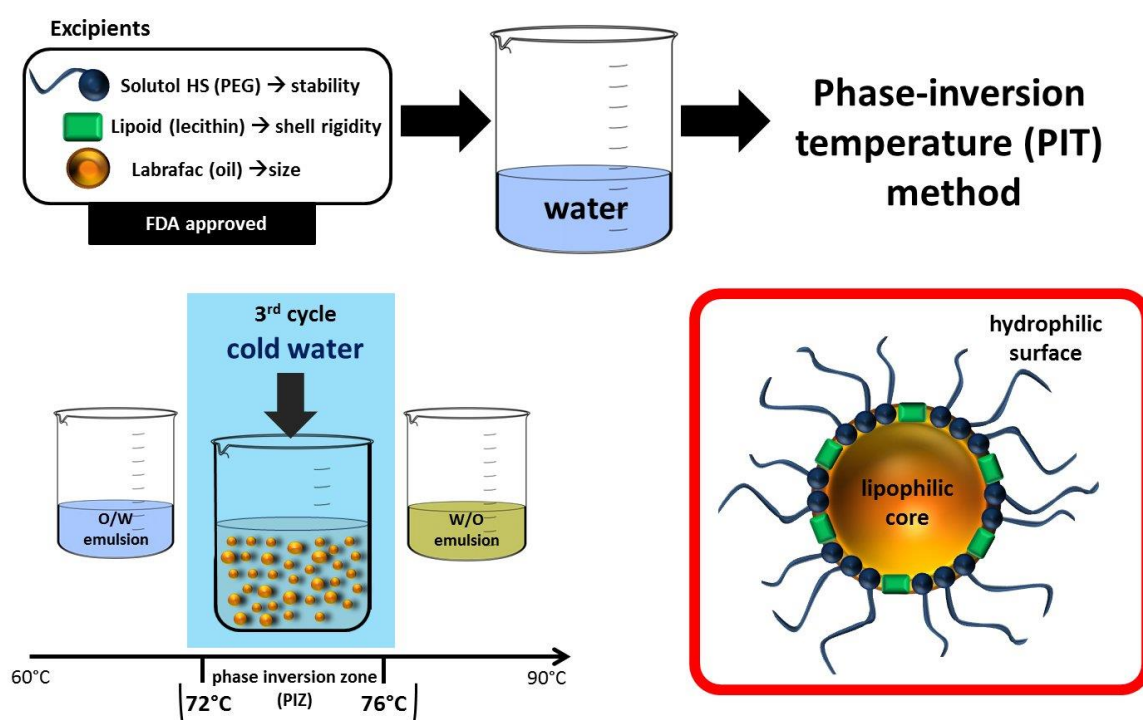
Figure 6. The phase-inversion temperature method to produce LNCs.
The phase inversion temperature (PIT) method is a solvent free and low energy process. Solutol HS®, Lipoid® and Labrafac® are mixed together. Then, the emulsion is heated and cooled between 60 °C and 90 °C. Higher temperatures lead to water in oil emulsions (dehydration of the polar surfactant heads) while lower temperatures lead to oil in water emulsions (hydration of the polar surfactant heads). After 3 temperature cycles, rapid dilution with cold water (4 °C) is performed at temperature corresponding to the PIT (between 72 °C and 76 °C). The final LNCs show a lipophilic core (Labrafac®) and an hydrophilic surface (Solutol HS® + Lipoid®).

4.3 Advantages of nanomedicines in NSC differentiation-based therapies

Nanomedicines have emerged to overcome some of the limitations cited above that are showed by conventional medicines.

Nanostructured scaffolds are promising candidates to mimic the *in vivo* extracellular conditions by selecting appropriate nanoscale material and architecture; thus they can be used to increase the correlation between *in vitro* and *in vivo* NSC behaviour. They could increase the viability of the transplanted NSCs and ensure their differentiation. Moreover, nanostructured scaffold could boost neurogenesis in non-neurogenetic regions (e.g., the striatum of PD patients [154]) and be associated to active drugs (e.g. chemotrophic proteins [155]) which can guide and maintain the migration and integration of NSC-differentiated cells *via* sustained drug release.

Some of the molecules used to stimulate NSC differentiation listed in Table 2 can be poorly soluble in water (vitamins) or highly sensitive (proteins). The nanoscale size reduction of low soluble drugs (e.g., simvastatin [156]) improves the dissolution rate of the molecules in aqueous media, facilitating their administration. The nanoencapsulation protects growth factors from the environment [157] and increases their levels in the CNS, preserving their activity [158]. Another critical factor is the capacity of a molecule to reach the dose in the required timeframe to allow a therapeutic NSC differentiation. Drug release can be controlled by different nanoparticulate systems (e.g., nanospheres or nanocapsules), the structure (e.g., monolayer or multilayers) and composition of the system (e.g., chitosan or hyaluronic acid-based polymers) [159]. Drug association with nanoparticulate systems led to an increased half-life and bioavailability compared to the free forms (e.g., for retinoic acid [160]). Furthermore, the nanoscale size can enhance the cellular uptake of the drug [161].

Nanotechnology-based real-time imaging can be used to develop non-invasive tools for the monitoring of NSC differentiation dynamics after *in vivo* transplantation. The real-time traceability of NSCs offers spatial and temporal information of the processes involved in differentiation, as well as the interactions between exogenous NSCs and endogenous cells. Consequently, it would improve the knowledge about the mechanisms of NSC differentiation.

The development of systems able to specifically target and stimulate endogenous NSC differentiation is a promising solution to overcome the previously described transplantation-associated issues (3.4 Challenges). Nanomedicines are suitable for surface modifications by

covalent or non-covalent grafting. Nanomedicine-associated drugs could cross the blood-brain barrier e.g. *via* OX26 [162] or lipoprotein [163] functionalization and reach endogenous NSCs *via* a NSC-targeting molecule. Moreover, selective targeting would allow the administration of smaller doses by increasing the efficacy of the drug and decreasing its side effects.

However, it has been clearly established that size, shape and composition of nanomedicines play an important role on the safety of human health by directly impacting their biological reactivity and accumulation/clearance in the body [164]. Size reduction and increase of surface area can induce an inflammatory response and genotoxicity for a same dose of medicine [165]. Indeed, one of the critical point is the potential activation of the immune system. It could nullify the expected therapeutic effect of nanomedicines (e.g., by macrophage sequestration) or induce acute immunotoxicity (e.g., anaphylactic and hypersensitivity reactions) [166]. Nevertheless, strategies can be used to limit the negative impact of nanoparticles on the immune system by modifying their size, by using less-immunogenic materials and by modifying their surface. For instance, the PEGylation of nanoparticle surface is widely used to reduce opsonisation and thus to "hide" nanoparticles from the immune system recognition [167].

4.4 Current nanomedicine-based studies aiming at NSC differentiation for therapeutic purposes

Nanostructured scaffolds have been developed for *in vivo* transplantation of NSCs. The first carbon-nanotube structured PLGA matrix made by Landers *et al.* induced the differentiation of iPSC-derived NSCs into neuronal cells after electric stimuli *in vitro* [168]. This nanostructured scaffold is a promising candidate to improve cell survival and functional integration in patients with neurodegenerative diseases who are receiving NSC transplantation (e.g., PD). Recently, Hoveizi *et al.* produced PLA/gelatin nanofibers seeded with iPSC-derived NSCs to investigate the influence of the nanostructured scaffold on NSC differentiation [169]. The authors demonstrated that iPSC-derived NSC were able to attach, proliferate, and differentiate on the PLA/gelatin fibers and that the system was a potential cell carrier for transplantation. In another work, Raspa *et al.* used self-assembling peptides (Ac-FAQ) in association with poly(ε-caprolactone)- poly(D,L-lactide-co-glycolide) (PCL–PLGA) to produce electrospun fibers [170]. The nanofibrous systems were highly biocompatible *in vivo* when implanted in rats and they promoted NSC differentiation *in vitro* after NSCs were seeded onto flat electrospun covered coverslips.

Bernardino and Ferreira were the first to produce retinoic acid-loaded nanoparticles [171,172]. Pro-neurogenic gene expression was increased after the intracranial injection of nanoparticles into the mouse SVZ due to the activation of nuclear retinoic acid receptors. Recently, a neuroprotective effect and an enhanced vascular regulation induced by their formulation was reported in PD [173] and IS [96] mouse models, respectively. Moreover, they also showed the advantage of the synergy between blue light exposure and light-reactive RA-loaded nanoparticles which potentiates neurogenesis in the SVZ [174]. Curcumin-loaded nanoparticles can also modulate NSC differentiation and are associated with the recovery of functional deficits in an AD rat model [175]. The administration of these nanoparticles *via* intraperitoneal injection increased the expression of genes involved in neuronal differentiation (neurogenin, neuroD1, etc.) and reversed learning and memory impairments probably *via* the activation of the Wnt/β-catenin pathway. Papadimitriou *et al*. developed two different types of polymeric nanoparticles, crosslinked to form a nanogel or self-assembled to form a block micelle system, which were loaded with retinoic acid and tested *in vitro* on NSCs of the SVZ of mice [176]. The authors demonstrated that both the nanogel and the block micelle system reached the cytoplasm and ensured a higher bioavailability of the retinoic acid, which increased the NSC differentiation into MAP-2 (neuronal marker) positive cells.

Fe_3O_4 magnetic nanoparticles in association with ELFEFs enhanced neural [177] and osteogenic [178] differentiation of bone marrow-derived mesenchymal stem cells. Since ELFEFs already showed the efficacy of inducing NSC neural differentiation, its association with magnetic nanoparticles could potentially be even more efficient at stimulating NSC differentiation. Genome editing of iPSCs *via* nanoparticle-based drug delivery systems has also been developed as a promising reprogramming strategy for personalized medicine [179,180].

Direct delivery of mRNA or microRNA into human iPSCs have provided human models for specific disease phenotypes, including neurodegenerative diseases, which are useful to design the most appropriate therapy by understanding their mechanisms and pathogenesis [181]. Moreover, genome editing of iPSC-derived NSCs using nanomedicines would supply an unlimited source of any human cell type, avoiding the cross-species issues of animal-derived models, and most of the ethical concerns related to stem cells (e.g., the utilization of human embryos) [182]. Direct delivery of nucleic acids to the CNS increased neuron regeneration and/or slow the progression of neurological impairments. Although transfection methods

mediated by viral vectors are efficiently applied to induce NSC differentiation (as shown in 3.2 [69,70,85]), from a clinical point of view, non-viral vectors are preferred [183].

Nanomedicines provide non-viral vectors, such as nanoparticle-based systems, which are suitable for cell reprogramming. Li *et al*. induced mature neuron differentiation *via* a biodegradable nanoparticle-mediated transfection method [184]. They delivered neurogenin 2 (bHLH transcription factor) to transplanted human fetal tissue-derived NSCs in the lesion site of a rat brain and generated a significantly larger number of neurofilament (neuronal marker) positive cells.

Saravia *et al*. reported for the first time the ability of a nanoparticle-based formulation to deliver miR-124 and to modulate the endogenous neurogenic niche in PD animal model [185]. They demonstrated not only neurogenesis at the SVZ-olfactory bulb axis but also the migration and maturation of new neurons into the lesioned striatum and the enhancement of the motor functions in PD-like mice. Fernandez and Chari recently achieved the highest transfection level (54%) reported so far on NSCs [186]. They demonstrated that the association between DNA microcircles, which are small DNA vectors without a bacterial backbone, and magnetic nanoparticles resulted in a sustained gene expression for 4 weeks. These results are really promising and bide well for a clinical translation of their system.

Recently, gold nanoparticles with deoxythymidine oligonucleotides Gd(III) and Cy3 have been shown to be useful for MRI imaging of transplanted NSCs [187]. A majority of transplanted NSCs (71%) was detectable in the brain over 2 weeks post-transplantation. In another work, the differentiation peak time (12 days post-transplantation) and the migration/apoptosis phases of the transplanted NSCs were identified [188]. The authors developed a polymeric nanovehicle that induced NSC differentiation (loaded with retinoic acid) and was detectable in real-time imaging (bicistronic vector TUPIS) [188]. Umashankar *et al*. proposed a live-imaging method to monitor superparamagnetic iron oxide/ Molday ION Rhodamine B (USPIO/MIRB)-labelled NSCs after transplantation [189]. NSCs were incubated with USPIO/MIRB nanoparticles and then identified by dual magnetic resonance and optical imaging. Although USPIO/MIRB may have advantageous labelling and detection features for NSC tracking, the immunoresponse produced *in vivo* needs further examinations before their utilization in the clinic. Jiráková *et al*. demonstrated that poly-L-lysine-γFe2O3 coated nanoparticles are a potential tool for the detection and monitoring of transplanted iPSC-derived NSCs [190]. Contrarily to cobalt zinc ferrite coated nanoparticles, poly-L-lysine-

γFe2O3 coated nanoparticles did not affect cell proliferation and differentiation. By making NSCs detectable by magnetic resonance without affecting the cellular behaviour, they provide a suitable non-invasive tool for cell tracking in NSC-based therapies.

Table 5. Nanomedicine-based approaches for the modulation of NSC differentiation

Strategy	System	Study design	Outcomes	Reference
nanostructured scaffold	DNA-peptide nanotubes	*in vitro*	NSC differentiation in neurons	[193] 2014
	carbon nanotubes	*in vivo*	actuation of NSC differentiation	[168] 2014
	graphene nanofibers	*in vitro*	NSC differentiation in oligodendrocytes	[194] 2014
	PLA/gelatin nanofibers	*in vitro*	iPSC differentiation in neuronal-like cells	[169] 2016
	rolled graphene oxide foams and electric stimuli	*in vitro*	NSC proliferation and differentiation	[195] 2016
	patterned porous silicon photonic crystals	*in vitro*	NSC differentiation	[196] 2016
	self-assembling peptide -PCL–PLGA nanofibers	*in vivo* implantation	NSC proliferation and differentiation in neurons and oligodendrocytes	[170] 2016
	self-assembling peptide nanofibers	*in vivo* implantation	robust survival and neurite outgrowth	[197] 2016
	salmon fibrin fibers	*in vivo* implantation	NSC proliferation and differentiation, vessel growth	[198] 2016
	collagen scaffold tethered with a collagen-binding epidermal growth factor receptor antibody	*in vivo* implantation	retain NSCs at the injury sites and promote neuronal differentiation	[202] 2017
	aligned nanofibrous PLGA scaffolds	*in vitro*	NSC proliferation and differentiation	[203] 2017
nanoparticulate drug delivery system	nilo1-titanium dioxide nanoparticles	*in vitro*	NSC recognition in co-culture	[191] 2011
	neurogenin2-loaded biodegradable nanoparticles	*in vitro*	increased neurofilamnet expression	[184] 2016
	polymeric nanoparticle-based nanogel loaded in retinoic acid	*in vitro*	increased number of MAP-2 positive cells	[176] 2016
	polymeric nanoparticle-based bloc micelle system loaded in retinoic acid	*in vitro*	increased number of MAP-2 positive cells	[176] 2016
	DNA microcircle magnetic nanoparticles	*in vitro*	sustained gene expression	[186] 2016
	retinoic-acid loaded polymeric nanoparticles	*in vivo* (intracranial)	NSC differentiation, neuroprotection, AD deficit recovery	[174] 2016; [173] 2015; [172] 2012
	miR-124-nanoparticles	*in vivo* (intracerebral)	neurogenic niche modulation, PD deficit recovery	[185] 2016

	curcumin-loaded nanoparticles	*in vivo* (intraperitoneal and intracranial)	NSC differentiation in neurons, AD deficit recovery	[175] 2013
	Nurr1 plasmid DNA/Rex1 siRNA-silica nanoparticles	*in vitro*	iPSC differentiation in dopaminergic neurons	[204] 2017
	SDF-1 PLGA nanoparticles	*in vivo* (intracranial injections)	NSC recruitment at brain lesioned site	[205] 2017
nanotechnology-based real-time imaging	bicistronic vector TUPIS functionalized nanovehicle	*in vivo*	NSC differentiation imaging	[188] 2015
	deoxythymidine oligonucleotides Gd(III)/Cy3 functionalized gold nanoparticles	*in vivo*	NSC differentiation imaging	[187] 2016
	USPIO/MIRB nanoparticle	*in vivo*	tracking of NSC behavior after neuronal transplantation	[189] 2016
	DNA–gadolinium–gold nanoparticles	*in vivo*	*in vivo* T1 magnetic resonance imaging of transplanted NSC	[199] 2016
	poly-L-lysine-γFe2O3 coated nanoparticles	*in vivo*	*in vivo* magnetic resonance imaging of iPSC-derived NSC	[190] 2016
	poly(aspartic acid-dimethylethanediamine) SPION-loaded micelles	*in vivo*	MRI tracking of NSCs	[206] 2017
mixed	3D graphene oxide-encapsulated gold nanoparticle	*in vitro*	NSC differentiation monitoring	[200] 2013
	nanotopographical siRNA delivery	*in vitro*	NSC differentiation in neurons	[192] 2013
	gold nanoparticle-decorated scaffold	*in vitro*	NSC differentiation in neurons	[201] 2015
	hybrid polyacrilammide-chitosan scaffolds grafted with PLGA nanoparticles grafted with transactivator of transcription von Hippel-Lindau peptide	*in vitro*	iPSC differentiation in neurons	[207] 2017

PLA, polylactic acid; PCL, polycaprolactone; PLGA, poly(lactic-co-glycolic acid); USPIO, ultrasmall superparamagnetic iron oxide ; MIRB, Molday ION Rhodamine B; SPION, Superparamagnetic iron oxide nanoparticles.

4.5 Conclusion

The field of nanomedicines offers many tools to overcome the limitations of the conventional NSC differentiation-based treatments, as well as the comprehension of the biological mechanisms behind NSC differentiation. Nanostructured scaffolds, nanoparticulate drug delivery systems, and nanotechnology-based real-time imaging have successfully improved NSC-based therapies. Nevertheless, the design of NSC-targeting systems could significantly increase the safety and the efficacy of those therapies.

5. *IN SITU* NSC DIFFERENTIATION *VIA* ENDOGENOUS NSC TARGETING

5.1 Endogenous NSC targeting

The development of systems able to target endogenous NSCs and to induce their differentiation *in situ* represents a promising strategy to overcome conventional medicine-associated limits as well as transplantation-associated issues. In particular, the risk of death or rejection of transplanted NSCs would be totally excluded. Also, the procedural limitations derived from *in vitro* manipulation of NSCs before their transplantation (e.g., the cultivation in restricted conditions or the risk of genetic modifications) would be avoided. Moreover, endogenous NSC targeting would increase the efficacy of the treatments by enhancing the highly efficient localized delivery and, consequently, limiting off target effects. Considering that people affected by neurodegenerative diseases are often physically debilitated, the development of less invasive strategies, such as *in situ* NSC differentiation *via* targeting nanomedicines, could be a successful approach.
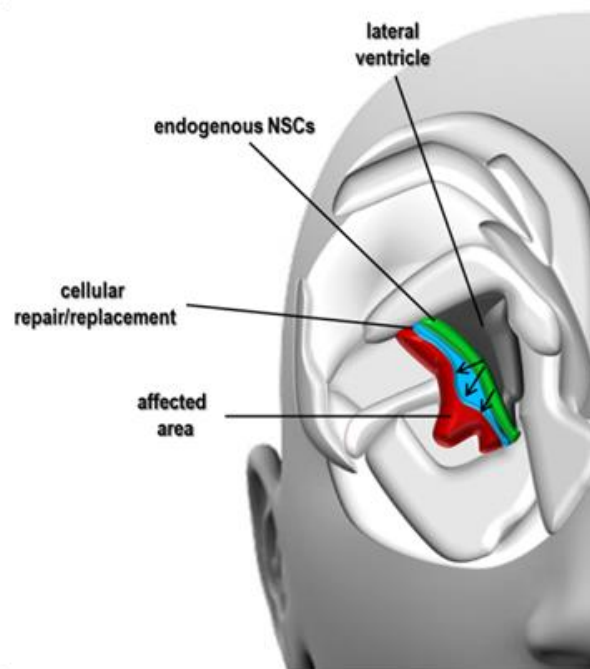

Figure 6. *In situ* NSC differentiation in the brain.
Endogenous NSCs of the subventricular zone of the brain (in green) could be stimulated to differentiate in specialized neuronal cells (neurons, astrocytes and oligodendrocytes) and, consequently, they could replace (in light blue) the damaged cells present in the surrounding lesioned areas (in red).

Endogenous NSC differentiation is considered one of the most promising approaches for the treatment of neurodegenerative diseases. However, not one system based on this approach has yet reached the clinical phase. The lack of NSC-targeting molecules is the primarily limitation toward the development of selective systems. Only one nanoparticle-based system has been designed to target endogenous NSCs and to deliver active molecules directly to the neurogenic niches: titanium dioxide nanoparticles coupled to Nilo1 [208]. Although these nanoparticles selectively interacted with NSCs *in vitro* [208], no further information is available on the *in vivo* efficacy of such system. Thus, significant results have been achieved *in vitro* for several nanoparticulate drug delivery systems, but the *in vivo* proof-of-principle is lacking.

Recently, for the first time, a new peptide, NFL-TBS.40-63, has been identified as selectively targeting endogenous NSCs of the brain *in vitro* and *in vivo* [209]. It represents an alternative and promising molecule to design nanomedicines targeting endogenous NSCs.

5.2 The NFL-TBS.40-63 peptide

The NFL-TBS.40-63 (NFL) peptide is a positively charged (+2) 24-aminoacid peptide corresponding to the tubulin-binding site located on the light subunit of neurofilaments [210] which are the major component of the neural cytoskeleton. The peptide, in its free form or associated with nanoparticles, can massively enter glioblastoma cells *via* active pathways (*in vitro* [211]) and reduces the tumor size in animal bearing glioblastoma (*in vivo* [212]) by disrupting the microtubule network of the tumor cells. NFL uptake by healthy cells (astrocytes and neurons) is not significant and shows no major toxicity on these cells. Recent works have also shown that NFL penetrates oligodendrocytes by clathrin-dependent endocytosis promoting their cellular growth, differentiation and survival *in vitro* [213,214]. Physicochemical studies carried on NFL indicated a strong correlation structure – activity (by alanine-scanning assay) and a dependency of the ratio alpha helix/beta sheet to the environmental conditions (by circular dichroism) [209].

Interestingly, NFL penetrates massively into NSCs of the subventricular zone (SVZ-NSCs) of the brain by direct translocation, increasing their adhesion and differentiation (*in vitro,* Figure 6A). It also localises in the NSC niche of the SVZ of the brain after intra-lateral ventricle injection (*in vivo,* Figure 6B) [209]. Although NFL has a high affinity for SVZ-NSCs, it does not induce yet an identified therapeutic effect *in vivo*. In addition, the strong correlation structure – activity limits chemical coupling between NFL and bioactive molecules that would be able to induce SVZ-NSC differentiation.
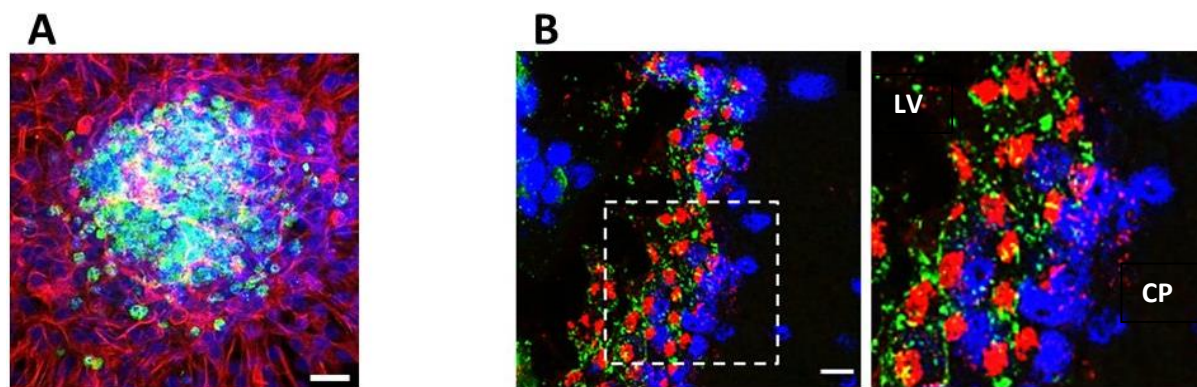
Figure 7. NSC targeting by the peptide NFL *in vitro* and *in vivo*.
A) Confocal microscopy of neurospheres incubated with 20 µmol/l 5-FAM-labeled NFL (green) immunostained with anti-α-tubulin (red) to reveal the microtubule network. The nuclei were stained with DAPI (blue). Scale bars = 20 µm. B) Confocal microscope localization of the 5-FAM-labeled NFL (green) in the subventricular zone of adult rats 1 hour after its injection in the right lateral ventricle. Immunofluorescence analysis of nestin (red; neural stem cells), and DAPI (blue). LV, lateral ventricle. CP, caudoputamen. Scale bars = 10 µm. [209]

Although the direct therapeutic application of the peptide is still not excluded for NSC differentiation, its association with a drug delivery system could potentially be a useful strategy for selective delivery of bioactive molecules and differentiation of NSCs. Moreover, NFL was recently related to the cell-penetrating peptides (CPPs) such as TAT [215] and VIM [216] (due to the characteristics it shares with them such as the positive charge, the low molecular weight and the balance between endocytosis and direct translocation in cell penetration [217]) which have been successfully used to enhance the cellular delivery of a large variety of cargos including nanoparticles [218].

6. AIM OF THE THESIS

The safety and the efficacy of the current NSC-based therapies would be greatly increased by the development of endogenous NSC-targeting drug delivery systems.

According to the information present in the scientific literature and summarized in this chapter, on one hand, NFL would represent a promising NSC-targeting ligand to functionalize drug delivery systems aiming at NSC targeting and differentiation. On the other hand, LNCs are a versatile drug delivery system suitable for targeting compound functionalization that does not necessarily requires covalent cross-linking.

Consequently, **our hypothesis is that a NSC-targeting drug delivery system, able to target endogenous NSCs and induce NSC differentiation *via* bioactive molecule delivery could be produced by the combination of both NFL and LNCs.** Retinoic acid would be a potent candidate to induce NSC differentiation as well as a compatible drug (lipophilic) to be encapsulated and delivered by LNCs.

7. PLAN OF THE PHD

The objective of this work is to provide a drug delivery system able both to target and to induce NSC differentiation for therapeutic purposes.

1) To produce a NSC-targeting nanovector. We adsorbed the NSC-targeting peptide NFL-TBS.40-63 (NFL) on the surface of the lipid nanocapsules (LNCs) by simple incubation. NFL-LNCs has been physicochemically characterize in size, PDI and zeta-potential. The stability of the system as well as of the binding between NFL and LNCs have been evaluated at different physiologic-mimicking conditions.
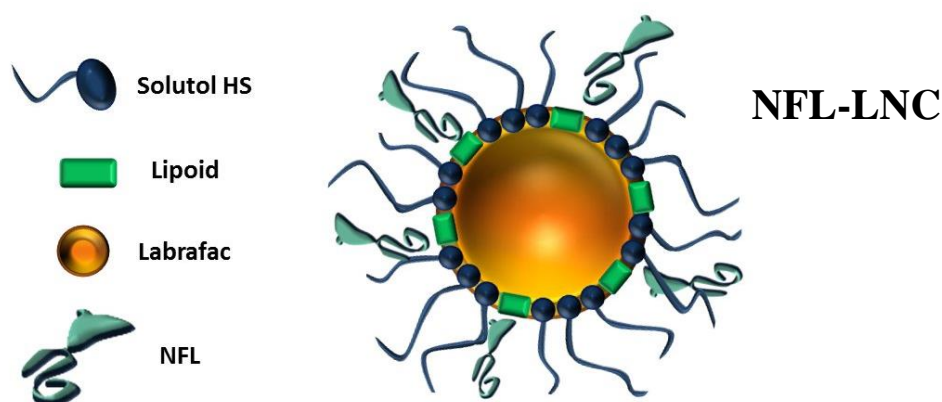
2) To evaluate NFL-LNC targeting efficiency *in vitro* and *in vivo*. NFL-LNC have been labelled with DiD to trace the nanoparticles during our tests. *In vitro*, NFL-LNC has been incubated with primary neural stem cells (NSCs) isolated from the subventricular zone of the brain (SVZ-NSCs) and from the central canal of the spinal cord (CC-NSCs). The targeting efficiency has been evaluated both by flow cytometry and by confocal imaging. *In vivo*, NFL-LNC has been injected either in the right lateral ventricle of the brain or at T10 of the spinal cord of adult rats.
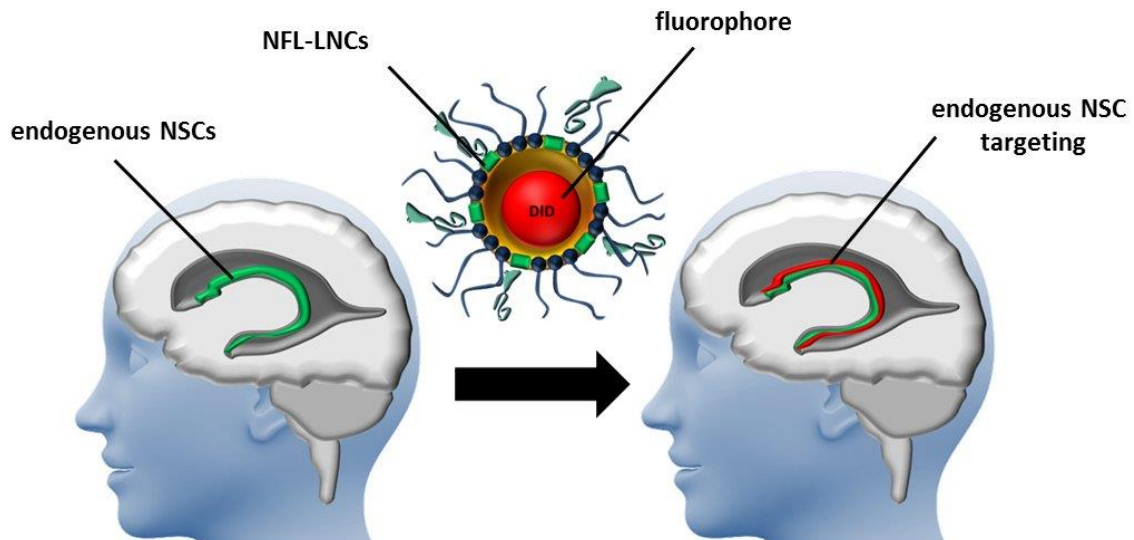
3) To evaluate the therapeutic potential of NFL-LNCs by encapsulating and delivering retinoic acid to endogenous NSCs. Retinoic acid (RA) was selected among several active molecules for its neurogenic potentials as well as compatibility with LNCs. RA was loaded into NFL-LNCs and tested *in vitro* on primary SVZ-NSCs. The differentiation efficiency has been evaluated by microscopic morphologic observation and immunocytochemistry. *In vivo*, RA-loaded NFL-LNCs have been injected in the demyelinated brain of adult rats. The differentiation efficiency is under evaluation by immunohistochemistry.
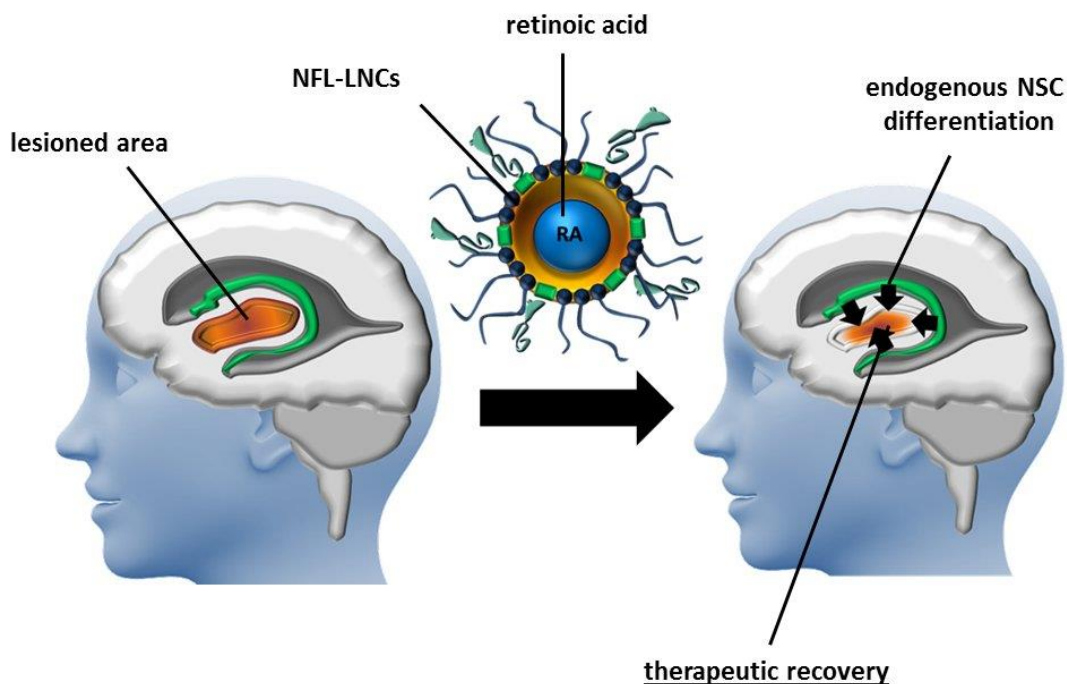
8. REFERENCES

[1] Smart, I.; Leblond, C. P. Evidence for division and transformations of neuroglia cells in the mouse brain, as derived from radioautography after injection of thymidine-H3. Journal of Comparative Neurology 1961, 116 (3), 349-367.

[2] Altman, J.; Das, G. D. Autoradiographic and histological evidence of postnatal hippocampal neurogenesis in rats. Journal of Comparative Neurology 1965, 124 (3), 319-335.

[3] Kaplan, M. S.; Hinds, J. W. Neurogenesis in the adult rat: electron microscopic analysis of light radioautographs. Science 1977, 197 (4308), 1092-1094.

[4] Goldman, S. A.; Nottebohm, F. Neuronal production, migration, and differentiation in a vocal control nucleus of the adult female canary brain. Proceedings of the National Academy of Sciences 1983, 80 (8), 2390-2394.

[5] Gould, E.; Cameron, H. A.; Daniels, D. C.; Woolley, C. S.; McEwen, B. S. Adrenal hormones suppress cell division in the adult rat dentate gyrus. The journal of neuroscience 1992, 12 (9), 3642-3650.

[6] Kuhn, H. G.; Dickinson-Anson, H.; Gage, F. H. Neurogenesis in the dentate gyrus of the adult rat: age-related decrease of neuronal progenitor proliferation. The journal of neuroscience 1996, 16 (6), 2027-2033.

[7] Nixon, K.; Crews, F. T. Binge ethanol exposure decreases neurogenesis in adult rat hippocampus. Journal of neurochemistry 2002, 83 (5), 1087-1093.

[8] Kempermann, G.; Kuhn, H. G.; Gage, F. H. More hippocampal neurons in adult mice living in an enriched environment. Nature 1997, 386 (6624), 493-495.

[9] Kuhn, H. G.; Winkler, J. G.; Kempermann, G.; Thal, L. J.; Gage, F. H. Epidermal growth factor and fibroblast growth factor-2 have different effects on neural progenitors in the adult rat brain. The journal of neuroscience 1997, 17 (15), 5820-5829.

[10] Kilpatrick, T. J.; Bartlett, P. F. Cloning and growth of multipotential neural precursors: requirements for proliferation and differentiation. Neuron 1993, 10 (2), 255-265.

[11] Reynolds, B. A.; Weiss, S. Generation of neurons and astrocytes from isolated cells of the adult mammalian central nervous system. Science 1992, 255 (5052), 1707-1710.

[12] Thored, P. J.; Wood, J.; Arvidsson, A.; Cammenga, J. Z.; Kokaia, Z.; Lindvall, O. Long-term neuroblast migration along blood vessels in an area with transient angiogenesis and increased vascularization after stroke. Stroke 2007, 38 (11), 3032-3039.

[13] Arvidsson, A.; Collin, T.; Kirik, D.; Kokaia, Z.; Lindvall, O. Neuronal replacement from endogenous precursors in the adult brain after stroke. Nature medicine 2002, 8 (9), 963-970.

[14] Murrell, W.; Palmero, E.; Bianco, J.; Stangeland, B.; Joel, M.; Paulson, L.; Thiede, B.; Grieg, Z.; Ramsnes, I.; Skjellegrind, H. K. Expansion of multipotent stem cells from the adult human brain. PloS one 2013, 8 (8), e71334.

[15] Kukekov, V. G.; Laywell, E. D.; Suslov, O.; Davies, K.; Scheffler, B.; Thomas, L. B.; O'brien, T. F.; Kusakabe, M.; Steindler, D. A. Multipotent stem/progenitor cells with similar properties arise from two neurogenic regions of adult human brain. Experimental neurology 1999, 156 (2), 333-344.

[16] Palmer, T. D.; Markakis, E. A.; Willhoite, A. R.; Safar, F.; Gage, F. H. Fibroblast growth factor-2 activates a latent neurogenic program in neural stem cells from diverse regions of the adult CNS. The journal of neuroscience 1999, 19 (19), 8487-8497.

[17] Shenghui, H. E.; Nakada, D.; Morrison, S. J. Mechanisms of stem cell self-renewal. Annual Review of Cell and Developmental 2009, 25, 377-406.

[18] Wagers, A. J.; Weissman, I. L. Plasticity of adult stem cells. Cell 2004, 116 (5), 639-648.

[19] Christian, K. M.; Song, H.; Ming, G. l. Functions and dysfunctions of adult hippocampal neurogenesis. Annual review of neuroscience 2014, 37, 243-262.

[20] Lehtinen, M. K.; Zappaterra, M. W.; Chen, X.; Yang, Y. J.; Hill, A. D.; Lun, M.; Maynard, T.; Gonzalez, D.; Kim, S.; Ye, P. The cerebrospinal fluid provides a proliferative niche for neural progenitor cells. Neuron 2011, 69 (5), 893-905.

[21] Silva-Vargas, V.; Maldonado-Soto, A. R.; Mizrak, D.; Codega, P.; Doetsch, F. Age-dependent niche signals from the choroid plexus regulate adult neural stem cells. Cell stem cell 2016, 19 (5), 643-652.

[22] Grassi, C.; D'Ascenzo, M.; Torsello, A.; Martinotti, G.; Wolf, F.; Cittadini, A.; Azzena, G. B. Effects of 50Hz electromagnetic fields on voltage-gated Ca 2+ channels and their role in modulation of neuroendocrine cell proliferation and death. Cell Calcium 2004, 35 (4), 307-315.

[23] Gonçalves, J. T.; Schafer, S. T.; Gage, F. H. Adult neurogenesis in the hippocampus: From stem cells to behavior. Cell 2016, 167 (4), 897-914.

[24] Bonaguidi, M. A.; Wheeler, M. A.; Shapiro, J. S.; Stadel, R. P.; Sun, G. J.; Ming, G. l.; Song, H. In vivo clonal analysis reveals self-renewing and multipotent adult neural stem cell characteristics. Cell 2011, 145 (7), 1142-1155.

[25] Calzolari, F.; Michel, J.; Baumgart, E. V.; Theis, F.; Götz, M.; Ninkovic, J. Fast clonal expansion and limited neural stem cell self-renewal in the adult subependymal zone. Nature neuroscience 2015, 18 (4), 490-492.

[26] Yamaguchi, M.; Seki, T.; Imayoshi, I.; Tamamaki, N.; Hayashi, Y.; Tatebayashi, Y.; Hitoshi, S. Neural stem cells and neuro/gliogenesis in the central nervous system: understanding the structural and functional plasticity of the developing, mature, and diseased brain. The Journal of Physiological Sciences 2016, 66 (3), 197-206.

[27] Lim, D. A.; Alvarez-Buylla, A. The adult ventricular-subventricular zone (V-SVZ) and olfactory bulb (OB) neurogenesis. Cold Spring Harbor perspectives in biology 2016, 8 (5), a018820.

[28] Merkle, F. T.; Mirzadeh, Z.; Alvarez-Buylla, A. Mosaic organization of neural stem cells in the adult brain. Science 2007, 317 (5836), 381-384.

[29] DeCarolis, N. A.; Mechanic, M.; Petrik, D.; Carlton, A.; Ables, J. L.; Malhotra, S.; Bachoo, R.; G+Âtz, M.; Lagace, D. C.; Eisch, A. J. In vivo contribution of nestin- and GLAST-lineage cells to adult hippocampal neurogenesis. Hippocampus 2013, 23 (8), 708-719.

[30] Deng, W.; Aimone, J. B.; Gage, F. H. New neurons and new memories: how does adult hippocampal neurogenesis affect learning and memory? Nature Reviews Neuroscience 2010, 11 (5), 339-350.

[31] Sahay, A.; Scobie, K. N.; Hill, A. S.; O'carroll, C. M.; Kheirbek, M. A.; Burghardt, N. S.; Fenton, A. A.; Dranovsky, A.; Hen, R. Increasing adult hippocampal neurogenesis is sufficient to improve pattern separation. Nature 2011, 472 (7344), 466-470.

[32] Aimone, J. B.; Deng, W.; Gage, F. H. Resolving new memories: a critical look at the dentate gyrus, adult neurogenesis, and pattern separation. Neuron 2011, 70 (4), 589-596.

[33] Butti, E.; Cusimano, M.; Bacigaluppi, M.; Martino, G. Neurogenic and non-neurogenic functions of endogenous neural stem cells. Adult neurogenesis twenty years later: physiological function versus brain repair 2015, 75.

[34] Qin, Y.; Zhang, W.; Yang, P. Current states of endogenous stem cells in adult spinal cord. Journal of neuroscience research 2015, 93 (3), 391-398.

[35] Götz, M.; Nakafuku, M.; Petrik, D. Neurogenesis in the Developing and Adult Brain-Similarities and Key Differences. Cold Spring Harbor perspectives in biology 2016, 8 (7), a018853.

[36] und Halbach, O. v. B. Immunohistological markers for proliferative events, gliogenesis, and neurogenesis within the adult hippocampus. Cell and tissue research 2011, 345 (1), 1-19.

[37] Abrous, D. N.; Koehl, M.; Le Moal, M. Adult neurogenesis: from precursors to network and physiology. Physiological reviews 2005, 85 (2), 523-569.

[38] Chaker, Z.; Codega, P.; Doetsch, F. A mosaic world: puzzles revealed by adult neural stem cell heterogeneity. Wiley Interdisciplinary Reviews: Developmental Biology 2016, 5 (6), 640-658.

[39] Lendahl, U.; Zimmerman, L. B.; McKay, R. D. CNS stem cells express a new class of intermediate filament protein. Cell 1990, 60 (4), 585-595.

[40] Roskams, A. J. I.; Cai, X.; Ronnett, G. V. Expression of neuron-specific beta-III tubulin during olfactory neurogenesis in the embryonic and adult rat. Neuroscience 1998, 83 (1), 191-200.

[41] Rao, M. S.; Shetty, A. K. Efficacy of doublecortin as a marker to analyse the absolute number anddendritic growth of newly generated neurons in the adult dentate gyrus. European Journal of Neuroscience 2004, 19 (2), 234-246.

[42] Seki, T. Expression patterns of immature neuronal markers PSA-NCAM, CRMP-4 and NeuroD in the hippocampus of young adult and aged rodents. Journal of neuroscience research 2002, 70 (3), 327-334.

[43] Gage, F. H.; Coates, P. W.; Palmer, T. D.; Kuhn, H. G.; Fisher, L. J.; Suhonen, J. O.; Peterson, D. A.; Suhr, S. T.; Ray, J. Survival and differentiation of adult neuronal progenitor cells transplanted to the adult brain. Proceedings of the National Academy of Sciences 1995, 92 (25), 11879-11883.

[44] Weyer, A.; Schilling, K. Developmental and cell type-specific expression of the neuronal marker NeuN in the murine cerebellum. Journal of neuroscience research 2003, 73 (3), 400-409.

[45] Liedtke, W.; Edelmann, W.; Bieri, P. L.; Chiu, F. C.; Cowan, N. J.; Kucherlapati, R.; Raine, C. S. GFAP is necessary for the integrity of CNS white matter architecture and long-term maintenance of myelination. Neuron 1996, 17 (4), 607-615.

[46] Ghandour, M. S.; Langley, O. K.; Labourdette, G.; Vincendon, G.; Gombos, G. Specific and artefactual cellular localizations of S100 protein: an astrocyte marker in rat cerebellum. Developmental neuroscience 1981, 4 (1), 66-78.

[47] Brunner, C.; Lassmann, H.; Waehneldt, T. V.; Matthieu, J.; Linington, C. Differential ultrastructural localization of myelin basic protein, myelin/oligodendroglial glycoprotein, and 2'-, 3'-cyclic nucleotide 3'-phosphodiesterase in the CNS of adult rats. Journal of neurochemistry 1989, 52 (1), 296-304.

[48] Ellis, P.; Fagan, B. M.; Magness, S. T.; Hutton, S.; Taranova, O.; Hayashi, S.; McMahon, A.; Rao, M.; Pevny, L. SOX2, a persistent marker for multipotential neural stem cells derived from embryonic stem cells, the embryo or the adult. Developmental neuroscience 2005, 26 (2-4), 148-165.

[49] Kanemura, Y.; Yamasaki, M.; Mori, K.; Fujikawa, H.; Hayashi, H.; Nakano, A.; Matsumoto, T.; Tamura, K.; Arita, N.; Sakakibara, S. i. Musashi1, an evolutionarily conserved neural RNA-binding protein, is a versatile marker of human glioma cells in determining their cellular origin, malignancy, and proliferative activity. Differentiation 2001, 68 (2-3), 141-152.

[50] Sansom, S. N.; Griffiths, D. S.; Faedo, A.; Kleinjan, D. J.; Ruan, Y.; Smith, J.; Van Heyningen, V.; Rubenstein, J. L.; Livesey, F. J. The level of the transcription factor Pax6 is essential for controlling the balance between neural stem cell self-renewal and neurogenesis. PLoS Genet 2009, 5 (6), e1000511.

[51] Lee, A.; Kessler, J. D.; Read, T. A.; Kaiser, C.; Corbeil, D.; Huttner, W. B.; Johnson, J. E.; Wechsler-Reya, R. J. Isolation of neural stem cells from the postnatal cerebellum. Nature neuroscience 2005, 8 (6), 723-729.

[52] Dimou, L.; Gallo, V. NG2-glia and their functions in the central nervous system. Glia 2015, 63 (8), 1429-1451.

[53] Sayegh, A. I.; Ritter, R. C. Morphology and distribution of nitric oxide synthase-, neurokinin-1 receptor-, calretinin-, calbindin-, and neurofilament-M-immunoreactive neurons in the myenteric and submucosal plexuses of the rat small intestine. The Anatomical Record Part A: Discoveries in Molecular, Cellular, and Evolutionary Biology 2003, 271 (1), 209-216.

[54] Van den Pol, A. N.; Herbst, R. S.; Powell, J. F. Tyrosine hydroxylase-immunoreactive neurons of the hypothalamus: a light and electron microscopic study. Neuroscience 1984, 13 (4), 1117-1156.

[55] Chen, W.; Aoki, C.; Mahadomrongkul, V.; Gruber, C. E.; Wang, G. J.; Blitzblau, R.; Irwin, N.; Rosenberg, P. A. Expression of a variant form of the glutamate transporter GLT1 in neuronal cultures and in neurons and astrocytes in the rat brain. Journal of Neuroscience 2002, 22 (6), 2142-2152.

[56] Ranscht, B.; Clapshaw, P. A.; Price, J.; Noble, M.; Seifert, W. Development of oligodendrocytes and Schwann cells studied with a monoclonal antibody against galactocerebroside. Proceedings of the National Academy of Sciences 1982, 79 (8), 2709-2713.

[57] Demars, M.; Hu, Y.; Gadadhar, A.; Lazarov, O. Impaired neurogenesis is an early event in the etiology of familial Alzheimer's disease in transgenic mice. Journal of neuroscience research 2010, 88 (10), 2103-2117.

[58] Hollands, C.; Bartolotti, N.; Lazarov, O. Alzheimer's Disease and Hippocampal Adult Neurogenesis; Exploring Shared Mechanisms. Frontiers in neuroscience 2016, 10.

[59] Giuliani, D.; Neri, L.; Canalini, F.; Calevro, A.; Ottani, A.; Vandini, E.; Sena, P.; Zaffe, D.; Guarini, S. NDP-α-MSH induces intense neurogenesis and cognitive recovery in Alzheimer transgenic mice through activation of melanocortin MC 4 receptors. Molecular and Cellular Neuroscience 2015, 67, 13-21.

[60] Jin, H.; Pei, L.; Shu, X.; Yang, X.; Yan, T.; Wu, Y.; Wei, N.; Yan, H.; Wang, S.; Yao, C. Therapeutic intervention of learning and memory decays by salidroside stimulation of neurogenesis in aging. Molecular neurobiology 2016, 53 (2), 851-866.

[61] Thier, M.; Wörsdörfer, P.; Lakes, Y. B.; Gorris, R.; Herms, S.; Opitz, T.; Seiferling, D.; Quandel, T.; Hoffmann, P.; Nöthen, M. M. Direct conversion of fibroblasts into stably expandable neural stem cells. Cell stem cell 2012, 10 (4), 473-479.

[62] Kageyama, R.; Ohtsuka, T.; Hatakeyama, J.; Ohsawa, R. Roles of bHLH genes in neural stem cell differentiation. Experimental cell research 2005, 306 (2), 343-348.

[63] Imayoshi, I.; Ishidate, F.; Kageyama, R. Real-time imaging of bHLH transcription factors reveals their dynamic control in the multipotency and fate choice of neural stem cells. Frontiers in cellular neuroscience 2015, 9.

[64] Ito, K.; Suda, T. Metabolic requirements for the maintenance of self-renewing stem cells. Nature reviews Molecular cell biology 2014, 15 (4), 243-256.

[65] Carpenter, M. K.; Cui, X.; Hu, Z. Y.; Jackson, J.; Sherman, S.; Seiger, A.; Wahlberg, L. U. In vitro expansion of a multipotent population of human neural progenitor cells. Experimental neurology 1999, 158 (2), 265-278.

[66] Gage, F. H. Mammalian neural stem cells. Science 2000, 287 (5457), 1433-1438.

[67] Gattazzo, F.; Urciuolo, A.; Bonaldo, P. Extracellular matrix: a dynamic microenvironment for stem cell niche. Biochimica et Biophysica Acta (BBA)-General Subjects 2014, 1840 (8), 2506-2519.

[68] Shimazaki, T.; Okano, H. Heterochronic microRNAs in temporal specification of neural stem cells: application toward rejuvenation. npj Aging and Mechanisms of Disease 2016, 2, 15014.

[69] Zhao, C.; Sun, G.; Li, S.; Shi, Y. A feedback regulatory loop involving microRNA-9 and nuclear receptor TLX in neural stem cell fate determination. Nature structural & molecular biology 2009, 16 (4), 365-371.

[70] Liu, C.; Teng, Z. Q.; McQuate, A. L.; Jobe, E. M.; Christ, C. C.; von Hoyningen-Huene, S. J.; Reyes, M. D.; Polich, E. D.; Xing, Y.; Li, Y. An epigenetic feedback regulatory loop involving microRNA-195 and MBD1 governs neural stem cell differentiation. PloS one 2013, 8 (1), e51436.

[71] Liu, Y.; Wang, L.; Long, Z.; Zeng, L.; Wu, Y. Protoplasmic astrocytes enhance the ability of neural stem cells to differentiate into neurons in vitro. PloS one 2012, 7 (5), e38243.

[72] Lairson, L. L.; Lyssiotis, C. A.; Zhu, S.; Schultz, P. G. Small Molecule-Based Approaches to Adult Stem Cell Therapies. Pharmacology and Toxicology 2013, 53.

[73] Ning, Y.; Huang, J.; Kalionis, B.; Bian, Q.; Dong, J.; Wu, J.; Tai, X.; Xia, S.; Shen, Z. Oleanolic Acid Induces Differentiation of Neural Stem Cells to Neurons: An Involvement of Transcription Factor Nkx-2.5. Stem cells international 2015, 2015, 1.

[74] Warashina, M.; Min, K. H.; Kuwabara, T.; Huynh, A.; Gage, F. H.; Schultz, P. G.; Ding, S. A synthetic small molecule that induces neuronal differentiation of adult hippocampal neural progenitor cells. Angewandte Chemie International Edition 2006, 45 (4), 591-593.

[75] Jung, G. A.; Yoon, J. Y.; Moon, B. S.; Yang, D. H.; Kim, H. Y.; Lee, S. H.; Bryja, V.; Arenas, E.; Choi, K. Y. Valproic acid induces differentiation and inhibition of proliferation in neural progenitor cells via the beta-catenin-Ras-ERK-p21Cip/WAF1 pathway. BMC cell biology 2008, 9 (1), 66.

[76] Chu, T.; Zhou, H.; Wang, T.; Lu, L.; Li, F.; Liu, B.; Kong, X.; Feng, S. In vitro characteristics of Valproic acid and all-trans-retinoic acid and their combined use in promoting neuronal differentiation while suppressing astrocytic differentiation in neural stem cells. Brain research 2015, 1596, 31-47.

[77] Xu, C.; Loh, H. H.; Law, P. Y. Effects of addictive drugs on adult neural stem/progenitor cells. Cellular and Molecular Life Sciences 2016, 73 (2), 327-348.

[78] Xu, C.; Zheng, H.; Loh, H. H.; Law, P. Morphine Promotes Astrocyte-Preferential Differentiation of Mouse Hippocampal Progenitor Cells via PKCε-Dependent ERK Activation and TRBP Phosphorylation. Stem Cells 2015, 33 (9), 2762-2772.

[79] Dabe, E. C.; Majdak, P.; Bhattacharya, T. K.; Miller, D. S.; Rhodes, J. S. Chronic D-amphetamine administered from childhood to adulthood dose-dependently increases the survival of new neurons in the hippocampus of male C57BL/6J mice. Neuroscience 2013, 231, 125-135.

[80] Trivedi, M.; Zhang, Y.; Lopez-Toledano, M.; Clarke, A.; Deth, R. Differential neurogenic effects of casein-derived opioid peptides on neuronal stem cells: implications for redox-based epigenetic changes. The Journal of Nutritional Biochemistry 2016, 37, 39-46.

[81] Leone, L.; Fusco, S.; Mastrodonato, A.; Piacentini, R.; Barbati, S. A.; Zaffina, S.; Pani, G.; Podda, M. V.; Grassi, C. Epigenetic modulation of adult hippocampal neurogenesis by extremely low-frequency electromagnetic fields. Molecular neurobiology 2014, 49 (3), 1472-1486.

[82] Piacentini, R.; Ripoli, C.; Mezzogori, D.; Azzena, G. B.; Grassi, C. Extremely low-frequency electromagnetic fields promote in vitro neurogenesis via upregulation of Ca+2 channel activity. Journal of cellular physiology 2008, 215 (1), 129-139.

[83] Xie, C.; Cong, D.; Wang, X.; Wang, Y.; Liang, H.; Zhang, X.; Huang, Q. The effect of simvastatin treatment on proliferation and differentiation of neural stem cells after traumatic brain injury. Brain research 2015, 1602, 1-8.

[84] Ibrahim, W. N. W.; Tofighi, R.; Onishchenko, N.; Rebellato, P.; Bose, R.; Uhlén, P.; Ceccatelli, S. Perfluorooctane sulfonate induces neuronal and oligodendrocytic differentiation in neural stem cells and alters the expression of PPARγ in vitro and in vivo. Toxicology and applied pharmacology 2013, 269 (1), 51-60.

[85] Soundarapandian, M. M.; Selvaraj, V.; Lo, U. G.; Golub, M. S.; Feldman, D. H.; Pleasure, D. E.; Deng, W. Zfp488 promotes oligodendrocyte differentiation of neural progenitor cells in adult mice after demyelination. Scientific reports 2011, 1.

[86] Bain, G.; Ray, W. J.; Yao, M.; Gottlieb, D. I. Retinoic acid promotes neural and represses mesodermal gene expression in mouse embryonic stem cells in culture. Biochemical and biophysical research communications 1996, 223 (3), 691-694.

[87] Okada, Y.; Shimazaki, T.; Sobue, G.; Okano, H. Retinoic-acid-concentration-dependent acquisition of neural cell identity during in vitro differentiation of mouse embryonic stem cells. Developmental biology 2004, 275 (1), 124-142.

[88] Gong, M.; Bi, Y.; Jiang, W.; Zhang, Y.; Chen, L.; Hou, N.; Chen, J.; Li, T. Retinoic acid receptor beta mediates all-trans retinoic acid facilitation of mesenchymal stem cells neuronal differentiation. The international journal of biochemistry & cell biology 2013, 45 (4), 866-875.

[89] Zhang, S.; Chen, X.; Hu, Y.; Wu, J.; Cao, Q.; Chen, S.; Gao, Y. All-trans retinoic acid modulates Wnt3A-induced osteogenic differentiation of mesenchymal stem cells via activating the PI3K/AKT/GSK3 signalling pathway. Molecular and cellular endocrinology 2016, 422, 243-253.

[90] Gudas, L. J.; Wagner, J. A. Retinoids regulate stem cell differentiation. Journal of cellular physiology 2011, 226 (2), 322-330.

[91] Bastien, Julie, and Cécile Rochette-Egly. "Nuclear retinoid receptors and the transcription of retinoid-target genes." Gene 328 (2004): 1-16.

[92] Cunningham, Thomas J., and Gregg Duester. "Mechanisms of retinoic acid signalling and its roles in organ and limb development." Nature reviews Molecular cell biology 16.2 (2015): 110-123.

[93] Sharow, K. A.; Temkin, B.; Asson-Batres, M. A. Retinoic acid stability in stem cell cultures. International Journal of Developmental Biology 2012, 56 (4), 273-278.

[94] Wohl, C. A.; Weiss, S. Retinoic acid enhances neuronal proliferation and astroglial differentiation in cultures of CNS stem cell-derived precursors. Journal of neurobiology 1998, 37 (2), 281-290.

[95] Muindi, J.; Frankel, S.; Miller, W. J.; Jakubowski, A.; Scheinberg, D. A.; Young, C.; Dmitrovsky, E.; Warrell, R. J. Continuous treatment with all-trans retinoic acid causes a progressive reduction in plasma drug concentrations: implications for relapse and retinoid" resistance" in patients with acute promyelocytic leukemia [published erratum appears in Blood 1992 Aug 1; 80 (3): 855]. Blood 1992, 79 (2), 299-303.

[96] R. Ferreira, M.C. Fonseca, T. Santos, J. Sargento-Freitas, R. Tjeng, F. Paiva, M. Castelo-Branco, L. Ferreira, L. Bernardino, Retinoic acid-loaded polymeric nanoparticles enhance vascular regulation of neural stem cell survival and differentiation after ischaemia, Nanoscale 8 (2016) 8126-8137.

[97] Lange, C.; Garcia, M. T.; Decimo, I.; Bifari, F.; Eelen, G.; Quaegebeur, A.; Boon, R.; Zhao, H.; Boeckx, B.; Chang, J. Relief of hypoxia by angiogenesis promotes neural stem cell differentiation by targeting glycolysis. The EMBO journal 2016, 35 (9), 924-941.

[98] Cuccurazzu, B.; Leone, L.; Podda, M. V.; Piacentini, R.; Riccardi, E.; Ripoli, C.; Azzena, G. B.; Grassi, C. Exposure to extremely low-frequency (50Hz) electromagnetic fields enhances adult hippocampal neurogenesis in C57BL/6 mice. Experimental neurology 2010, 226 (1), 173-182.

[99] Podda, M. V.; Leone, L.; Barbati, S. A.; Mastrodonato, A.; Li Puma, D. D.; Piacentini, R.; Grassi, C. Extremely low-frequency electromagnetic fields enhance the survival of newborn neurons in the mouse hippocampus. European Journal of Neuroscience 2014, 39 (6), 893-903.

[100]   Wu, C. C.; Lien, C. C.; Hou, W. H.; Chiang, P. M.; Tsai, K. J. Gain of BDNF function in engrafted neural stem cells promotes the therapeutic potential for Alzheimer's disease. Scientific Reports 2016, 6.

[101] Lilja, A. M.; Malmsten, L.; Röjdner, J.; Voytenko, L.; Verkhratsky, A.; Ogren, S. O.; Nordberg, A.; Marutle, A. Neural Stem Cell Transplant-Induced Effect on Neurogenesis and Cognition in Alzheimer Tg2576 Mice Is Inhibited by Concomitant Treatment with Amyloid-Lowering or Cholinergic 7 Nicotinic Receptor Drugs. Neural plasticity 2015, 2015.

[102] Chen, B.; Wang, X.; Wang, Z.; Wang, Y.; Chen, L.; Luo, Z. Brain-derived neurotrophic factor stimulates proliferation and differentiation of neural stem cells, possibly by triggering the Wnt/β-catenin signaling pathway. Journal of neuroscience research 2013, 91 (1), 30-41.

[103] Zhang, P.; Wu, C.; Liu, N.; Niu, L.; Yan, Z.; Feng, Y.; Xu, R. Protocadherin 11 x regulates differentiation and proliferation of neural stem cell in vitro and in vivo. Journal of Molecular Neuroscience 2014, 54 (2), 199-210.

[104] Huang, H.; Liu, L.; Li, B.; Zhao, P. P.; Xu, C. M.; Zhu, Y. Z.; Zhou, C. H.; Wu, Y. Q. Ketamine Interferes with the Proliferation and Differentiation of Neural Stem Cells in the Subventricular Zone of Neonatal Rats. Cellular Physiology and Biochemistry 2015, 35 (1), 315-325.

[105] Cohen, A.; Soleiman, M. T.; Talia, R.; Koob, G. F.; George, O.; Mandyam, C. D. Extended access nicotine self-administration with periodic deprivation increases immature neurons in the hippocampus. Psychopharmacology 2015, 232 (2), 453-463.

[106] Ramos, A. D.; Andersen, R. E.; Liu, S. J.; Nowakowski, T. J.; Hong, S. J.; Gertz, C. C.; Salinas, R. D.; Zarabi, H.; Kriegstein, A. R.; Lim, D. A. The long noncoding RNA Pnky regulates neuronal differentiation of embryonic and postnatal neural stem cells. Cell stem cell 2015, 16 (4), 439-447.

[107] Giusto, E.; Donegà, M.; Cossetti, C.; Pluchino, S. Neuro-immune interactions of neural stem cell transplants: from animal disease models to human trials. Experimental neurology 2014, 260, 19-32.

[108] Barreau, K.; Lépinoux-Chambaud, C.; Joël, E. Review of Clinical Trials Using Neural Stem Cells. JSM Biotechnology & Biomedical Engineering 2016, 3 (3).

[109] Qiao, L. y.; Huang, F. j.; Zhao, M.; Xie, J. h.; Shi, J.; Wang, J.; Lin, X. z.; Zuo, H.; Wang, Y. l.; Geng, T. c. A two-year follow-up study of cotransplantation with neural stem/progenitor cells and mesenchymal stromal cells in ischemic stroke patients. Cell transplantation 2014, 23 (1), S65-S72.

[110] Mazzini, L.; Gelati, M.; Profico, D. C.; Sgaravizzi, G.; Pensi, M. P.; Muzi, G.; Ricciolini, C.; Nodari, L. R.; Carletti, S.; Giorgi, C. Human neural stem cell transplantation in ALS: initial results from a phase I trial. Journal of translational medicine 2015, 13 (1), 17.

[111] Namba, H.; Kawaji, H.; Yamasaki, T. Use of genetically engineered stem cells for glioma therapy (Review). Oncology letters 2016, 11 (1), 9-15.

[112] Morshed, R. A.; Gutova, M.; Juliano, J.; Barish, M. E.; Hawkins-Daarud, A.; Oganesyan, D.; Vazgen, K.; Yang, T.; Annala, A.; Ahmed, A. U. Analysis of glioblastoma tumor coverage by oncolytic virus-loaded neural stem cells using MRI-based tracking and histological reconstruction. Cancer gene therapy 2015, 22 (1), 55-61.

[113] Bagó, J. R.; Alfonso-Pecchio, A.; Okolie, O.; Dumitru, R.; Rinkenbaugh, A.; Baldwin, A. S.; Miller, C. R.; Magness, S. T.; Hingtgen, S. D. Therapeutically engineered induced neural stem cells are tumour-homing and inhibit progression of glioblastoma. Nature communications 2016, 7.

[114] Weil, Z. M.; Norman, G. J.; DeVries, A. C.; Nelson, R. J. The injured nervous system: a Darwinian perspective. Progress in neurobiology 2008, 86 (1), 48-59.

[115] Bonfanti, L. From hydra regeneration to human brain structural plasticity: a long trip through narrowing roads. The Scientific World Journal 2011, 11, 1270-1299.

[116] Trounson, Alan, and Natalie D. DeWitt. "Pluripotent stem cells progressing to the clinic." Nature Reviews Molecular Cell Biology 17.3 (2016): 194-200.

[117] Amariglio, Ninette, et al. "Donor-derived brain tumor following neural stem cell transplantation in an ataxia telangiectasia patient." PLoS Med 6.2 (2009): e1000029.

[118] Simonson, O. E.; Domogatskaya, A.; Volchkov, P.; Rodin, S. The safety of human pluripotent stem cells in clinical treatment. Annals of medicine 2015, 47 (5), 370-380.

[119] Herberts, C. A.; Kwa, M. S.; Hermsen, H. P. Risk factors in the development of stem cell therapy. Journal of translational medicine 2011, 9 (1), 29.

[120] Abbott, A. Italian stem-cell trial based on flawed data. Nature News doi 2013, 10.

[121] Cattaneo, E.; Bonfanti, L. Therapeutic potential of neural stem cells: greater in people's perception than in their brains? 2014.

[122] European Medicines Agency, http://www.ema.europa.eu/docs/en_GB/document_library/Regulatory_and_procedural_guideline/2010/01/WC500069728.pdf (Accessed 14 April 2017)

[123]   European   Science   Foundation, http://archives.esf.org/fileadmin/Public_documents/Publications/Nanomedicine.pdf (Accessed 14 April 2017)

[124] Couvreur, P. "Nanoparticles in drug delivery: past, present and future." Advanced drug delivery reviews 65.1 (2013): 21-23.

[125] National Science and Technology Council, http://www.nano.gov/nanotech-101/what/definition (Accessed 14 April 2017)

[126] European Commission http://ec.europa.eu/research/industrial_technologies/policy_en.html (Accessed 14 April 2017)

[127] Alapan, Yunus, Kutay Icoz, and Umut A. Gurkan. "Micro-and nanodevices integrated with biomolecular probes." Biotechnology advances 33.8 (2015): 1727-1743.

[128] Saccardo, Paolo, et al. Development of artificial viruses for nanomedicine and gene therapy. (2015).

[129] Watanabe, Kunihiko. Bacterial membrane vesicles (MVs): novel tools as nature-and nano-carriers for immunogenic antigen, enzyme support, and drug delivery. Applied microbiology and biotechnology 100.23 (2016): 9837-9843.

[130] Shah, Dhaval A., Sharad B. Murdande, and Rutesh H. Dave. A review: pharmaceutical and pharmacokinetic aspect of nanocrystalline suspensions. Journal of Pharmaceutical Sciences (2015).

[131] Castro, Emilio, and Arun Kumar. Nanoparticles in drug delivery systems. Nanomedicine in drug delivery (2013): 1-22.

[132] Matougui, Nada, et al. Lipid-based nanoformulations for peptide delivery. International journal of pharmaceutics 502.1 (2016): 80-97.

[133] Allen, Theresa M., and Pieter R. Cullis. Liposomal drug delivery systems: from concept to clinical applications. Advanced drug delivery reviews 65.1 (2013): 36-48.

[134] Bulbake, Upendra, et al. Liposomal Formulations in Clinical Use: An Updated Review. Pharmaceutics 9.2 (2017): 12.

[135] Pabst, Georg, et al., eds. Liposomes, lipid bilayers and model membranes: from basic research to application. CRC Press, 2014.

[136] Gill, Kanwaldeep K., Amal Kaddoumi, and Sami Nazzal. PEG–lipid micelles as drug carriers: physiochemical attributes, formulation principles and biological implication. Journal of drug targeting 23.3 (2015): 222-231.

[137] Gupta, Ankur, et al. Nanoemulsions: formation, properties and applications. Soft matter 12.11 (2016): 2826-2841.

[138] Singh, Yuvraj, et al. Nanoemulsion: Concepts, development and applications in drug delivery. Journal of Controlled Release (2017).

[139] Weber, S., A. Zimmer, and J. Pardeike. Solid lipid nanoparticles (SLN) and nanostructured lipid carriers (NLC) for pulmonary application: a review of the state of the art. European Journal of Pharmaceutics and Biopharmaceutics 86.1 (2014): 7-22.

[140] Huynh, Ngoc Trinh, et al. Lipid nanocapsules: a new platform for nanomedicine. International journal of pharmaceutics 379.2 (2009): 201-209.

[141] Roger, Emilie, et al. Reciprocal competition between lipid nanocapsules and P-gp for paclitaxel transport across Caco-2 cells. European Journal of Pharmaceutical Sciences 40.5 (2010): 422-429.

[142] Anton, Nicolas, et al. Aqueous-core lipid nanocapsules for encapsulating fragile hydrophilic and/or lipophilic molecules. Langmuir 25.19 (2009): 11413-11419.

[143] Allard, Emilie, et al. Lipid nanocapsules loaded with an organometallic tamoxifen derivative as a novel drug-carrier system for experimental malignant gliomas. Journal of Controlled Release 130.2 (2008): 146-153.

[144] Béduneau, Arnaud, et al. Pegylated nanocapsules produced by an organic solvent-free method: Evaluation of their stealth properties. Pharmaceutical research 23.9 (2006): 2190-2199.

[145] Hirsjärvi, Samuli, et al. Surface modification of lipid nanocapsules with polysaccharides: from physicochemical characteristics to in vivo aspects. Acta biomaterialia 9.5 (2013): 6686-6693.

[146] Balzeau, Julien, et al. The effect of functionalizing lipid nanocapsules with NFL-TBS. 40-63 peptide on their uptake by glioblastoma cells. Biomaterials 34.13 (2013): 3381-3389.

[147] Hirsjärvi, Samuli, et al. Tumour targeting of lipid nanocapsules grafted with cRGD peptides. European Journal of Pharmaceutics and Biopharmaceutics 87.1 (2014): 152-159.

[148] Groo, Anne-Claire, et al. Fate of paclitaxel lipid nanocapsules in intestinal mucus in view of their oral delivery. International journal of nanomedicine 8.1 (2013): 4291.

[149] David, Stephanie, et al. siRNA LNCs–a novel platform of lipid nanocapsules for systemic siRNA administration. European Journal of Pharmaceutics and Biopharmaceutics 81.2 (2012): 448-452.

[150] Barras, A., et al. Formulation and characterization of polyphenol-loaded lipid nanocapsules. International journal of pharmaceutics 379.2 (2009): 270-277.

[151] Bastiat, Guillaume, et al. A new tool to ensure the fluorescent dye labeling stability of nanocarriers: a real challenge for fluorescence imaging. Journal of Controlled Release 170.3 (2013): 334-342.

[152] Ballot, Sandrine, et al. 99mTc/188Re-labelled lipid nanocapsules as promising radiotracers for imaging and therapy: formulation and biodistribution. European journal of nuclear medicine and molecular imaging 33.5 (2006): 602-607.

[153] Peltier, Sandra, et al. Enhanced oral paclitaxel bioavailability after administration of paclitaxel-loaded lipid nanocapsules. Pharmaceutical research 23.6 (2006): 1243-1250.

[154] Xu, Chi, et al. Morphine Promotes Astrocyte-Preferential Differentiation of Mouse Hippocampal Progenitor Cells via PKCε-Dependent ERK Activation and TRBP Phosphorylation. Stem Cells 33.9 (2015): 2762-2772.

[155] E. Tamariz, A.C. Wan, Y.S. Pek, M. Giordano, G. Hernández-Padrón, A. Varela-Echavarría, I. Velasco, V.M. Castaño, Delivery of chemotropic proteins and improvement of dopaminergic neuron outgrowth through a thixotropic hybrid nano-gel, J. Mater. Sci. Mater. Med. 22 (2011) 2097-2110.

[156] A. Fattahi, J. Karimi-Sabet, A. Keshavarz, A. Golzary, M. Rafiee-Tehrani, F. Dorkoosh, Preparation and characterization of simvastatin nanoparticles using rapid expansion of supercritical solution (RESS) with trifluoromethane, J. Supercrit. Fluids 107 (2016) 469-478.

[157] Z. Liu, X. Gao, T. Kang, M. Jiang, D. Miao, G. Gu, Q. Hu, Q. Song, L. Yao, Y. Tu, H. Chen, X. Jiang, B6 peptide-modified PEG-PLA nanoparticles for enhanced brain delivery of neuroprotective peptide, J. Chen, Bioconj. Chem. 24 (2013) 997-1007.

[158] I. Khalin, R. Alyautdin, T.W. Wong, J. Gnanou, G. Kocherga, J. Kreuter, Brain-derived neurotrophic factor delivered to the brain using poly (lactide-co-glycolide) nanoparticles improves neurological and cognitive outcome in mice with traumatic brain injury, Drug Deliv. 23 (2016) 3520-3528.

[159] N. Kamaly, B. Yameen, J. Wu, O.C. Farokhzad, Degradable controlled-release polymers and polymeric nanoparticles: Mechanisms of controlling drug release, Chem. Rev. 116 (2016) 2602-2663.

[160] L. Hu, X. Tang, F. Cui, Solid lipid nanoparticles (SLNs) to improve oral bioavailability of poorly soluble drugs, J. Pharm. Pharmacol. 56 (2004) 1527-1535.

[161] H. Hoshyar, S. Gray, H. Han, G. Bao, The effect of nanoparticle size on in vivo pharmacokinetics and cellular interaction, Nanomedicine 11 (2016) 673-692.

[162] A. Béduneau, P. Saulnier, F. Hindré, A. Clavreul, J.C. Leroux, J.B. Benoit, Design of targeted lipid nanocapsules by conjugation of whole antibodies and antibody Fab'fragments, Biomaterials 28 (2007) 4978-4990.

[163] J. Kreuter, T. Hekmatara, S. Dreis, T. Vogel, S. Gelperina, K. Langer, Covalent attachment of apolipoprotein AI and apolipoprotein B-100 to albumin nanoparticles enables drug transport into the brain, J. Control. Release, 118 (2007) 54–58.

[164] H. Godwin, C. Nameth, D. Avery, L.L. Bergeson, D. Bernard, E. Beryt, W. Boyes, S. Brown, A.J. Clippinger, Y. Cohen, M. Doa, C.O. Hendren, P. Holden, K. Houck, A.B. Kane, F. Klaessig, T. Kodas, R. Landsiedel, I. Lynch, T. Malloy, M.B. Miller, J. Muller, G. Oberdorster, E.J. Petersen, R.C. Pleus, P. Sayre, V. Stone, K.M. Sullivan, J. Tentschert, P. Wallis, A.E. Nel, Nanomaterial categorization for assessing risk potential to facilitate regulatory decision-making , ACS Nano 9 (2015) 3409-3417.

[165] V. Iswarya, J. Manivannan, A. De, S. Paul, R. Roy, J.B. Johnson, R. Kundu, N. Chandrasekaran, A. Mukherjee, A. Mukherjee, Surface capping and size-dependent toxicity of gold nanoparticles on different trophic levels, Environ. Sci. Pollu.t Res. Int. 23 (2016) 4844-4858.

[166] M.A. Dobrovolskaia, M. Shurin, A.A. Shvedova, Current understanding of interactions between nanoparticles and the immune system, Toxicol. Appl. Pharmacol. 15 (2016) 78-89.

[167] Q. Jiao, L. Li, Q. Mu, Q. Zhang, Immunomodulation of nanoparticles in nanomedicine applications, Biomed. Res. Int. (2014) 426028. doi: 10.1155/2014/426028.

[168] J. Landers, J.T. Turner, G. Heden, A.L. Carlson, N.K. Bennett, P.V. Moghe, A.V. Neimark, Carbon nanotube composites as multifunctional substrates for in situ actuation of differentiation of human neural stem cells, Adv. Healthc. Mater. 3 (2014) 1745-1752.

[169] E. Hoveizi, S. Ebrahimi-Barough, S. Tavakol, K. Sanamiri, In Vitro Differentiation of Human iPS Cells into Neural like Cells on a Biomimetic Polyurea , Mol. Neurobiol. (2016) 1-7.

[170] A. Raspa, A. Marchini, R. Pugliese, M. Mauri, M. Maleki, R. Vasita, F. Gelain, A biocompatibility study of new nanofibrous scaffolds for nervous system regeneration, Nanoscale 8 (2016) 253-265.

[171] J. Maia, T. Santos, S. Aday, F. Agasse, L. Cortes, J.O. Malva, L. Bernardino, L. Ferreira, Controlling the neuronal differentiation of stem cells by the intracellular delivery of retinoic acid-loaded nanoparticles, ACS Nano 5 (2010) 97-106.

[172] T. Santos, R. Ferreira, J. Maia, F. Agasse, S. Xapelli, L. Cortes, J. Bragança, J.O. Malva, L. Ferreira, L. Bernardino, Polymeric nanoparticles to control the differentiation of neural stem cells in the subventricular zone of the brain, ACS Nano 6 (2012) 10463-10474.

[173] M. Esteves, A.C. Cristóvão, T. Saraiva, S.M. Rocha, G. Baltazar, L. Ferreira, L. Bernardino, Retinoic acid-loaded polymeric nanoparticles induce neuroprotection in a mouse model for Parkinson's disease, Front. Aging Neurosci. 7 (2015).

[174] Santos, Tiago, et al. "Blue light potentiates neurogenesis induced by retinoic acid-loaded responsive nanoparticles." Acta Biomaterialia (2017).

[175] S.K. Tiwari, S. Agarwal, B. Seth, A. Yadav, S. Nair, P. Bhatnagar, M. Karmakar, M. Kumari, L.K. Chauhan, D.K. Patel, V. Srivastava, D. Singh, S.K. Gupta, A. Tripathi, R.K. Chaturvedi, K.C. Gupta, Curcumin-loaded nanoparticles potently induce adult neurogenesis and reverse cognitive deficits in Alzheimer's disease model via canonical Wnt/β-catenin pathway, ACS Nano 8 (2013) 76-103.

[176] S.A. Papadimitriou, M.P. Robin, D. Ceric, R.K. O'Reilly, S. Marino, M. Resmini, Fluorescent polymeric nanovehicles for neural stem cell modulation, Nanoscale 8 (2016) 17340-17349.

[177] Y.K. Choi, D.H. Lee, Y.K. Seo, H. Jung, J.K. Park, H. Cho, Stimulation of Neural Differentiation in Human Bone Marrow Mesenchymal Stem Cells by Extremely Low-Frequency Electromagnetic Fields Incorporated with MNPs, Appl. Biochem. Biotechnol. 174 (2014) 1233-1245.

[178] M.O. Kim, H. Jung, S.C. Kim, J.K. Park, Y.K. Seo, Electromagnetic fields and nanomagnetic particles increase the osteogenic differentiation of human bone marrow-derived mesenchymal stem cells, Int. J. Mol. Med. 35 (2015) 153-160.

[179] M. Silva, L. Daheron, H. Hurley, K. Bure, R. Barker, A.J. Carr, D. Williams, H.W. Kim, A. French, P.J. Coffey, J.J. Cooper-White, B. Reeve, M. Rao, E.Y. Snyder, K.S. Ng, B.E. Mead, J.A. Smith, J.M. Karp, D.A. Brindley, I. Wall, Generating iPSCs: Translating Cell Reprogramming Science into Scalable and Robust Biomanufacturing Strategies, Cell Stem cell 16 (2015) 13–17.

[180] W.T. Hendriks, C.R. Warren, C.A. Cowan, Genome Editing in Human Pluripotent Stem Cells: Approaches, Pitfalls, and Solutions, Cell Stem Cell 18 (2016) 53-65.

[181] K. Saha, R. Jaenisch, Technical challenges in using human induced pluripotent stem cells to model disease, Cell Stem Cell 5 (2009) 584-95.

[182] K.M. Haston, S. Finkbeiner, Clinical Trials in a Dish: The Potential of Pluripotent Stem Cells to Develop Therapies for Neurodegenerative Diseases, Annu. Rev. Pharmacol. Toxicol. 56 (2016) 489–510.

[183] J.Y. Tan, D.L. Sellers, B. Pham, S.H. Pun, P.J. Horner, Non-Viral Nucleic Acid Delivery Strategies to the Central Nervous System, Front. Mol. Neurosci. 9 (2016) 108.

[184] X. Li, S.Y. Tzeng, X. Liu, M. Tammia, Y.H. Cheng, A. Rolfe, D. Sun, N. Zhang, J.J. Green, X. Wen, H.Q. Mao, Nanoparticle-mediated transcriptional modification enhances neuronal differentiation of human neural stem cells following transplantation in rat brain, Biomaterials,84 (2016) 157-166.

[185] C. Saraiva, J. Paiva, T. Santos, L. Ferreira, L. Bernardino, MicroRNA-124 loaded nanoparticles enhance brain repair in Parkinson's disease, J. Control. Rel. 235 (2016) 291-305.

[186] A.R. Fernandes, D.M. Chari, Part I: Minicircle vector technology limits DNA size restrictions on ex vivo gene delivery using nanoparticle vectors: Overcoming a translational barrier in neural stem cell therapy, J. Control. Rel. 238 (2016) 289-299.

[187] F.J. Nicholls, M.W. Rotz, H. Ghuman, K.W. MacRenaris, T.J. Meade, M. Modo, DNA-gadolinium-gold nanoparticles for in vivo T1 MR imaging of transplanted human neural stem cells, Biomaterials 77 (2016) 291-306.

[188] Z. Wang, Y. Wang, Z. Wang, J. Zhao, J.S. Gutkind, A. Srivatsan, G. Zhang, H.S. Liao, X. Fu, A. Jin, X. Tong, G. Niu, X. Chen, Polymeric Nanovehicle Regulated Spatiotemporal Real-Time Imaging of the Differentiation Dynamics of Transplanted Neural Stem Cells after Traumatic Brain Injury, ACS Nano 9 (2015) 6683-6695.

[189] A. Umashankar, M.J. Corenblum, S. Ray, M. Valdez, E.S. Yoshimaru, T.P. Trouard, L. Madhavan, Effects of the iron oxide nanoparticle Molday ION Rhodamine B on the viability and regenerative function of neural stem cells: relevance to clinical translation, Int. J. Nanomedicine 11 (2016) 1731-1748.

[190] K. Jiráková, M. Šeneklová, D. Jirák, K. Turnovcová, M. Vosmanská, M. Babič, D. Horák, P. Veverka, P. Jendelová, The effect of magnetic nanoparticles on neuronal differentiation of induced pluripotent stem cell-derived neural precursors, Int. J. Nanomedicine 11 (2016) 6267-6281.

[191] G. Elvira, B. Moreno, I.D. Valle, J.A. Garcia-Sanz, M. Canillas, E. Chinarro, J.R. Jurado, A.J. Silva, Targeting neural stem cells with titanium dioxide nanoparticles coupled to specific monoclonal antibodies, J. Biomater. App. 26 (2011) 1069-1089.

[192] A. Solanki, S. Shah, P.T. Yin, K.B. Lee, Nanotopography-mediated reverse uptake for siRNA delivery into neural stem cells to enhance neuronal differentiation, Sci. Rep. 3 (2013).

[193] N. Stephanopoulos, R. Freeman, H.A. North, S. Sur, S.J. Jeong, F. Tantakitti, J.A. Kessler, S.I. Stupp, Bioactive DNA-peptide nanotubes enhance the differentiation of neural stem cells into neurons, Nano Lett. 15 (2014) 603-609.

[194] S. Shah, P.T. Yin, T.M. Uehara, S.T. Chueng, L. Yang, K.B. Lee, Guiding stem cell differentiation into oligodendrocytes using graphene-nanofiber hybrid scaffolds, Adv. Mater. 26 (2014) 3673-3680.

[195] O. Akhavan, E. Ghaderi, S.A. Shirazian, R. Rahighi, Rolled graphene oxide foams as three-dimensional scaffolds for growth of neural fibers using electrical stimulation of stem cells, Carbon 97 (2016) 71-77.

[196] T.H. Huang, Y. Pei, D. Zhang, Y. Li, K.A. Kilian, Patterned porous silicon photonic crystals with modular surface chemistry for spatial control of neural stem cell differentiation, Nanoscale 8 (2016) 10891-10895.

[197] N.L. Francis, N.K. Bennett, A. Halikere, Z.P. Pang, P.V. Moghe, Self-Assembling Peptide Nanofiber Scaffolds for 3-D Reprogramming and Transplantation of Human Pluripotent Stem Cell-Derived Neurons, ACS Biomater. Sci. Eng. 2 (2016) 1030-1038.

[198] J. Arulmoli, H.J. Wright, D.T. Phan, U. Sheth, R.A. Que, G.A. Botten, M. Keating, E.L. Botvinick, M.M. Pathak, T. Zarembinski, D.S. Yanni, O.V. Razorenova, C.C. Hughes, L.A. Flanagan, Combination scaffolds of salmon fibrin, hyaluronic acid, and laminin for human neural stem cell and vascular tissue engineering, Acta Biomaterialia 43 (2016): 122-138.

[199] F.J. Nicholls, M.W. Rotz, H. Ghuman, K.W. MacRenaris, T.J. Meade, M. Modo, DNA-gadolinium-gold nanoparticles for in vivo T1 MR imaging of transplanted human neural stem cells, Biomaterials 77 (2016) 291-306.

[200] T.H. Kim, K.B. Lee, J.W. Choi, 3D graphene oxide-encapsulated gold nanoparticles to detect neural stem cell differentiation, Biomaterials 34 (2013) 8660-8670.

[201] Baranes, Koby, et al. Gold nanoparticle-decorated scaffolds promote neuronal differentiation and maturation. Nano letters 16.5 (2015): 2916-2920.

[202] Xu, Bai, et al. A Dual Functional Scaffold Tethered with EGFR Antibody Promotes Neural Stem Cell Retention and Neuronal Differentiation for Spinal Cord Injury Repair. Advanced Healthcare Materials (2017).

[203] Sperling, Laura E., et al. "Influence of random and oriented electrospun fibrous poly (lactic-co-glycolic acid) scaffolds on neural differentiation of mouse embryonic stem cells." Journal of Biomedical Materials Research Part A (2017).

[204] Chang, Jen-Hsuan, et al. Dual Delivery of siRNA and Plasmid DNA using Mesoporous Silica Nanoparticles to Differentiate Induced Pluripotent Stem Cells into Dopaminergic Neurons. Journal of Materials Chemistry B (2017).

[205] Zamproni, Laura N., et al. Injection of SDF-1 loaded nanoparticles following traumatic brain injury stimulates neural stem cell recruitment."International journal of pharmaceutics 519.1 (2017): 323-331.

[206] Mohammadi, Marzieh, et al. Biocompatible polymersomes-based cancer theranostics: Towards multifunctional nanomedicine. International journal of pharmaceutics (2017).

[207] Kuo, Yung-Chih, and Chun-Wei Chen. Neuroregeneration of Induced Pluripotent Stem Cells in Polyacrylamide-Chitosan Inverted Colloidal Crystal Scaffolds with Poly (lactide-co-glycolide) Nanoparticles and Transactivator of Transcription von Hippel-Lindau Peptide. Tissue Engineering Part A (2017).

[208] G. Elvira, B. Moreno, I.D. Valle, J.A. Garcia-Sanz, M. Canillas, E. Chinarro, J.R. Jurado, A.J. Silva, Targeting neural stem cells with titanium dioxide nanoparticles coupled to specific monoclonal antibodies, J. Biomater. App. 26 (2011) 1069-1089.

[209] Lépinoux-Chambaud, Claire, Kristell Barreau, and Joël Eyer. The Neurofilament-Derived Peptide NFL-TBS. 40-63 Targets Neural Stem Cells and Affects Their Properties. Stem cells translational medicine 5.7 (2016): 901-913.

[210] Berges, Raphael, et al. Structure-function analysis of the glioma targeting NFL-TBS. 40-63 peptide corresponding to the tubulin-binding site on the light neurofilament subunit. PloS one 7.11 (2012): e49436.

[211] Lépinoux-Chambaud, Claire, and Joël Eyer. The NFL-TBS. 40-63 anti-glioblastoma peptide enters selectively in glioma cells by endocytosis. International journal of pharmaceutics 454.2 (2013): 738-747.

[212] Rivalin, Romain, et al. The NFL-TBS. 40-63 anti-glioblastoma peptide disrupts microtubule and mitochondrial networks in the T98G glioma cell line. PloS one 9.6 (2014): e98473.

[213] Fressinaud, Catherine, and Joël Eyer. Neurofilaments and NFL-TBS. 40–63 peptide penetrate oligodendrocytes through clathrin-dependent endocytosis to promote their growth and survival in vitro. Neuroscience 298 (2015): 42-51.

[214] Fressinaud, Catherine, and Joël Eyer. Neurofilament-tubulin binding site peptide NFL-TBS. 40–63 increases the differentiation of oligodendrocytes in vitro and partially prevents them from lysophosphatidyl choline toxiciy. Journal of neuroscience research 92.2 (2014): 243-253.

[215] Rizzuti, Mafalda, et al. Therapeutic applications of the cell-penetrating HIV-1 Tat peptide. Drug discovery today 20.1 (2015): 76-85.

[216] Saini, Avneet, et al. Insights on the structural characteristics of Vim-TBS (58-81) peptide for future applications as a cell penetrating peptide. Bioscience trends 7.5 (2013): 209-220.

[217] Bechara, Chérine, and Sandrine Sagan. Cell-penetrating peptides: 20years later, where do we stand?. FEBS letters 587.12 (2013): 1693-1702.

[218] Copolovici, Dana Maria, et al. Cell-penetrating peptides: design, synthesis, and applications. ACS nano 8.3 (2014): 1972-1994.

CHAPTER 2

NFL-LIPID NANOCAPSULES FOR BRAIN NEURAL STEM CELL TARGETING *

TABLE OF CONTENTS

1. PREFACE

Although endogenous NSC differentiation is considered one of the most promising strategies for the treatment of neurodegenerative diseases, the lack of NSC-targeting molecules primarily promotes the development of non-selective systems.

Thus, the aim of this work was to produce a pharmaceutical system able to target endogenous neural stem cells (NSCs) and to potentially deliver a wide choice of bioactive compounds.

Lipid nanocapsules (LNCs) were selected as drug delivery system due to their high biocompatibility and versatility while cell-penetrating peptides (TAT and VIM), known to increase nanoparticle-uptake, and the peptide NFL-TBS.40-63 (NFL), known for its NSCs-targeting property, were used to functionalize the system. The evaluation of the targeting efficiency of the different combinations LNCs-peptides was performed *in vitro* and only the most efficient was tested *in vivo*. Primary NSCs from the brain (subventricular zone) or from the spinal cord (central canal) were used for the *in vitro* tests while injections in the lateral ventricle of the brain or in the T10 of the spinal cord were performed for the *in vivo* evaluations.

We showed that only LNCs on which NFL was stably adsorbed, NFL-LNCs, were able to interact *in vitro* and *in vivo* with NSCs of the brain while the other peptides did not show such a unique functionalization of the nanoparticles. Surprisingly, when the NFL-LNCs were tested on NSCs of the spinal cord, they failed to penetrate in these cells.

This study indicates for the first time the possibility to selectively interact with NSCs of the brain *in vitro* and *in vivo* with a versatile drug delivery system. Moreover, the preferential interaction towards NSCs of the brain over NSCs of the spinal cord suggests interesting differences between the two types of cells which would worth to investigate.

2. ABSTRACT

The replacement of injured neurons by the selective stimulation of neural stem cells *in situ* represents a potential therapeutic strategy in the treatment of neurodegenerative diseases. The peptide NFL-TBS.40-63 showed specific interactions towards neural stem cells of the subventricular zone. The aim of our work was to produce a NFL-based drug delivery system able to target neural stem cells through the selective affinity between the peptide and these cells. NFL-TBS.40-63 (NFL) was adsorbed on lipid nanocapsules (LNCs) whom targeting efficiency was evaluated on neural stem cells from the subventricular zone (brain) and from the central canal (spinal cord). NFL-LNC were incubated with primary neural stem cells *in vitro* and injected either in adult rat's brain (right lateral ventricle) or spinal cord (T10) *in vivo*. NFL-LNC interactions with neural stem cells were different depending on the origin of the cells. NFL-LNC showed a preferential uptake by neural stem cells of the brain while they did not interact with neural stem cells of the spinal cord. The results obtained *in vivo* correlated with the results observed *in vitro*. NFL-LNCs are thus a promising therapeutic tool to selectively deliver bioactive molecules to brain neural stem cells.
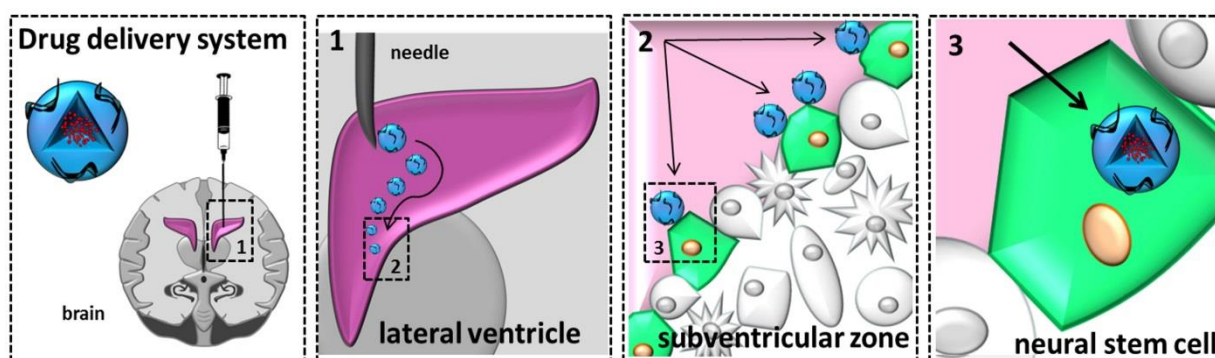
3. INTRODUCTION

Stem cells are characterized by self-renewal [1] and differentiation into specialized cells [2]. Stem cell classification can be related to their developmental stage (embryonic, fetal or adult) [3], plasticity (totipotent, pluripotent, multipotent or unipotent) [4] and anatomical localization [5]. In an adult mammalian organism, neural stem cells (NSC) are multipotent self-renewing cells, localized in the central nervous system, that are able to differentiate into neurons, astrocytes and oligodendrocytes [6]. NSC are confined in places called niches such as the subventricular (SVZ) and the subgranular zones in the brain [7], and central canal (CC) in the spinal cord [8]. Neurogenesis can occur during the adulthood in these niches [9]. NSC can be isolated and cultivated as floating aggregates named neurospheres [10]. The absence of growing factors (EGF and FGF) as well as the presence of serum induces NSC to differentiate into specialized neuronal cells [11]. The regenerative potential of these cells [12], due to their differentiation property, makes them a suitable tool for the treatment of neurodegenerative diseases [13]. NSC can potentially replace and repair injured neurons [14]. The most common NSC-based therapeutic approach consists in allogenic NSC transplantation at the site of interest [15-18]. Unfortunately this method is strongly limited by the dangers their transplantation represents (development of metastases, immune-mediated rejections, death of the transplanted cells [19]) and by their availability as well [20]. Thus, new strategies have emerged aiming at the *in situ* stimulation of endogenous NSC to induce their differentiation [21, 22]. Although this approach would solve most of the issues associated with NSC transplantation, the lack of selective NSC targeting greatly slows the progresses in that direction.

Recently NFL-TBS.40-63 (NFL), a synthetic 24-aminoacid peptide corresponding to the tubulin-binding site of the neurofilament light subunit [23], shows a strong specificity for NSC of the SVZ (SVZ-NSC) [24]. *In vitro*, NFL penetrated massively in SVZ-NSC by direct translocation increasing their adhesion and differentiation whereas it did not enter in astrocytes and neurons. *In vivo*, after intra-lateral ventricle injection (in rat brain), it localized specifically in the SVZ-NSC niche. NFL induced no toxicity both *in vitro* and *in vivo*. NFL was also tested as anti-glioblastoma drug, alone [25, 26] or associated with nanoparticulate systems [27]. The active uptake of the peptide by cancerous cells induced the inhibition of the tumor growth because of the disruption of microtubule and mitochondrial networks [28]. The cytotoxic effect was not observed on healthy cells. The peptide also showed *in vitro* affinity for oligodendrocytes, in which it penetrated by clathrin-dependent endocytosis promoting the

cellular growth and survival [29, 30]. The reason of the affinity between NFL and these three kinds of cells (SVZ-NSC, glioblastoma cells and oligodendrocytes) is not well understood yet, neither the reason of the different mechanisms of penetration (passive in the first case and active in the second and third case). Physicochemical studies carried on NFL indicated a strong correlation structure – activity (by alanine-scanning assay) and a dependency of the ratio alpha helix/beta sheet to the environmental conditions (by circular dichroism) [31]. Although NFL has high affinity for SVZ-NSC, it did not induce yet an identified therapeutic effect. Moreover, the strong correlation structure – activity [31] limits chemical coupling between NFL and bioactive molecules that would be able to induce SVZ-NSC differentiation. While a direct therapeutic application of the peptide is still not excluded, its association with a drug delivery system could potentially be a useful strategy for selective delivery of bioactive molecules to NSC.

Lipid nanocapsules (LNC) are the drug delivery system that has been selected for this purpose. The excipients used to produce LNC are approved by the FDA (for oral, topical and parenteral administration). The formulation is highly stable and the process of production is organic solvent-free and follows a phase inversion temperature method [32-35]. LNC are a versatile vector promoting a nanoencapsulation or a nanoassociation of a wide range of therapeutics (hydrophilic, lipophilic or amphiphilic [36]). Furthermore this nanoparticulate system can be easily made traceable by fluorescent labelling. DiD is one of the most used fluorescent dye for LNC tracking [37] and its compatibility with *in vivo* experiment (e.g. for intra-lateral ventricle injection in the brain) is well known [38]. NFL was recently related to the cell-penetrating peptides (CPP) [26] due the characteristics it shares with them: the positive charge, the low molecular weight and the balance between endocytosis and direct translocation in cell penetration [39]. CPP have been successfully used to enhance the cellular delivery of a large variety of cargos including nanoparticles [40]. Hence we decided to compare LNC presenting NFL at their surface (NFL-LNC) with LNC decorated with other described CPP such as TAT [41] and VIM [42].

Thus, the objective of this work was to evaluate whether the LNC-based drug delivery system is able to selectively interact with NSC. NFL-LNC targeting efficiency was tested on NSC from the SVZ (brain) and from the CC (spinal cord) *in vitro*. The mechanism of interaction between NFL-LNC and NSC was characterized *in vitro*. Then, NFL-LNC were injected in adult rat brain (right lateral ventricle) and spinal cord (T10) to determine if they specifically target endogenous NSC.

4. MATERIALS AND METHODS

4.1 Materials

Biotinylated NFL-TBS.40-63 (NFL), biotinylated VIM-TBS.58-81 (VIM), biotinylated TAT (TAT), 5-FAM-labeled scramble NFL (SCR NFL), 5-FAM-labeled TAT (fluoTAT), 5-FAM-labeled NFL-TBS.40-63 (fluoNFL) and 5-FAM-labeled VIM-TBS.58-81 (fluoVIM) were purchased from GeneCust (Luxembourg, Luxembourg). Labrafac® was purchased from Gattefosse SA (Saint-Priest, France). Lipoïd® was purchased from Lipoid Gmbh (Ludwigshafen, Germany). Solutol HS was purchased from BASF (Ludwigshafen, Germany). Sodium chloride (NaCl) was purchased from Prolabo (Fontenay-sous-bois, France). D-glucose, Phalloidin-Rhodamine and primary antibodies mouse anti-alpha tubulin, anti-nestin, anti-GFAP and anti-vimentin were purchased from Sigma (Saint-Louis, Missouri). DiD' solid; DiIC18(5) solid (1,1'-Dioctadecyl-3,3,3',3'-Tetramethylindodicarbocyanine, 4-Chlorobenzenesulfonate Salt) (DiD), secondary antibodies anti-mouse Alexa Fluor 488, Alexa Fluor 568 and DAPI, HEPES, Pen/Strept, Na Pyruvate, B27, MEM alpha (no nucleosides), 0.05 % Trypsin-EDTA (1x), DNAse and ProLong Gold antifade were purchased from Thermo Fisher Scientific (Waltham, Massachusetts). EGF and bFGF were purchased from Tebu-Bio (Le Perray en Yvelines, France). BD CellTak was purchased from Corning Inc (New York, New York). BCA Uptima was purchased from Interchim (Montluçon, France). CellTiter 96® AQueous One Solution Cell Proliferation Assay was purchased from Promega (Fitchburg, Wisconsin). Amicon Ultra-0.5 ml 100K filters were purchased from Merck Millipore (Billerica, Massachusetts). The isolation of NSC and *in vivo* experiments were performed according to Directive 2010/63/EU, to guidelines of the French and Belgian Government following the approval by the local committee of Pays de la Loire for Ethic on Animal Experiments or by the ethical committee for animal care of the faculty of medicine of the Université catholique de Louvain.

4.2 Preparation and characterization of LNC presenting CPP at their surface

Preparation of DiD-labeled lipid nanocapsule stock solution (stock-LNC). Stock-LNC was prepared according to the protocol developed by Heurtault et al. [32]. Briefly, 0.846 g Solutol HS15, 0.075 g Lipoïd®, 0.089 g NaCl, 1.028 g Labrafac® and 2.962 ml of water were mixed under magnetic stirring for 5 min at 30 °C. Temperature cycles (a minimum of 3) of progressive heating/cooling were done between 60 °C and 90 °C. During the cooling of the last cycle, at 80 °C 27.5 µl of DiD solution (1 mg/ml in absolute ethanol) and at 74 °C 12.5 ml

of cold water were added, under high speed stirring, respectively. The nanoparticles were filtered by 0.2 µm filter and stored at 4 °C.

Preparation of CPP DiD-labeled lipid nanocapsules (CPP-LNC). TAT-, VIM- and NFL-LNC were produced by incubating 369 µl of 1 mM peptide solution (in water) overnight with 1 ml of stock-LNC under gentle stirring. LNC without peptide (negative control) were produced incubating 369 µl of water overnight with 1 ml of DiD-labelled lipid nanocapsule stock solution under gentle stirring.

CPP-LNC physicochemical properties. Size, z-potential and PDI of CPP-LNC were characterized using a Malvern Zetasizer Nano Serie DTS 1060 (Malvern Instruments). For the measurement of size and PDI, nanoparticles were diluted 1/100 (v/v) in water. For the measurement of z-potential, nanoparticles were diluted 1/100 (v/v) in NaCl 10 mM. Peptide concentration at LNC surface was indirectly measured by BCA Uptima quantification [27]. Briefly, CPP-LNC were filtered by centrifugation at 4000 g during 30 min using an Amicon Ultra-0.5 ml 100K filter. The water phase containing the unbound peptide was collected. The positive control consisted of free peptide (NFL, TAT or VIM).

Characterization of NFL interactions with LNC. NFL-LNC size was measured after dilution 1/100 (v/v) in water or in NaCl 1 M. Neutral LNC (nLNC) and NFL-nLNC were prepared following the same protocol as described above but without Lipoïd®. Size and PDI were measured in different concentrations of Tris or NaCl (0, 0.005, 0.05, 0.15, 0.25, 0.5 and 1 M).

4.3 Impact of CPP on LNC interactions with NSC primary cultures

Isolation of SVZ-NSC. SVZ-NSC were isolated according to a protocol developed by Guo et al. [43]. Briefly, new-born rats (from 1 to 5 day-old) were sacrificed by decapitation. The brain was removed and put in dissection buffer (1.25 ml of D-glucose 1 M, 750 µl of HEPES and 500 µl Pen/Strept in 50 ml of HBSS medium). It was then cut into 400 µm coronal sections and the SVZ was dissected and placed in 1 ml of dissection buffer. The tissue was vortexed and centrifuged for 5 min at 344 g. The supernatant was removed and 1 ml of stem cell culture medium (1.25 ml of D-glucose 1 M, 750 µl of HEPES, 500 µl Pen/Strept, 500 µl Na Pyruvate, 500 µl of B27 and 10 ng/ml of EGF in 50 ml of MEM alpha no nucleosides medium) was added. The pellet was mechanically triturated using a 26 G needle. The cells were seeded at 2.10^5 to 3.10^5 cells/Petri 60 mm in 5 ml of cell culture medium. SVZ-NSC

were cultivated as floating neurospheres which appeared after 5 days. The percentage of NSC (Nestin positive cells) was between 71 and 76 % (Supplementary data 1).

Isolation of CC-NSC. CC-NSC were isolated according to a protocol developed by Hugnot [44]. Briefly new-born rats were sacrificed by decapitation. The spinal cords were removed and put in a 1.5 ml tube with 500 µl of HBSS (two spinal cords/tube). In each tube, 130 µl of hyaluronidase, 130 µl of trypsin and 25 µl of DNAse were added. The samples were incubated at 37 °C for 30 min, transferred in a 15 ml tube containing 12 ml of HBSS and centrifuged at 380 g for 5 min. The supernatant was eliminated and the pellet was suspended in 600 µl of HBSS and mechanically dissociated. A 40 µm filter was used to filter the suspension which was then centrifuged at 380 g for 5 min. The supernatant was eliminated and the pellet was suspended in 2 ml of 25 % sucrose solution. The suspension was centrifuged at 780 g for 30 min. The supernatant was removed and 1 ml of stem cell culture medium (with 10 ng of bFGF) was added. The cells were seeded at 2.10^5 to 3.10^5 cells/T25 flask and floating neurospheres appeared after 5 days. The percentage of NSC was between 75 and 82 % (Supplementary data 1).

Cell viability. SVZ-NSC and CC-NSC viability was measured following incubation during 24 hours with NFL, LNC and NFL-LNC at different concentrations (0.63, 1.26 and 2.52 mg/ml) and with 10 mM sodium azide in the presence of 6 mM 2-deoxy-D-glucose to deplete cellular ATP (ATP depl solution) using CellTiter 96® AQueous One Solution Cell Proliferation assay.

FACS analyses. BD FACSCalibur™ flow cytometer (BD Biosciences) was used to measure the percentage of 5-FAM positive NSC (after incubation with fluorescent CPP) or DiD positive NSC (after their incubation with nanoparticle formulations). The fluorescent CPP and the nanoparticles were used at a final concentration of 10 µM and of 1.26 mg/ml in cell culture medium respectively. All the *in vitro* experiments were done using 6 to 7-day old neurospheres with a concentration of +/- 2900 neurospheres/ml (corresponding to +/- 4.10^5cells/ml). Before FACS analyses, neurospheres were washed 3 times with PBS, dissociated with a 26 G needle and re-suspended in 50 µg/mL propidium iodide.

Characterization of the interactions between the CPP or CPP-LNC and SVZ-NSC. 5-FAM-labeled CPP (NFL, SCR NFL, VIM or TAT) were incubated 1 h with SVZ-NSC. FACS was used to measure the percentage of 5-FAM positive cells. CPP-LNC (TAT-LNC or NFL-LNC) were incubated 1 h with SVZ-NSC. FACS was used to measure the percentage of DiD

positive NSC. FluoNFL or NFL-LNC were incubated during 5, 20 and 60 min with SVZ-NSC or CC-NSC to evaluate the kinetic of interaction with the cells. To study the mechanism of interactions between NFL or NFL-LNC and NSC, SVZ-NSC and CC-NSC were pre-incubated at 4 °C or pre-treated to deplete cellular ATP for 30 min before to be incubated for 1 h with fluoNFL or NFL-LNC. To study the effect of NFL pre-treatment on SVZ-NSC affinity towards CPP and nanoparticles, SVZ-NSC were pre-treated for 5 min with NFL solution before to be incubated for 5 min with 5-FAM-labeled CPP (NFL or VIM) or nanoparticle formulations (LNC and NFL-LNC). Pre-treatment was also performed with VIM as control. FACS was used to measure the percentage of 5-FAM and DiD positive NSC respectively.

Confocal microscopy evaluation of NFL-LNC association to NSC. Neurospheres from SVZ-NSC or CC-NSC were incubated 1 h with NFL-LNC. Neurospheres were washed 3 times with cell medium and fixed with 4 % PFA for 15 min. They were then incubated 2 h with 100 nM rhodamine-phalloidin, and mounted with VECTASHIELD® antifade mounting medium. The visualization of NFL-LNC association with NSC was also performed on adherent SVZ-NSC which were seeded on lamellae coated with BD CellTak. Pictures were taken with a Zeiss Cell Observer Spinning Disk microscope (Carl Zeiss). Two pictures/condition were taken randomly.

4.4 Impact of NFL on LNC specific interactions with NSC *in vivo*

Injection of NFL-LNC in the brain right ventricle. Six week-old Sprague Dawley female rats were anesthetized using 1 µl/g of ketamine:xylazine (50:50) by intraperitoneal injection. The rat head was stabilized in a stereotactic frame. Twenty µl of LNC or NFL-LNC (126 mg/ml) were injected at -0.8 mm anteroposterior, 1.5 mm mediolateral and 4 mm dorsoventral respect to bregma using a convection-enhanced delivery (CED) microinjector (Harvard Apparatus) at 0.5 µl/min (32 G needle). Brains were retrieved 1 h or 6 h after injection and cryopreserved. Twelve µm sections were collected and fixed in methanol for 10 min. Samples were stained against nestin (mouse anti-nestin, 1/50), vimentin (mouse anti-vimentin, 1/200) or glial fibrillary acid protein (GFAP) (mouse anti-GFAP, 1/200). Antigen detection was performed with Alexa Fluor 488 anti-mouse IgG (1/200) at 4 °C. DAPI (1/300 in PBS) was used to stain cell nuclei. Sections were mounted with ProLong Gold antifade and pictures were acquired by TCS-SP8 Leica (Leica Microsystems) confocal microscopy. A minimum of 5 pictures/condition were taken.

Injections of NFL-LNC in the spinal cord. Six week-old Sprague Dawley female rats were anesthetized with 80 µl of Temgesic® (0.03 mg/ml) by intraperitoneal injection. Isoflurane (2.5 %) was administered during the whole operation by aerosol. Vertebral laminectomy was performed at T10. Five µl of LNC or NFL LNC (126 mg/ml) were injected at 0.5 mm mediolateral and 1.2 mm dorsoventral respect to T10 midline using a CED microinjector (Harvard Apparatus) at 0.8 µl/min (33 G). Twelve µm sections were collected and fixed in methanol for 10 min. Samples were stained against nestin, vimentin and GFAP. Sections were finally covered with VECTASHIELD® and fixed on microscope slides. Pictures were taken with a Zeiss Cell Observer Spinning Disk microscope (Carl Zeiss). Two pictures/condition were taken randomly.

4.5 Statistical analyses

All the experiments were repeated at least 3 times. Error bars represent standard error of the mean (SEM). $p* < 0.05$, $p** < 0.01$ and $p*** < 0.001$ were calculated with Mann-Whitney test by using Prism 5.00 (GraphPad software, San Diego, CA).

5. RESULTS AND DISCUSSION

To selectively target endogenous NSC, NFL was selected among several cell-penetrating peptides (CPP) and was adsorbed at the surface of LNC.

5.1 Enhancement of LNC interactions with NSC

We compared different CPP to select the best peptide to functionalize LNC and to efficiently interact with NSC. NFL was tested because of its specificity towards SVZ-NSC [24], TAT for its detailed description in the literature [45], VIM for its ability to target the cell nucleus [42] and SCR NFL for its amino-acid composition, which is the same as NFL but in a random sequence [31]. The selection of the most appropriate CPP was done in three steps: evaluating i) its ability to interact with SVZ-NSC, ii) its capacity to interact with LNC surface and iii) CPP-LNC efficiency to interact with SVZ-NSC. NFL, VIM and TAT, but not SCR NFL, interacted with SVZ-NSC *in vitro* (Figure 1A). As already demonstrated for glioblastoma cells [31], SCR NFL showed a lower cellular uptake compared to NFL. The interaction with SVZ-NSC seems to be influenced also by the amino-acid organization of the peptides. Seventy to 93 % of the cells were positive for 5-FAM after 1 h of incubation with NFL, VIM and TAT and no significant differences were observed among them. Then, NFL, VIM and

TAT were incubated with LNC. NFL and TAT significantly increased LNC size and z-potential (+4 to +9 nm and +2 to +3 mV respectively) but not VIM (Figure 1B). After centrifugation of the nanoparticles, 54.1 % of NFL, 100 % of VIM and 61.7 % of TAT were recovered (Figure 1B). NFL and TAT interacted with LNC surface but not VIM. VIM could present specific folds [46], which hide its positively charged residues and prevent its interaction with the LNC surface. The percentage of non-bound NFL we observed is similar to the one reported by Balzeau et al. (54.1% versus 51.7 %, respectively) [27]. While less TAT was adsorbed at LNC surface, the LNC size increase was higher in presence of TAT than when incubated with NFL. We hypothesized that the size increase of LNC in presence of TAT or NFL is not necessarily linked to the absolute amount of peptide adsorbed at the LNC surface. Indeed, a different conformation of TAT at the surface of the LNC and a higher hydration of the peptide due to its more positive profile (+8 for TAT and +2 for NFL) could increase the hydrodynamic size of the LNC in a higher extent compared to NFL. Moreover, the spatial accumulation of the peptide and water molecules could hide the active sites of TAT from the NSC membrane preventing the interaction between TAT-LNC and SVZ-NSC.

NFL-LNC and TAT-LNC were incubated with primary cultures of SVZ-NSC. Significantly more cells were positive for DiD when LNC were decorated with NFL (60 %) than with TAT (10 %) (Figure 1C). Thus, TAT did not provide LNC the affinity for SVZ-NSC observed with TAT alone.

SCR NFL, VIM and TAT were sequentially eliminated because of their low affinity for SVZ-NSC, inability to interact with LNC surface and lack of interaction of the final CPP-based system with SVZ-NSC, respectively. We confirmed the ability of NFL to interact with SVZ-NSC [24] and to adsorb on LNC surface [27]. Moreover we showed that this peptide conferred to LNC the ability to interact with SVZ-NSC.
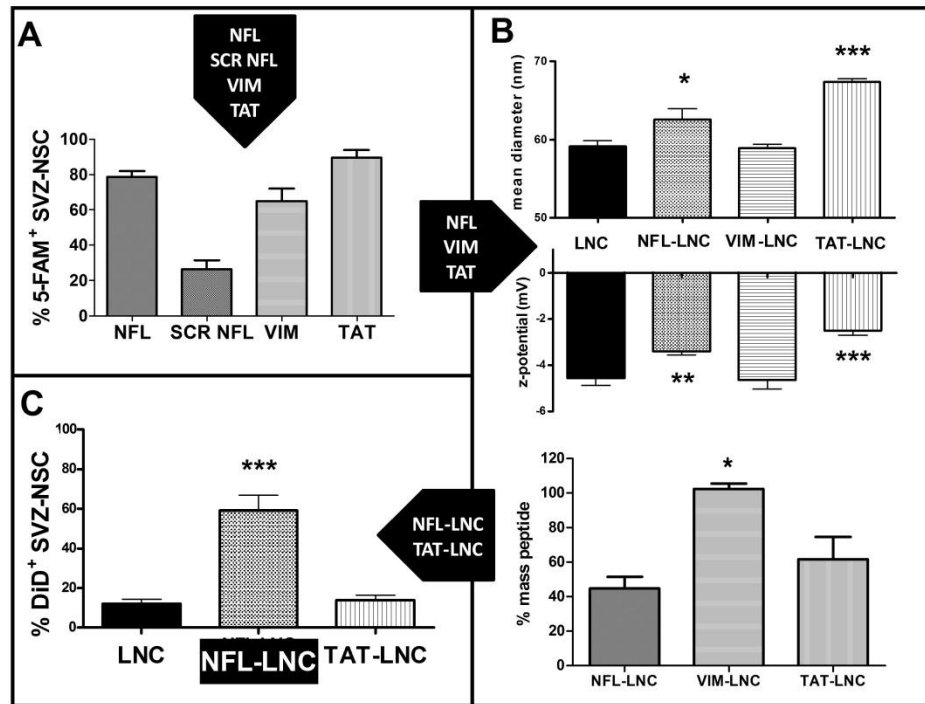
Figure 1: Enhancement of LNC interactions with NSC *via* CPP functionalization. A: 5-FAM-labelled NFL, scramble NFL, VIM and TAT were incubated at 37 °C for 1 h with SVZ-NSC. B: NFL, VIM and TAT were incubated overnight with LNC and the resulting CPP-LNC were physicochemical characterized (p* < 0.05, p** < 0.01 and p*** < 0.001 compared to LNC, n=12). C: NFL-LNC and TAT-LNC were incubated at 37 °C for 1 h with SVZ-NSC (p*** < 0.001 compared to LNC, n=7).

5.2 Characterization of NFL interaction with LNC

LNC have a size of 60 nm ± 4, a PDI of 0.01 and a z- potential of -8.5 mV ± 1.5 (Table 1). Adsorption of NFL significantly increased LNC size (+ 6 nm) and PDI as well as z-potential (+ 2.5 mV). The experimental conditions are comparable (particle concentrations, continuous phase viscosity, electrolyte concentrations, temperature) and the accuracy of the apparatus is +/- 2% of the size of the nanoparticle (www.malvern.com). Thus, a difference of 6 nm (10 % of LNC size) is significant and it is a reliable indication of NFL adsorption on LNC surface. NFL did not change neutral LNC (nLNC) physicochemical properties (Table 1).

The influence of NFL on DiD-labelling was evaluated as well as the stability of the system in different conditions. Whatever the incubation time and the lipidic phase, no significant amount of DiD leaked from the nanocapsules (Supplementary Data 2), confirming the correspondence DiD – LNC in FACS and confocal evaluations. No variation was observed in the physicochemical properties of NFL-LNC when incubated in cell culture medium and artificial cerebrospinal fluid (aCSF[47]) (Supplementary Data 3).

Table 1. Physiochemical characteristics of the nanoparticles

	size (nm)	PDI	z-potential (mV)
LNC	60 ± 4	0.01	-8.5 ± 1.5
NFL-LNC	66 ± 4*	0.18-0.21***	-6.0 ± 1.5**
nLNC	65 ± 1.6	0.136	-1.5 ± 1.5
NFL-nLNC	67 ± 0.6	0.112	-1.5± 2

Size and PDI were characterized by DLS diluting the nanoparticles 1/100 (v/v) in water. The z-potential was measured by diluting the nanoparticles 1/100 (v/v) in NaCl 10 mM (p* < 0.05, p** < 0.01 and p*** < 0.001 compared to LNC, n=12).

The adsorption of NFL on LNC surface is due to the interaction between the peptide and the polar PEG groups of the Solutol®, as previously shown by tensiometry studies [27]. Since the peptide is positively charged and the LNC is slightly negatively charged, we hypothesized that ionic interactions drove NFL adsorption at LNC surface. To study the importance of electrostatic interactions in NFL − LNC association, NFL-LNC were incubated in 1 M NaCl. NFL-LNC size (66 nm) significantly decreased to the LNC size (60 nm) (Figure 2A). We can suppose that the hydration of the peptide is significantly modified by the electrolytes leading to a modification of its secondary structure (the hydrodynamic diameter of the whole particle is lower). It can be also hypothesized that the peptide was removed from the nanoparticle surface by the high ionic strength of the solution. We tested then the ability of the peptide to interact with LNC presenting a neutral surface (nLNC). The resulting formulation did not show any significant physicochemical variation compared to nLNC alone, suggesting that no peptide adsorbed on LNC surface. These results underlined the critical role played by electrostatic interactions between NFL and LNC. As a consequence, NFL could be washed away from the surface or replaced by other molecules/ions [48], so NFL-LNC were incubated at different salt concentrations. The size of NFL-LNC was unaffected by an increase of ionic strength up to 0.25 M of NaCl and 0.005 M of Tris buffer (Figure 2B). Higher concentrations of these salts affected the size of the system decreasing it. Tris and NaCl have the same ionic strength (1 M) at pH 7 but Tris impacted NFL-LNC more than NaCl. This could be an indication that the interactions between NFL and LNC do not depend only on electrostatic interactions. So-called "weak interactions" (e.g. Wan der Waals forces) could also be involved in NFL and LNC interactions and cannot be neglected. Importantly, in the experimental settings used in this study, NFL-LNC interactions were preserved.
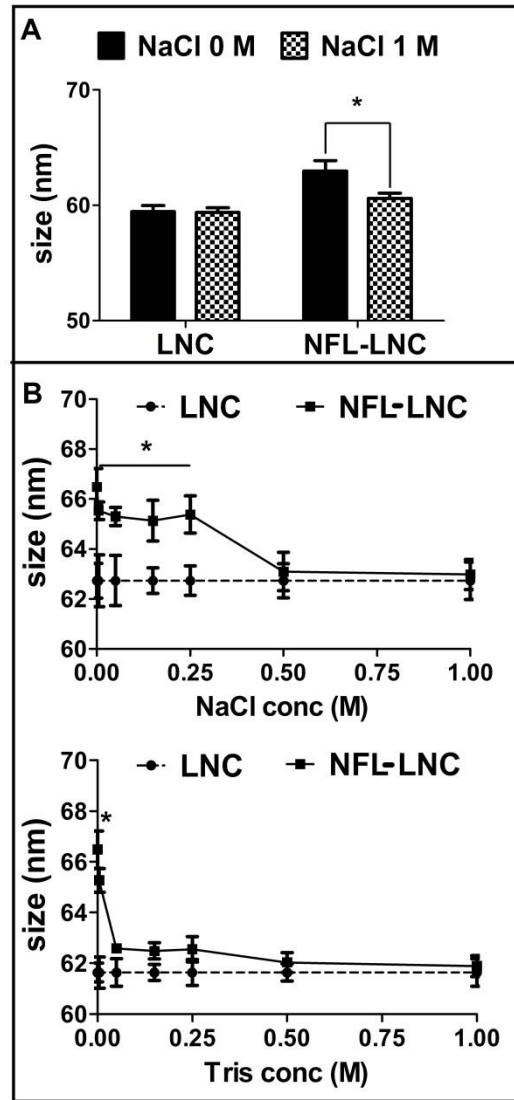
Figure 2: Impact of salt concentration on NFL interaction with LNC. A: LNC and NFL-LNC size was measured before and after incubation with 1 M NaCl (p* < 0.05, n=18). B: LNC and NFL-LNC size was measured in different salts (NaCl and Tris) and at different salt concentrations (p* < 0.05 compared to LNC, n=3).

5.3 Interactions between NFL-LNC and NSC *in vitro*

First, the impact of NFL, LNC and NFL-LNC at different concentrations on NSC viability was evaluated for 24h of incubation. Whatever the condition, viability of SVZ-NSC was at least 100 % (Figure 3A). Viability of CC-NSC (Figure 3B) was generally lower than the one observed for SVZ-NSC but stayed above 70%. Incubation of CC-NSC with NFL-LNC at the highest concentration (2.52 mg/ml) decreased NSC viability (70 %), while for the other conditions, it remained above 80 %. Moreover, no significant difference was observed between the percentage of propidium iodide positive NSC treated cells and the control in FACS analyses (data not shown). So, NFL, LNC and NFL-LNC showed no significant

toxicity on SVZ-NSC at any concentrations while NFL-LNC significantly decreased the viability of CC-NSC only at the highest concentration.
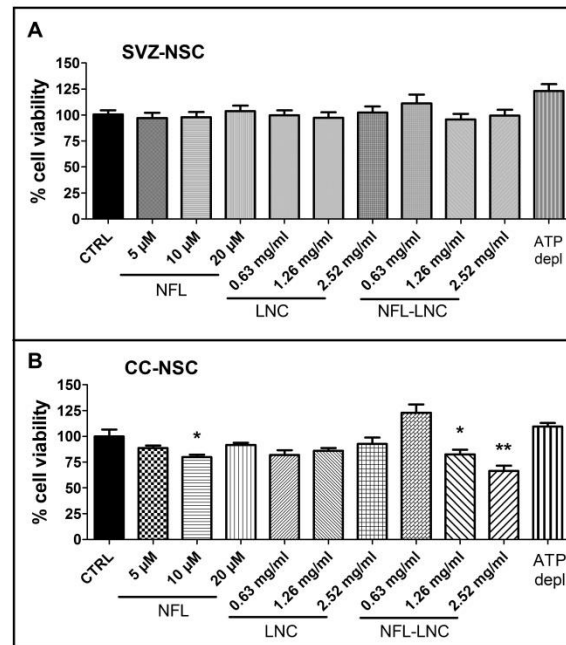

Figure 3: Impact of NFL, LNC and NFL-LNC on NSC viability. A: viability of SVZ-NSC evaluated by MTS assay after 24-h incubation with different compounds (NFL, LNC, NFL-LNC, and ATP depl solution) at different concentrations. B: viability of CC-NSC evaluated by MTS assay after 24-hour incubation with different compounds (NFL, LNC, NFL-LNC, and ATP depl solution) at different concentrations ($p^* < 0.05$ compared to CTRL, n=3). NFL concentrations in 0.63, 1.26, and 2.52 mg/ml of NFL-LNC correspond to 1.35, 2.7, and 5.4 μM respectively.

Then, the kinetic of NFL, LNC and NFL-LNC interactions with NSC was analysed and the impact of energy deprivation on their interaction was evaluated. NFL interacted very quickly with SVZ-NSC (after 5 min 43 % of SVZ-NSC were positive to 5-FAM) while it was slower with CC-NSC (less than 5 % were positive to 5-FAM) (Figure 4A top). After 20 min, the percentage of 5-FAM positive CC-NSC was similar to the percentage of 5-FAM positive SVZ-NSC (54 %). From 20 min to 1 h, the percentage of 5-FAM positive cells steadily increased and no difference were observed between CC- and SVZ-NSC, to reach 80 % of positive cells. The percentage of 5-FAM positive SVZ-NSC was not affected by the energetic conditions (Figure 4A bottom): 37 °C (normal condition, n.c.), ATP depletion (ATP depl) and 4 °C. The interaction between NFL and CC-NSC were significantly decreased (more than 50 %) when the incubation was performed at 4 °C (30 % of 5-FAM positive cells). Thus, the kinetic of interactions between NFL and NSC was influenced by cell origin and energetic conditions for CC-NSC. CPP can penetrate plasmatic membranes by different pathways,

mostly by energy-independent mechanisms [39, 40] but the mechanisms are cell type-dependent. For instance, NFL penetrates passively in SVZ-NSC but actively in oligodendrocytes and glioblastoma cells [24, 26, 29]. We hypothesized that plasma membrane composition could change depending on cell type and consequently, impact cell-CPP interactions. Up to now, only the plasma membrane of SVZ-NSC has been partially characterized [49]. Thus, so far, it is not possible to compare the membrane composition of both types of cells and to draw conclusions about its influence.
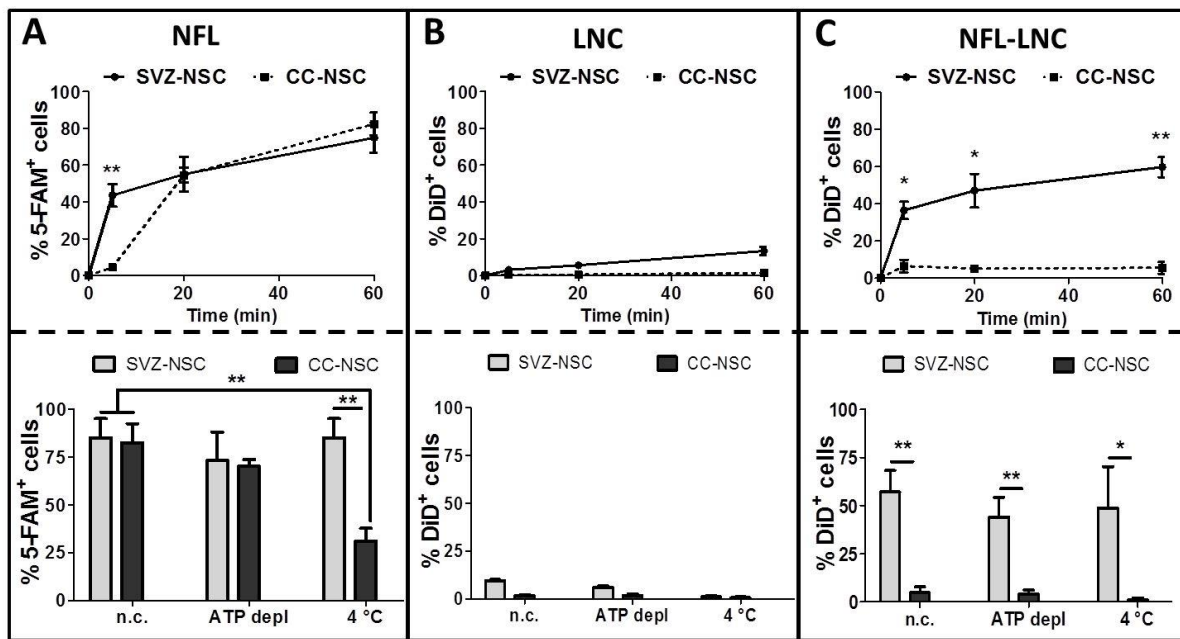

Figure 4: Interaction between NFL, LNC, and NFL-LNC and NSC. A, top: kinetic of peptide internalization by SVZ-NSC and CC-NSC over time ($p^{**} < 0.01$ compared to CC-NSC, n=3). A, bottom: peptide internalization by SVZ-NSC and CC-NSC at different energetic conditions ($p^{**} < 0.01$, n=3). B, top: kinetic of LNC internalization by SVZ-NSC and CC-NSC over time. B, bottom: LNC internalization by SVZ-NSC and CC-NSC at different energetic conditions. C, top: kinetic of NFL-LNC internalization by SVZ-NSC and CC-NSC over time ($p^{*} < 0.05$ and $p^{**} < 0.01$ compared to CC-NSC, n=3). C, bottom: NFL-LNC internalization by SVZ-NSC and CC-NSC at different energetic conditions ($p^{*} < 0.05$ and $p^{**} < 0.01$, n=3).

LNC did not interact with NSC, whatever the cell type and the incubation time (Figure 4B). Only 12 % of SVZ-NSC were positive for DiD after 1 h of incubation with LNC. LNC were reported to interact with cancer cells [50] and mesenchymal stem cells [51] while they did not with NSC. NSC could have different proteins/lipids involved in specific pathways of internalization compared to these cells. It has already been demonstrated that nanoparticle uptake can be affected also by the cell type [52]: e.g. HepG2 cells have no endogenous caveolin, so they are unable to uptake nanoparticles by caveolae mediated endocytosis [53].

NFL-LNC showed an affinity only for SVZ-NSC (Figure 4C). The kinetic of interaction between NFL-LNC and SVZ-NSC was similar to the one observed for NFL (Figure 4C, top).

After 5 min, more than 35 % of SVZ-NSC were positive for DiD. The percentage of positive cells increased over time from 47 % after 20 min, to 60 % after 1 h. The interaction between NFL-LNC and SVZ-NSC were not significantly affected by the energetic conditions of the incubation (Figure 4C, bottom). The percentage of the cells positive to DiD remained around 50 %. Thus, only NFL conferred LNC targeting toward SVZ-NSC. NFL adsorption at LNC surface allowed LNC to interact with SVZ-NSC *via* energetic-independent mechanisms, but no interaction of LNC was observed with CC-NSC despite the presence of NFL. As hypothesized for NFL alone, SVZ-NSC and CC-NSC could have a different lipid/protein membrane composition that could account for these results.

We hypothesized that the presence of NFL-specific receptors at the SVZ-NSC surface may be responsible for the rapid association of NFL or NFL-LNC with SVZ-NSC. To test this hypothesis, we evaluated the effect of cell pre-incubation with NFL to determine if it would be possible to saturate those potential receptors or interaction sites. SVZ-NSC were first pre-treated with NFL for 5 min and then incubated with VIM, NFL, LNC or NFL-LNC. The effect of the pre-treatment with NFL was measured comparing the percentage of 5-FAM (NFL and VIM) or DiD (LNC and NFL-LNC) positive SVZ-NSC between pre-treated and not pre-treated cells. The percentage of cells that interacted with NFL or VIM significantly increased (Figure 5A) when they were pre-treated with NFL (from 50% to more than 80%) but not after VIM pre-treatment (Figure 5A). If NFL and NSC interactions were receptor-mediated, we expected that peptide internalization would have been lower after NFL pre-treatment. Since it was not the case, NFL did not penetrate NSC *via* receptor-mediated pathways. NFL and VIM could have different mechanisms of interaction with NSC. The percentage of 5-FAM positive cells was similar after 1-hour incubation with NFL or VIM while it was differently affected by 5-min incubation with these peptides (47 % for NFL and 15 % for VIM). We hypothesize that NFL pre-treatment could modify the cell membrane structure and thus increase peptide penetration while VIM pre-treatment could not. As for the adsorption on LNC surface, VIM could present specific folds that hide its positively charged residues and consequently affect its interaction with the plasmatic membrane.

To the contrary of NFL and VIM, LNC and NFL-LNC interactions with SVZ-NSC were not affected by pre-incubation with NFL or VIM (Figure 5B). NFL and VIM have a mean diameter of 2 nm (2.7 kDa) while nanoparticle size was around 65 nm. The effect of CPP on the plasma membrane (e.g. the production of pores already reported for antimicrobial peptides [51]) might only affect the penetration of small molecules. The same experiment was

performed also on CC-NSC and no significant effect was observed at any condition (data not shown).
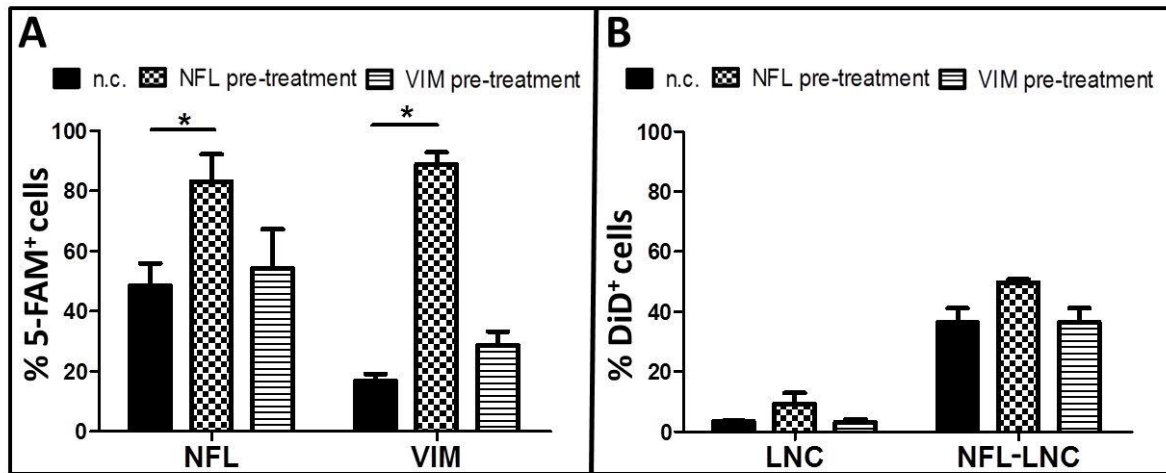

Figure 5: Effect of NFL pre-treatment on SVZ-NSC affinity for NFL and NFL-LNC. A: percentage of 5-FAM positive SVZ-NSC after 5-min incubation with NFL or VIM following pre-treatment with NFL or VIM ($p* < 0.05$, n=3). B: percentage of DiD positive SVZ-NSC after their incubation with LNC or NFL-LNC following pre-treatment with NFL or VIM.

To localize NFL-LNC after incubation with NSC, NSC treated with NFL-LNC were observed by confocal microscopy. No DiD signal was detected in SVZ-NSC neurospheres (Figure 6A) when they were incubated with LNC, while DiD was clearly visible when the incubation was performed with NFL-LNC. The same observations were made on adherent SVZ-NSC (Figure 6B). Both floating and adherent NSC cultures were tested to evaluate the influence of the spatial organization of the cells on the interaction with NFL-LNC. No significant difference was observed between the three-dimensional (floating) and the bi-dimensional (adherent) organisation of SVZ-NSC. Moreover, culture of adherent NSC is an *in vitro* model widely used that can be employed to assess the potential of bioactive molecule-loaded NFL-LNC on NSC differentiation. NFL-LNC can be seen around NSC (Figure 6C) and in the cells (Figure 6D). It is crucial to know where the NFL-LNCs are localized in the cells to choose appropriate active biomolecules for the design of future NFL-LNC-based therapeutic systems. As observed by FACS, no NFL-LNCs were associated with CC-NSC (Supplementary data 4).
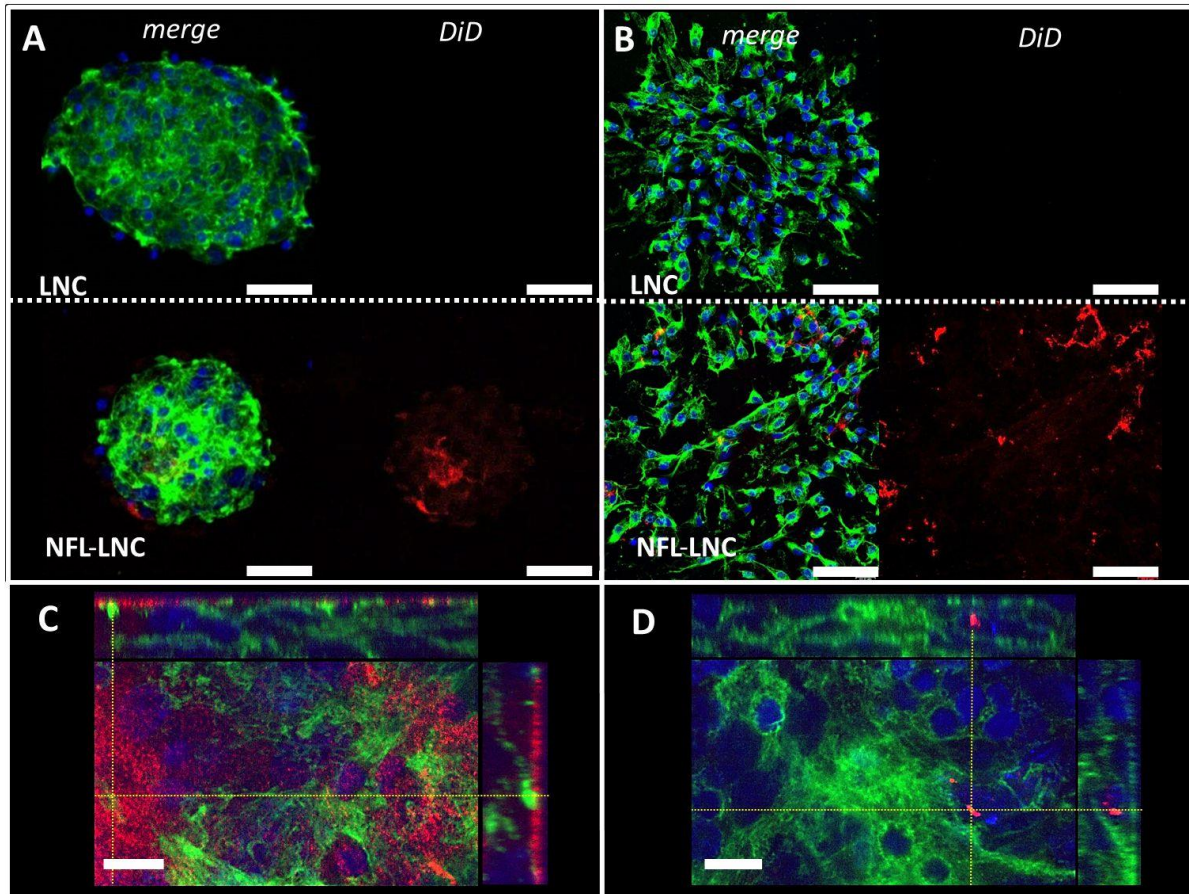
Figure 6: Visualization of interactions between NFL-LNC and SVZ-NSC. A: SVZ-NSC neurospheres were incubated 1 h with LNC and with NFL-LNC (blue is DAPI, cell nucleus; green is Rh-Ph, F-actin, cytoskeleton; red is DiD, LNC). Barr = 50 µm. B: SVZ-NSC adherent cells were incubated 1 h with LNC and NFL-LNC (blue is DAPI, cell nucleus; green is alpha-tubulin, cytoskeleton; red is DiD, LNC). Scale Bar = 50 µm for A and B. C and D: Orthogonal sections of SVZ-NSC neurospheres incubated 1 h with NFL-LNC (blue is DAPI, cell nucleus; green is Rh-Ph, F-actin, cytoskeleton; red is DiD, LNC). C: NFL-LNC localization on SVZ NSC surface. D: NFL-LNC localization into SVZ-NSC cytoplasm. Scale Bar = 10 µm for C-D.

5.4 In vivo targeting of SVZ-NSC by NFL-LNC

We demonstrated that NFL-LNC targeted SVZ-NSC *in vitro* but this result had to be confirmed *in vivo*. Thus, we injected LNC and NFL-LNC in rat brain right ventricle (Figure 7). One and 6 h post-injection, brains were retrieved and LNC and NFL-LNC localization was analysed by confocal microscopy. In our work we used different markers (GFAP, vimentin and nestin) to identify cellular components of the SVZ (astrocytes, ependymal cells and NSC, respectively). According to the cell architecture of the SVZ [54], cells expressing nestin correspond to a subpopulation of astrocytes (type B1), which reside adjacent to the ependymal cells (type E). In rodents, type B1 cells proliferate and give rise to progenitor cells (type C),

which in turn generate neuroblasts (type A) that afterwards differentiate into neurons [55]. For that reason they are considered *bona fide* NSC.

LNCs were still visible in the ventricle 1 h post-injection only when LNC were decorated with NFL (Figure 7B). The preferential localization of NFL-LNC on nestin positive cells was also visible 6 h after the injection (Figure 7C). NFL-LNCs were co-localized with nestin-positive cells (NSC) but not with GFAP- or vimentin-positive cells (astrocytes and ependymal cells, respectively) (Figure 7D). These observations confirmed the specificity of NFL-LNC interactions with SVZ-NSC observed *in vitro*. The initial accumulation of NFL-LNC in the ventricle, as observed 1 h post-injection (Figure 7B), might be due to a spatial obstruction in the ventricle resulted from the first interactions nanoparticles-cells. Over time, cerebrospinal fluid flow probably washed away unbound NFL-LNC. Thus, only NFL-LNC that interacted with SVZ-NSCs were visible (Figure 7C). NFL-LNCs were not observed in the left ventricle 6 h after their injection in the brain (Supplementary data 5). NFL-LNCs were not able to diffuse in the ventricular cavity at the doses we tested. DiD signal was limited to the ependymal and sub-ependymal layer and no diffusion was observed in the parenchyma while opposite results were obtained testing DiD alone [38] suggesting the integrity of our system. *In vitro* results were also confirmed for CC-NSC: no NFL-LNCs were visible in the spinal cord (Supplementary data 6).

In situ NSC differentiation stimulated by nanoparticle drug delivery systems is a relatively new strategy. One article described nanoparticle-driven NSC differentiation *in situ* [56] and only one study, to the best of our knowledge, reported nanoparticles targeting endogenous NSC [57]. Titanium dioxide nanoparticles decorated with Nilo1 (monoclonal antibody specifically targeting NSC) successfully targeted NSC *in vitro* but no further information was available regarding *in vivo* targeting. In this work we demonstrated for the first time according to our knowledge that NFL-LNC are able to target SVZ-NSC *in vitro* and *in vivo*.

The objective of this work was to demonstrate in vivo the specific affinity of NFL-LNC towards SVZ-NSC. In that perspective, nanoparticles were administered by intracranial injection. Nevertheless, for an easier translation to clinical applications, less invasive routes of administration, e.g. nasal [58], should be explored. NFL-LNC biodistribution and crossing of the blood-brain barrier were not investigated. But we believe that mucosal delivery might be more promising than systemic administration for LNC delivery into the brain. Thus, NFL-LNC represents a versatile drug delivery system able to carry a wide range of therapeutics

(hydrophilic, lipophilic and amphiphilic) in one of the most neurogenic region of the organism, the SVZ. NFL-LNC could be a useful tool in the development of SVZ-NSC-based therapeutic approaches for the treatment of several neurodegenerative diseases.
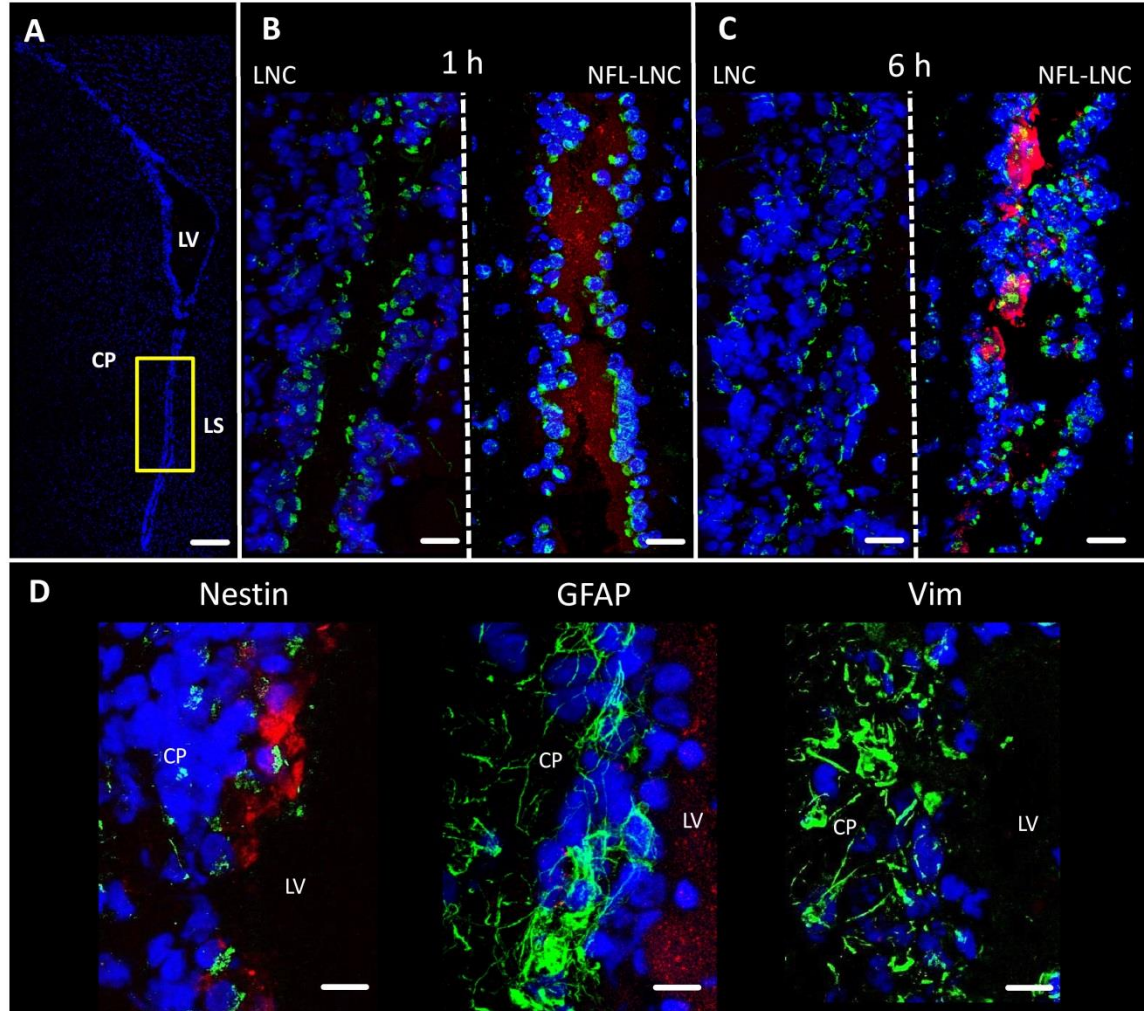

Figure 7: *In vivo* targeting of SVZ-NSC by NFL-LNC. A: right lateral ventricle (blue is DAPI, cell nucleus). Scale Bar = 200 μm. B e C: section of the right lateral ventricle 1 h (B) or 6 h (C) after LNC or NFL-LNC injection. (blue is DAPI, cell nucleus; green is Alexa 488, nestin, *bona fide* NSC; red is DiD, LNC). Scale Bar = 20 μm. D: co-localisation of NFL-LNC with different cell populations present in the right lateral ventricle 6 h after NFL-LNC injection (blue is DAPI, nucleus; green is Alexa 488, nestin/GFAP/vimentin; red is DiD, LNC). The pictures were taken in different areas of the SVZ. Scale Bar = 10 μm. CP, caudoputamen; LV, lateral ventricle; LS, lateral septal nucleus.

6. CONCLUSION

We developed a drug delivery system that selectively targets endogenous SVZ NSC *in vitro* and *in vivo*. NFL was selected among several cell-penetrating peptides. NFL interacted with LNC by electrostatic interactions and entered NSC *via* an energy-independent mechanism. A

sustained interaction of NFL-LNC with the NSC of the SVZ was observed. For therapeutic applications this system can be loaded with active biomolecules that could induce *in situ* differentiation of endogenous NSC. NFL-LNC is thus a promising drug delivery system for stem cell-based therapy for the treatment of neurodegenerative diseases.

ACKNOWLEDGMENTS

7. REFERENCES

[1] Shenghui, H. E., Nakada, D., & Morrison, S. J. (2009). Mechanisms of stem cell self-renewal. *Annual Review of Cell and Developmental*, 25, 377-406.

[2] Wagers, A. J., & Weissman, I. L. (2004). Plasticity of adult stem cells. *Cell*, 116(5), 639-648.

[3] Bissels, U., Eckardt, D., & Bosio, A. (2013). Characterization and classification of stem cells, in: G Steinhoff (Ed), *Regenerative Medicine: From Protocol to Patient,* Springer Netherlands, Dordrecht, 155-176

[4] Mariano, E. D., Teixeira, M. J., Marie, S. K. N., & Lepski, G. (2015). Adult stem cells in neural repair: Current options, limitations and perspectives. *World journal of stem cells*, 7(2), 477.

[5] Morrison, S. J., & Spradling, A. C. (2008). Stem cells and niches: mechanisms that promote stem cell maintenance throughout life. *Cell*, 132(4), 598-611.

[6] Gage, F. H. (2000). Mammalian neural stem cells. *Science*, 287(5457), 1433-1438.

[7] Fuentealba, L. C., Obernier, K., & Alvarez-Buylla, A. (2012). Adult neural stem cells bridge their niche. *Cell stem cell*, 10(6), 698-708.

[8] Sabelström, H., Stenudd, M., & Frisén, J. (2014). Neural stem cells in the adult spinal cord. *Experimental neurology*, 260, 44-49.

[9] Bond, A. M., Ming, G. L., & Song, H. (2015). Adult mammalian neural stem cells and neurogenesis: five decades later. *Cell stem cell*, 17(4), 385-395.

[10] Gil-Perotín, S., Duran-Moreno, M., Cebrián-Silla, A., Ramírez, M., García-Belda, P., & García-Verdugo, J. M. (2013). Adult neural stem cells from the subventricular zone: a review of the neurosphere assay. *The Anatomical Record*, 296(9), 1435-1452.

[11] Hinsch, K., & Zupanc, G. K. (2006). Isolation, cultivation, and differentiation of neural stem cells from adult fish brain. *Journal of neuroscience methods*, 158(1), 75-88.

[12] Bond, A. M., Ming, G. L., & Song, H. (2015). Adult mammalian neural stem cells and neurogenesis: five decades later. *Cell stem cell*, 17(4), 385-395.

[13] Suksuphew, S., & Noisa, P. (2015). Neural stem cells could serve as a therapeutic material for age-related neurodegenerative diseases. *World journal of stem cells*, 7(2), 502.

[14] Mendonça, L. S., Nóbrega, C., Hirai, H., Kaspar, B. K., & de Almeida, L. P. (2015). Transplantation of cerebellar neural stem cells improves motor coordination and neuropathology in Machado-Joseph disease mice. *Brain*, 138(2), 320-335.

[15] Iwai, H., Shimada, H., Nishimura, S., Kobayashi, Y., Itakura, G., Hori, K., et al. (2015). Allogeneic Neural Stem/Progenitor Cells Derived From Embryonic Stem Cells Promote Functional Recovery After Transplantation Into Injured Spinal Cord of Nonhuman Primates. *Stem cells translational medicine*, sctm-2014.

[16] Zhang, W., Gu, G. J., Shen, X., Zhang, Q., Wang, G. M., & Wang, P. J. (2015). Neural stem cell transplantation enhances mitochondrial biogenesis in a transgenic mouse model of Alzheimer's disease–like pathology. *Neurobiology of aging*, 36(3), 1282-1292.

[17] Lindvall, O. (2015). Treatment of Parkinson's disease using cell transplantation. *Philosophical Transactions of the Royal Society B,* 370(1680), 20140370.

[18] Kim, J. A., Ha, S., Shin, K. Y., Kim, S., Lee, K. J., Chong, Y. H. et al. (2015). Neural stem cell transplantation at critical period improves learning and memory through restoring synaptic impairment in Alzheimer's disease mouse model. *Cell death & disease*, 6(6), e1789

[19] Herberts, C. A., Kwa, M. S., & Hermsen, H. P. (2011). Risk factors in the development of stem cell therapy. *Journal of Translational Medicine*, 9(1), 29.

[20] Lo, B., & Parham, L. (2013, July). Ethical issues in stem cell research. Endocrine Society.

[21] Rochette-Egly, C. (2015). Retinoic acid signaling and mouse embryonic stem cell differentiation: Cross talk between genomic and non-genomic effects of RA. *Biochimica et Biophysica Acta (BBA)-Molecular and Cell Biology of Lipids*, 1851(1), 66-75.

[22] Chambers, S. M., Mica, Y., Lee, G., Studer, L., & Tomishima, M. J. (2016). Dual-SMAD inhibition/WNT activation-based methods to induce neural crest and derivatives from human pluripotent stem cells. *Human Embryonic Stem Cell Protocols*, 329-343.

[23] Bocquet A, Berges R, Frank R, Robert P, Peterson AC, and Eyer J. Neurofilaments bind tubulin and modulate its polymerization. *Journal of Neuroscience* 2009; 29:11043-11054.

[24] Lépinoux-Chambaud C, Barreau K, Eyer J. The neurofilament-derived peptide NFL-TBS.40-63 targets neural stem cells and affects their properties. *Stem Cells Transl Med.* 2016 May 13. pii: sctm.2015-0221.

[25] Berges, R., Balzeau, J., Peterson, A. C., & Eyer, J. (2012). A tubulin binding peptide targets glioma cells disrupting their microtubules, blocking migration, and inducing apoptosis. *Molecular Therapy*, 20(7), 1367-1377.

[26] Lépinoux-Chambaud, C., & Eyer, J. (2013). The NFL-TBS. 40-63 anti-glioblastoma peptide enters selectively in glioma cells by endocytosis. *International journal of pharmaceutics*, 454(2), 738-747.

[27] Balzeau, J., Pinier, M., Berges, R., Saulnier, P., Benoit, J. P., & Eyer, J. (2013). The effect of functionalizing lipid nanocapsules with NFL-TBS. 40-63 peptide on their uptake by glioblastoma cells. *Biomaterials*, 34(13), 3381-3389.

[28] Rivalin, R., Lepinoux-Chambaud, C., Eyer, J., & Savagner, F. (2014). The NFL-TBS. 40-63 anti-glioblastoma peptide disrupts microtubule and mitochondrial networks in the T98G glioma cell line. *PloS ONE*, 9(6), e98473.

[29] Fressinaud, C., & Eyer, J. (2015). Neurofilaments and NFL-TBS. 40–63 peptide penetrate oligodendrocytes through clathrin-dependent endocytosis to promote their growth and survival in vitro. *Neuroscience*, 298, 42-51.

[30] Fressinaud, C., & Eyer, J. (2014). Neurofilament-tubulin binding site peptide NFL-TBS. 40–63 increases the differentiation of oligodendrocytes in vitro and partially prevents them from lysophosphatidyl choline toxiciy. *Journal of neuroscience research*, 92(2), 243-253.

[31] Berges, R., Balzeau, J., Takahashi, M., Prevost, C., & Eyer, J. (2012). Structure-function analysis of the glioma targeting NFL-TBS. 40-63 peptide corresponding to the tubulin-binding site on the light neurofilament subunit. *PLoS ONE* 7(11): e49436. doi:10.1371/journal.pone.0049436

[32] Heurtault B, Saulnier P, Pech B, Proust JE, Richard J, & Benoit JP. Lipidic nanocapsules: preparation process and use as Drug Delivery Systems. Patent No. WO02688000.

[33] Minkov, I., Ivanova, T., Panaiotov, I., Proust, J., & Saulnier, P. (2005). Reorganization of lipid nanocapsules at air–water interface: Part 2. *Properties of the formed surface film. Colloids and Surfaces B: Biointerfaces*, 44(4), 197-203.

[34] Shinoda, K., & Saito, H. (1969). The stability of O/W type emulsions as functions of temperature and the HLB of emulsifiers: the emulsification by PIT-method. *Journal of Colloid and Interface Science*, 30(2), 258-263.

[35] Huynh NT, Passirani C, Saulnier P, and Benoit JP. Lipid nanocapsules: A new platform for nanomedicine. *International Journal of Pharmaceutics* 2009; 379: 201-209.

[36] Anton, N., Saulnier, P., Gaillard, C., Porcher, E., Vrignaud, S., & Benoit, J. P. (2009). Aqueous-core lipid nanocapsules for encapsulating fragile hydrophilic and/or lipophilic molecules. *Langmuir*, 25(19), 11413-11419.

[37] Bastiat, G., Pritz, C. O., Roider, C., Fouchet, F., Lignières, E., Jesacher, A. et al. (2013). A new tool to ensure the fluorescent dye labeling stability of nanocarriers: a real challenge for fluorescence imaging. *Journal of Controlled Release*, 170(3), 334-342.

[38] Carradori, D., Barreau, K., & Eyer, J. (2016). The carbocyanine dye DiD labels in vitro and in vivo neural stem cells of the subventricular zone as well as myelinated structures following in vivo injection in the lateral ventricle. *Journal of neuroscience research*, 94(2), 139-148.

[39] Ramsey, J. D., & Flynn, N. H. (2015). Cell-penetrating peptides transport therapeutics into cells. *Pharmacology & therapeutics*, 154, 78-86.

[40] Farkhani, S. M., Valizadeh, A., Karami, H., Mohammadi, S., Sohrabi, N., & Badrzadeh, F. (2014). Cell penetrating peptides: efficient vectors for delivery of nanoparticles, nanocarriers, therapeutic and diagnostic molecules. *Peptides*, 57, 78-94.

[41] Lee, D., Pacheco, S., & Liu, M. (2014). Biological effects of Tat cell-penetrating peptide: a multifunctional Trojan horse?. Nanomedicine, 9(1), 5-7.

[42] Balzeau, J., Peterson, A., & Eyer, J. (2012). The vimentin-tubulin binding site peptide (Vim-TBS. 58-81) crosses the plasma membrane and enters the nuclei of human glioma cells. *International journal of pharmaceutics*, 423(1), 77-83.

[43] Guo, W., Patzlaff, N. E., Jobe, E. M., & Zhao, X. (2012). Isolation of multipotent neural stem or progenitor cells from both the dentate gyrus and subventricular zone of a single adult mouse. *Nature protocols*, 7(11), 2005-2012.

[44] Hugnot, J. P. (2013). Isolate and culture neural stem cells from the mouse adult spinal cord. *In Neural Progenitor Cells* (pp. 53-63). Humana Press.

[45] Rizzuti, M., Nizzardo, M., Zanetta, C., Ramirez, A., & Corti, S. (2015). Therapeutic applications of the cell-penetrating HIV-1 Tat peptide. *Drug discovery today*, 20(1), 76-85.

[46] Saini, A., R. Jaswal, R., Negi, R., & S. Nandel, F. (2013). Insights on the structural characteristics of Vim-TBS (58-81) peptide for future applications as a cell penetrating peptide. *Bioscience trends*, 7(5), 209-220.

[47] Synthetic aCSF was prepared according to Hájos, N., & Mody, I. (2009). Establishing a physiological environment for visualized in vitro brain slice recordings by increasing oxygen supply and modifying aCSF content. *Journal of neuroscience methods*, 183(2), 107-113.

[48] Sperling, R. A., & Parak, W. J. (2010). Surface modification, functionalization and bioconjugation of colloidal inorganic nanoparticles. *Philosophical Transactions of the Royal Society of London A: Mathematical, Physical and Engineering Sciences*, 368(1915), 1333-1383.

[49] Langelier, B., Linard, A., Bordat, C., Lavialle, M., & Heberden, C. (2010). Long chain-polyunsaturated fatty acids modulate membrane phospholipid composition and protein localization in lipid rafts of neural stem cell cultures. *Journal of cellular biochemistry*, 110(6), 1356-1364.

[50] Hirsjärvi, S., Belloche, C., Hindré, F., Garcion, E., & Benoit, J. P. (2014). Tumour targeting of lipid nanocapsules grafted with cRGD peptides. *European Journal of Pharmaceutics and Biopharmaceutics*, 87(1), 152-159.

[51] Clavreul, A., Montagu, A., Lainé, A. L., Tétaud, C., Lautram, N., Franconi, F. et al. (2015). Targeting and treatment of glioblastomas with human mesenchymal stem cells carrying ferrociphenol lipid nanocapsules. *International journal of nanomedicine*, 10, 1259.

[52] Kou, L., Sun, J., Zhai, Y., & He, Z. (2013). The endocytosis and intracellular fate of nanomedicines: Implication for rational design. *Asian Journal of Pharmaceutical Sciences*, 8(1), 1-10.

[53] Fujimoto, T., Kogo, H., Nomura, R., & Une, T. (2000). Isoforms of caveolin-1 and caveolar structure. *Journal of Cell Science*, 113(19), 3509-3517.

[54] Capilla-Gonzalez, V., Cebrian-Silla, A., Guerrero-Cazares, H., Garcia-Verdugo, J. M., & Quiñones-Hinojosa, A. (2014). Age-related changes in astrocytic and ependymal cells of the subventricular zone. Glia, 62(5), 790-803.

[55] Garcıa-Verdugo, J. M., Doetsch, F., Wichterle, H., Lim, D. A., & Alvarez-Buylla, A. (1998). Architecture and cell types of the adult subventricular zone: in search of the stem cells. *J. Neurobiol*, 36, 234-248.

[56] Santos, T., Ferreira, R., Maia, J., Agasse, F., Xapelli, S., Cortes, L. et al. (2012). Polymeric nanoparticles to control the differentiation of neural stem cells in the subventricular zone of the brain. *ACS nano*, 6(12), 10463-10474.

[57] Elvira, G., Moreno, B., del Valle, I., Garcia–Sanz, J. A., Canillas, M., Chinarro, E. et al. (2011). Targeting neural stem cells with titanium dioxide nanoparticles coupled to specific monoclonal antibodies. *Journal of biomaterials applications*, 0885328210393294.

[58] Gartziandia, O., Egusquiaguirre, S. P., Bianco, J., Pedraz, J. L., Igartua, M., Hernandez, R. M., et al. (2016). Nanoparticle transport across in vitro olfactory cell monolayers. *International journal of pharmaceutics*, 499(1), 81-89.
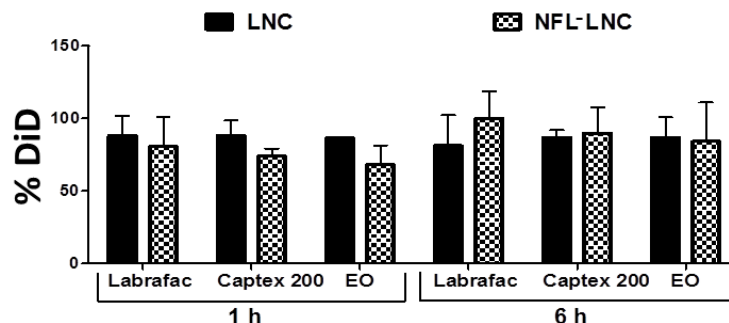
8. SUPPLEMENTARY DATA

Supplementary data 1: Qualitative analysis of NSC cultures. SVZ-NSC and CC-NSC (2900 neurospheres/ml corresponding to $4*10^5$cells/ml) were fixed in PFA 4 % and incubated 30 min in Triton 0.05 %. NSC were treated 1 h in BSA 1 % and subsequently NSC were incubated 2 hours with anti-nestin primary antibody (1/50 in BSA 1 %) and 2 hours with Alexa fluor 488 secondary antibody (1/200 in BSA 1 %). BD FACSverse™ flow cytometer was used to measure the % of Alexa fluor 488$^+$ NSC.
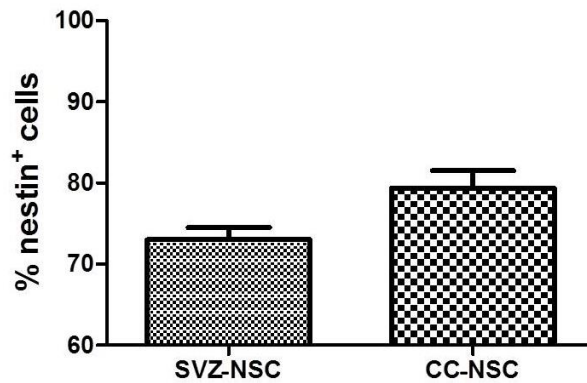
Supplementary data 1: Percentage of NSC in primary NSC cultures. SVZ-NSC and CC-NSC positive to nestin.

Supplementary Data 2: DiD-labelling stability. The stability of the labelling was evaluated following the protocol developed by Bastiat et al. [37]. Briefly, 1 ml of NFL-LNC suspension was mixed with 1 ml of a lipidic solution (Labrafac® WL 1349, Captex® 200 or ethyl oleate). The mixture was incubated 6 h and centrifuged (4800 g, 30 min) until the separation of the phases was obtained. DiD fluorescence intensity was measured in the nanoparticle solution at 644/665 nm by Spectramax M2 (Molecular Devices).


Supplementary data 2: Stability of DiD-labeling of LNC. Fluorescence intensity of LNC and NFL-LNC was measured at 644/665 nm before and after incubation in lipidic solutions (Labrafac®, Captex 200® or EO).

*Supplementary Data 3: NFL-LNC physicochemical property stability at different conditions.* The size, z-potential and PDI of NFL-LNC were measured over the time at 4 °C, at room temperature (not diluted), in cell culture media, and in artificial cerebrospinal fluid (aCSF) at 37 °C (diluted 1/100).
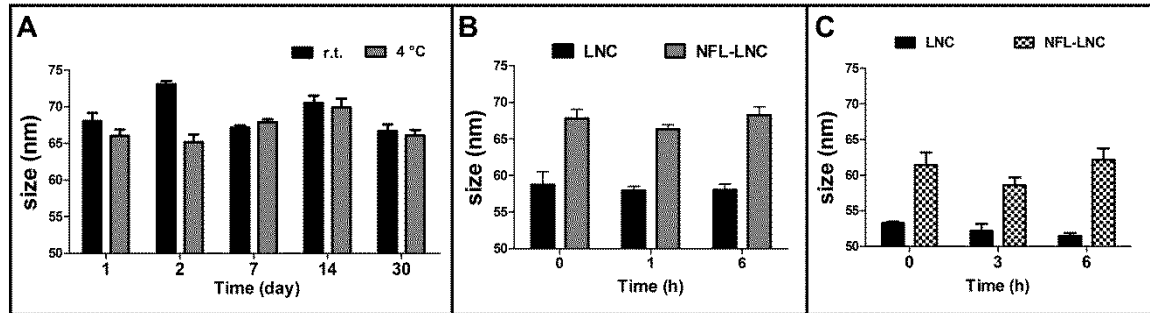
Supplementary data 3: NFL-LNC stability at different conditions. A: NFL-LNC stability over time. The size was measured after incubation at 4 °C or room temperature over time (p* < 0.05 compared to day 1, n=3). B: Stability of NFL-LNC in cell culture medium. Size of LNC and NFL-LNC were measured over time after dilution in cell culture medium (1/100) at 37 °C. C: Stability of NFL-LNC in aCSF. Size of LNC and NFL-LNC were measured over time after dilution in cell aCSF (1/100) at 37 °C.
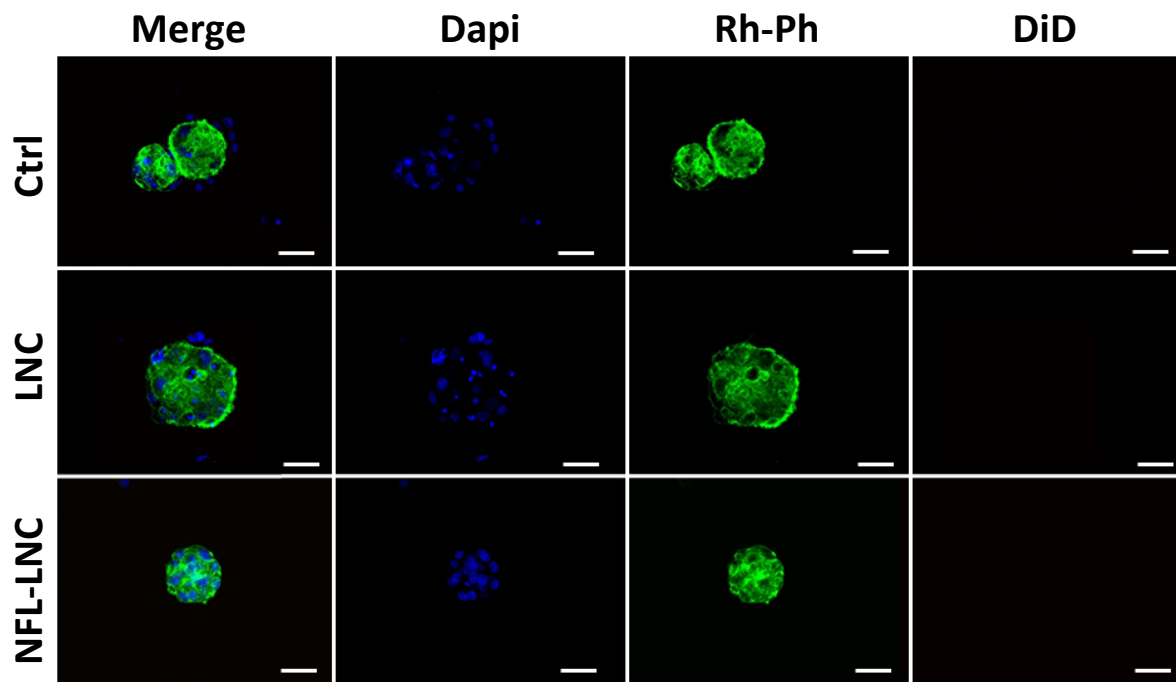
Supplementary data 4: **Interactions between NFL-LNC and CC-NSC by confocal imaging.** CC-NSC neurospheres incubated 1 h with LNC and with NFL-LNC (blue is DAPI, cell nucleus; green is Rh-Ph, F-actin, cytoskeleton; red is DiD, LNC). Scale bar = 50 µm.
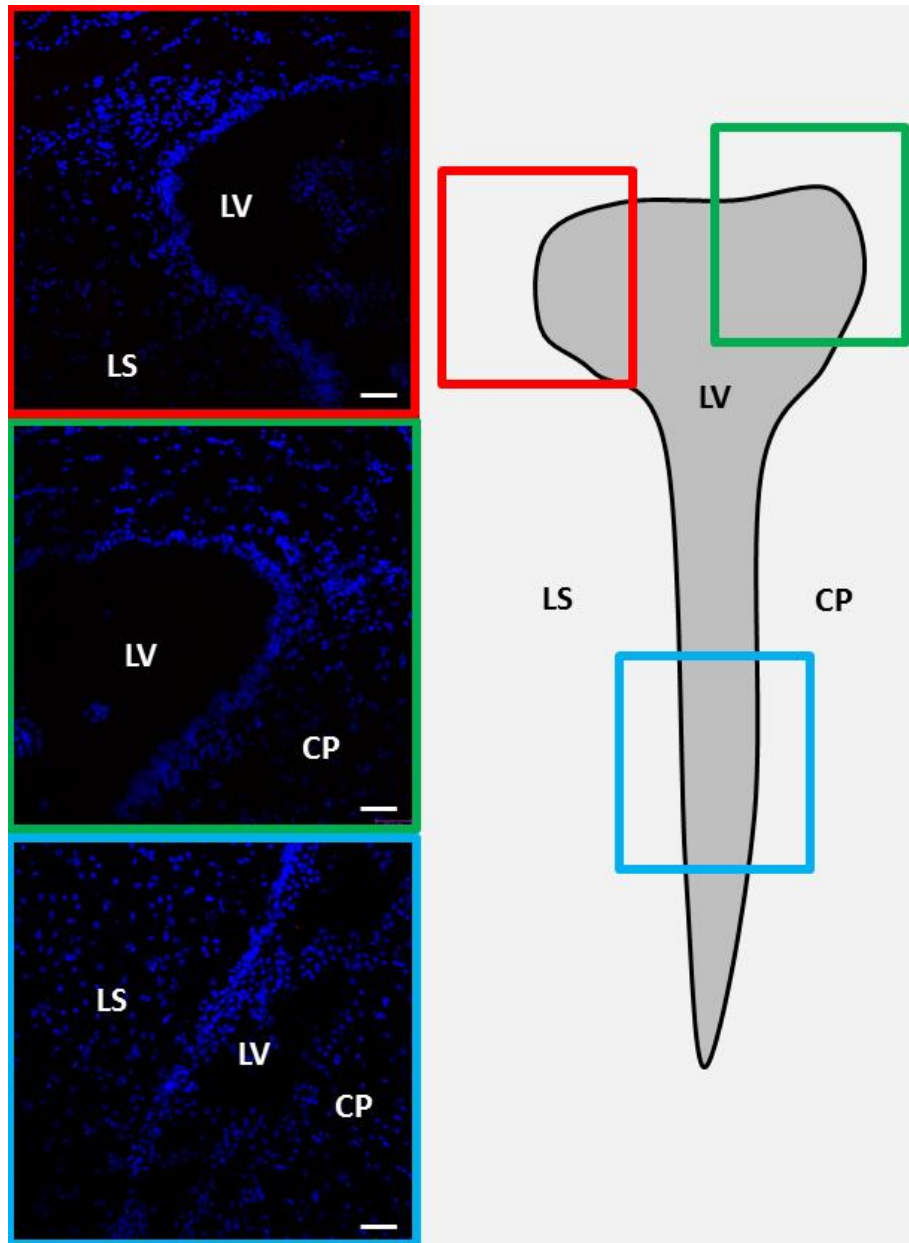
Supplementary data 5: Sections of the left lateral ventricle. Section of the left lateral ventricle 6 h after the injection of NFL-LNC in the right lateral ventricle (blue is DAPI, cell nucleus; red is DiD, LNC). Scale bar = 50 μm. LV, lateral ventricle; CP, caudoputament; LS, lateral septal nucleus.
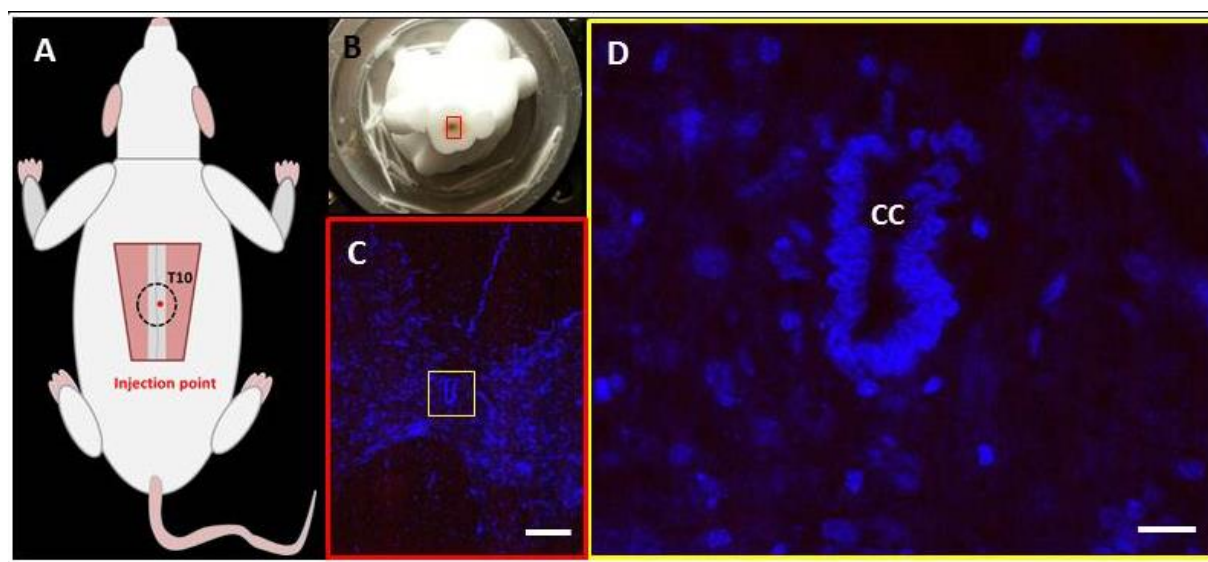
Supplementary data 6: Spinal cord central canal 1 hour after NFL-LNC injection. A: site of the injection performed with Harvard Apparatus. B: coronal sections of the spinal cord. C: central canal of the spinal cord 1 h after NFL-LNC injection (blue is DAPI, cell nucleus). Scale bar = 200 μm. D: high magnification of the central canal (CC) of the spinal 1 h after NFL-LNC injection (blue is DAPI, cell nucleus; red is DiD, LNC). Scale bar = 50 μm.

Supplementary Data 7: composition of LNC. LNC are classically composed of 3 principal components: the oily phase (Labrafac®), the aqueous phase (distilled water) and the nonionic surfactant (Solutol® HS). Labrafac® is composed of triglycerides of capric and caprylic acids. Solutol® HS is a mixture of free PEG 660 and PEG 660 hydroxystearate. The aqueous phase consists of distilled water plus NaCl. In this study, another surfactant, Lipoid®, composed of 69% phosphatidylcholine soya bean lecithin, is used in small proportions. Each component has different roles on LNC formulation (see Table s1).

Table s1. Role of the compounds in the formulation of LNCs.

Compounds	Effects
Solutol®	Major influence on LNC formation and stability
Labrafac®	Increase of LNC size
NaCl	Decrease of phase-inversion temperature
Lipoid®	Stabilizing the LNC rigid shell and slight decrease of the z-potential

Supplementary Data 8: peptide properties.

Table s2. NFL, SCR NFL, VIM, and TAT properties

Peptide	Sequence	Molecular weight	Iso-electric point	Net charge at pH 7
NFL	YSSYSAPVSSSLSVRRSYSSSSGS	2488.58 g/mo	9.87 pH	+2
SCR NFL	SLGSPSSSVRASYSSSRSYVYSSS	2488.58 g/mo	9.87 pH	+2
VIM	GGAYVT RSSAVRLRSSVPGVRLLQ	2529.9 g/mol	12.11 pH	+4
TAT	GRKKRRQRRRPPG	1647.94 g/mol	12.81 pH	+8

CHAPTER 3

THE CHARACTERISTICS OF NEURAL STEM CELL PLASMA MEMBRANE AFFECT THEIR INTERACTION WITH NFL-LIPID NANOCAPSULES *

TABLE OF CONTENTS

1. PREFACE

In our previous work (Chapter 2), we produced a neural stem cell (NSC)-targeting drug delivery system by adsorbing the peptide NFL-TBS.40-63 (NFL) on the surface of lipid nanocapsules (LNCs). NFL-LNCs interact with NSCs of the subventricular zone (SVZ-NSCs) *in vitro* and *in vivo* while they do not interact with NSCs of the central canal (CC-NSCs). This result was surprising as no data were found in the literature that could explain this difference. To understand how the characteristics of each NSC type could impact so dramatically their interactions with NFL-LNC, we compared the plasma membrane of SVZ-NSCs and CC-NSCs.

Although many plasma membrane characteristics could play a crucial role in the interaction between compounds and cells (such as membrane protein, lateral/transversal asymmetry), passive internalization is mostly related to the lipidic composition and organisation of the cell membrane.

As NFL and NFL-LNC showed passive translocation and energetic-independent interactions with SVZ-NSCs respectively, our hypothesis was that the lipidic composition of the two types of NSCs was different and would thus modulate the interaction with NFL-LNC by impacting the fluidity and rigidity of their membrane.

The aim of this work was to characterize the plasma membrane of both type of cells and to identify the factor(s) modulating the selective interaction between NFL-LNC and SVZ-NSCs.

2. ABSTRACT

NFL-LNC is a drug delivery system penetrating NSCs of the subventricular zone (SVZ-NSCs) of the brain, *in vitro* and *in vivo*, but not NSCs of the central canal (CC-NSCs) of the spinal cord. The objective of the present work was to investigate the reason(s) of the selective interaction between NFL-LNCs and SVZ-NSCs, focusing on their lipid plasma membrane characterization. A significantly higher proportion of ceramides and a lower content in phosphatidylcholines were detected in SVZ-NSCs compared to CC-NSCs while no significant differences in the amount of phospholipids and cholesterol were observed. Lipid composition is known to influence plasma membrane characteristics modulating the interactions nanoparticle-cell. Consequently, we measured physical state and permeability (by generalized polarization of laurdan and permeability to fluorescent dextran respectively) and their variation after NSC incubation with NFL, LNCs and NFL-LNCs. The study showed a significantly different generalized polarization of laurdan between the two types of cells and a cell-dependent impact of LNCs on the physical state. While the steady state of the permeability between SVZ-NSCs and CC-NSCs was similar, SVZ-NSCs showed a significant increase of the permeability after incubation with NFL. We concluded that the different amount of phosphatidylcholines and ceramides detected in CC-NSCs and SVZ-NSCs could play a role in the interaction towards NFL-LNCs by impacting the physical state and the permeability of the plasma membranes.
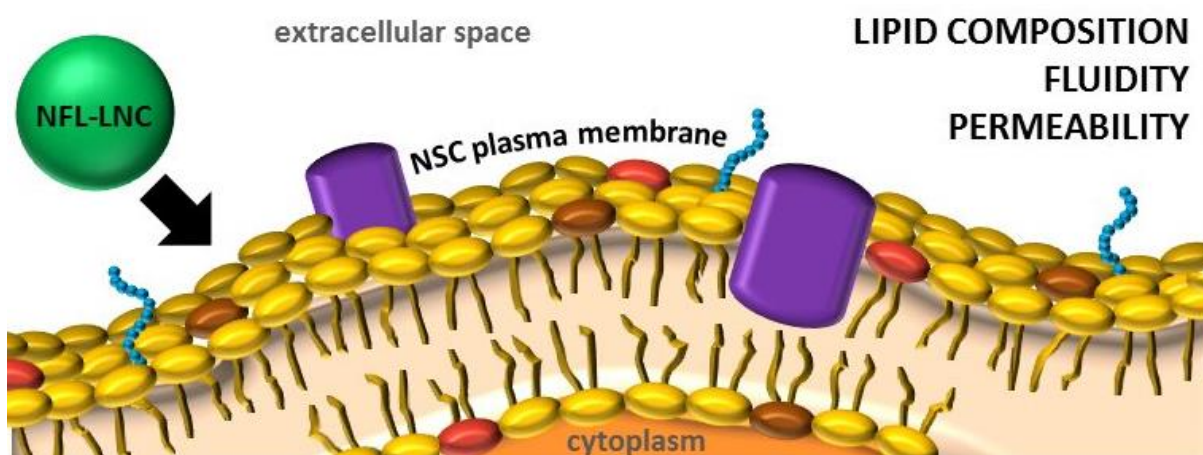
3. INTRODUCTION

Neural stem cells (NSCs) are located in restricted neurogenic areas of the central nervous system (CNS) such as the central canal (CC), in the spinal cord, and the subventricular zone (SVZ), in the brain. NSCs can undergo self-renewal and differentiate into specialized neural cells (astrocytes, oligodendrocytes and neurons) [1]. NSC differentiation plays a crucial role in the neurogenesis process during both the development and the maintenance of the mammalian CNS [2]. The therapeutic relevance of NSCs rose when many studies clearly demonstrated that the stimulation of the neurogenesis resulted in the partial recovery of injured neuronal networks [3] and in the enhancement of behavioral performances (e.g., learning and memory) [4]. Their impact on neurogenesis made NSCs an attractive tool for the treatment of CNS diseases characterized by progressive lesion/loss of neural tissue and deterioration of neurological functions [5]. Consequently, NSCs have been investigated to replace injured cells and to restore neurological functions. Different strategies have been developed which essentially depend on whether NSCs are exogenous (induced from other somatic cells or isolated from neurogenic niches) or endogenous (niche-localized) [6]. Exogenous NSC differentiation occurs after transplantation of *in vitro* expanded/stimulated cells while endogenous NSC differentiation occurs *in situ* after local stimulation. *In situ* differentiation of endogenous NSCs remains one of the most promising strategies for the treatment of neurodegenerative diseases since it avoids both the transplantation-associated issues (e.g., cell sources and cell viability) [7] and the procedural limitations derived from the *in vitro* manipulation of exogenous NSCs (e.g., the cultivation in restricted conditions or the risk of genetic modifications) [8]. Although many drugs and drug delivery systems have been tested in CNS disease animal models to induce *in situ* differentiation of endogenous NSCs [9,10], no treatment based on this strategy has reached the clinical phase yet [11]. The lack of NSC-targeting molecules mostly promoted non-selective systems that might present off-target associated side-effect or inefficiency.

Recently, the 24-aminoacid peptide NFL-TBS.40-63 (NFL), corresponding to the tubulin-binding site of the neurofilament light subunit [12], showed a strong interaction with NSCs of the SVZ (SVZ-NSCs) of the brain [13]. *In vitro*, NFL massively penetrated SVZ-NSCs by direct translocation and induced NSC differentiation while *in vivo,* it localized in SVZ-NSC niches after intra-lateral ventricle injection in rat brain. NFL was not detected in astrocytes and neurons and it showed no significant toxicity both *in vitro* and *in vivo*. NFL was also tested as anti-glioblastoma drug, alone [14,15] or in association with lipid nanocapsules [16].

Interestingly, the peptide showed a different mechanism of internalization in the glioblastoma cells compared to SVZ-NSCs. NFL was actively taken up and induced tumour growth inhibition *via* microtubule and mitochondrial network disruption [17] while no major toxicity was observed on healthy cells (rat astrocytes and neurons). NFL actively penetrates in oligodendrocytes by clathrin-dependent endocytosis and induces their differentiation *in vitro* [18]. The reason behind the selective interactions between NFL and these three types of cells (SVZ-NSCs, glioblastoma cells and oligodendrocytes) or the different mechanisms of penetration (passive for SVZ-NSCs and active for glioblastoma and oligodendrocytes) is not well understood yet.

NFL can be associated to cell-penetrating peptides due to the positive charge, low molecular weight and balance between endocytosis and direct translocation in cell penetration mechanisms [19]. Physicochemical analysis performed by alanine-scanning assay and circular dichroism indicated a strong structure-activity correlation and a dependency to the environmental conditions of the ratio alpha helix/beta sheet, respectively [20]. Although NFL massively penetrates SVZ-NSCs, it did not show yet an identified therapeutic effect *in vivo* on these cells. Moreover, the strong structure-activity correlation limits chemical coupling between NFL and bioactive molecules. A direct therapeutic application of the peptide is still not excluded but its association with a drug delivery system represents a potential strategy for the selective delivery of bioactive molecules to NSCs.

Lipid nanocapsules (LNCs) are a versatile drug delivery system due to their long stability (more than 18 months), ability to deliver both lipophilic and hydrophilic drugs, and biocompatibility [21]. They are produced by a solvent-free method, called phase-inversion temperature method, and they have a lipid core of caprylic/capric triglycerides (Labrafac®) and a shell of lecithin (Lipoid®) and PEG_{600}/PEG stearate derivatives (Kolliphor®).

In our previous work [22], we adsorbed the peptide NFL on LNC surface producing a drug delivery system, NFL-LNC, able to target SVZ-NSCs *in vitro* and *in vivo*. Interestingly, NFL-LNCs did not interact with NSCs from the central canal (CC-NSCs) of the spinal cord. *In vitro*, the analysis of the association between NFL/LNCs/NFL-LNCs and SVZ-NSCs/CC-NSCs highlighted significant differences in the kinetic and in the mechanism of interaction. NFL interacted faster with SVZ-NSCs (5 min, 43% cells) than with CC-NSCs (5 min, < 5% cells) but from 20 min to 1 h the values were similar for both types of cells (from 54% to 80%). LNCs were not detected in significant amounts whatever the cell type and incubation

time while NFL-LNCs interacted only with SVZ-NSCs, following the same kinetic than NFL alone. The mechanistic study of the association process showed that the interactions of NFL and NFL-LNCs with SVZ-NSCs did not shown any significant variation when incubated at 37 °C, 4 °C or in ATP depletion while NFL interaction with CC-NSCs significantly decreased at 4 °C exclusively. Moreover, pre-incubations with NFL increased the penetration of the peptide itself in SVZ-NSCs but not in CC-NSCs.

These results highlight the differences between SVZ-NSC and CC-NSC interactions with NFL and NFL-LNCs. We hypothesized that they could be related to different plasma membrane characteristics. Unfortunately, it was not possible to find information in the literature to support this hypothesis. Up to now, only the lipids and the proteins of brain NSCs have been characterized but no distinction was made between SVZ-NSCs and the other brain NSCs (e.g., from the subgranular zone) [23].

Thus, the objective of this work was to characterize and compare the plasma membranes of SVZ-NSCs and CC-NSCs to identify the possible factor(s) modulating the interactions with NFL-LNCs.

4. MATERIALS AND METHODS

4.1 Materials

Biotinylated NFL-TBS.40-63 (NFL) was purchased from GeneCust (Luxembourg, Luxembourg). Labrafac® was purchased from Gattefosse SA (Saint-Priest, France). Lipoïd® was purchased from Lipoid Gmbh (Ludwigshafen, Germany). Kolliphor HS® was purchased from Sigma (Saint-Louis, Missouri, USA). Sodium chloride (NaCl) was purchased from Prolabo (Fontenay-sous-bois, France). Egg sphingomyelin (eSM), *1*-palmitoyl-*2*-oleoyl-sn-glycero-*3*-phosphocholine (POPC), and cholesterol (Chol) were purchased from Avanti Polar Lipids (Birmingham, Alabama, USA). *6*-dodecanoyl-*2*-dimethyl-aminonaphthalene (Laurdan) was purchased from Molecular Probes (Carlsbad, California, USA). 3137-0050 oak ridge tubes were purchased from Thermo Fisher Scientific (Waltham, Massachusetts, USA). DAPI, HEPES, Pen/Strept, Na Pyruvate, B27, MEM alpha (no nucleosides), 0.05 % Trypsin-EDTA (1x), DNAse and ProLong Gold antifade were purchased from Thermo Fisher Scientific (Waltham, Massachusetts, USA). Fluorescein isothiocyanate–dextran 4 kDa (FD4), 10KDa (FD10) and 40 kDa (FD40) were purchased from Sigma (Saint-Louis, Missouri, USA). EGF

and bFGF were purchased from Tebu-Bio (Le Perray en Yvelines, France). BD CellTak was purchased from Corning Inc (New York, New York, USA). BCA Uptima was purchased from Interchim (Montluçon, France). CellTiter 96® AQueous One Solution Cell Proliferation Assay was purchased from Promega (Fitchburg, Wisconsin, USA). Amicon Ultra-0.5 ml 100K filters were purchased from Merck Millipore (Billerica, Massachusetts, USA). The isolation of NSCs were performed according to Directive 2010/63/EU, to guidelines of the French and Belgian Government following the approval by the ethical committee for animal care of the faculty of medicine of the University catholique de Louvain.

4.2 Preparation of lipidic nanocapsules

LNC-stock was prepared according to the protocol developed by Heurtault et al. [24]. Briefly, 0.846 g Kolliphor HS®, 0.075 g Lipoïd®, 0.089 g NaCl, 1.028 g Labrafac® and 2.962 ml of water were mixed under magnetic stirring for 5 min at 40°C. Temperature cycles (a minimum of 3) of progressive heating/cooling were done between 60°C and 90°C. During the cooling of the last cycle, 12.5 ml of water (4°C) were added at 74°C under high speed stirring. The nanoparticles were filtered on 0.2 μm filter and stored at 4°C. NFL-LNCs were produced by incubating 369 μl of 1 mM NFL solution (in water) overnight with 1 ml of stock-LNC under gently stirring. LNCs without peptide (control) were produced by incubating 369 μl of water overnight with 1 ml of LNC-stock solution under gently stirring.

4.3 Preparation of liposomes

Liposomes were made according to the protocol described by Hope et al. [25]. The amount of lipids and Laurdan required to reach a final concentration of 10 mM and 0.01 mM, respectively, was dissolved in 1 ml of chloroform. After drying the lipid mixture with nitrogen, the lipid film was placed overnight in a vacuum desiccator to remove remaining solvent traces. The lipid film was hydrated with 1 ml of phosphate-free buffer (10 mM Tris, 0.1 M NaCl, pH 7) and incubated at 50°C for 30 min. The suspension was subjected to five cycles of freezing/thawing to obtain multilamellar vesicles. Liposomes were obtained by extrusion through polycarbonate filters (Nucleopore Track-Etch Membrane Whatman®, Brentford, UK) with a pore diameter of 0.1 μm. Phospholipid concentrations were determined according to the protocol developed by Bartlett G.R. [26]. Liposomes were stored at 4°C and used within 2 days after their preparation. Different lipid molar ratios of POPC/eSM/Chol were used (Table 1).

Table 1. Lipid composition of the liposomes

Liposomes	POPC (%)	eSM (%)	Chol (%)
1	33	33	33
2	15	75	15
3	70	15	15
4	15	15	70
5	0	50	50
6	50	50	0
7	50	0	50
8	50	25	25
9	25	50	25
10	25	25	50

Egg sphingomyelin (eSM), *1*-palmitoyl-*2*-oleoyl-sn-glycero-*3*-phosphocholine (POPC), and cholesterol (Chol).

4.4 LNC and liposome physicochemical characterization.

Size, ζ-potential and PDI of LNCs and liposomes were characterized using a Malvern Zetasizer Nano Serie DTS 1060 (Malvern Instruments). For the measurement of size and PDI, samples were diluted 1/100 (v/v) in water. For the measurement of ζ-potential, samples were diluted 1/100 (v/v) in NaCl 10 mM.

4.5 Isolation of NSCs

SVZ-NSC isolation. SVZ-NSCs were isolated according to a protocol presented by Guo et al. [27]. Briefly, new-born rats (from 1 to 5 day-old) were sacrificed by decapitation and the brain was removed and put in the dissection buffer (1.25 ml of D-glucose 1 M, 750 µl of HEPES and 500 µl Pen/Strept in 50 ml of HBSS medium). Brains were cut into 400 µm coronal sections and the SVZ was dissected and placed in 1.5 ml tubes with 0.5 ml of dissection buffer. The tubes were centrifuged for 5 min at 400 g. The supernatant was removed and 1 ml of stem cell culture medium (1.25 ml of D-glucose 1 M, 750 µl of HEPES, 500 µl Pen/Strept, 500 µl Na Pyruvate, 500 µl of B27 and 10 ng/ml of EGF in 50 ml of MEM alpha no nucleosides medium) was added. The pellet was mechanically triturated using a 26 G needle and the cells were seeded at $2*10^5$ to $3*10^5$ cells/T75 flask in 12 ml of cell culture medium.

CC-NSC isolation. CC-NSCs were isolated according to a protocol described by Hugnot [28]. Briefly new-born rats were sacrificed by decapitation. The spinal cords were removed and put in a 1.5 ml tube with 500 µl of HBSS (two spinal cords/tube). In each tube, 130 µl of hyaluronidase, 130 µl of trypsin and 25 µl of DNAse were added. The samples were incubated at 37 °C for 30 min, transferred in a 15 ml tube containing 12 ml of HBSS and centrifuged at 380 g for 5 min. The supernatant was eliminated and the pellet was suspended in 600 µl of HBSS and mechanically dissociated. A 40 µm filter was used to filter the suspension which was then centrifuged at 380 g for 5 min. The supernatant was eliminated and the pellet was suspended in 2 ml of 25 % sucrose solution. The suspension was centrifuged at 780 g for 30 min. The supernatant was removed and 1 ml of stem cell culture medium (with 10 ng of bFGF) was added. The cells were seeded at $2*10^5$ to $3*10^5$ cells/T75 flask in 12 ml of cell culture medium.

The isolation of SVZ-NSCs and CC-NSCs has been performed on the same animals. NSCs were cultivated as floating neurospheres, which appeared after 5 days, and used 7 days after their isolation.

4.6 Isolation of NSC plasma membranes

The isolation of NSC plasma membrane was performed following the protocol presented by Susky et al. [29]. Briefly, $3*10^7$ SVZ-NSCs or CC-NSCs were collected in a 50 ml falcon and centrifuged (5804R centrifuge, Eppendorf) for 5 min at 500 g. Supernatants were eliminated and 200 µl of lysis buffer (730 mM sucrose, 20 mM Tris-HCl, 100 µM EDTA) were added. The cells were left on ice during 30 min. Then, 30 ml of distilled water were added, keeping the tube on ice for another 30 min. Samples were centrifuged for 5 min at 800 g; supernatants were recovered and centrifuged again for 5 min at 800 g. Supernatants were transferred in a 3137-0050 oak ridge tube and centrifuged (Avanti J-E, Beckman) for 10 min at 10000 g (rotor JA-20, Beckman). Supernatants were recovered and centrifuged again for 10 min at 10000 g before to be recovered and centrifuged for 20 min at 25000 g. The pellets were suspended in 15 ml of ice-cold starting buffer (SB) (225 mM mannitol, 75 mM sucrose, and 30 mM Tris-HCl) and centrifuged for 20 min at 25000 g. The pellets were recovered in 0.5 ml of plasma membrane resuspension buffer (5mM Bis-Tris and 0.2 mM EDTA, pH6), placed on the top of a sucrose gradient (from the bottom: 3 ml of sucrose 53%, 4 ml of sucrose 43%, and 4 ml of sucrose 38%) in a Ultra-Clear centrifuge tube (ref 344059) and centrifuged (Optima XL-100K, Beckman) 2 h and 30 min at 95000 g (rotor SW40, Beckman). Centrifugation in

sucrose gradient resulted in three bands (from the bottom: plasma membrane, mitochondria and plasma-membrane associated microdomains). Top and bottom bands were recovered using a pipette. The bands were diluted up to 1 ml in SB.

4.7 Lipidic composition of NSC plasma membranes

Phospholipid concentration in NSC PMs was determined by phosphorus assay following the protocol described by Bartlett G.R. [26] while the cholesterol concentration was determined by Amplex® Red Cholesterol Assay Kit (Thermo Fisher Scientific) following supplier instructions. HPLC-MS preliminary data have been obtained by extracting the lipids from the PM and analyzing them as described by Mutemberezi *et al.* [30]. The lipid fraction was analyzed by a LTQ-Orbitrap mass spectrometer (ThermoFisher Scientific) coupled to an Accela HPLC system (ThermoFisher Scientific). Analyte separation was achieved using a C-18 Supelguard pre-column and a kinetex LC-18 column (5μm, 4.6 × 150 mm) (Phenomenex) and a gradient of acidified methanol and water.

4.8 Fluidity characterization of NSC plasma membranes

NSC plasma membrane fluidity was studied by measuring the generalized polarization (GP) of Laurdan, a lipophilic fluorescent probe, according to the method presented by Parasassi et al. [31]. Briefly, $1*10^6$/ml of SVZ-NSCs or CC-NSCs were incubated with 1% BSA for 1 h and then centrifuged at 500 g for 5 min. Pellets were suspended in 2.5 μM Laurdan in HBSS and incubated for 45 min at room temperature. NSCs were centrifuged again at 500 g for 5 min and suspended in HBSS at $1*10^6$/ml. The cell suspension was placed into a fluorometric cuvette with a 10 mm optical path length. Laurdan emission spectra were recorded at 4°C or at 37°C using λex = 360 nm, and λem = 440 nm (emission in blue, I_B) and 490 nm (emission in red, I_R), where I_B and I_R are the fluorescence intensities emitted by Laurdan in the gel phase and liquid crystalline phase, respectively. GP was calculated using the following formula:

$$GP = (I_B-I_R)/(I_B+I_R).$$

The risk of interferences between the lipid nanoparticles and Laurdan was avoided with the elimination of the excess of the probe by NSC centrifugation and resuspension in fresh buffer after plasma membrane labelling. The concentrations of the compounds were fixed below the limit of toxicity previously evaluated [13,22].

4.9 Impact of NFL, LNCs and NFL-LNCs on membrane fluidity

On cells. SVZ-NSCs and CC-NSCs were treated as described in 5.8. The impact of NFL, LNCs and NFL-LNCs on NSC plasma membrane fluidity was studied by measuring the variation of GP before and after incubations (5 min) with different concentration of NFL, LNCs and NFL-LNCs. Laurdan emission spectra were recorded as previously described.

On liposomes. Liposomes (Table 1) were diluted 1/10 in 1 ml HBSS (final volume, 1 ml; final lipid concentration, 1 mM) and were incubated (5 min) with NFL, LNCs and NFL-LNCs. Laurdan emission spectra were recorded as previously described.

4.10 Permeability characterization of NSC plasma membranes

NSC plasma membrane permeability was analysed by measuring the penetration of fluorescein isothiocyanate–dextrans (FD) into NSCs according to the method developed by Jia et al. [32]. Briefly, SVZ-NSCs and CC-NSCs were seeded at 2900 neurospheres/ml (corresponding to $2.5*10^5$ cells/ml) in NSC medium with FD 4 kDa, FD10 kDa or FD 40 kDa at 20 µM for 10 min. The neurospheres were centrifuged at 500 g for 5 min and the pellets resuspended in FD-free NSC medium. Before BD FACSCalibur™ flow cytometer (BD Biosciences) analysis, neurospheres were washed 3 times with PBS and dissociated with a 26 G needle.

4.11 Impact of NFL, LNCs and NFL-LNCs on plasma membrane permeability

SVZ-NSCs and CC-NSCs were treated as described in 4.10. Impact of NFL, LNCs and NFL-LNCs on NSC plasma membrane permeability was analyzed by measuring the variation of fluorescence before and after 5 min incubation with different concentrations of NFL, LNCs and NFL-LNCs. SVZ-NSCs incubated with NFL at 20 µM in NSC medium supplemented with FD4 at 20 µM were analyzed by confocal microscopy (Zeiss Cell Observer Spinning Disk microscope, Carl Zeiss). Neurospheres were washed 3 times with PBS and fixed with 4 % PFA for 15 min. They were mounted with VECTASHIELD® antifade mounting medium and 2 pictures/condition were taken randomly. To evaluate NSC permeability recovery, SVZ-NSCs were seeded at 2900 neurospheres/ml (corresponding to $2.5*10^5$ cells/ml) in FD-free NSC medium and incubated at 37°C during 5 min with NFL at 20 µM. Neurospheres were centrifuged at 500 g for 5 min, the pellet was resuspended in FD-free NSC medium and incubated at 37°C for 6 h. Then, neurospheres were centrifuged at 500 g for 5 min, resuspended in FD4 (20 µM)-supplemented NSC medium and incubated at 37°C for 5 min.

Neurospheres were finally centrifuged at 500 g for 5 min and the pellet was suspended in FD-free NSC medium. Before BD FACSCalibur™ flow cytometer (BD Biosciences) analysis, neurospheres were washed 3 times with PBS and dissociated with a 26 G needle.

4.12 Statistical analyses

All the experiments were repeated at least 3 times. Error bars represent standard error of the mean (SEM). $p^* < 0.05$, $p^{**} < 0.01$ and $p^{***} < 0.001$ were calculated with Mann-Whitney test or with ANOVA one-way (with a Bonferroni correction to adapt the first order risk) by using Prism 5.00 (GraphPad software, San Diego, CA).

5 RESULTS AND DISCUSSION

5.1 Characterization of LNCs and liposomes

LNCs had a size of 59 nm ± 4 , a PDI of 0.08 and a zeta-potential of -9.0 mV ± 1.5 while the adsorption of NFL increased LNC size (+ 6 nm) and PDI as well as ζ-potential (+ 2 mV) (Table 1), as previously observed [22]. Liposomes showed a size of 140 nm ± 10, a PDI of 0.15 and a ζ-potential of -15.0 mV ± 6 (Table 2), as previously observed [33,34].

Table 2. Physiochemical characteristics of the nanoparticles

	size (nm)	PDI	ζ-potential (mV)
LNCs	59 ± 4	0.08	-9.0 ± 1.5
NFL-LNCs	65 ± 4	0.18-0.2	-7.0 ± 1.5
Liposomes	140 ± 10	0.15	-15 ± 6

Size and PDI were characterized by DLS diluting the nanoparticles and liposomes 1/100 (v/v) in water. The ζ-potential was measured by diluting the nanoparticles and liposomes 1/100 (v/v) in NaCl 10 mM

5.2 Plasma membrane lipidic composition depends of NSC origin

Although many plasma membrane characteristics could play a crucial role in the interaction between compounds and cells (such as lipid/protein composition, lipid rafts and transversal asymmetry), passive internalization is mostly related to the lipidic composition of the cell membrane [40]. As NFL and NFL-LNC showed passive translocation and interactions with SVZ-NSCs, respectively [13,22], to decipher why NFL-LNCs would target SVZ-NSCs and not CC-NSCs, we studied NSC plasma membrane lipid composition.

Plasma membranes from SVZ-NSCs and CC-NSCs have been isolated and collected from the same new born rats to limit variabilities. The purity of NSC cultures was evaluated before plasma membrane isolation by counting the percentage of Nestin^{+} cells (73.5 and 78.5 % for SVZ-NSCs and CC-NSCs respectively). To the best of our knowledge, no NSC isolation protocol provides cultures 100% Nestin[+], consequently, the possible influence of non-NSCs must be always taken into account. The amount of phospholipids detected after plasma membrane isolation was similar and constant between SVZ- and CC-NSCs (Figure 1A).

Cholesterol is a key component of animal cell membranes, present at different proportions, depending on cell type. It can affect membrane mechanical properties (e.g., fluidity) as well as permeability to water and small molecules [35]. Cholesterol concentrations were not statistically different between SVZ-NSC and CC-NSC plasma membranes despite the higher amount detected in SVZ-NSCs (Figure 1B), excluding a major role of this lipid in the interactions between NFL-LNCs and NSCs.
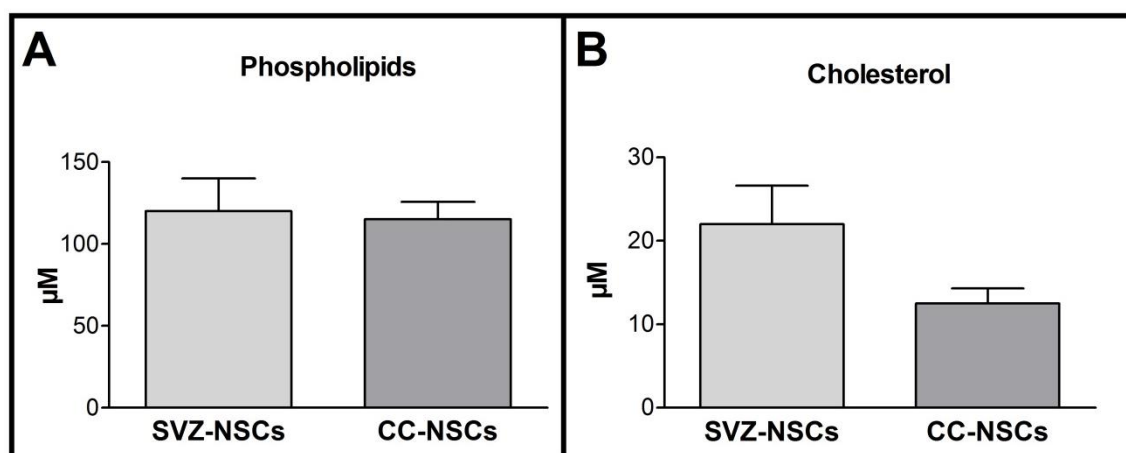

Figure 1. Phospholipid and cholesterol quantification in SVZ-NSC and CC-NSC plasma membranes. A, phospholipid quantification in SVZ-NSC and CC-NSC plasma membranes. B, cholesterol quantification in SVZ-NSC and CC-NSC plasma membrane. $p > 0.05$. One way ANOVA test (Bonferroni comparison between SVZ-NSCs and CC-NSCs). N=5, n=2 and n=3 for phospholipid and cholesterol quantification respectively.

The comparison of the lipidic composition of SVZ- and CC-NSC plasma membrane highlighted differences in the ceramide and phosphatidylcholine content between the two types of cells. On the one hand, a significantly higher amount of C18:0 ceramide was detected in SVZ-NSCs as well as a higher content of other ceramides (C16:0, C18:1, C20:0, C22:0 and C24:1) compared to CC-NSC plasma membrane (Figure 2A). On the other hand, a significantly higher amount of C36:0, C38:1, C38:3, C38:4, C40:4 and C40:6 phosphatidylcholines were detected in CC-NSCs (Figure 2B) as well as a higher amount of other phosphatidylcholines (C32:0, C34:0, C34:1, C36:2, C36:3, C36:4, C36:5, C38:2, C38:5 and C40:5) (Figure S1) compared to SVZ-NSCs. The quantification of sphingomyelins did not show any significant difference between the two types of cells (Figure S2).
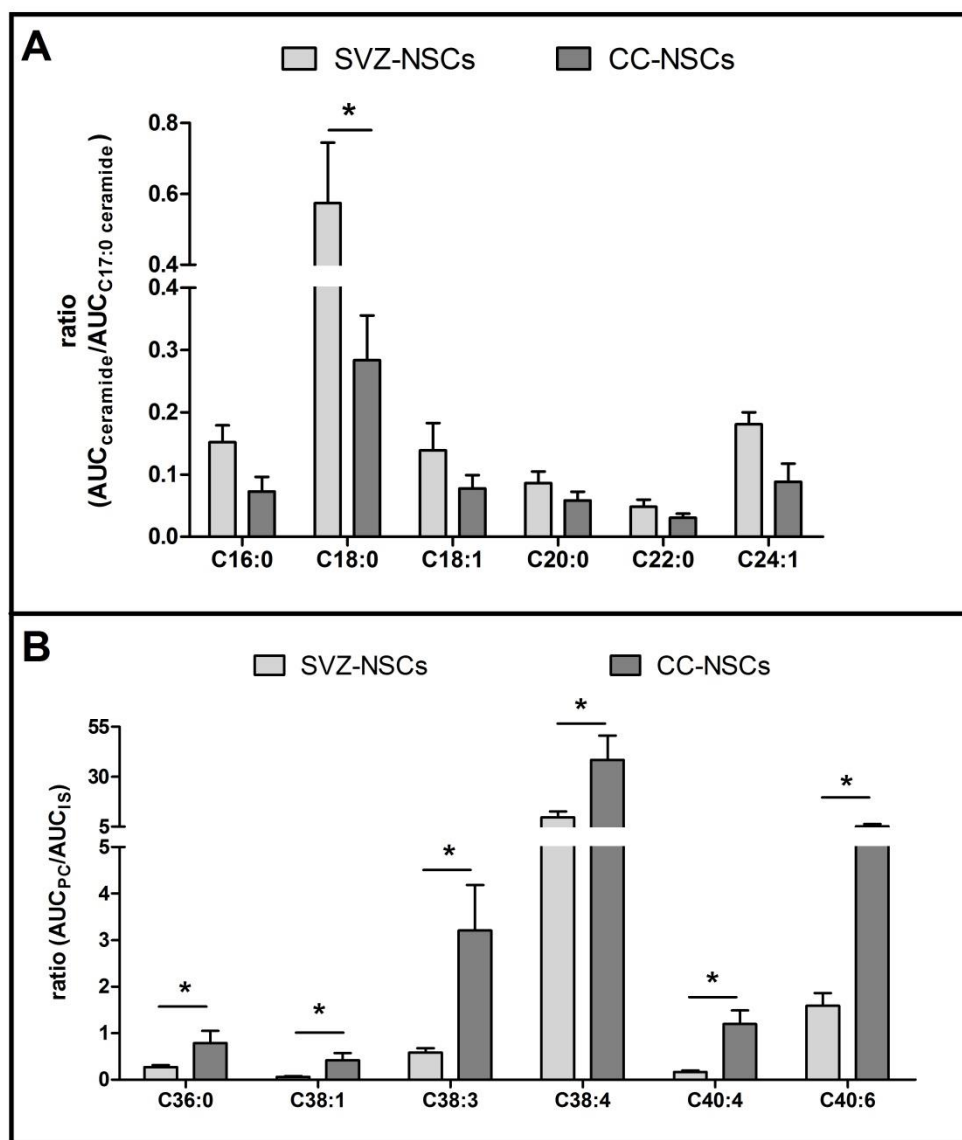
Figure 2. Ceramides and phosphatidylcholines quantification in SVZ-NSC and CC-NSC plasma membrane by HPLC-MS. A, ceramides. B, phosphatidylcholines. p* < 0.05. One way ANOVA test (Bonferroni comparison between SVZ-NSCs and CC-NSCs). N=5, n=5.

Ceramides are a family of lipids composed by sphingosine and a fatty acid while phosphatidylcholines are a class of phospholipids that incorporate choline as a head group. Both of those lipids significantly affect membrane properties, such as fluidity and permeability [36-38] in a dose-dependent form [39] which are critical for nanoparticle-cell interactions [40]. Ceramide and phosphatidylcholine proportion in NSC membrane could thus impact the ability of NFL-LNCs to target NSCs *via* its influence on NSC fluidity and permeability.

5.3 NSC plasma membrane fluidity impacts interactions between NSCs and both LNCs and NFL-LNCs

We then evaluated and compared SVZ- and CC-NSC membrane fluidity and permeability before and after incubations with NFL, LNCs and NFL-LNCs.

The fluidity of both SVZ- and CC-NSC plasma membranes is related to the GP of laurdan whose maximal emission depends on the polarity of the environment [41]. GP is sensitive to the water content of cellular membranes. Consequently, it can be used to quantitatively determine the relative amount of solid and liquid phases in plasma membranes [42]. CC-NSC GP was significantly higher ($p*<0.05$) than the GP value of SVZ whatever the temperature (Figure 3), suggesting that SVZ-NSC plasma membrane was significantly more fluid than CC-NSC plasma membrane and both were significantly more rigid at 4 °C (GP 0.53-0.65) than at 37 °C (GP 0.32-0.40). This result showed that the physical state of NSCs was different depending on the temperature and the cell type.
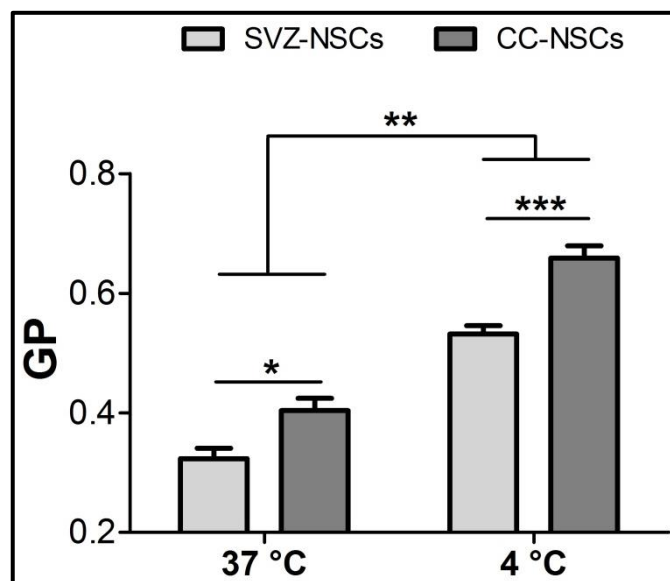

Figure 3. Fluidity characterization of SVZ-NSC and CC-NSC plasma membranes by the generalized polarization (GP) of Laurdan. Fluidity of both SVZ-NSCs and CC-NSCs was measured at 37 °C or at 4 °C. $p* < 0.05$, $p** < 0.01$, $p*** < 0.001$. Mann-Whitney test. N=3, n=2.

Catapano *et al*. observed that ceramides increase the rigidity of lipid membranes [43] while Pinto *et al*. showed that laurdan is excluded from the rigid ceramide-rich domains, resulting in a higher fraction of the probe in the fluid phase [44]. We could thus hypothesize that the low GP of SVZ-NSC membrane, despite the higher amount of ceramides, could be due to the exclusion of laurdan from the rigid domains.

The different fluidity of NSCs could be one of the factors regulating the selective targeting of NFL-LNCs toward SVZ-NSCs. Variations of GP (ΔGP) provide information on the interactions compound-cell [45]. So, SVZ-NSC and CC-NSC GPs were measured at 4° and 37 °C, before and after incubation with NFL, LNCs and NFL-LNCs at different concentrations. The increase of ΔGP is usually associated with a lower bilayer packing and higher polarity (increase of membrane fluidity) whereas a decrease of ΔGP corresponds to the opposite [42].

NFL had no significant impact on NSC ΔGP whatever the condition (Figure 4) despite the demonstration of the peptide penetration into SVZ-NSCs [13]. The dissociation of the neurospheres in single cells, necessary to measure NSC GPs, could impact the integrity of the plasma membranes. Consequently, we hypothesized that the effect on the fluidity induced by the dissociation would hinder the effect of the peptide. Therefore, the action of NFL on SVZ-NSC and CC-NSC membrane fluidity might be no detectable following this method.

LNCs and NFL-LNCs (≥ 1.26 mg/ml of nanoparticles) significantly decreased the ΔGP of SVZ-NSC and CC-NSC membrane at 37 °C, while no major variation was measured at 4 °C (Figure 4). Even if LNCs and NFL-LNCs increased the rigidity of both membranes, the effect of the nanoparticles on SVZ-NSC GP (+ 40%) (Figure 4A) was significantly higher (p* <0.05) than the effect on CC-NSC GP (+ 26%) (Figure 4B). When looking at the GP values pre-incubation (Figure 3), it seemed that the lowest the GP value, the highest the impact of LNCs and NFL-LNCs.

Thus, we propose that nanoparticles could preferentially interact with SVZ-NSCs compared to CC-NSCs due to the higher ceramide content and lower phosphatidylcholine amount resulting in different membrane fluidity.
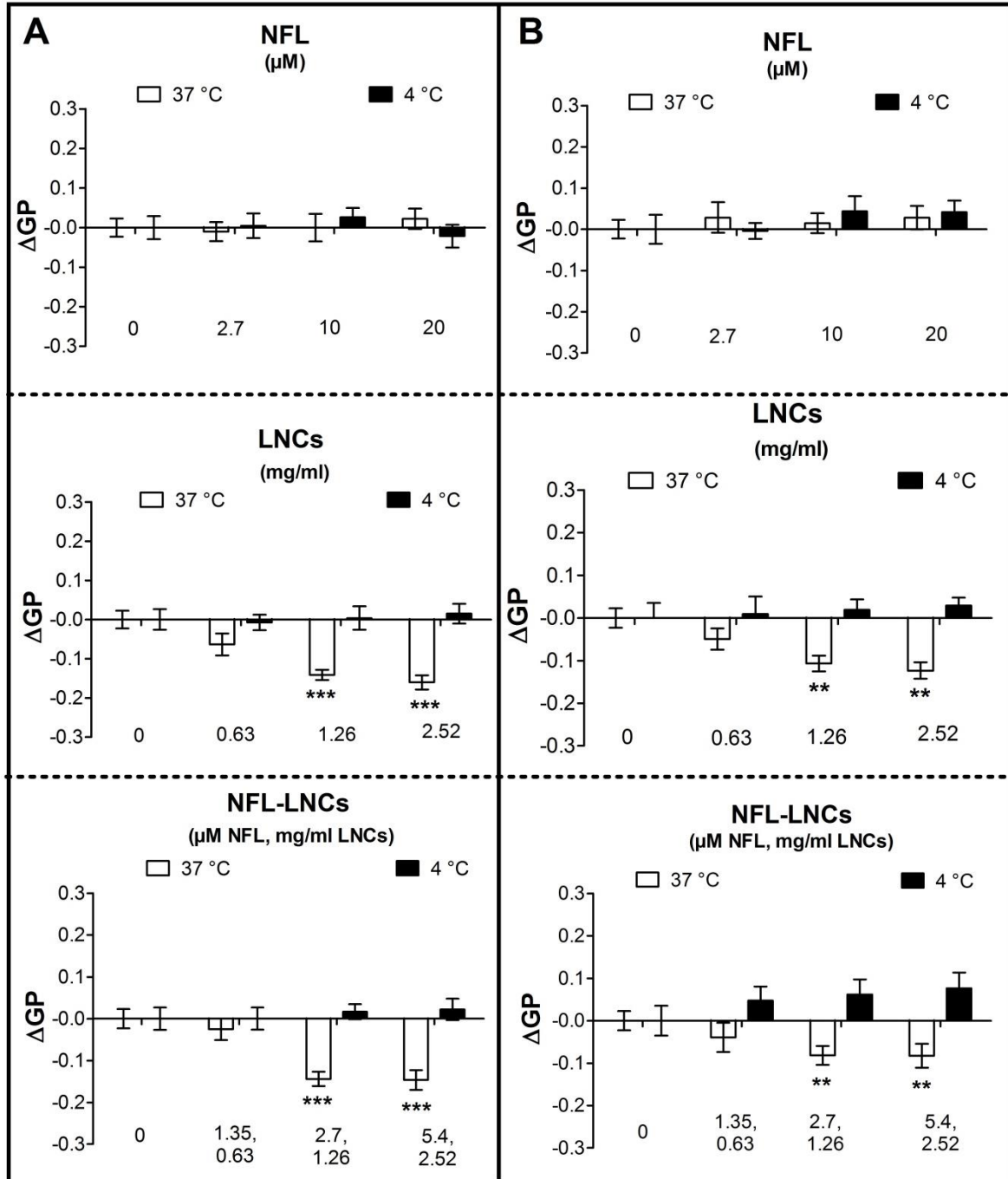
Figure 4. Impact of NFL, LNCs and NFL-LNCs on ΔGP of SVZ-NSC and CC-NSC lipid fluidity. The impact on the plasma membrane fluidity was measured incubating SVZ-NSCs (A) and CC-NSCs (B) with NFL (2.7, 10, and 20 μM), LNCs (0.63, 1.26 and 2.52 mg/ml) and NFL-LNCs (1.35 +0.63, 2.7+1.26, 5.4 +2.52, NFL + mg/ml LNCs) at 4 °C and 37 °C (ΔGP = GP before incubation – GP after incubation). P** < 0.01, p*** < 0.001. Mann-Whitney test. N=3, n=2.

On the one hand, we demonstrated that plasma membrane fluidity was significantly more affected by LNCs and NFL-LNCs for SVZ-NSCs than for CC-NSCs. On the other hand, NFL presence in the formulation did not show any major effect on the membrane fluidity, despite the selective targeting brought by the peptide [22].

To confirm the role of plasma membrane fluidity on NSC interaction with LNCs and NFL-LNCs, we performed membrane-modelling using liposomes. Liposomes can mimic many aspects of cellular membranes [46] and for that reason, they have already been used as models to investigate the interactions between molecules/nanoparticles and cells [47,48]. Different ratios of POPC, eSM and Chol were used to produce liposomes with different GPs (from 0.15 to 0.62) [49] (Figure 5A). The lipid mixture required to produce liposome 4 did not produce the phospholipid bilayer, therefore liposome 4 was not used.

Liposome ΔGPs were measured to evaluate the role of membrane fluidity on the interactions with NFL, LNCs and NFL-LNCs (Figure 5B). No trend related to the liposome composition was observed. NFL did not show major effects on the ΔGP of the liposomes at this concentration (2.7 μM) while LNCs and NFL-LNCs significantly increased the rigidity of liposomes with GP lower than 0.448 (Figure 5B), as already shown in NSCs. Moreover, the impact on the fluidity of NFL-LNCs was higher compared to LNCs as the liposome GPs were low (liposome 6 and 3). NFL-LNCs decreased GP values of liposome 1 while LNCs and NFL-LNCs decreased GP values of liposome 5. Also in this case, the effect depended on the initial liposome fluidity but with an opposite impact on the GP: the higher the initial GP ($\geq$ 0.506), the higher the fluidizing effect of LNCs.

Liposomes with GPs between 0.33 and 0.4 did not show any significant ΔGPs after incubation with the treatments. Interestingly, liposome GPs close to the SVZ-NSC GP were more impacted compared to liposome GPs close to CC-NSC GP.

Using liposomes with different GPs as models for cell membranes highlighted the relation between membrane fluidity and interaction with LNC. The lower the GP, the higher the rigidity induced by LNCs, while the higher the GP, the higher the fluidity. The use of liposomes with different ceramide and phosphatidylcholine content could be used to highlight the relation between LNC impact on ΔGP and the variation of ceramide/phosphatidylcholine ratios.
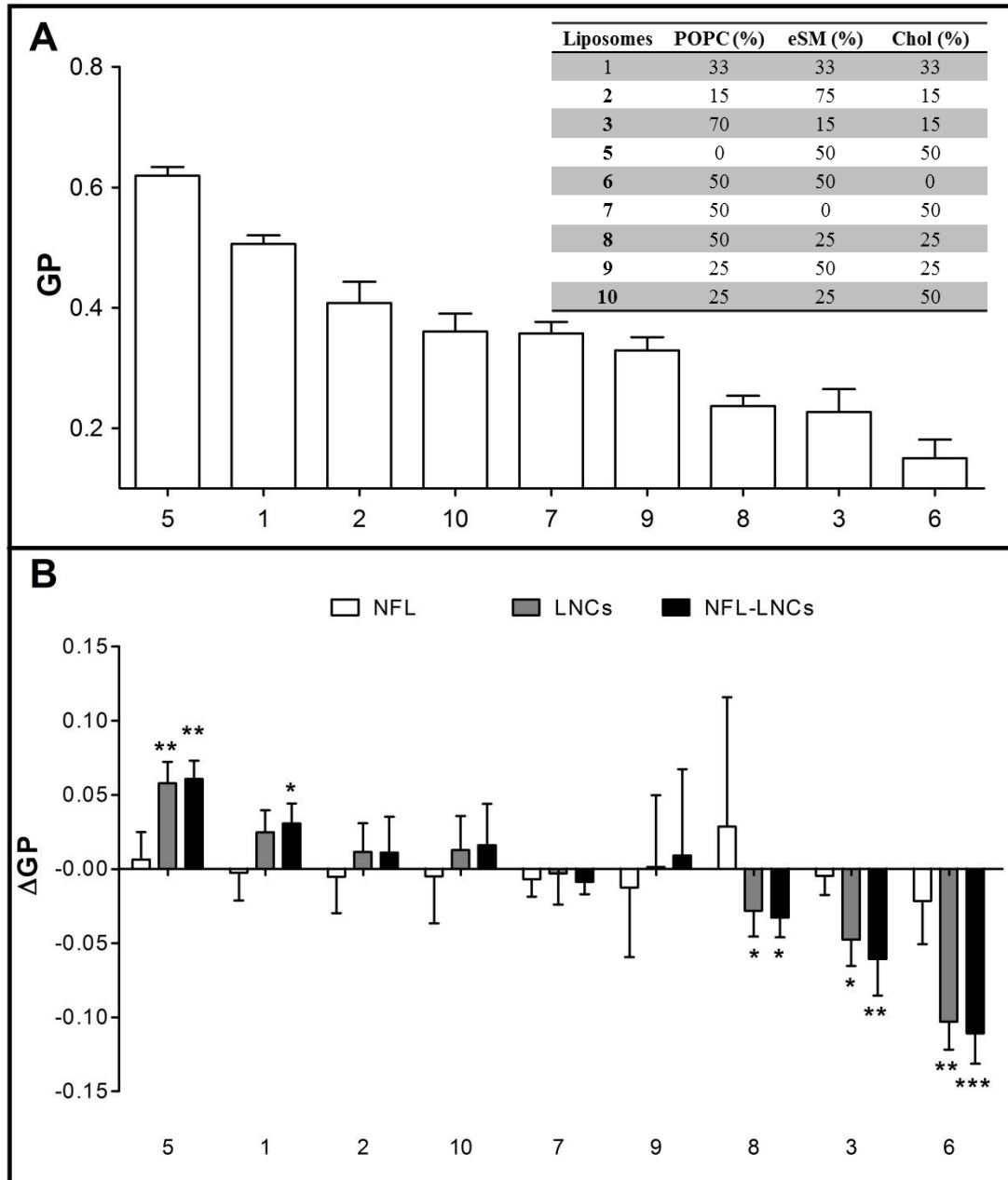
The table inside panel A:

Liposomes	POPC (%)	eSM (%)	Chol (%)
1	33	33	33
2	15	75	15
3	70	15	15
5	0	50	50
6	50	50	0
7	50	0	50
8	50	25	25
9	25	50	25
10	25	25	50

Figure 5. Impact of NFL, LNCs and NFL-LNCs on liposome lipid fluidity. A, table of liposomes made at different ratios of POPC, eSM and Cho, with their respective GPs. N = 4. B, impact of NFL (2.7 μM), LNCs (1.26mg/ml) and NFL-LNCs (2.7 μM NFL + 1.26 mg/ml LNCs) on liposome lipid fluidity at 25 °C. p* < 0.05, p** <0.01, p***<0.001. One way ANOVA test (Bonferroni comparison between compounds and CTRL of each liposome). N=4.

SVZ-NSCs have a significantly different GP compared to CC-NSCs, probably due to the higher amount of ceramides and lower content of phosphatidylcholines. NFL impact on the membrane fluidity was not detectable while LNCs and NFL-LNCs showed a GP-dependent impact on both NSCs and liposomes. Thus, we conclude that physical state of the membrane is a factor impacting the interactions between NFL-LNCs and NSCs.

5.4 NFL affects NSC plasma membrane permeability

Molecule internalization into cells is regulated, in part, by plasma membrane permeability which, in turn, depends on its lipid composition [50]. Ceramides can increase plasma membrane permeability by detergent solubilization effects, induction of nonlamellar structures and generation of structural defects between rigid and fluid lipid phases [51]. Consequently, we hypothesized that SVZ-NSCs and CC-NSCs could have different plasma membrane permeability due to the different amount of ceramides detected in those cells.

Plasma membrane permeability to FD4, FD10 and FD40 did not show any significant difference between the two types of NSCs. The percentage of positive cells was close to the baseline of the instrument (below 13%) for all conditions (Figure 6). Thus, the different amount of ceramides detected in SVZ-NSCs and CC-NSCs would not be directly related to the cell steady state permeability for those compounds. However, we cannot exclude different NSC permeability for lower molecular weight molecules (< 4kDa).
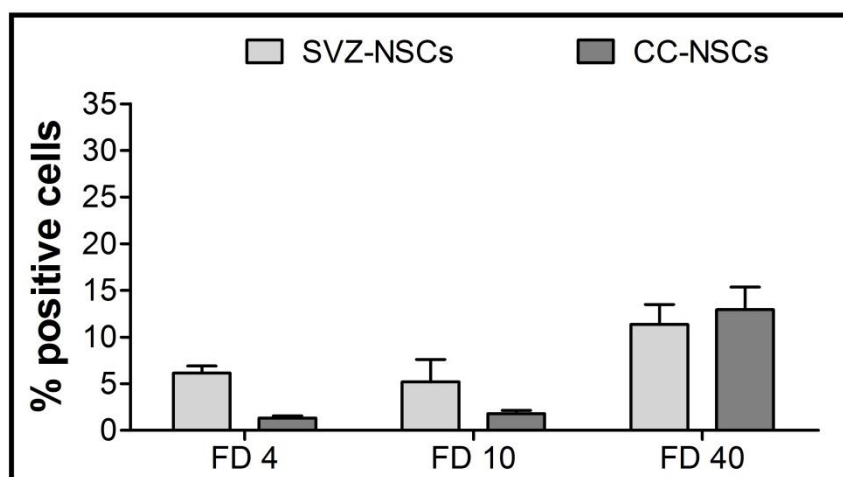

Figure 6. Permeability of SVZ-NSCs and CC-NSCs to fluorescent dextrans. Percentage of positive NSCs to different molecular weight fluorescent dextrans (FD4, FD10 and FD40) obtained by flux cytometry. N=4.

Hence, we measured the variation of NSC permeability before and after incubation with NFL, LNCs and NFL-LNCs. While membrane permeability of both cell types to FD4, FD10 and FD 40 did not show any major difference after incubation with LNCs and NFL-NCs (data not shown), the treatment with NFL at 20 μM significantly increased the penetration of FD4 in 29% of SVZ-NSCs (Figure 7A). This result was also confirmed by confocal imaging (Figure 7B).

Cell penetrating peptides can produce pores of different sizes on the plasma membrane of the cells, depending on the condition of incubation (e.g., concentration) [52]. Only 20 μM of NFL

allowed the penetration of FD4 (4 kDa), suggesting the ability of the peptide to make pores but only above this concentration. However, in our previous work we showed that pre-incubations with 10 µM NFL allowed the penetration of 1.6-2.7 kDa molecules [22]. Consequently, we hypothesized that NFL could modulate SVZ-NSC plasma membrane permeability by producing pores with concentration-depending sizes. Unfortunately it was not possible to perform NSCs incubation with higher concentrations of NFL due to its toxicity [13]. The modification of SVZ-NSC permeability by NFL was totally recovered after 6 hours (Figure 7C), indicating that the effect of the peptide was transient.
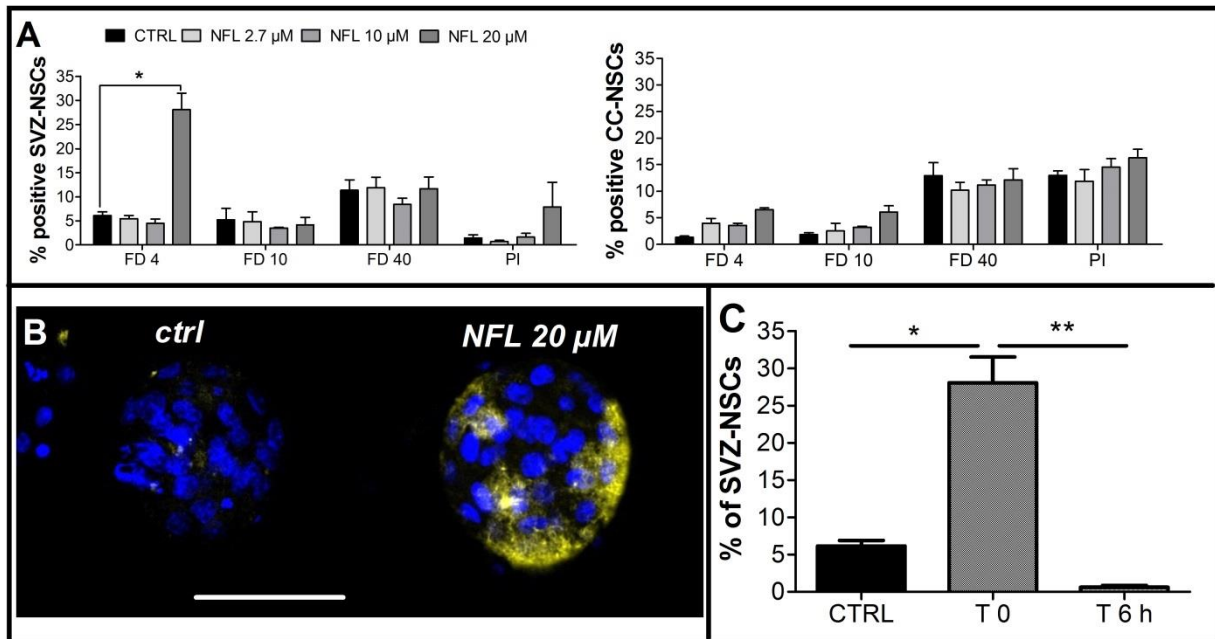

Figure 7. Impact of NFL on NSC permeability. A, percentage of positive NSCs to fluorescent dextran (FD) of different molecular weights (4, 10 and 40 kDa) after incubation with increasing concentration of NFL (2.7, 10, 20 µM). p* < 0.05. One way ANOVA test (Bonferroni comparison between all the columns with the respective CTRL). N=4. B, confocal imaging of SVZ-NSCs treated with NFL 20 µM. Blue is DAPI, nucleus. Yellow is fluorescein isothiocyanate, FD4. Scale barr = 50 µm. C, permeability recovery 6 hours after the treatment with NFL 20 µM in presence of FD4. p* < 0.05, p** <0.01. Mann-Whitney test. N=3.

Although ceramides are associated with higher membrane permeability [51], no significant difference was observed between the SVZ-NSC and CC-NSC steady state permeability for FD4, FD10 and FD40. Despite LNCs and NFL-LNCs did not show any major effect, NFL significantly increased the permeability of SVZ-NSCs, suggesting a preferential permeabilizant effect of the peptide on those cells compared to CC-NSCs. Interestingly, the higher (but not significant) presence of Chol observed in SVZ-NSC did not hinder the permeabilizant effect of the peptide NFL despite the fact that this lipid usually decreases the permeability of the plasma membranes [35]. Pae *et al.* showed that ceramides increase the

uptake of arginine-rich CPPs while prevent the internalization of amphipathic CPPs [53]. Due to the presence of arginines in the structure of NFL, we can hypothesize that the higher amount of ceramides detected in SVZ-NSCs could enhances NFL penetration and thus impact the permeability of those cells.

6. CONCLUSIONS

NFL-LNCs selectively interact with SVZ-NSCs and not with CC-NSCs. The characterization of the plasma membrane of both cell types highlighted interesting differences in the lipid compositions which, in turn, have an impact on the physical state and permeability of the cells. Higher ceramide content as well as lower phosphatidylcholine amount were observed in SVZ-NSC plasma membrane compared to CC-NSCs. The interaction between NSCs and nanoparticles depends on the initial physical state of the plasma membrane while NFL preferentially increases the permeability of SVZ-NSC plasma membrane. The implementation of plasma membrane characterization (e.g., by proteomic) or the comparison with other cells (e.g., glioblastoma cells) would provide additional information to understand and explain NFL-LNC interaction towards SVZ-NSCs.

7. REFERENCES

[1] Murrell, Wayne, et al. "Expansion of multipotent stem cells from the adult human brain." PloS one 8.8 (2013): e71334.

[2] Bond, Allison M., Guo-li Ming, and Hongjun Song. "Adult mammalian neural stem cells and neurogenesis: five decades later." Cell Stem Cell 17.4 (2015): 385-395.

[3] Arvidsson, Andreas, et al. "Neuronal replacement from endogenous precursors in the adult brain after stroke." Nature medicine 8.9 (2002): 963-970.

[4] Giuliani, Daniela, et al. "NDP-α-MSH induces intense neurogenesis and cognitive recovery in Alzheimer transgenic mice through activation of melanocortin MC 4 receptors." Molecular and Cellular Neuroscience 67 (2015): 13-21.

[5] Kim, Seung U., Hong J. Lee, and Yun B. Kim. "Neural stem cell-based treatment for neurodegenerative diseases." Neuropathology 33.5 (2013): 491-504.

[6] Carradori, Dario, et al. "The therapeutic contribution of nanomedicine to treat neurodegenerative diseases via neural stem cell differentiation." Biomaterials 123 (2017): 77-91.

[7] Herberts, Carla A., Marcel SG Kwa, and Harm PH Hermsen. "Risk factors in the development of stem cell therapy." Journal of translational medicine 9.1 (2011): 29.

[8] Simonson, Oscar E., et al. "The safety of human pluripotent stem cells in clinical treatment." Annals of medicine 47.5 (2015): 370-380.

[9] Xie, Chuncheng, et al. "The effect of simvastatin treatment on proliferation and differentiation of neural stem cells after traumatic brain injury." Brain research 1602 (2015): 1-8.

[10] Saraiva, C., et al. "MicroRNA-124 loaded nanoparticles enhance brain repair in Parkinson's disease." Journal of Controlled Release 235 (2016): 291-305.

[11] Barreau, Kristell, Claire Lépinoux-Chambaud, and Eyer Joël. "Review of Clinical Trials Using Neural Stem Cells." JSM Biotechnology & Biomedical Engineering 3.3 (2016).

[12] Bocquet, Arnaud, et al. "Neurofilaments bind tubulin and modulate its polymerization." Journal of Neuroscience 29.35 (2009): 11043-11054.

[13] Lépinoux-Chambaud, Claire, Kristell Barreau, and Joël Eyer. "The Neurofilament-Derived Peptide NFL-TBS. 40-63 Targets Neural Stem Cells and Affects Their Properties." Stem cells translational medicine 5.7 (2016): 901-913.

[14] Berges, Raphael, et al. "A tubulin binding peptide targets glioma cells disrupting their microtubules, blocking migration, and inducing apoptosis." Molecular Therapy 20.7 (2012): 1367-1377.

[15] Lépinoux-Chambaud, Claire, and Joël Eyer. "The NFL-TBS. 40-63 anti-glioblastoma peptide enters selectively in glioma cells by endocytosis." International journal of pharmaceutics 454.2 (2013): 738-747.

[16] Balzeau, Julien, et al. "The effect of functionalizing lipid nanocapsules with NFL-TBS. 40-63 peptide on their uptake by glioblastoma cells." Biomaterials 34.13 (2013): 3381-3389.

[17] Rivalin, Romain, et al. "The NFL-TBS. 40-63 anti-glioblastoma peptide disrupts microtubule and mitochondrial networks in the T98G glioma cell line." PloS one 9.6 (2014): e98473.

[18] Fressinaud, Catherine, and Joël Eyer. "Neurofilaments and NFL-TBS. 40–63 peptide penetrate oligodendrocytes through clathrin-dependent endocytosis to promote their growth and survival in vitro." Neuroscience 298 (2015): 42-51.

[19] Ramsey, Joshua D., and Nicholas H. Flynn. "Cell-penetrating peptides transport therapeutics into cells." Pharmacology & therapeutics 154 (2015): 78-86.

[20] Berges, Raphael, et al. "Structure-function analysis of the glioma targeting NFL-TBS. 40-63 peptide corresponding to the tubulin-binding site on the light neurofilament subunit." PloS one 7.11 (2012): e49436.

[21] Huynh, Ngoc Trinh, et al. "Lipid nanocapsules: a new platform for nanomedicine." International journal of pharmaceutics 379.2 (2009): 201-209.

[22] Carradori, Dario, et al. "NFL-lipid nanocapsules for brain neural stem cell targeting in vitro and in vivo." Journal of Controlled Release 238 (2016): 253-262.

[23] Langelier, Bénédicte, et al. "Long chain-polyunsaturated fatty acids modulate membrane phospholipid composition and protein localization in lipid rafts of neural stem cell cultures." Journal of cellular biochemistry 110.6 (2010): 1356-1364.

[24] Heurtault B, Saulnier P, Pech B, Proust JE, Richard J, & Benoit JP. Lipidic nanocapsules: preparation process and use as Drug Delivery Systems. Patent No. WO02688000.

[25] Hope, M. J., et al. "Production of large unilamellar vesicles by a rapid extrusion procedure. Characterization of size distribution, trapped volume and ability to maintain a membrane potential." Biochimica et Biophysica Acta (BBA)-Biomembranes 812.1 (1985): 55-65.

[26] Bartlett, Grant R. "Phosphorus assay in column chromatography." Journal of Biological Chemistry 234 (1959): 466-468.

[27] Guo, Weixiang, et al. "Isolation of multipotent neural stem or progenitor cells from both the dentate gyrus and subventricular zone of a single adult mouse." Nature protocols 7.11 (2012): 2005-2012.

[28] Hugnot, Jean-Philippe. "Isolate and culture neural stem cells from the mouse adult spinal cord." Neural progenitor cells: methods and protocols (2013): 53-63.

[39] Suski, Jan M., et al. "Isolation of plasma membrane–associated membranes from rat liver." nature protocols 9.2 (2014): 312-322.

[30] Mutemberezi, Valentin, et al. "Development and validation of an HPLC-MS method for the simultaneous quantification of key oxysterols, endocannabinoids, and ceramides: variations in metabolic syndrome." Analytical and bioanalytical chemistry 408.3 (2016): 733-745.

[31] Parasassi, T., et al. "Quantitation of lipid phases in phospholipid vesicles by the generalized polarization of Laurdan fluorescence." Biophysical journal 60.1 (1991): 179-189.

[32] Jia, Y., et al. "Comparison of cell membrane damage induced by the therapeutic ultrasound on human breast cancer MCF-7 and MCF-7/ADR cells." Ultrason Sonochem. (2015):128-35.

[33] Etzerodt, Thomas P., et al. "A GALA lipopeptide mediates pH-and membrane charge dependent fusion with stable giant unilamellar vesicles." Soft Matter 8.21 (2012): 5933-5939.

[34] Cuco, Andreia, et al. "Interaction of the Alzheimer Aβ (25–35) peptide segment with model membranes." Colloids and Surfaces B: Biointerfaces 141 (2016): 10-18.

[35] Magarkar, Aniket, et al. "Cholesterol level affects surface charge of lipid membranes in saline solution." Scientific reports 4 (2014): 5005.

[36] van Blitterswijk, Wim J., et al. "Ceramide: second messenger or modulator of membrane structure and dynamics?." Biochemical Journal 369.2 (2003): 199-211.

[37] Silva, Liana, et al. "Ceramide-platform formation and-induced biophysical changes in a fluid phospholipid membrane." Molecular membrane biology 23.2 (2006): 137-148.

[38] Van Meer, Gerrit, Dennis R. Voelker, and Gerald W. Feigenson. "Membrane lipids: where they are and how they behave." Nature reviews Molecular cell biology 9.2 (2008): 112-124.

[39] Holopainen, Juha M., Jukka YA Lehtonen, and Paavo KJ Kinnunen. "Lipid microdomains in dimyristoylphosphatidylcholine–ceramide liposomes." Chemistry and physics of lipids 88.1 (1997): 1-13.

[40] Peetla, Chiranjeevi, Sivakumar Vijayaraghavalu, and Vinod Labhasetwar. "Biophysics of cell membrane lipids in cancer drug resistance: Implications for drug transport and drug delivery with nanoparticles." Advanced drug delivery reviews 65.13 (2013): 1686-1698.

[41] Owen, Dylan M., et al. "Quantitative imaging of membrane lipid order in cells and organisms." Nature protocols 7.1 (2012): 24-35.

[42] Bagatolli, L. A. "LAURDAN fluorescence properties in membranes: a journey from the fluorometer to the microscope." Fluorescent methods to study biological membranes. Springer Berlin Heidelberg, 2012. 3-35.

[43] Catapano, Elisa R., et al. "Solid character of membrane ceramides: a surface rheology study of their mixtures with sphingomyelin." Biophysical journal 101.11 (2011): 2721-2730.

[44] Pinto, Sandra N., et al. "A combined fluorescence spectroscopy, confocal and 2-photon microscopy approach to re-evaluate the properties of sphingolipid domains." Biochimica et Biophysica Acta (BBA)-Biomembranes 1828.9 (2013): 2099-2110.

[45] Kovács, Eugenia, et al. "Interaction of gentamicin polycation with model and cell membranes." Bioelectrochemistry 87 (2012): 230-235.

[46] Bangham, A. D., M. W. Hill, and N. G. A. Miller. "Preparation and use of liposomes as models of biological membranes." Methods in membrane biology. Springer US, 1974. 1-68.

[47] Kristl, J., et al. "Interactions of solid lipid nanoparticles with model membranes and leukocytes studied by EPR." International journal of pharmaceutics 256.1 (2003): 133-140.

[48] Van Meer, Gerrit, Dennis R. Voelker, and Gerald W. Feigenson. "Membrane lipids: where they are and how they behave." Nature reviews Molecular cell biology 9.2 (2008): 112-124.

[49] Madani, Fatemeh, et al. "Mechanisms of cellular uptake of cell-penetrating peptides." Journal of Biophysics 2011 (2011).

[50] Smith, Dennis, et al. "Passive lipoidal diffusion and carrier-mediated cell uptake are both important mechanisms of membrane permeation in drug disposition." Molecular pharmaceutics 11.6 (2014): 1727-1738.

[51] Contreras, F-Xabier, et al. "Sphingosine increases the permeability of model and cell membranes." Biophysical journal 90.11 (2006): 4085-4092.

[52] Herce, H. D., et al. "Arginine-rich peptides destabilize the plasma membrane, consistent with a pore formation translocation mechanism of cell-penetrating peptides." Biophysical journal 97.7 (2009): 1917-1925.

[53] Pae, Janely, et al. "Translocation of cell-penetrating peptides across the plasma membrane is controlled by cholesterol and microenvironment created by membranous proteins." Journal of Controlled Release 192 (2014): 103-113.

8. SUPPLEMENTARY DATA

Figure S1. Lipid characterization of SVZ-NSC and CC-NSC plasma membranes by HPLC-MS. Quantification of different phosphatidylcholines in the plasma membrane of SVZ-NSCs and CC-NSCs. N=5, n=5.
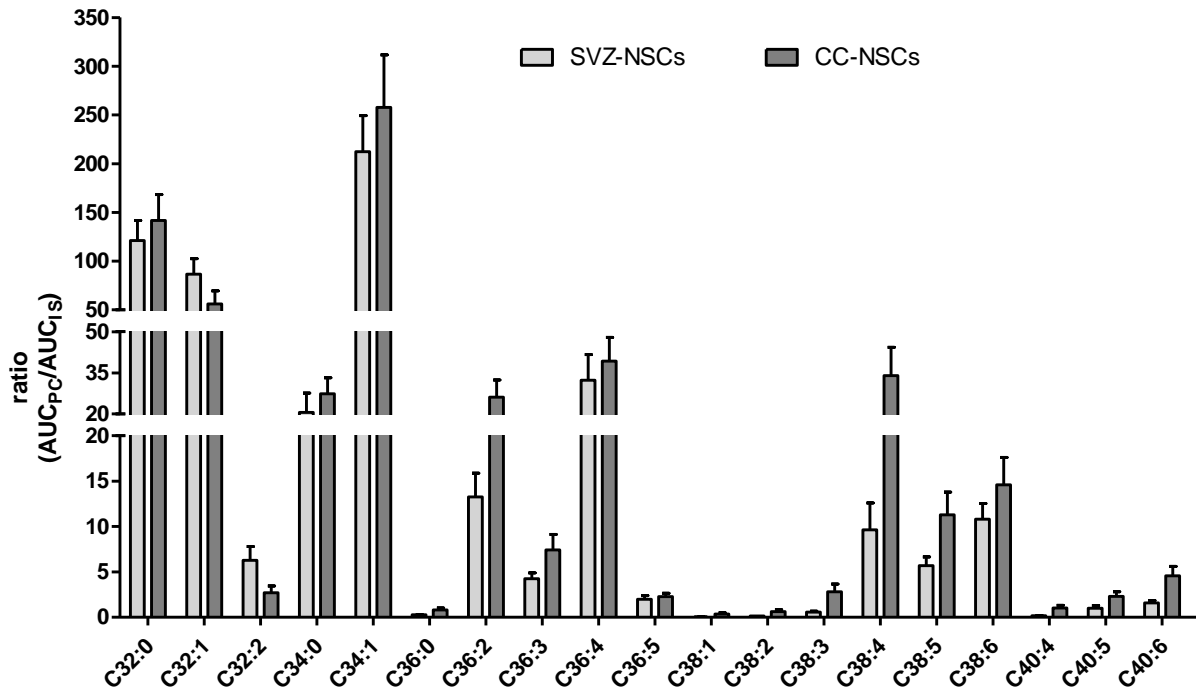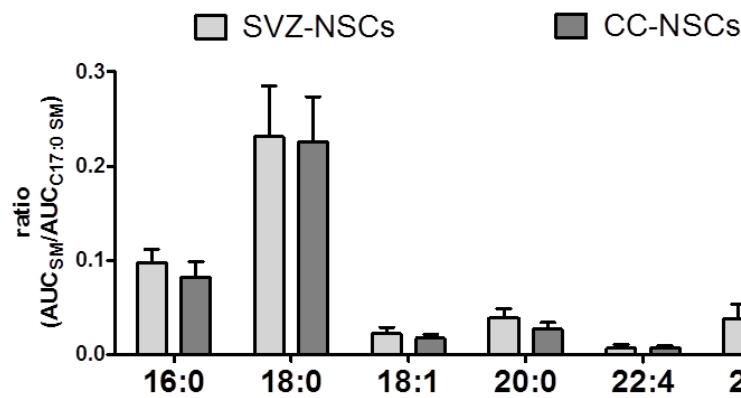

Figure S2. Lipid characterization of SVZ-NSC and CC-NSC plasma membranes by HPLC-MS. Quantification of different sphingomyelins in the plasma membrane of SVZ-NSCs and CC-NSCs. N=5, n=5.

CHAPTER 4

RETINOIC ACID -LOADED NFL-LIPID NANOCAPSULES INDUCE NEURAL STEM CELL DIFFERENTIATION TOWARDS THE OLIGODENDROCYTE LINEAGE *

TABLE OF CONTENTS

1. PREFACE

Central nervous system (CNS) diseases are mostly characterized by the chronic loss and lesion of specialized neural cells such as neurons, astrocytes and oligodendrocytes. In this case, neural stem cells (NSCs) are of great interest due to their differentiation property by which they could replace those lesioned cells. The therapeutic strategy based on the stimulation of endogenous NSCs is one of the most promising because it would avoid some of the limiting issues associated to exogenous NSC-based approaches (e.g., source of cells, viability post-transplantation).

The production of a system able to target endogenous NSCs and to stimulate their differentiation *via* the delivery of a bioactive molecule would represent an important step forward in NSC-based therapy.

In our previous work, we developed and characterized a NSC-interacting drug delivery system by adsorbing the peptide NFL-TBS.40-63 (NFL) on the surface of lipid nanocapsules (LNCs). When injected in the brain, NFL-LNCs specifically co-localize with Nestin^{+} cells which are considered the bona fide neural stem cells of the subventricular zone (SVZ-NSCs). The SVZ is one of the most neurogenic regions of the CNS. It is thus an interesting target for the modulation of NSC differentiation and NFL-LNC represents a promising way to deliver bioactive drugs in this area.

The aim of this work was to provide the proof of concept of this hypothesis by loading retinoic acid, a molecule active on NSC differentiation, into NFL-LNCs and inducing SVZ-NSC differentiation towards specialized neural cells.

2. ABSTRACT

Neural stem cells (NSCs) are located in restricted areas of the central nervous system such as the subventricular zone (SVZ) of the brain where they undergo self-renew or differentiate into specialized neural cells (neurons, astrocytes and oligodendrocytes). The stimulation of endogenous NSCs is one of the most promising NSC-based therapeutic approaches to restore neurological functions in patients affected by neurodegenerative diseases. Unfortunately, the lack of drugs/systems able both to target and to induce NSC differentiation limits the clinical translation of this strategy. Recently, the combination between the peptide NFL-TBS.40-63 (NFL) and lipid nanocapsules (LNCs) produced a nanoscale vector able to co-localize with the NSCs of the SVZ (SVZ-NSCs). The aim of this work was to induce NSC differentiation by delivering retinoic acid (RA) to SVZ-NSCs *via* NFL-LNCs. RA was successfully encapsulated into NFL-LNC and RA-loaded NFL-LNCs were incubated with primary newborn or adult rat SVZ-NSCs. The impact on NSC self-renewal and differentiation was investigated, either by light microscopy or by immunocytochemistry (2 and 7 days post-incubation). Treatment with RA-loaded NFL-LNCs significantly increased the number of GalC$^+$ (oligodendrocytic marker) cells while it decreased the number of Nestin$^+$ (neural stem cell marker) cells. Then, RA-loaded NFL-LNCs were injected in an *in vivo* rat model of white matter demyelination (lysolecithin injection in the caudoputamen) to evaluate the efficacy of our system on remyelination stimulation. The analysis of brain tissues is ongoing.
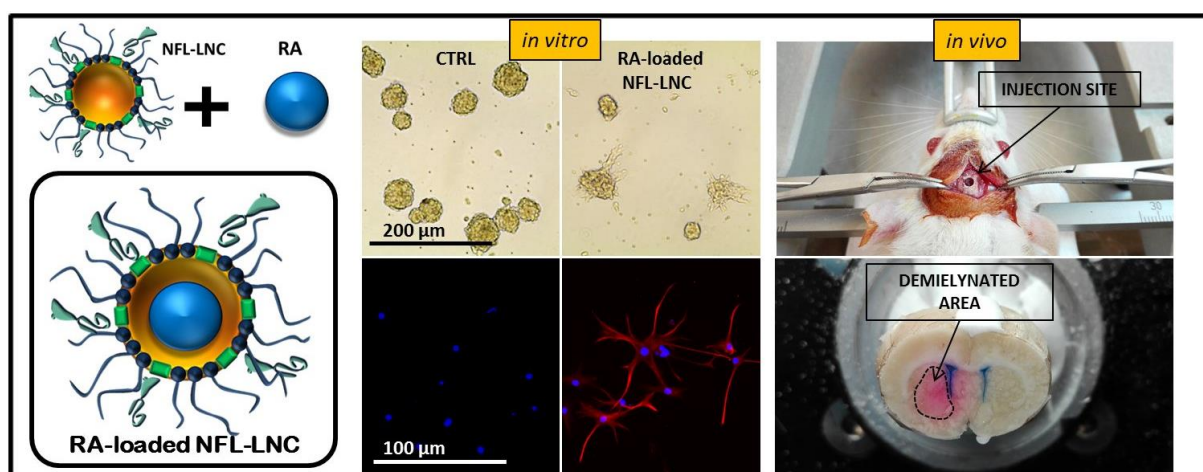
3. INTRODUCTION

CNS degenerative diseases are a heterogeneous group of disorders characterized by the progressive development of lesions and loss of specialized neural cells such as neurons, astrocytes and oligodendrocytes [1,2]. Oligodendrocytes are myelinating cells which modulate the axonal conduction and provide trophic support to neurons [3]. Myelin dysfunction and oligodendrocitic failure are primarily involved in the etiology of many demyelinating CNS diseases (e.g., multiple sclerosis and multiple system atrophy) which have high economic and social costs worldwide [4].

Neural stem cells (NSCs) have been investigated to treat such diseases since many studies demonstrated partial neurological function recovery after their transplantation in animal models [5]. NSCs are located in restricted neurogenic niches of the CNS (e.g., the central canal (CC) in the spinal cord and the subventricular zone (SVZ) and the subgranular zone (SGZ) in the brain). The therapeutic effect of NSCs is mostly related to their differentiation and proliferation, properties by which they can replace damaged cells and enhance the recovery of the affected areas [6]. Several NSC-based strategies have been developed to treat CNS diseases which especially depend on whether NSCs are exogenous (induced from other somatic cells or isolated from neurogenic niches) or endogenous (niche-localized) [7]. Basically, NSC differentiation is designed to occur either *in vivo* after transplantation of *in vitro* expanded/stimulated exogenous NSCs or *in situ* after endogenous NSC stimulation respectively.

In situ differentiation of endogenous NSCs is one of the most promising strategies to treat demyelinating diseases because it would avoid both the issues associated to the transplantation (e.g., cell sources and cell viability) [8] and the *in vitro* manipulations (e.g., risk of contamination and genetic modifications) of NSCs [9]. Nevertheless, the lack of drugs and systems combining endogenous NSCs targeting and differentiation strongly slows down the development of this therapeutic approach.

The peptide NFL-TBS.40-63 (NFL) is a 24-aminoacid peptide which corresponds to the tubulin-binding site of the neurofilament light subunit [10]. It selectively penetrates SVZ-NSCs by direct translocation *in vitro* while it localizes in SVZ-NSC niches after intra-lateral ventricle injection in rat brain *in vivo* [11]. Although NFL targets SVZ-NSCs and induces their differentiation into neurons and oligodendrocytes *in vitro*, it did not show yet an identified therapeutic effect *in vivo*. Moreover, the strong structure-activity correlation

evaluated by alanine-scanning assay and circular dichroism [12] limits chemical coupling between NFL and bioactive molecules. While the direct therapeutic application of the peptide to target and differentiate NSCs is still not excluded, its association with a drug delivery system represents a potential strategy for the selective delivery of bioactive molecules to SVZ-NSCs.

In a previous work [13], NFL was adsorbed on the surface of lipid nanocapsules (LNCs) which are a nanoscale vector characterized by long stability (more than 18 month), FDA-approved excipients, easy scale-up, versatility (compatible with lipophilic as well as hydrophilic drugs) [14], and suitable surface functionalization (e.g. with targeting ligands) [15]. The adsorption of NFL on the LNCs did not modify the NSC-targeting property of the peptide which, on the contrary, was extended to the whole system. NFL-LNC interacts with primary SVZ-NSCs, *in vitro*, and localizes on the NSCs of the SVZ after injection in the lateral ventricle of rat, *in vivo*. The SVZ is one of the most important neurogenic regions of the CNS that is involved in the origin/development of many CNS diseases [16-18]. Thus, the targeting of this area *via* NFL-LNC would be a good opportunity to induce NSC differentiation by delivering a bioactive molecule to SVZ-NSCs.

Retinoic acid (RA) is a lipophilic molecule that modulates neurogenesis by inducing neurite outgrowth and differentiation into specialized neural cells from different cell sources, such as embryonic stem cells [19-21] and mesenchymal stem cells [22-24]. In particular, RA has been shown to induce the differentiation of pluripotent stem cells [25] and neural progenitor cells [26] in myelinating oligodendrocytes. Although RA represents a promising bioactive drug to stimulate NSC differentiation and treat demyelinating diseases [27], many factors limit its utilisation as a free molecule *in vitro*, (e.g., its low solubility in aqueous media) and *in vivo* (e.g., the progressive decline of its plasmatic concentrations). One strategy to overcome these issues is to incorporate RA into nanoparticles. For instance, RA encapsulation in nanovectors showed an enhanced therapeutic effect in the treatment of cancer [28] or ischemia [29], highlighting the interest of RA-based systems.

Thus, the objectives of this work were (i) to encapsulate RA into NFL-LNCs and (ii) to evaluate their efficacy to stimulate NSC differentiation, first *in vitro*, on primary SVZ-NSCs, and then *in vivo*, and in a rat model of brain demyelinated lesions.

4. MATERIALS AND METHODS

4.1 Materials

Biotinylated NFL-TBS.40-63 (NFL) was purchased from GeneCust (Luxembourg, Luxembourg). Labrafac® provided by Gattefosse SA (Saint-Priest, France). Lipoïd® was provided by Lipoid Gmbh (Ludwigshafen, Germany). Kolliphor HS®, L-α-Lysolecithin, poly-D-Lysine hydrobromide, retinoic acid and Rhodamine B were purchased from Sigma (Saint-Louis, Missouri). Sodium chloride (NaCl) was purchased from Prolabo (Fontenay-sous-bois, France). Primary antibody mouse anti-GalC was purchased from Merck Millipore (Billerica, Massachusetts, USA). Primary antibodies mouse anti-PAN neurofilament and mouse anti-bIII tubulin were purchased from Biolegend (San Diego, California, USA). Primary antibodyes rabbit anti-Nestin and rabbit anti-GFAP were purchased from Abcam (Cambridge, United Kingdom). Secondary antibodyes Alexa 488 anti-mouse, Alexa 488 anti-rabbit, Alexa 594 anti-mouse and Alexa 594 anti-rabbit were purchased from ThermoFisher Scientific (Waltham, Massachusetts, USA). DiD' solid; DiIC18(5) solid (1,1'-Dioctadecyl-3,3,3',3'-Tetramethylindodicarbocyanine, 4-Chlorobenzenesulfonate Salt) (DiD), DAPI, HEPES, Pen/Strept, Na Pyruvate, B27, MEM alpha (no nucleosides), 0.05 % Trypsin-EDTA (1x), DNAse and ProLong Gold antifade were purchased from Thermo Fisher Scientific. EGF was purchased from Tebu-Bio (Le Perray en Yvelines, France). CellTiter 96® AQueous One Solution Cell Proliferation Assay was purchased from Promega (Fitchburg, Wisconsin, USA). Formaldeyde solution 37% was purchased from Carl Roth (Karlsruhe, Germany). Amicon Ultra-0.5 ml 100K filters were purchased from Merck Millipore (Billerica, Massachusetts, USA). The isolation of NSC and *in vivo* experiments were performed according to Directive 2010/63/EU, to guidelines of the Belgian Government following the approval by the ethical committee for animal care of the faculty of medicine of the Université catholique de Louvain.

4.2 Preparation of RA-loaded NFL-LNCs

NFL-LNCs. Stok-LNCs were prepared following the protocol developed by Heurtault et al. [30]. Briefly, Kolliphor HS15® (0.846 g), Lipoïd® (0.075 g), NaCl (0.089 g), Labrafac® (1.028 g) and water (2.962 g) were mixed under gentle magnetic stirring at 30°C for 5 min. The solution was progressively heated (90 °C) and cooled (60 °) three times. During the last cooling, cold water (12.5 g at 4 °C) was added at 72-74 °C under high speed stirring. The nanoparticles were filtered by 0.2 μm filter and stored at 4°C. NFL-LNCs were produced by incubating 369 μl of 1 mM peptide solution (in water) overnight with 1 ml of stock-LNC

under gently stirring while LNCs without peptide were produced incubating 369 µl of water. LNC concentration: 126 mg/ml of nanoparticles. NFL-LNC concentration: 270 µM NFL + 126 mg/ml of nanoparticles.

RA-loaded NFL-LNCs. RA was loaded into LNCs by adding 50 µl of RA stock solution (20 mg/ml in DMSO) at 75 °C during the last cooling of LNC preparation. RA-loaded NFL-LNCs were produced by following the same protocol as for NFL-LNCs. The concentration of RA-loaded LNC stock solution was 400 µM RA + 126 mg/ml of nanoparticles and of RA-loaded NFL-LNC stock solution was 400 µM RA + 270 µM NFL + 126 mg/ml of nanoparticles.

4.3 Characterization of LNC

Size, ζ-potential and PDI of nanoparticles were characterized using a Malvern Zetasizer Nano ZS (Malvern Instruments). For the measurement of size and PDI, samples were diluted 1/100 (v/v) in water. For the measurement of ζ-potential, samples were diluted 1/100 (v/v) in NaCl 10 mM.

4.4 Isolation of SVZ-NSCs

SVZ-NSCs were isolated according to a protocol described by Guo et al. [31]. Briefly rats from 5 day-old or 2 month-old were sacrificed by decapitation. The brain was removed and put in dissection buffer (1.25 ml of D-glucose 1 M, 750 µl of HEPES and 500 µl Pen/Strept in 50 ml of HBSS medium). The brain was cut into coronal sections of 400 µm and the SVZ was dissected and placed in 1 ml of dissection buffer. The tissue was centrifuged for 5 min at 344 g. The supernatant was removed to add 1 ml of stem cell culture medium (1.25 ml of D-glucose 1 M, 750 µl of HEPES, 500 µl Pen/Strept, 500 µl Na Pyruvate, 500 µl of B27 and 10 ng/ml of EGF in 50 ml of MEM alpha no nucleosides medium). The pellet was vortexed and mechanically triturated using a 26 G needle. The cells were seeded at $2*10^5$ cells/Petri 60 mm in 5 ml of cell culture medium. Either neurospheres or dissociated cells have been used during this study, depending on the aim of the experiment.

4.5 Impact of RA-loaded NFL-LNCs on SVZ-NSC viability

Five days after isolation, neurospheres corresponding to $3*10^5$ SVZ-NSCs/ml were incubated for 1 h at 37 °C with RA-loaded NFL-LNCs or their controls (PBS, NFL, LNCs, NFL-LNCs, RA and RA-LNCs) diluted 1/100 from stock solutions (final concentrations RA 4 µM, NFL 2.7 µM, LNCs 1.26 mg/ml, NFL-LNCs NFL 2.7 µM+ 1.26 mg/ml LNCs, RA-loaded LNCs

RA 4 μM + 1.26 mg/ml LNCs, RA-loaded NFL-LNCs RA 4 μM + 2.7 μM NFL + 1.26 mg/ml LNCs). Then, the neurospheres were washed, dissociated by using a 26 G needle, and seeded at $3*10^5$ cells/ml on poly-D-Lysine hydrobromide (0.1 mg/ml in water) coated 96-well plates. Cell viability was measured after 1h, 2 days and 7 days using the CellTiter 96® AQueous One Solution Cell Proliferation assay as per supplier instructions.

4.6 Effect of RA-loaded NFL-LNCs on SVZ-NSC self-renewal

Five days after isolation, neurospheres were treated as described in 4.5. Then, the neurospheres were seeded in 24-well plates at $3*10^5$ cells/ml or dissociated using a 26 G needle and seeded either at $3*10^5$ cells/ml (1st observation) or $1.5*10^5$ (2nd observation) on poly-L-Lysine coated 24-well plates. Evaluation of SVZ-NSC self-renewal was performed 2 and 7 days after the treatment.

Un-dissociated neurospheres were counted manually using bright-filter microscopy (Evos XL Core, Thermo Fisher Scientific). At least, 3 pictures/condition were taken.

Dissociated SVZ-NSCs were fixed with 4 % PFA for 10 min, treated 1 h with Triton 0.05% in BSA 1% and incubated overnight with mouse anti-Nestin (1/250) primary antibody in BSA 1%. The cells were incubated 2 h with Alexa 488 (1/400) anti-mouse secondary antibody in PBS and mounted with VECTASHIELD® antifade mounting medium (Vector Laboratories, Burlingame, California, USA). An EVOS fluorescent microscope was used to take at least 3 pictures/conditions. Nestin+ cells were counted manually.

4.7 Influence of RA-loaded NFL-LNCs on SVZ-NSC differentiation

Five days after isolation, neurospheres were treated as described in 4.5. Then, the neurospheres were dissociated by using a 26 G needle and seeded either at $3*10^5$ cells/ml (1st observation) or $1.5*10^5$ (2nd observation)on poly-D-Lysine hydrobromide coated 24-well plates.

Two days after treatment, SVZ-NSCs were fixed with 4 % PFA for 10 min, treated 1 h with Triton 0.05% in BSA 1% and incubated overnight with rabbit anti-GFAP (1/1000) and mouse anti-βIII tubulin (1/1000) primary antibodies in BSA 1%. The cells were incubated 2 h with Alexa 488 (1/400) anti-mouse and Alexa 594 (1/400) anti-rabbit secondary antibodies in PBS.

Seven days after the treatment, SVZ-NSCs were fixed with 4 % PFA for 10 min, treated 1 h with Triton 0.05% in BSA 1% for 30 and incubated overnight with (separately) mouse anti-pan-neurofilament (panNF) (1/500) and mouse anti-GalC (1/500) primary antibodies in BSA

1%. The cells were incubated 2 h with Alexa 488 anti-mouse (1/400) and Alexa 594 (1/400) anti-mouse secondary antibodies in PBS.

Samples were then mounted with VECTASHIELD® antifade mounting medium and pictures were acquired with an EVOS fluorescent microscope (at least 3 pictures/conditions). PanNF$^+$ and GalC$^+$ cells were counted manually.

4.8 Impact of RA-loaded NFL-LNCs on a focal brain white matter demyelinated lesion

Demyelinating lesion was induced in the caudoputamen of 2 month-old female Wistar rats by stereotaxic injection in the right caudate putamen (ML: +2.1; AP: -0.8; DV: +4) of 2 µl of 1% lysolecithin (0.5 µl/min) in PBS using a Harvard apparatus (Holliston, Massachusetts). Three days after the lesion, the rats received 20 µl of RA-loaded NFL-LNCs (400 µM RA + 270 µM NFL + 126 mg/ml LNCs) (0.5 µl/min) or their controls by a second stereotaxic injection in the right lateral ventricle (ML: +1.5; AP: -0.8; DV: +4). Five days after the treatment (7 days after the lesion), the animals were sacrificed by overdose of isoflurane and intracardially perfused with 4% paraformaldehyde in NaCl buffer. Brains were recovered, post-fixed 6 hours and cryoprotected in 30% sucrose before storage at −80 °C in OCT.

The impact of RA-loaded NFL-LNCs on focal brain white matter demyelinated lesion will be evaluated on 20-µm brain section by comparing the number of oligodendrocytes (Olig1 and Olig2$^+$ cells) and the amount of myelin (MAG and MBP$^+$ cells) in brains treated with the controls and with RA-loaded NFL-LNCs. This is currently ongoing.

4.9 Statistical analyses

All experiments were repeated at least 3 times. Error bars represent standard error of the mean (SEM). p* < 0.05, p** < 0.01 and p*** < 0.001 were calculated with Mann-Whitney test or with ANOVA one-way (Bonferroni correction to take into account the test multiplicity) by using Prism 5.00 (GraphPad software, San Diego, CA).

5. RESULTS AND DISCUSSION

5.1 Characterization of LNCs

Table 1. Physiochemical characteristics of the nanoparticles

	size (nm)	PDI	ζ-potential (mV)
LNCs	57 ± 4	0.027	-8.5 ± 1.5
NFL-LNCs	65 ± 4	0.175	-4.2 ± 0.5
RA-loaded LNCs	55 ± 3	0.093	-11.0 ± 2.5
RA-loaded NFL-LNCs	63 ± 4	0.2	-15 ± 6

Size and PDI were characterized by DLS diluting the nanoparticles 1/100 (v/v) in water. The ζ-potential was measured by diluting the nanoparticles 1/100 (v/v) in NaCl 10 mM. N=3, n=3

LNCs had a size of 57 nm ± 4 , a PDI of 0.027 and a ζ-potential of -8.5 mV ± 1.5 while the adsorption of NFL increased LNC size (+ 8 nm) and PDI as well as ζ-potential (+ 4 mV) (Table 1), as previously observed [22]. RA encapsulation did not influence LNC size and PDI but slightly decreased ζ-potential values (p > 0.05).

5.2 Impact of RA-loaded NFL-LNCs on SVZ-NSC viability

Cell viability was evaluated 1 hour, 2 days and 7 days after SVZ-NSCs incubation. These time points were chosen to investigate acute (1 h) and chronic (2 d and 7 d) effect during the evaluation of NSC self-renewal and differentiation. LNC concentrations were selected below the threshold of toxicity [13].

None of the treatments had major effects on NSC viability (Figure 1A) as well as RA-loaded NFL-LNCs at higher concentration (1/50) (Figure 1B).
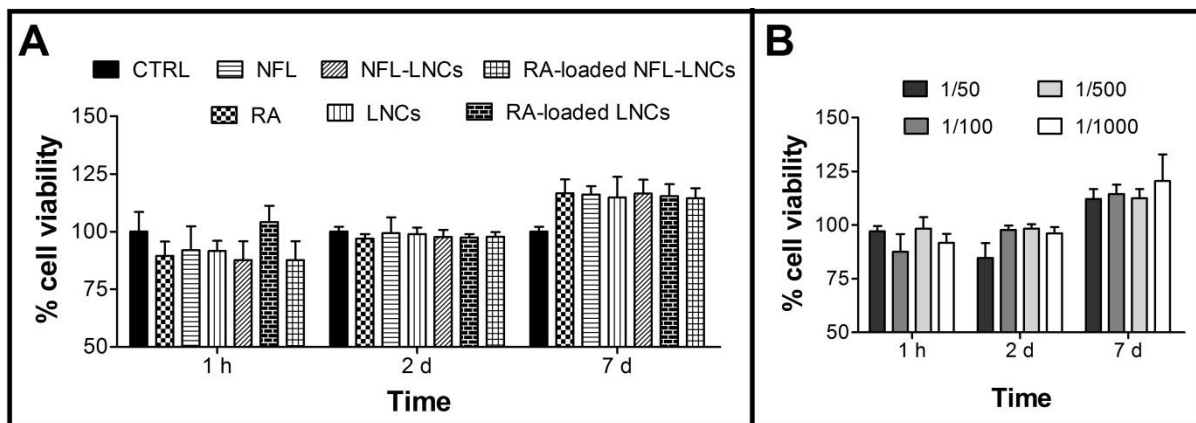

Figure 1: Impact of RA-loaded NFL-LNCs or their controls on NSC viability. A: viability of SVZ-NSCs incubated 1 hour with different treatments: RA (4 μM), NFL (2.7 μM), LNCs (1.26 mg/ml), NFL-LNCs (2.7

µM NFL + 1.26 mg/ml LNCs), RA-loaded LNCs (4 µM RA + 1.26 mg/ml LNCs) and RA-loaded NFL-LNCs (4 µM RA + 2.7 µM NFL and 1.26 mg/ml LNCs). The evaluation was performed 1 hour, 2 days and 7 days after the incubation by MTS. B: viability of SVZ-NSCs incubated 1 hour with RA-loaded NFL-LNCs (400 µM RA + 270 µM NFL + 126 mg/ml LNCs) at different dilutions (1/50, 1/100, 1/500 and 1/1000). The evaluation was performed 1 hour, 2 days and 7 days after the incubation by MTS assay. N=3, n=3. (p > 0.05).

5.3 RA-loaded NFL-LNCs modulate SVZ-NSC self-renewal

RA, NFL, NFL-LNCs and RA-loaded NFL-LNCs significantly decreased the number of neurospheres after 2 days (Figure 2A). After 7 days, NFL, NFL-LNCs and RA-loaded NFL-LNCs but not RA anymore significantly reduced the percentage of neurospheres (Figure 2B). The highest decrease was observed for NFL-LNCs at 2 days post-treatment but the percentage of neurospheres was not significantly lower anymore for this condition after 7 days.

Self-renewal is the ability of stem cells to proliferate by maintaining an undifferentiated state and its loss typically accompanies stem cell differentiation into specialized cells [32]. The negative impact of NFL on the neurosphere-forming property was already observed in SVZ-NSCs [11] while the effect of RA on those cells was not described before, to the extent of our knowledge. The reduction of self-renewal was higher 2 days than 7 days after the treatments, suggesting the capacity of NSCs to partially recover their property. Only NFL, NFL-LNCs and RA-loaded NFL-LNCs kept their negative modulation on SVZ-NSC self-renewal probably due to the presence of the peptide either as free molecule or associated to LNCs (NFL-LNCs and RA-loaded NFL-LNCs).

Another indication of NSC differentiation was the decrease of the percentage of Nestin$^+$ cells (Figure 2C-D, Figure 1S). NFL-LNCs and RA-loaded NFL-LNCs significantly decreased the number of Nestin$^+$ cells after 2 (Figure 2C) and 7 days (Figure 2D), while the other treatments showed no major effect.

The absolute number of neurospheres and Nestin$^+$ cells decreased from the 1st to the 2nd (-20% and -15% respectively) observation due to the percentage of NSCs that differentiate during cultivation [33].

Important *in vitro* NSC characteristics such as the capacity to form neurospheres [34] and to express Nestin [35] are indicators of the balance proliferation-differentiation. The reduction of those characteristics was an indication of SVZ-NSC transition from the undifferentiated state to the differentiating state. Thus, NFL-LNCs and RA-loaded NFL-LNCs would induce NSC differentiation.
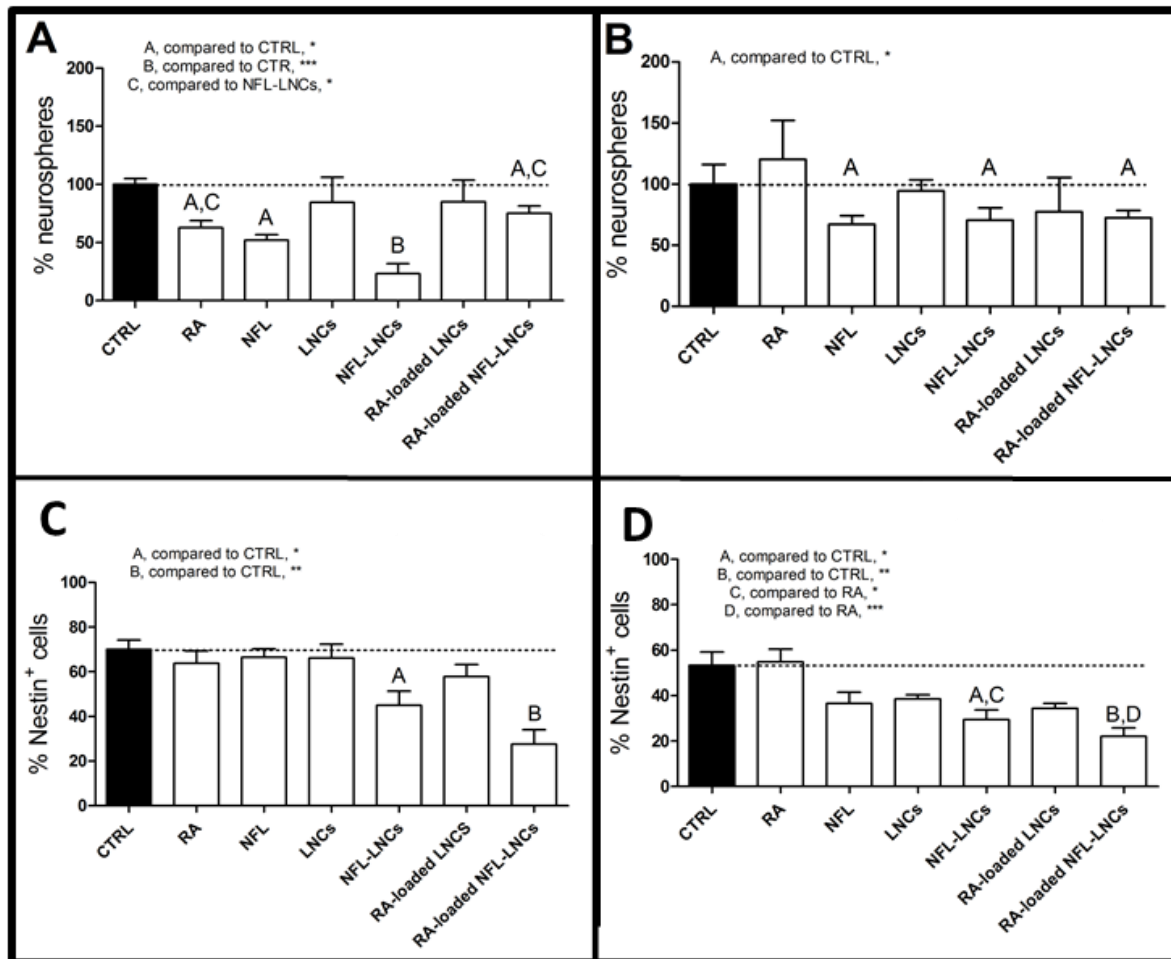
Figure 2: Impact of RA-loaded NFL-LNCs on SVZ-NSC self-renewal. SVZ-NSCs have been incubated 1 hour with different treatments: RA (4 μM), NFL (2.7 μM), LNCs (1.26 mg/ml), NFL-LNCs (2.7 μM NFL + 1.26 mg/ml LNCs), RA-loaded LNCs (4 μM RA + 1.26 mg/ml LNCs) and RA-loaded NFL-LNCs (4 μM RA + 2.7 μM NFL and 1.26 mg/ml LNCs). A: number of neurospheres 2 day after the treatment. B: number of neurospheres 7 days after the treatment. C: percentage of Nestin$^+$ cells 2 days after the treatment. D: percentage of Nestin$^+$ cells 7 days after the treatment. . $p^* < 0.05$, $p^{**} < 0.01$, $p^{***} < 0.001$ compared to CTRL. One-way ANOVA test. N=4. n=2 for A and B. N=4, n=3 for C and D.

5.4 RA-loaded NFL-LNCs affect SVZ-NSC differentiation

β III Tubulin is a marker associated to early neuronal developmental stages while neurofilaments (NF) and galactocerebroside (GalC) are expressed by mature neurons and

oligodendrocytes, respectively [36,37]. The glial fibrillary acid protein (GFAP) is commonly used to identify mature astrocytes [38] but it is also an early marker for astroglia and oligodendroglia due to their phenotype overlap at their early stage [39].

2 day time point (1ˢᵗ observation). The impact of RA-loaded NFL-LNCs on NSC differentiation was evaluated by βIII Tubulin and GFAP immunostaining 2 days after treatment. NFL and RA-loaded NFL-LNCs significantly increased the percentage of both β III Tubulin⁺ and GFAP⁺ cells (Figure 3).

We hypothesized that RA encapsulation in LNCs would allow SVZ-NSC differentiation in GFAP⁺ and βIII Tubulin⁺ cells. Indeed, RA as a free drug shows many limitations *in vitro* such as precipitation in aqueous media and adsorption on glass and plastic wares.

RA-loaded NFL-LNC significantly increased the percentage of GFAP⁺ cells compared to free RA but not to RA-loaded LNCs. GFAP⁺ cells induced by RA-loaded LNCs could be due to the RA carried into the cells *via* the small amount of un-functionalized LNCs (10%) able to penetrate SVZ-NSCs [13]. An increase of βIII Tubulin⁺ cells was observed when NSCs were treated with NFL and RA-loaded NFL-LNC. We propose that the highest percentage of GFAP⁺ and βIII Tubulin⁺ cells observed when NSCs were treated with RA-loaded NFL-LNCs could be due to a synergetic effect between NFL and RA. The ability of NFL to induce NSC differentiation towards oligodendrocyte and neuronal phenotypes has already been reported [11]. Consequently, the effect on both markers is not surprising as well as the low percentage of GFAP⁺ cells induced by NFL-LNC could be due to the presence of the peptide on LNC surface.

We thus hypothesised that RA-loaded NFL-LNCs showed higher percentage of GFAP⁺ cells compared to NFL probably because of the synergy between NFL and RA. It would be interesting to test the effect of RA-loaded LNCs in presence of NFL to confirm this hypothesis.

Figure 3: Impact of RA-loaded NFL-LNC on SVZ-NSC differentiation in GFAP$^+$ and β III$^+$ cells evaluated at 2 day time point. SVZ-NSCs have been incubated 1 hour with different treatments: RA (4 μM), NFL (2.7 μM), LNCs (1.26 mg/ml), NFL-LNCs (2.7 μM NFL + 1.26 mg/ml LNCs), RA-loaded LNCs (4 μM RA + 1.26 mg/ml LNCs) and RA-loaded NFL-LNCs (4 μM RA + 2.7 μM NFL and 1.26 mg/ml LNCs). Cell were immunostained for GFAP (green), β III Tubulin (red) and DAPI (blue). The number of positive cells has been counted manually. p* < 0.05, p** < 0.01, p*** < 0.001. One way ANOVA test (Bonferroni post-test). N=4, n=3.

7 day time point. The percentage of GFAP$^+$ and GalC$^+$ cells was evaluated 7 days after treatment. The percentage of GalC$^+$ cells significantly increased after incubation with RA-loaded NFL-LNCs (Figure 4A) while no significant effect was observed for the other treatments. Moreover, SVZ-NSCs treated with RA-loaded NFL-LNCs presented morphology similar to immature oligodendrocytes 7 days after treatment (Figure 4B). The percentage of GFAP$^+$ cells was not significantly impacted whatever the condition ($p > 0.05$), even if treatment of NSCs with RA-loaded LNCs and RA-NFL-LNCs tended to reduce the percentage of GFAP$^+$ cells while treatments with RA, NFL, LNCs and NFL-LNCs tended to increase the number of GFAP$^+$ cells (Figure 4A). Compared to the observation performed 2 day after the treatment, the percentage of GFAP$^+$ increased for the CTRL (from 4 to 12%). The co-expression of both markers remained below 15% for all conditions.
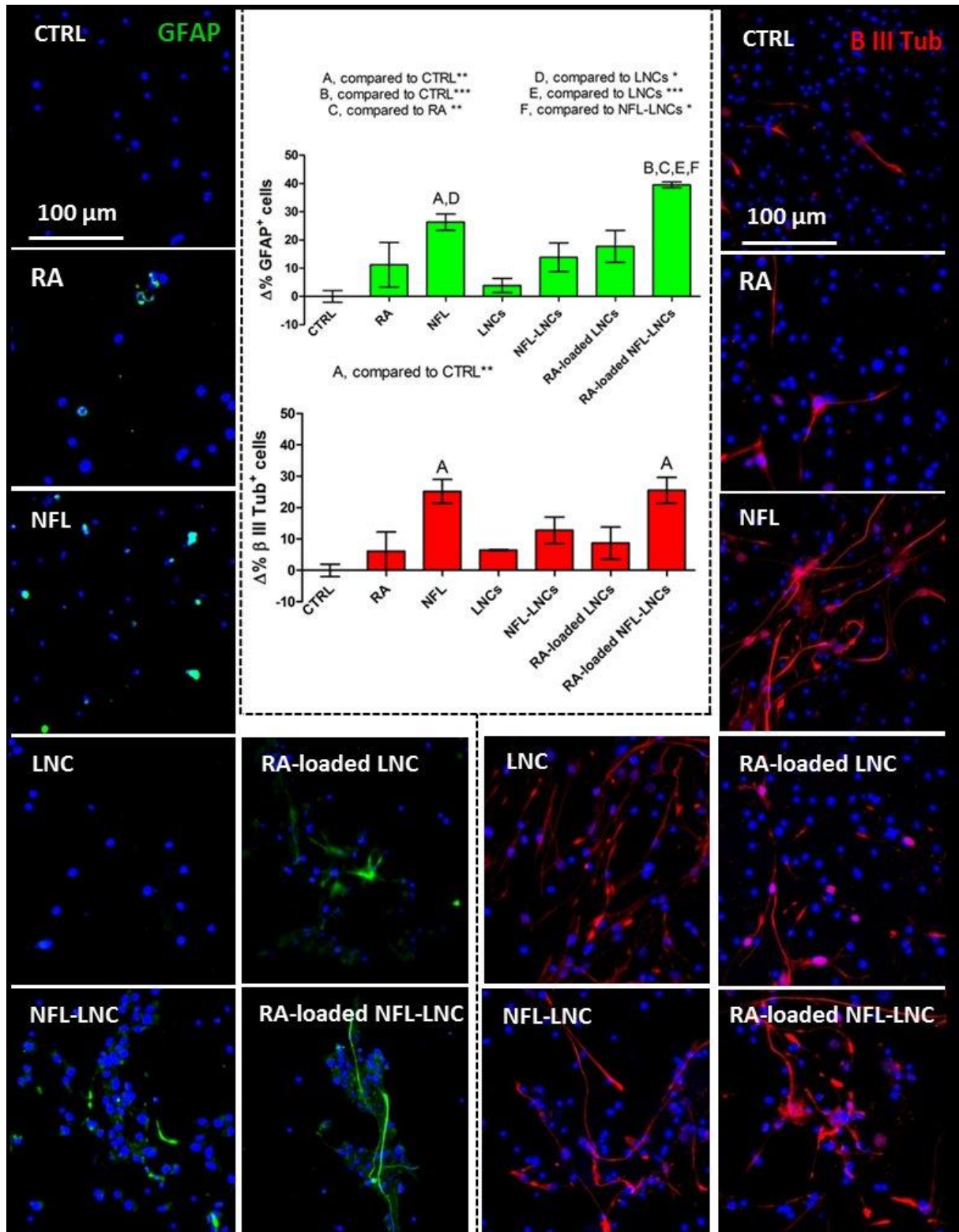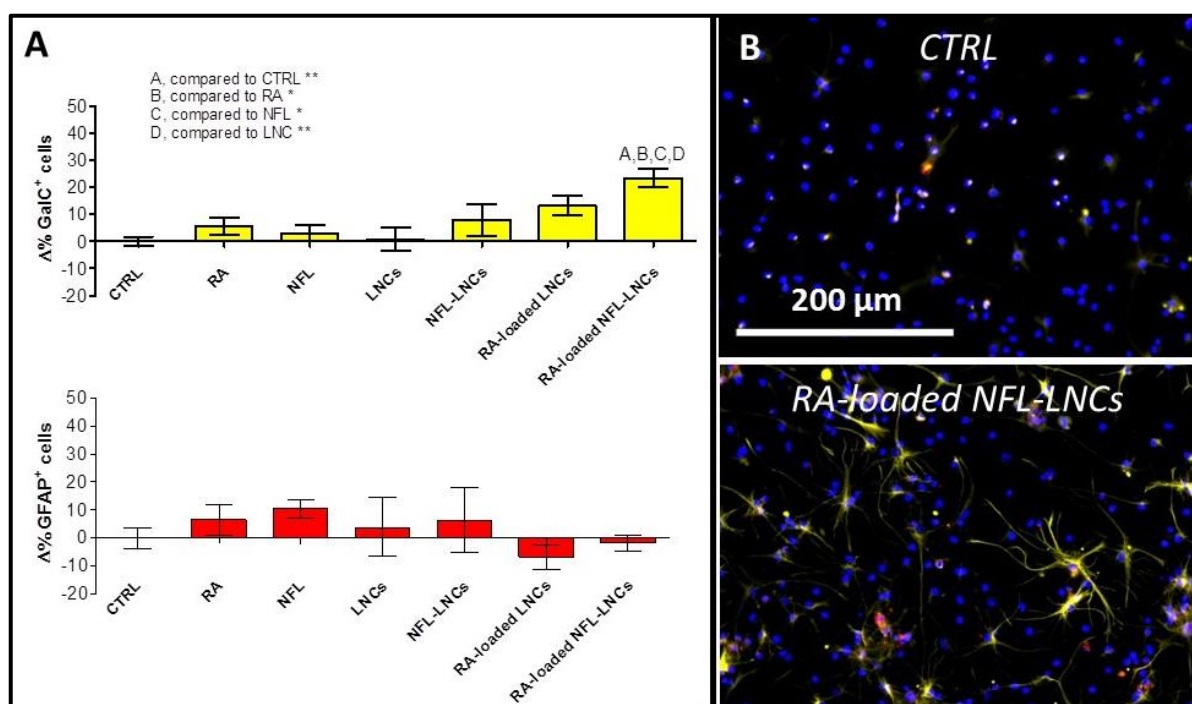

Figure 4: Impact of RA-loaded NFL-LNC on SVZ-NSC differentiation in GFAP$^+$ and GalC$^+$ cells evaluated at 7 day time point. SVZ-NSCs have been incubated 1 hour with different treatments: RA (4 μM), NFL (2.7 μM), LNCs (1.26 mg/ml), NFL-LNCs (2.7 μM NFL + 1.26 mg/ml LNCs), RA-loaded LNCs (4 μM RA + 1.26 mg/ml LNCs) and RA-loaded NFL-LNCs (4 μM RA + 2.7 μM NFL and 1.26 mg/ml LNCs). Cells were immunostained for GalC (yellow), GFAP (red) and DAPI (blue). A: the number of GalC$^+$, GFAP$^+$ and GalC/GFAP$^+$ cells after treatment. $p^* < 0.05$, $p^{**} < 0.01$, $p^{***} < 0.001$ compared to CTRL. One-way ANOVA test. N=4, n=3. B: confocal imaging of SVZ-NSCs treated with RA-loaded NFL-LNCs compared to non-treated cells.

NF immunostaining was performed to measure the percentage of neuron-like cells 7 days after the treatment of SVZ-NSCs but no neuron was detected whatever the condition (Figure

2S). Longer treatments and late observations could be necessary to detect the neuronal phenotype [40]

Although self-renewal and differentiation properties were evaluated on 5-day old rat NSCs, RA-loaded NFL-LNCs incubated with SVZ-NSCs either from 5-day old or from 2-month old rats did not show any significant difference in the percentage of GalC$^+$ cells (Figure 3S). Moreover, decreasing concentration of RA-loaded NFL-LNCs induced lower NSC differentiation into oligodendrocytes (Figure 4S).

The evaluation of the differentiation has been performed by immunostaining with early and mature specialized cell markers to observe the development of the process over time. The "2 days" time point was chosen because morphological modifications were already visible under bright filter light while the "7 days" time point was one of the most frequent used to detect NSC differentiation in the literature. RA-loaded NFL-LNCs increased the expression of early (GFAP and β III Tub) and mature (GalC) glial markers and, in the same time, decreased the number of neurospheres and Nestin$^+$ cells. Moreover, it had similar differentiating effect on both newborn and adult NSCs *in vitro*. Hence, RA-loaded NFL-LNCs would represent a promising system to induce SVZ-NSC differentiation into oligodendrocytes and treat demyelinating diseases. The *in vivo* proof of concept is ongoing.

6. CONCLUSION

Myelin dysfunction and oligodendrocitic loss are primarily involved in the etiology of many demyelinating CNS diseases which have high economic and social costs worldwide. The encapsulation of RA into NFL-LNCs provides a drug delivery system able to selectively interact with SVZ-NSCs and to induce their differentiation into the oligodendrocyte lineage *in vitro*. RA-loaded NFL-LNC represents a promising tool to treat demyelinating disease *via* endogenous NSC differentiation. The impact of RA-loaded NFL-LNCs on focal brain white matter demyelinating lesion in under evaluation.

7. REFERENCES

[1] Vadakkan, Kunjumon I. "Neurodegenerative disorders share common features of "loss of function" states of a proposed mechanism of nervous system functions." Biomedicine & Pharmacotherapy 83 (2016): 412-430.

[2] Barnham, Kevin J., Colin L. Masters, and Ashley I. Bush. "Neurodegenerative diseases and oxidative stress." Nature reviews Drug discovery 3.3 (2004): 205-214.

[3] Fünfschilling, Ursula, et al. "Glycolytic oligodendrocytes maintain myelin and long-term axonal integrity." Nature 485.7399 (2012): 517-521.

[4] Ettle, Benjamin, Johannes CM Schlachetzki, and Jürgen Winkler. "Oligodendroglia and myelin in neurodegenerative diseases: more than just bystanders?." Molecular neurobiology 53.5 (2016): 3046-3062.

[5] Vishwakarma, Sandeep K., et al. "Current concept in neural regeneration research: NSCs isolation, characterization and transplantation in various neurodegenerative diseases and stroke: A review." Journal of advanced research 5.3 (2014): 277-294.

[6] Murrell, Wayne, et al. "Expansion of multipotent stem cells from the adult human brain." PloS one 8.8 (2013): e71334. (2013): e71334.

[7] Carradori, Dario, et al. "The therapeutic contribution of nanomedicine to treat neurodegenerative diseases via neural stem cell differentiation." Biomaterials 123 (2017): 77-91.

[8] Herberts, Carla A., Marcel SG Kwa, and Harm PH Hermsen. "Risk factors in the development of stem cell therapy." Journal of translational medicine 9.1 (2011): 29.

[9] Simonson, Oscar E., et al. "The safety of human pluripotent stem cells in clinical treatment." Annals of medicine 47.5 (2015): 370-380.

[10] Bocquet, Arnaud, et al. "Neurofilaments bind tubulin and modulate its polymerization." Journal of Neuroscience 29.35 (2009): 11043-11054.

[11] Lépinoux-Chambaud, Claire, Kristell Barreau, and Joël Eyer. "The Neurofilament-Derived Peptide NFL-TBS. 40-63 Targets Neural Stem Cells and Affects Their Properties." Stem cells translational medicine 5.7 (2016): 901-913.

[12] Berges, Raphael, et al. "Structure-function analysis of the glioma targeting NFL-TBS. 40-63 peptide corresponding to the tubulin-binding site on the light neurofilament subunit." PloS one 7.11 (2012): e49436.

[13] Carradori, Dario, et al. "NFL-lipid nanocapsules for brain neural stem cell targeting in vitro and in vivo." Journal of Controlled Release 238 (2016): 253-262.

[14] Huynh, Ngoc Trinh, et al. "Lipid nanocapsules: a new platform for nanomedicine." International journal of pharmaceutics 379.2 (2009): 201-209.

[15] Béduneau, Arnaud, et al. "Design of targeted lipid nanocapsules by conjugation of whole antibodies and antibody Fab'fragments." Biomaterials 28.33 (2007): 4978-4990.

[16] Curtis, Maurice A., Richard LM Faull, and Peter S. Eriksson. "The effect of neurodegenerative diseases on the subventricular zone." Nature Reviews Neuroscience 8.9 (2007): 712-723

[17] Gonzalez-Perez, Oscar, and Arturo Alvarez-Buylla. "Oligodendrogenesis in the subventricular zone and the role of epidermal growth factor." Brain research reviews 67.1 (2011): 147-156.

[18] Maki, Takakuni, et al. "Mechanisms of oligodendrocyte regeneration from ventricular-subventricular zone-derived progenitor cells in white matter diseases." Frontiers in cellular neuroscience 7 (2013): 275.

[19] Corcoran, J.; Maden, M. Nerve growth factor acts via retinoic acid synthesis to stimulate neurite outgrowth. Nature neuroscience 1999, 2 (4), 307-308.

[20] Bain, G.; Ray, W. J.; Yao, M.; Gottlieb, D. I. Retinoic acid promotes neural and represses mesodermal gene expression in mouse embryonic stem cells in culture. Biochemical and biophysical research communications 1996, 223 (3), 691-694.

[21] Okada, Y.; Shimazaki, T.; Sobue, G.; Okano, H. Retinoic-acid-concentration-dependent acquisition of neural cell identity during in vitro differentiation of mouse embryonic stem cells. Developmental biology 2004, 275 (1), 124-142.

[22] Gong, M.; Bi, Y.; Jiang, W.; Zhang, Y.; Chen, L.; Hou, N.; Chen, J.; Li, T. Retinoic acid receptor beta mediates all-trans retinoic acid facilitation of mesenchymal stem cells neuronal differentiation. The international journal of biochemistry & cell biology 2013, 45 (4), 866-875.

[23] Zhang, S.; Chen, X.; Hu, Y.; Wu, J.; Cao, Q.; Chen, S.; Gao, Y. All-trans retinoic acid modulates Wnt3A-induced osteogenic differentiation of mesenchymal stem cells via activating the PI3K/AKT/GSK3 signalling pathway. Molecular and cellular endocrinology 2016, 422, 243-253.

[24] Su, Z. y.; Li, Y.; Zhao, X. l.; Zhang, M. All-trans retinoic acid promotes smooth muscle cell differentiation of rabbit bone marrow-derived mesenchymal stem cells. Journal of Zhejiang University Science B 2010, 11 (7), 489-496.

[25] Douvaras, Panagiotis, et al. "Efficient generation of myelinating oligodendrocytes from primary progressive multiple sclerosis patients by induced pluripotent stem cells." Stem Cell Reports 3.2 (2014): 250-259.

[26] Davis, Scott F., et al. "Isolation of adult rhesus neural stem and progenitor cells and differentiation into immature oligodendrocytes." Stem cells and development 15.2 (2006): 191-199.

[27] Sharow, K. A.; Temkin, B.; Asson-Batres, M. A. Retinoic acid stability in stem cell cultures. International Journal of Developmental Biology 2012, 56 (4), 273-278.

[28] Huang, Hai, et al. "Co-delivery of all-trans-retinoic acid enhances the anti-metastasis effect of albumin-bound paclitaxel nanoparticles." Chemical Communications 53.1 (2017): 212-215.

[29] R. Ferreira, M.C. Fonseca, T. Santos, J. Sargento-Freitas, R. Tjeng, F. Paiva, M. Castelo-Branco, L. Ferreira, L. Bernardino, Retinoic acid-loaded polymeric nanoparticles enhance vascular regulation of neural stem cell survival and differentiation after ischaemia, Nanoscale 8 (2016) 8126-8137.

[30] Heurtault B, Saulnier P, Pech B, Proust JE, Richard J, & Benoit JP. Lipidic nanocapsules: preparation process and use as Drug Delivery Systems. Patent No. WO02688000.

[31] Guo, Weixiang, et al. "Isolation of multipotent neural stem or progenitor cells from both the dentate gyrus and subventricular zone of a single adult mouse." Nature protocols 7.11 (2012): 2005-2012.

[32] Ito, Keisuke, and Toshio Suda. "Metabolic requirements for the maintenance of self-renewing stem cells." Nature reviews Molecular cell biology 15.4 (2014): 243-256.

[33] Xiong, Fangling, et al. "Optimal time for passaging neurospheres based on primary neural stem cell cultures." Cytotechnology 63.6 (2011): 621-631.

[34] Pastrana, Erika, Violeta Silva-Vargas, and Fiona Doetsch. "Eyes wide open: a critical review of sphere-formation as an assay for stem cells." Cell stem cell 8.5 (2011): 486-498.

[35] Johansson, Clas B., et al. "Identification of a neural stem cell in the adult mammalian central nervous system." Cell 96.1 (1999): 25-34.

[36] Sayegh, Ayman I., and Robert C. Ritter. "Morphology and distribution of nitric oxide synthase-, neurokinin-1 receptor-, calretinin-, calbindin-, and neurofilament-M-immunoreactive neurons in the myenteric and submucosal plexuses of the rat small intestine." The Anatomical Record Part A: Discoveries in Molecular, Cellular, and Evolutionary Biology 271.1 (2003): 209-216.

[37] Ranscht, B., et al. "Development of oligodendrocytes and Schwann cells studied with a monoclonal antibody against galactocerebroside." Proceedings of the National Academy of Sciences 79.8 (1982): 2709-2713.

[38] Xu, Kexing, et al. "Glial fibrillary acidic protein is necessary for mature astrocytes to react to β- amyloid." Glia 25.4 (1999): 390-403.

[39] Badrah Alghamdi, Robert Fern. "Phenotype overlap in glial cell populations: astroglia, oligodendroglia and NG-2 (+) cells." Frontiers in neuroanatomy 9 (2015).

[40] Mahabadi, Vahid Pirhajati, et al. "In Vitro Differentiation of Neural Stem Cells into Noradrenergic-Like Cells." International journal of molecular and cellular medicine 4.1 (2015): 22.

8. SUPPLEMENTARY DATA
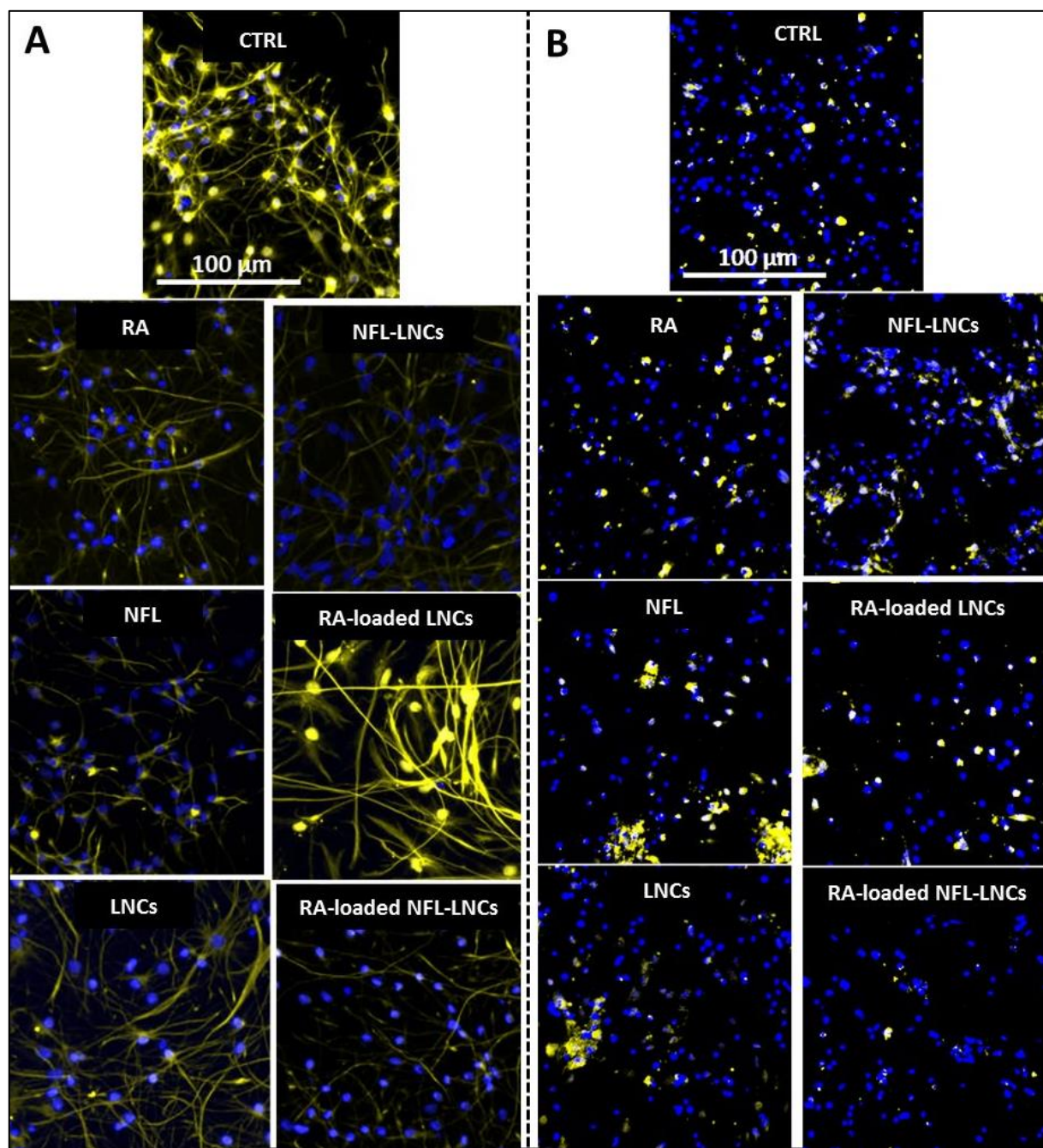
Figure 1S: Impact of RA, NFL, LNCs, NFL-LNCs, RA-loaded LNCs and RA-loaded NFL-LNC on the percentage of Nestin+ cells. SVZ-NSC have been incubated 1 hour with different compounds (RA 4 µM, NFL 2.7 µM, LNCs 1.26 mg/ml, NFL-LNCs NFL 2.7 µM+ 1.26 mg/ml LNCs, RA-loaded LNCs RA 4 µM + 1.26 mg/ml LNCs, RA-loaded NFL-LNCs RA 4 µM + 2.7 µM NFL + 1.26 mg/ml LNCs). The immunostaining was performed 2 days (A) and 7 days (B) after the treatment. Blue: DAPI, nucleus. Yellow, Alexa 488, Nestin. Scale barr: 100 µm.
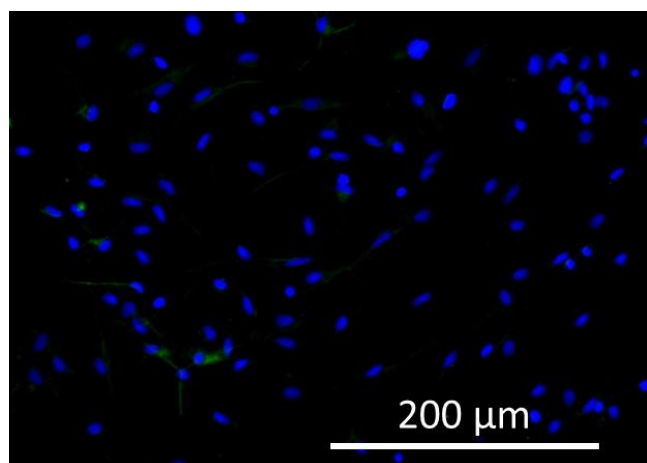
Figure2S: representative picture of NF expression in SVZ-NSC 7 days after treatment. SVZ-NSCs have been incubated 1 hour with different compounds (RA 4 μM, NFL 2.7 μM, LNCs 1.26 mg/ml, NFL-LNCs NFL 2.7 μM+ 1.26 mg/ml LNCs, RA-loaded LNCs RA 4 μM + 1.26 mg/ml LNCs, RA-loaded NFL-LNCs RA 4 μM + 2.7 μM NFL + 1.26 mg/ml LNCs) and immunostained for NF (green) and DAPI (blue).
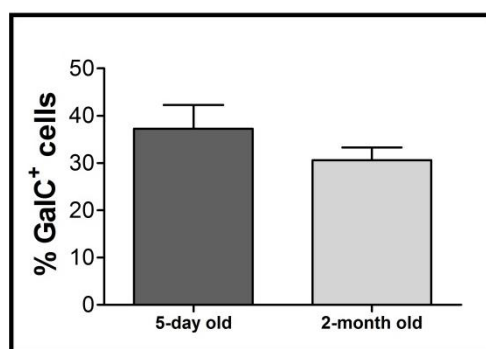
Figure3S: GalC expression in SVZ-NSC isolated from 5-day old and 2-month old rats 7 days after treatment. Both types of SVZ-NSCs have been incubated 1 hour with RA-loaded NFL-LNCs (RA 4 μM + 1.26 mg/ml LNCs, RA-loaded NFL-LNCs RA 4 μM + 2.7 μM NFL + 1.26 mg/ml LNCs) and immunostained for GalC. The number of GalC$^+$ was evaluated by manual counting. N=3, n=3.
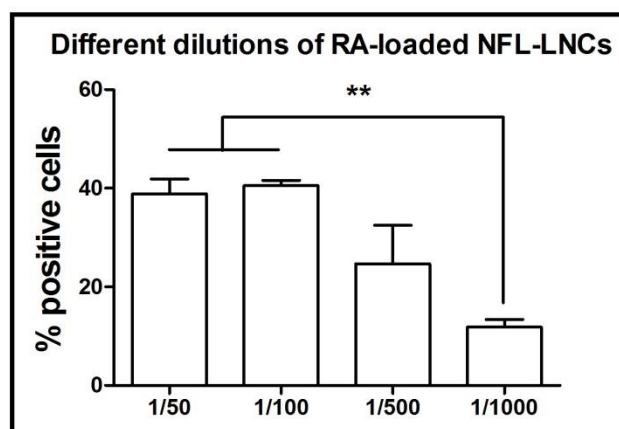
Figure4S: GalC expression in SVZ-NSCs treated with RA-loaded NFL-LNCs at different concentrations. SVZ-NSCs have been incubated 1 hour with RA-loaded NFL-LNCs (400 µM RA + 270 µM NFL + 126 mg/ml LNCs) at different dilutions (1/50, 1/100, 1/500 and 1/1000). Cells were immunostained for GalC. The number of GalC$^+$ was evaluated by manual counting. N=3.

Discussion

As reviewed in the introduction of this manuscript, the discovery of neural stem cells (NSCs) and their contribution in the neurogenesis process has represented a step forward in the regenerative medicine of the central nervous system (CNS). NSCs can undergo self-renewal and differentiate into specialized neural cells such as neurons, astrocytes and oligodendrocytes. Consequently, NSCs have been investigated to replace loss or lesioned neuronal cells and to treat neurodegenerative diseases *via* their differentiation property. Several NSC-based strategies have been developed which basically depend on whether the differentiation is designed to occur after transplantation of *in vitro* cultivated exogenous NSCs or *in situ* after endogenous NSC stimulation.

The exogenous NSC-based strategy shows many limitations derived either from the *in vitro* manipulation of the cells (e.g., risk of contaminations and genetic modifications) or from their *in vivo* transplantation (e.g., viability and immunoreactions). Endogenous NSC-based approach would avoid all of these issues aiming at directly stimulating the NSCs present in the niches of the CNS. Unfortunately, the lack of NSC-targeting molecules primarily promoted non-selective drugs/systems which limited the medical translation.

A system able to target endogenous NSCs and to induce their differentiation *in situ* would represent a promising therapeutic tool for the treatment of neurodegenerative diseases. Moreover, it would increase the efficacy and the safety of the treatments by enhancing the localized drug delivery and, consequently, by limiting the side effects.

The aim of this work was to contribute to the development of neural stem cell (NSC)-based therapy by providing a drug delivery system able both to target endogenous NSCs and to induce their differentiation *in situ*.

The goals of this thesis were i) to produce and characterize a drug delivery system targeting NSCs, ii) to investigate the mechanism behind the selective interaction NSCs-drug delivery system and iii) to induce endogenous NSC differentiation *in situ* by delivering a bioactive molecule.

1. MAIN ACHIEVEMENTS

We provided a drug delivery system penetrating neural stem cells of the subventricular zone *in vitro* and co-localizing with Nestin^{+} cells after intra-lateral ventricle injection in the brain *in vivo*.

Although there is no drug delivery system able to selectively target endogenous NSCs yet, several nanoparticle-based therapeutics successfully induced NSC differentiation *in vivo* (see Chapter 1, 4.4) [1-5]. Only one nanoparticle-based system showed efficient NSC targeting *in vitro* but no further information is available *in vivo* (see Chapter 1, 5.1) [6]. NFL-LNC was designed to target endogenous NSCs. Although the *in vitro* proof of principle must be strengthen (e.g. by NSC co-culture with another neural cell type), the co-localization with Nestin^{+} cells after intra-lateral ventricle injection in the brain *in vivo* is a promising result concerning the ability of NFL-LNC to selectively interact with endogenous NSCs.

1) Nanoparticle functionalization with targeting ligands can be obtained following different technics. Most of them require complex chemical manipulations of both the nanoparticle and the targeting ligand to allow their covalent and stable combination (e.g., *via* nanoparticle DSPE-PEG-maleimide post-insertion and peptide/protein thiolation [7]). NFL-TBS.40-63 (NFL) can be adsorbed on the surface of lipid nanocapsules (LNCs) by simple incubation. The functionalization is due to electrostatic interactions and the binding between NFL and LNCs is not significantly affected by the ionic force of the physiologic fluids. The major physicochemical properties of NFL-LNC are stable over the time and at different physiologic-mimicking conditions. All the excipients used for the formulation of LNCs are FDA approved for oral, topical and parenteral administration. Hence, <u>NFL-LNCs are easy to produce and suitable for *in vivo* studies</u>.

2) While it shows no interactions for NSCs of the central canal (CC-NSCs) of the spinal cord, NFL-LNC co-localizes with NSCs from the subventricular zone (SVZ-NSCs) of the brain which is one of the most neurogenic regions of the nervous system [8]. Most of the neurodegenerative diseases induce a substantial downregulation of SVZ cell proliferation. Consequently, this area is an important target for therapeutic intervention [9]. <u>The interaction with Nestin^{+} cells of the SVZ *via* NFL-LNC would offer the best opportunity to induce, in an adult organism, NSC differentiation into neural cells and to study their migration and integration into functional brain circuits</u>.

3) Due to the versatility of the carrier, NFL-LNC can deliver a wide range of molecules (lipophilic, hydrophilic and amphiphilic compounds). Many drugs have shown different impacts on NSC differentiation and most of them would be compatible with NFL-LNC. NSC differentiation could be then oriented towards specific neural cell types (neurons, astrocytes or oligodendrocytes) depending on the drug encapsulated in NFL-LNC and on the targeted disease.

Thus, NFL-LNC is a versatile tool that could potentially be translated to clinic and treat different types of neurodegenerative diseases *via* endogenous NSC differentiation.

We characterized the plasma membranes of SVZ-NSCs and CC-NSCs and we identified some of the factors regulating the selective interactions between SVZ-NSCs and NFL-LNC.

The evaluation of the plasma membrane lipid composition, fluidity and permeability represents the first physicochemical characterization of both SVZ-NSCs and CC-NSCs, to the best of our knowledge. The comparison between SVZ-NSCs and CC-NSCs, before and after incubation with NFL, LNCs and NFL-LNCs, highlighted the role of plasma membrane characteristics on the interactions between NSCs and these treatments.

1) Although there are similarities among all eukaryotic cellular membranes, each cell has peculiar plasma membrane characteristics which provide unique features [10]. Significant differences in the plasma membrane lipid composition of SVZ-NSCs and CC-NSCs were observed. Consequently, the lipid contents differently impacted fluidity and permeability of those two types of cells. On the one hand, changes in temperature and osmolarity cause plasma membrane fluidity fluctuations which are critical to the initiation of the regulatory reactions and environmental acclimation [11]. On the other hand, little variation in ceramide content would impact several cellular processes such as peptide translocation, cell proliferation, apoptosis and inflammation [12]. Consequently, SVZ-NSCs and CC-NSCs could have different regulatory mechanisms as well as sensibility to the action of the environmental stimuli. These data improve the general background of NSC biology and provide the first physicochemical characterization of SVZ-NSCs and CC-NSCs allowing the comprehension/prediction of their behavior at specific conditions.

2) The differences emerged between SVZ-NSCs and CC-NSCs provide new elements to design alternative NSC-targeting strategies. For instance, liposomal formulations have been

produced to target cancer cell plasma membranes (whose fluidity is higher than in healthy cell) and decrease tumor proliferation [13]. Plasma membrane lipid composition and physical state are peculiar characteristics to which a drug delivery system could be selectively directed.

3) NFL, LNCs and NFL-LNCs would preferentially interact with SVZ-NSCs because their plasma membrane has peculiar characteristics. Consequently, other cells with similar characteristics could be potentially targeted by NFL-LNCs. The comprehension of the interactions nanoparticle-target is required for the safe use of nanomaterials in therapy. In the event of a systemic administration of NFL-LNC, the information provided by this study could anticipate or exclude eventual out-of-target interactions allowing a safer administration of NFL-LNC.

Hence, this study contributes to the improvement of the NSC biology knowledge, it provides crucial information to produce novel NSC-targeting systems and it identifies some of the factors regulating SVZ-NSC targeting.

We induced SVZ-NSC differentiation towards oligodendrocyte lineage after treatment with retinoic acid (RA)-loaded NFL-LNCs.

Most of the nanoparticle-based drug delivery systems induce significant *in vitro* NSC differentiation after treatments longer than 8 hours (see Chapter 1, 4.4) [14,15]. RA-loaded NFL-LNC is the first treatment able to induce significant *in vitro* NSC differentiation after 1 hour only, to the extent of our knowledge.

1) RA is a commercial and inexpensive drug which is a promising neurogenesis modulator. It is loaded into LNCs by addition of this molecule into the excipient mixture. The high lipophilicity of RA assures high drug encapsulation efficiency and retention inside the LNCs. The surface functionalization with NFL is not affected by RA loading in LNCs. Thus, RA-loaded NFL-LNC is low cost and easy to produce.

2) SVZ-NSCs differentiate into immature oligodendrocytes 1 week after incubation with RA-loaded NFL-LNCs *in vitro*. Oligodendrocytes represent around 75% of all glial cells in the adult CNS and their main function is the production of myelin [16]. The lesion/loss of oligodendrocytes is related to many demyelinating diseases (e.g., multiple sclerosis) which have high social and economic costs worldwide. The possibility to replace those damaged cells *via* oligodendrocyte-oriented NSC differentiation would represent a promising therapeutic strategy to treat those neurodegenerative diseases.

3) The evaluation of the *in vivo* efficacy of RA-loaded NFL-LNC on lysolecithin demyelinated animal model is ongoing. <u>In the event that there will be a recovery/remyelination of the affected areas due to NSC differentiation, RA-loaded NFL-LNCs would represent the first system able both to target endogenous NSCs and to induce their differentiation for therapeutic purpose. Thus, the aim of this thesis would have been fully addressed.</u> In the event that no biological effect is detected, the reason should be investigated. On the one hand it could depend on the lack of correspondence between the *in vitro* and *in vivo* behavior of NSCs, already observed for many other promising therapeutic approaches. On the other hand it could be due to an inappropriate therapeutic schedule. In this case, several parameters (such as the dose of RA-loaded NFL-LNC, the number of the injections, the time-points of the treatment) could be adapted to induce a therapeutic effect.

2. PERSPECTIVES

Less invasive administration route would greatly increase the safety of NFL-LNC-based therapies.

Although intracranial injections are currently used in therapy (e.g., brain cancer), less invasive ways of administration could be explored. The intravenous administration would be suitable in those neurodegenerative diseases presenting increased blood-brain barrier (BBB) permeability (e.g., ALS [17]) which would allow NFL-LNC brain accumulation *via* passive targeting. Alternatively, the intranasal administration of lipid-based nanoparticles has been successfully performed to target the brain of PD patients [18]. Moreover, NFL-LNC targeting/accumulation in SVZ-NSCs could be improved by increasing both the half-life of the carrier (e.g., *via* LNC shell modification with longer chain PEG [19]) and the passage through the BBB (e.g., *via* focused ultrasound permeabilization [20] or BBB-crossing ligand surface functionalization [21]).

The detection of NFL-LNC during the biodistribution studies (e.g., *via* non-invasive tomographic imaging or positron emission tomography) will depend on the type of tracking agent used for LNC labelling (e.g., fluorescent [22] or radioactive [23]).

Further plasma membrane characterization would provide additional information on the interactions between NFL-LNC and cells.

Proteins have a crucial role in the transport, signaling and cell interactions with the environment [24]. Therefore, the proteomic evaluation of SVZ-NSC and CC-NSC plasma membranes would enrich the study on the factors modulating the interaction. Mass spectroscopy-based methods combined with other technics (e.g., chromatographic or 2-D electrophoresis [25]) are powerful tools for plasma membrane proteomic mapping and expression before and after incubation with NFL-LNCs. Consequently, the impact of the plasma membrane proteins on the interactions towards NFL-LNC, if any, would be revealed.

The characterization of the plasma membrane could be extended also to glioblastoma cells, which are massively penetrated by NFL-LNCs *via* active mechanisms. In this work we compared cells penetrated (SVZ-NSCs) or not (CC-NSCs) by NFL-LNCs, providing information about the preferential interaction between NFL-LNCs and SVZ-NSCs. The comparison of glioblastoma cells with SVZ-NSCs would provide information on the factor(s) regulating the type of the interaction (energetic-dependent and energetic-independent respectively).

The (co)encapsulation of other drugs in NFL-LNC could be used for the treatment of many neurodegenerative diseases.

The versatility of NFL-LNCs allows the encapsulation and the delivery of a wide range of active molecules to SVZ-NSCs. Lipophilic drugs are directly dissolved in the lipid phase (e.g., Labrafac®) while hydrophilic molecules can be pre-encapsulated into micelles which are then encapsulated into LNCs. The adaptation of the drug-encapsulation method to the chemical profile of the molecule does not significantly impact LNC major properties.

The combination of RA and valproic acid increased the rate of NSC differentiation *in vitro* due to their synergic effect [26]; thus, co-delivering those molecules *via* NFL-LNC could result in a more rapid and/or enhanced recovery of the demyelinating disorders compared to RA alone. Moreover, RA association to molecules known to promote neurite growth (e.g., brain-derived neurotrophic [27]) or neuroprotection (e.g., iron chelators [28]) would allow the treatment of both demyelination and demyelination-associated injuries, such as axonal loss in MS [29]. Importantly, inflammation often occurs during the development of demyelinating disorders as a local response driven by microglia [30]. Co-delivery of RA and anti-inflammatory molecules (e.g., nonsteroidal drugs [31]) *via* NFL-LNC could alleviate pain, heat, redness, swelling and loss of function during the treatment of the diseases.

Although RA-loaded NFL-LNCs show promising results for the treatment of demyelinating diseases, it would be worth to investigate the potential of other drugs. The ability to orient NSC differentiation towards specific neuronal cell types depending on the encapsulated molecule would make NFL-LNC a multivalent tool to treat different neurodegenerative diseases. While the combination of pramipexole, bone morphogenetic proteins 7 and growth factors induced NSC differentiation into dopaminergic neurons *in vitro* [32], neurotrophin-3 promoted NSC differentiation into cholinergic neurons *in vitro* [33]. The encapsulation and delivery of those molecules *via* NFL-LNC would represent a promising strategy for the treatment of PD and AD respectively.

By providing strengthened pre-clinical studies, RA-loaded NFL-LNCs have the potential to be tested in clinical trials.

RA-loaded NFL-LNCs induce NSC differentiation into GalC$^+$ cells *in vitro* while they restore the number of oligodendrocytes after focused white matter demyelination *in vivo* (preliminary results). Thus, inflammatory demyelinating diseases (e.g., multiple sclerosis [34]) could be the best target to evaluate the therapeutic effect of RA-loaded NFL-LNCs. However, before to reach the clinic, toxicity as well as therapeutic doses of RA-loaded NFL-LNCs should be determined in at least two different mammalian species (including one non-rodent species) to estimate the safe starting dose in humans [35]. In parallel, RA-loaded NFL-LNCs must be scalable and produced under good manufacturing practices (GMP) [36].

3. CONCLUSION

The safety and the efficacy of the current NSC-based therapies would be greatly increased by the development of endogenous NSC-targeting drug delivery systems able both to target endogenous NSC and to induce their differentiation *in situ*.

Here, we produced a stable and versatile drug delivery system directed towards endogenous NSCs by simply adsorbing the NSC-targeting peptide NFL on the surface of LNCs. NFL-LNC shows high affinity for endogenous SVZ-NSCs, representing the first drug delivery system with potential NSC-targeting ability *in vivo*.

We investigated the reasons of the preferential interaction performing a physicochemical study of NSC plasma membranes which provided new information in NSC biology as well as identified some of the factors modulating the preferential interaction.

We loaded RA into NFL-LNCs and we induced SVZ-NSC differentiated towards oligodendrocyte lineage *in vitro* 1 week after only 1 hour treatment with RA-loaded NFL-LNCs. The evaluation of the *in vivo* efficacy on demyelinated animal models is ongoing and, in the case remyelination/recovery will occur, the aim of our work would be totally addressed.

Nevertheless, independently of the *in vivo* results, we significantly contributed to the development of NSC-based therapy by providing a versatile drug delivery system able to interact with endogenous NSCs and, potentially, to deliver a wide range of active drugs for the treatment of neurodegenerative diseases.

4. REFERENCES

[1] T. Santos, R. Ferreira, J. Maia, F. Agasse, S. Xapelli, L. Cortes, J. Bragança, J.O. Malva, L. Ferreira, L. Bernardino, Polymeric nanoparticles to control the differentiation of neural stem cells in the subventricular zone of the brain, ACS Nano 6 (2012) 10463-10474.

[2] C. Saraiva, J. Paiva, T. Santos, L. Ferreira, L. Bernardino, MicroRNA-124 loaded nanoparticles enhance brain repair in Parkinson's disease, J. Control. Rel. 235 (2016) 291-305.

[3] S.K. Tiwari, S. Agarwal, B. Seth, A. Yadav, S. Nair, P. Bhatnagar, M. Karmakar, M. Kumari, L.K. Chauhan, D.K. Patel, V. Srivastava, D. Singh, S.K. Gupta, A. Tripathi, R.K. Chaturvedi, K.C. Gupta, Curcumin-loaded nanoparticles potently induce adult neurogenesis and reverse cognitive deficits in Alzheimer's disease model via canonical Wnt/β-catenin pathway, ACS Nano 8 (2013) 76-103.

[4] Chang, Jen-Hsuan, et al. Dual Delivery of siRNA and Plasmid DNA using Mesoporous Silica Nanoparticles to Differentiate Induced Pluripotent Stem Cells into Dopaminergic Neurons. Journal of Materials Chemistry B (2017).

[5] Zamproni, Laura N., et al. Injection of SDF-1 loaded nanoparticles following traumatic brain injury stimulates neural stem cell recruitment."International journal of pharmaceutics 519.1 (2017): 323-331.

[6] G. Elvira, B. Moreno, I.D. Valle, J.A. Garcia-Sanz, M. Canillas, E. Chinarro, J.R. Jurado, A.J. Silva, Targeting neural stem cells with titanium dioxide nanoparticles coupled to specific monoclonal antibodies, J. Biomater. App. 26 (2011) 1069-1089.

[7] Béduneau, Arnaud, et al. "Design of targeted lipid nanocapsules by conjugation of whole antibodies and antibody Fab'fragments." Biomaterials 28.33 (2007): 4978-4990.

[8] Lim, Daniel A., and Arturo Alvarez-Buylla. "The adult ventricular–subventricular zone (V-SVZ) and olfactory bulb (OB) neurogenesis." Cold Spring Harbor perspectives in biology 8.5 (2016): a018820.

[9] Curtis, Maurice A., Richard LM Faull, and Peter S. Eriksson. "The effect of neurodegenerative diseases on the subventricular zone." Nature Reviews Neuroscience 8.9 (2007): 712-723.

[10] de la Serna, Jorge Bernardino, et al. "There Is No Simple Model of the Plasma Membrane Organization." Frontiers in Cell and Developmental Biology 4 (2016).

[11] Los, Dmitry A., and Norio Murata. "Membrane fluidity and its roles in the perception of environmental signals." Biochimica et Biophysica Acta (BBA)-Biomembranes 1666.1 (2004): 142-157.

[12] Mencarelli, Chiara, and Pilar Martinez–Martinez. "Ceramide function in the brain: when a slight tilt is enough." Cellular and Molecular Life Sciences 70.2 (2013): 181-203.

[13] Garg, Sumit, et al. "Membrane fluidity in cancer cell membranes as a therapeutic target: validation using BPM 31510." Biophysical Journal 108.2 (2015): 246a.

[14] J. Maia, T. Santos, S. Aday, F. Agasse, L. Cortes, J.O. Malva, L. Bernardino, L. Ferreira, Controlling the neuronal differentiation of stem cells by the intracellular delivery of retinoic acid-loaded nanoparticles, ACS Nano 5 (2010) 97-106.

[15] S.A. Papadimitriou, M.P. Robin, D. Ceric, R.K. O'Reilly, S. Marino, M. Resmini, Fluorescent polymeric nanovehicles for neural stem cell modulation, Nanoscale 8 (2016) 17340-17349.

[16] de Hoz, Livia, and Mikael Simons. "The emerging functions of oligodendrocytes in regulating neuronal network behaviour." Bioessays 37.1 (2015): 60-69.

[17] Brettschneider, Johannes, et al. "Axonal damage markers in cerebrospinal fluid are increased in ALS." Neurology 66.6 (2006): 852-856.

[18] Gartziandia, Oihane, et al. "Chitosan coated nanostructured lipid carriers for brain delivery of proteins by intranasal administration." Colloids and Surfaces B: Biointerfaces 134 (2015): 304-313.

[19] Vonarbourg, A., et al. "Evaluation of pegylated lipid nanocapsules versus complement system activation and macrophage uptake." Journal of biomedical materials research Part A 78.3 (2006): 620-628.

[20] Nance, Elizabeth, et al. "Non-invasive delivery of stealth, brain-penetrating nanoparticles across the blood−brain barrier using MRI-guided focused ultrasound." Journal of controlled release 189 (2014): 123-132.

[21] Re, Francesca, et al. "Functionalization of liposomes with ApoE-derived peptides at different density affects cellular uptake and drug transport across a blood-brain barrier model." Nanomedicine: Nanotechnology, Biology and Medicine 7.5 (2011): 551-559.

[22] Bastiat, Guillaume, et al. "A new tool to ensure the fluorescent dye labeling stability of nanocarriers: a real challenge for fluorescence imaging." Journal of Controlled Release 170.3 (2013): 334-342.

[23] Ballot, Sandrine, et al. "99mTc/188Re-labelled lipid nanocapsules as promising radiotracers for imaging and therapy: formulation and biodistribution." European journal of nuclear medicine and molecular imaging 33.5 (2006): 602-607.

[24] Chattopadhyay, Amitabha, and Jean-Marie Ruysschaert. "Membrane proteins occupy a central role in cellular physiology. Introduction." Biochimica et biophysica acta 1848.9 (2015): 1727.

[25] Zhao, Yingxin, et al. "Proteomic analysis of integral plasma membrane proteins." Analytical chemistry 76.7 (2004): 1817-1823.

[26] Jung, Gyung-Ah, et al. "Valproic acid induces differentiation and inhibition of proliferation in neural progenitor cells via the beta-catenin-Ras-ERK-p21 Cip/WAF1 pathway." BMC cell biology 9.1 (2008): 66.

[27] Kamei, Naosuke, et al. "BDNF, NT-3, and NGF released from transplanted neural progenitor cells promote corticospinal axon growth in organotypic cocultures." Spine 32.12 (2007): 1272-1278.

[28] Dexter, David T., et al. "Clinically available iron chelators induce neuroprotection in the 6-OHDA model of Parkinson's disease after peripheral administration." Journal of neural transmission 118.2 (2011): 223-231.

[29] Brück, Wolfgang. "The pathology of multiple sclerosis is the result of focal inflammatory demyelination with axonal damage." Journal of neurology 252.5 (2005): v3-v9.

[30] Minghetti, Luisa. "Role of inflammation in neurodegenerative diseases." Current opinion in neurology 18.3 (2005): 315-321.

[31] Xu, Zhixiang, et al. "Design, synthesis and evaluation of a series of non-steroidal anti-inflammatory drug conjugates as novel neuroinflammatory inhibitors." International immunopharmacology 25.2 (2015): 528-537.

[32] Yang, HongNa, et al. "Dopaminergic Neuronal Differentiation from the Forebrain-Derived Human Neural Stem Cells Induced in Cultures by Using a Combination of BMP-7 and Pramipexole with Growth Factors." Frontiers in neural circuits 10 (2016).

[33] Yan, Yu-hui, et al. "Neurotrophin-3 promotes proliferation and cholinergic neuronal differentiation of bone marrow-derived neural stem cells via notch signaling pathway." Life sciences 166 (2016): 131-138.

[34] J.R. Plemel, W.Q. Liu and V.W. Yong. "Remyelination therapies: a new direction and challenge in multiple sclerosis." Nature Reviews Drug Discovery (2017) doi:10.1038/nrd.2017.115

[35] Atanasov, Atanas G., et al. "Discovery and resupply of pharmacologically active plant-derived natural products: A review." Biotechnology advances 33.8 (2015): 1582-1614.

[36] http://ec.europa.eu/growth/sectors/chemicals/good-laboratory-practice_it

ANNEX

The Carbocyanine Dye DiD Labels In Vitro and In Vivo Neural Stem Cells of the Subventricular Zone as Well as Myelinated Structures Following In Vivo Injection in the Lateral Ventricle

Dario Carradori, Kristell Barreau, and Joël Eyer★

Laboratoire Neurobiologie and Transgenèse, LUNAM, INSERM, UPRES-EA3143, Institut de Biologie en Santé, Bâtiment PBH-IRIS, Centre Hospitalier Universitaire, Angers, France

Carbocyanines are fluorescent lipophilic cationic dyes used since the early 1980s as neuronal tracers. Several applications of these compounds have been developed thanks to their low cell toxicity, lateral diffusion within the cellular membranes, and good photostability. 1,1'-Dioctadecyl-3,3,3',3'-tetramethylindodicarbocyanine 4-chlorobenzenesulfonate (DiD) is an interesting component of this family because, in addition to the classic carbocyanine properties, it has a longer wavelength compared with its analogues. That makes DiD an excellent carbocyanine for labeling cells and tissues with significant intrinsic fluorescence. Drug encapsulation, drug delivery, and cellular transplantation are also fields using DiD-based systems where having detailed knowledge about its behavior as a single entity is important. Recently, promising studies concerned neural stem cells from the subventricular zone of the lateral ventricle in the brain (their natural niche) and their potential therapeutic use. Here, we show that DiD is able to label these stem cells in vitro and present basilar information concerning its pharmacokinetics, concentrations, and microscope protocols. Moreover, when DiD is injected in vivo in the cerebrospinal fluid present in the lateral ventricle of rat, it also labels stem cells as well as myelinated structures of the caudoputamen. This analysis provides a database to consult when planning experiments concerning DiD and neural stem cells from the subventricular zone. © 2015 Wiley Periodicals, Inc.

Key words: neural stem cells; subventricular zone; myelin; carbocyanine; DiD

Carbocyanines represent a large class of lipophilic dyes composed of two positively charged indole groups connected by a short, unsaturated chain of carbon atoms. They can be partially soluble or insoluble in water depending on the length of the hydrocarbon chain, short in the first case, long in the second case. Initially these compounds were used to study the potential of cellular membranes (Sims et al., 1974) and diffusion within them (Axelrod et al., 1978). The main application that made these compounds popular was staining neurites (Schwartz and Agranoff, 1981). Because of their low toxicity, carbocyanines were also used in anterograde and retrograde neuron tracing (Hoing and Hume, 1986). The results suggested that these compounds diffused within cellular membranes through a translocation mechanism based on lateral diffusion. This hypothesis was then confirmed as a new method to stain neurons in fixed tissues (Godement et al., 1987). All these works focused on DiI (excited in green) and DiO (excited in blue), the most often used carbocyanines in that decade. During 1990s the number and type of applications increased: immunocytochemistry

SIGNIFICANCE

This work shows that SVZ SCs can be easily labeled in vitro as well as in vivo by the carbocyanine DiD. We highlight the critical points in the interpretation of the results produced by DiD labeling and provide detailed procedures as well as explications to avoid experimental errors. We also describe the interesting ability of DiD to identify and define myelinated structures in the caudoputamen. This property makes DiD a helpful tool in the study of neurodegenerative diseases, especially those characterized by alterations of myelinated structures.

and immunohistochemistry (Holmquist et al., 1992), intracellular labeling (Terasaki and Jaffe, 1991), cellular migration (Ragnarson et al., 1992), cellular transplantation (Heredia et al., 1991), cell–cell interactions (Spötl et al., 1995), and cell adhesion (Ramanathan et al., 1996). At the end of the twentieth century, DiI was used to stain ependymal cells of the subventricular zone (SVZ), focusing on astrocytes, which were identified as acting as stem-like cells (Doetsch et al., 1999). After 1999 carbocyanines were no longer related strictly to SVZ stem cells (SCs), but their application in neurobiology continued (Gan et al., 2000; Matsubayashi et al., 2008; Cheng et al., 2014).

DiD is an interesting component of this family of dyes because it has a longer wavelength compared with the other carbocyanines, which makes it better for labeling cells and tissues with important autofluorescence (The Molecular Probes Handbook, 2010). It shows less fluorescence when it is in water than when it is associated with cellular membranes (Simon et al., 2006), and it is a suitable probe for long-term labeling (Mäkinen et al., 2013). It also shows the typical carbocyanine characteristics, including low cell toxicity and lateral diffusion within the cellular membranes.

The recent interest in neural SCs is due largely to their potential application in therapy and as promising targets. In particular for CNS therapy, SVZ SCs were subjected to several manipulations (Ladran et al., 2013; Gage and Temple, 2013; Cave et al., 2014; Guerra, 2014). Surprisingly, although carbocyanine-based systems are developing rapidly (micelles: Yang et al., 2013; nanocapsules: Groo et al., 2013; virus: Soto et al., 2006) and their application will soon concern SVZ SCs, no detailed information is available concerning carbocyanines' properties as free molecules. In particular, it is important to determine their pharmacokinetic properties, concentrations, potential toxicity, and microscope visualization in order to elaborate adequate and powerful carbocyanine-based systems.

Here we show that DiD alone is able to label in vitro neural SCs isolated from the SVZ of newborn rats or in vivo following its stereotaxic injection in the lateral ventricle of adult rats. Moreover, we show that DiD is able to label myelinated structures surrounding the ven-tricular zone, indicating that this product is able to pass through the monolayer of ependymal cells lining the ventricular cavity. These in vitro and in vivo experiments provide basic and fundamental information concerning the pharmacokinetic, concentrations, protocols, and microscope imaging of this carbocyanine, which are essential for further use of this fluorescent marker alone or together with other systems including micelles or nanoparticles.

MATERIALS AND METHODS

Primary antibodies used in this work are described in Table I and secondary antibodies in Table II.

Animals

Primary SVZ SC cultures and in vivo experiments were performed according to Directive 2010/63/EU and to guidelines of the French Government following the approval by the local committee of Pays de la Loire for Ethics in Animal Experiments.

DiD Solution

DiD solid (Life Technologies, Grand Island, NY) was dissolved in 10 ml ethanol and then sonicated for 15 min. The final concentration was 1 mM. For the in vitro experiments, DiD solution was diluted in H_2O MilliQ. For the in vivo experiments, DiD solution was diluted in physiological sterile water.

Isolation of SVZ SCs

Neural SCs were isolated from the SVZ by using the protocol of Guo et al. (2012). Briefly, newborn rats (1–5 days old) were sacrificed by decapitation. The brain was removed and placed in the dissection buffer (1.25 ml D-glucose 1 M, 750 μl HEPES, and 500 μl Pen/Strept in 50 ml Hank's medium; Life Technologies). The brain was then cut into 400-μm coronal sections, and the SVZ was microdissected and placed in a tube filled with 1 ml dissection buffer. The tube was centrifuged for 5 min at 344g. The supernatant was removed, and 1 ml SC culture medium (1.25 ml of D-glucose 1 M, 750 μl HEPES, 500 μl Pen/Strept, 500 μl Na pyruvate, 500 μl B27, and 5 μl epidermal growth factor (EGF) in 50 ml MEM; Life Technologies) was added. The pellet was mechanically triturated with a syringe. The cells were counted in a counting chamber, seeded at 2–3×10^5 cells/60-mm-diameter Petri dish, and incubated at 37°C. SVZ SCs were cultivated as floating neurospheres, which appeared after 5 days. All in vitro experiments used 6- and 7-day-old neurospheres.

TABLE I. Primary Antibodies Used in This Work

Name	Target	Host	Cat. N°
Anti-α-tubulin	α-Tubulin	Mouse	T9026
Anti-GFAP	Glial fibrillary acidic protein	Mouse	G3893
Antinestin	Nestin	Rabbit	N5413
Antivimentin	Vimentin	Mouse	V6630

TABLE II. Secondary Antibodies Used in This Work

Name	Target	Host	Catalog No.	Manufacturer	RRID	Clone	Dilution
Alexa Fluor 488	Anti-mouse IgG IgM (H+L)	Goat	A10680	Life Technologies	AB11180055	Unknown	1/200
Alexa Fluor 488	Anti-rabbit IgG (H+L)	Goat	A11008	Life Technologies	AB10563748	Unknown	1/200

In Vitro FACS Analysis

Six-well plates were used for these experiments (1.5 ml/well), with a cellular concentration of $0.59–0.66 \times 10^6$ cells/well, or 4,390–4,850 neurospheres/well. For each condition, the dilution of the compound was 1/100 (15 µl/well). For the pharmacokinetic studies, SVZ SCs were incubated with DiD (0.015 µM) at 37 °C for different times (5 min, 10 min, 20 min, 40 min, 1 hr, 2 hr, 4 hr, 6 hr, and 8 hr). For the concentration study, SVZ SCs were incubated for 1 hr at 37 °C with different DiD concentrations (0.00075, 0.00375, 0.0075, 0.03, 0.06, and 0.15 µM). For the diffusion study in unfavorable conditions, SVZ SCs were incubated for 1 hr at 4 °C with DiD at 0.015 µM. A BD FACSCalibur flow cytometry system (RRID:SciRes_000153) was used for the evaluation.

In Vitro Confocal Imaging

Twenty-four-well plates and lamellae (13 mm diameter) were used in these experiments (0.5 ml/well), with a cellular concentration of $0.19–0.22 \times 10^6$ cells/well or 1,463–1,616 neurospheres/well. The lamellae were coated with BD CellTak (BD Biosciences) before cell seeding. For each condition, the dilution of the compounds was 1/100 (5 µl/well). For the imaging evaluation, SVZ SCs were incubated at 37 °C for different times (20 min, 1 hr, and 6 hr) with different DiD concentrations (0.015, 0.15, and 1.5 µM). A TCS-SP8 Leica confocal microscope (RRID:SciRes_000154) was used for the observations, and pictures were taken at ×63 magnification.

In Vitro Confocal Imaging Immunocytochemistry Protocol

At the end of the incubation, the lamellae were washed with SC culture medium three times (5 min each). The neurospheres were fixed with 4% paraformaldehyde for 15–20 min and then washed three times with PBS (5 min each). They were incubated for 30 min with different permeabilization agents (Triton 0.5%, saponin 1%, digitonin 0.01%, and no permeabilizer), then saturated with bovine serum albumin (BSA) 1% for 60 min and incubated overnight at 4 °C with a mouse anti α-tubulin solution (Sigma-Aldrich, St. Louis, MO; catalog No. T9026 RRID:AB_477593; 1/1,000 in 1% BSA). The neurospheres were washed three times with PBS (5 min each) and incubated in the dark for 90 min with an Alexa Fluor 488 solution (Life Technologies; catalog No. A10680; RRID:AB_11180055; 1/200 in 1% BSA). They were washed three times with phosphate-buffered saline (PBS; 5 min each) and incubated for 5 min in DAPI solution (Life Technologies; catalog No. D3571; RRID:AB_2307445; 1/300 in PBS). The neurospheres were washed once in PBS (for 5 min). The lamellae were finally removed from the wells, covered with ProLong Gold antifade (Life Technologies), and fixed on microscope slides.

In Vivo Intraventricle Injection

Sprague female rats (2–3 months old) were used for in vivo intraventricle injection. The animals were anesthetized with 1 µl/g ketamine:xylazine solution (50:50) by intraperitoneal injection. The head was stabilized in a stereotactic frame.

The stereotactic coordinates were −0.8 mm AP, 1.5 mm ML, and 4 mm DV with respect to the bregma. The injection was made with a CED microinjection apparatus (Harvard) at 0.5 µl/min rate (needle diameter 1.457 mm) for a total injected volume of 20 µl, as previously described for such injection protocols according to the good practices for animal experimentation by Wolfensohn and Lloyd (2008). Different concentrations of DiD solution were used (0.015 µM, 0.15 µl, and 1.5 µl). The animals were sacrificed 1 or 6 hr after the end of the injection. The brains were then removed and stored at −80 °C.

Ex Vivo Confocal Imaging

Approximately 150–210 sections (12 µm thick) were collected from each brain using a CM3050S Cryostat Leica and placed on microscope slides (three sections/slide). A preliminary screening verified the homogeneity of the distribution of DiD; the sections were analyzed by taking just a few of them at specific intervals to cover the whole series. The sections were fixed in methanol for 10 min, washed once in PBS for 5 min, stained with DAPI solution (1/300 in PBS) for 5 min, washed once in PBS for 5 min, covered with ProLong Gold antifade, and overlaid with coverslips. Once we had identified the range at which DiD signal was most visible, an immunohistochemistry protocol was performed on the sections. The evaluation used a Leica TCS SPE (RRID:SciRes_000154). Pictures were taken at different magnifications, ×7.5, × 20, and ×40.

Ex Vivo Confocal Imaging Immunohistochemistry Protocol

The sections were fixed in methanol for 10 min and then washed three times in PBS (3 min each). The sections were saturated with BSA 5% for 30 min and incubated overnight with different primary antibodies (one antibody for one slide): mouse anti-GFAP (Sigma-Aldrich; catalog No. G3893; RRID:AB_477010; 1/200 in 5% BSA), rabbit antinestin (Sigma-Aldrich; catalog No. N5413; RRID:AB_1841032; 1/50 in 5% BSA), and mouse antivimentin (Sigma-Aldrich; catalog No. V6630; RRID:AB_477627; 1/200 in 5% BSA). The slides were washed three times with PBS (5 min each) and incubated at 4 °C in the dark for 90 min with Alexa Fluor 488 (Life Technologies; catalog No. A10680; RRID:AB_11180055; 1/200 in 5% BSA) for mouse anti-GFAP and for mouse antivimentin, Alexa Fluor 488 (Life Technologies; catalog No. A11008; RRID:AB_10563748; 1/200 in 5% BSA) for rabbit antinestin. They were washed three times with PBS (3 min each) and incubated for 5 min with a DAPI solution (Life Technologies; catalog No. D3571; RRID:AB_2307445; 1/300 in PBS). The sections were finally covered with ProLong Gold antifade and overlaid with coverslips.

Myelin Identification

The sections were incubated 18 hr at 56 °C in a Luxol fast blue (BDH) solution according to Klüver and Barrera (1953). The slides were rinsed twice in alcohol 95% until complete rehydration differentiated first in lithium carbonate and then in alcohol 70%. They were rinsed in distilled water for 5 min before the counterstaining with nuclear red (Sigma). Slides
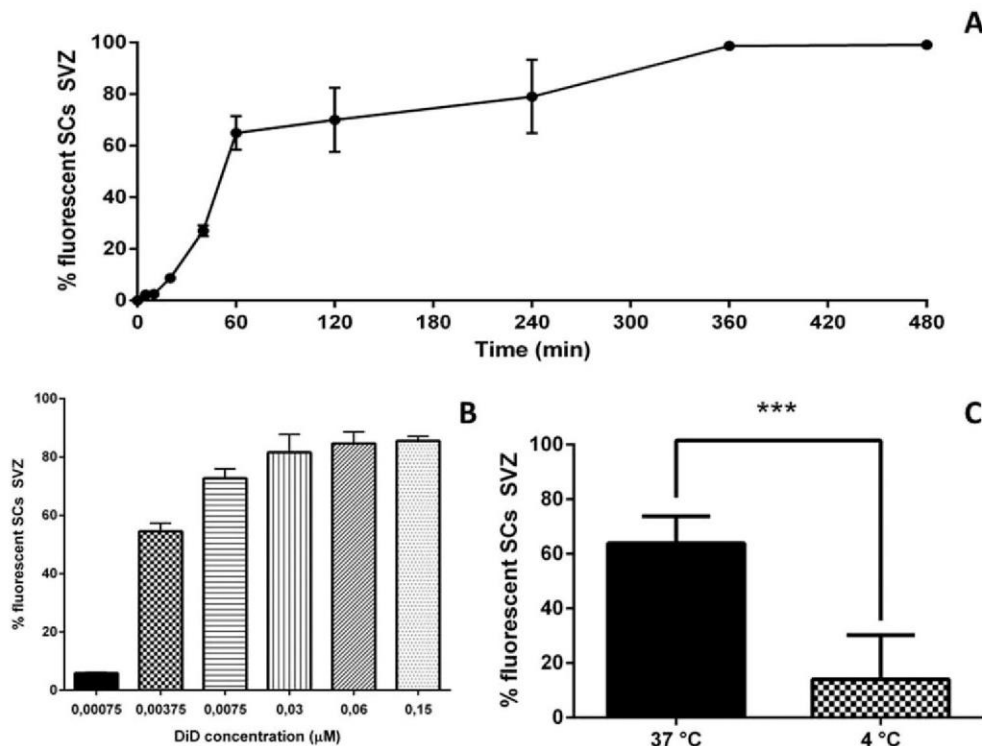
Fig. 1. **A**: Evolution of fluorescent stem cells (in percentage) after different incubation times at 37 °C with 0.015 μM DiD. **B**: Percentage of fluorescent SVZ SCs after 1 hr incubation at 37 °C with different DiD concentrations. **C**: Percentage of fluorescent SVZ SCs after 1 hr incubation at 37 °C or 4 °C with DiD 0.015 μM. ★★★$P < 0.001$.

were then washed in water and dehydrated by consecutive incubation with alcohol 70% (5 min), alcohol 95% (5 min), alcohol 100% (5 and 10 min) and xylene (10 and 15 min). The sections were covered with Eukitt and overlaid with coverslips. Pictures were taken with an Olympus BX50 microscope at × 10.

Statistical Analyses

All the experiments were performed at least three times for each condition. For the FACS analysis, 40,000 events/condition were analyzed. Error bars were produced using the standard error of mean (SEM) method. Statistical analysis in Figure 1C was performed with Student's t- test in Graphpad Prism (RRID:rid_000081; n = 4). For the confocal in vitro examination, at least two pictures/condition were taken randomly, and for the ex vivo observation several pictures of the lateral ventricle were taken for each condition and at different magnification of the SVZ and its periphery (caudoputamen and lateral septal nucleus).

RESULTS

In Vitro FACS Evaluation of SC Labeling by DiD

The pharmacokinetic study shows a progressively increased percentage of fluorescent SVZ SCs following their incubation with DiD at 0.015 μM (Fig. 1A). At this concentration no major difference or relevance was observed in terms of the percentage of fluorescent SVZ

SCs between 5 min and 10 min of incubation. The fluorescence started to be clearly measurable by FACS after 20 min of incubation, and 100% of cells were labeled after 6 hr. The concentrations study (Fig. 1B) shows that no relevant fluorescence was observed in cells with 0.00075 μM of DiD, whereas at concentrations over 0.06 μM no significant difference of fluorescent SVZ SCs (approximately 80%) was noted. In the range of 0.00375–0.03 μM, the percentage of fluorescent cells is related to the concentration of DiD. Under unfavorable conditions, a huge decrease of DiD diffusion in SVZ SCs occurred following 1 hr incubation at 4 °C compared with the incubation at 37 °C (Fig. 1C). According to the sensitivity of the instrument and to the experimental conditions, DiD could or could not be detected.

In Vitro Confocal Microscopy Analysis of Did Labeling

Different labeling of SCs by DiD can be obtained depending on the nature of the membrane permeabilization protocol. In particular, the immunocytochemistry protocols, which include Triton 0.5% or saponin 1%, are not suitable for visualizing DiD (Fig. 2A,B). On the other hand, good labeling occurred with digitonin 0.01%, or without membrane permeabilization (Fig. 2C,D). Although Triton has a nonspecific dissolving action on
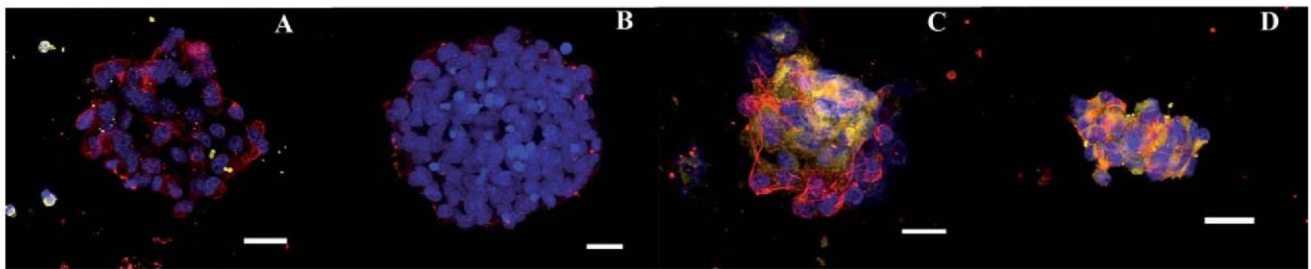
Fig. 2. SVZ SCs were incubated during 1 hr with DiD 1.5 μM and then treated with different permeabilizant agents at the beginning of the immunocytochemistry protocol, Triton 0.5% (**A**), saponin 1% (**B**), or digitonin 0.01% (**C**) or without permeabilizant agent (**D**). Blue is DAPI: nucleus. Red is anti-α-tubulin: cytoskeleton. Yellow is DiD. Scale bars = 20 μm. [Color figure can be viewed in the online issue, which is available at wileyonlinelibrary.com.]

the lipid bilayer, saponin and digitonin are specific permeabilizants, which act mostly on cholesterol.

Confocal microscopic analysis also shows that the DiD signal in neural SCs depends on the duration of incubation and DiD concentration. Although the very sensitive FACS analysis showed that most cells (approximately 60%) are labeled after 1 hr of incubation with 0.015 μM DiD (Fig. 1B), the confocal microscopic examination indicates that at this concentration only a faint labeling of cells occurred (Fig. 3D), whereas after 6 hr of incubation a massive penetration of DiD in all cells was observed for all the concentrations (Fig. 3G–I). Moreover, at 0.015 μM DiD (Fig. 3G), the visualization of the dye is more punctiform than at 1.5 μM DiD (Fig. 3H), which appears well diffused within cellular membranes. At higher concentration (1.5 μM DiD), the fluorescent dye massively penetrates in all cells after less than 20 min of incubation (Fig. 3C). Therefore, the 0.15 μM concentration of DiD is the best condition to avoid overpenetration in cells and saturation of the signal. To visualize SVZ SCs incubated for 6 hr with DiD at 1.5 μM, the gain of the confocal apparatus was significantly decreased because of signal saturation.

In Vivo Confocal Microscopic Analysis of Neural SCs Labeling Following Injection of DiD in the Lateral Ventricle

The labeling of the different types of cells by DiD after its stereotaxic injection in the lateral ventricle was evaluated by immunohistology with different antibodies. In particular, we detected the intermediate filaments specifically expressed by the different cells present in this region of the central nervous system: gliofilaments expressed in glial cells (GFAP[+]), vimentin expressed in neuronal precursor cells (Vim[+]), and nestin present in bona fide SCs (nestin[+]). As a general observation, the diffusion of the DiD from the lateral ventricle to the SVZ occurred without any particular preferences for one of the three type of cells identified by the expression of their characteristic intermediate filaments (Fig. 4). Moreover, in the immunolabeled pictures (nestin, vimentin, GFAP), DiD seems to be compartmentalized in some regions and

not in others. In fact, the reason is that the dye is passing from one layer to the next, apparently accumulating in them but in reality diffusing and labeling all of the cells step by step. The lack of a compartmentalization of the fluorophore probably is due to a similar composition of the cellular membranes of GFAP[+], nestin[+], and Vim^{+} cells, which allows DiD diffusion without specific obstacles or orientation in this zone.

The diffusion of DiD from the ventricle to the SVZ occurred in less than 1 hr (Fig. 4A,C), and its diffusion in the whole caudoputamen and lateral septal nucleus (LSr) occurred in less than 6 hr (Fig. 4B,D). In the first case DiD signal is well defined and limited to the SVZ, but in the second case the signal is weaker and widely diffused in the CP and the LSr. At concentrations higher than 1.5 μM, DiD causes a saturation of the signal, which makes these high concentrations useless for confocal evaluation under these conditions.

DiD signal is more accentuated around the injection zone (top of the lateral ventricle), but its diffusion along the whole surface of the ventricle is evident. To visualize DiD 1.5 μM, the gain was significantly decreased (not shown) because of the saturation of the signal. Brain sections of rats sacrificed 1 hr after the intraventricle injection show similar results but with different intensity according to the DiD concentration used: DiD signal is mostly limited to the subependymal zone. Nevertheless, a small portion of DiD diffused in the deep CP. Brain sections of rats sacrificed 6 hr after the intraventricle injection show, also in this case, similar results but with different intensity according to the DiD concentration used; if on one hand an increase of the diffusion was observed in the CP, on the other hand a general decrease of the signal intensity in the SVZ was observed as well.

During the confocal microscopic analysis for the evaluation of the DiD pharmacokinetics and distribution after its injection in the lateral ventricle, we noticed that characteristic DiD labeling was systematically present in the sections, with high or low intensity depending on the concentration of DiD used for the lateral ventricle injection. Because the localization was present only in the CP and not in the LSr, we further investigated these labeled structures. First, we found a symmetric disposition of
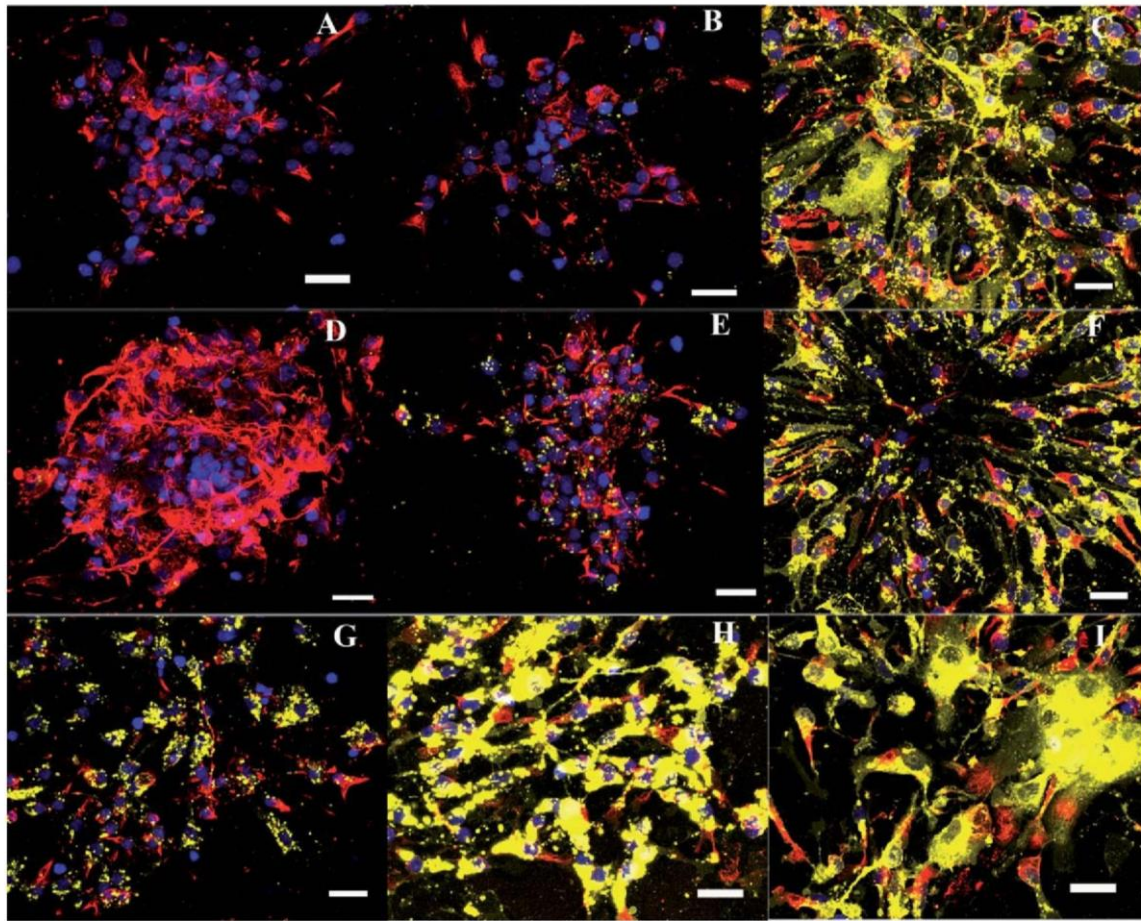
Fig. 3. SVZ SCs were incubated for different times (20 min, **A–C**; 1 hr, **D–F**; 6 hr, **G–I**) and with different DiD concentrations (0.015 µM, A,D,G; 0.15 µM, B,E,H; 1.5 µM, C,F,I). Blue is DAPI: nucleus. Yellow is DiD. Red is anti-α-tubulin: cytoskeleton. Scale bars = 20 µm. [Color figure can be viewed in the online issue, which is available at wileyonlinelibrary.com.]

these spots in brain sections taken consecutively (Fig. 5A,B) suggesting that they were actually 3D structures defined by DiD accumulation within them. Second, we identified the nature of these structures by staining them with Luxol fast blue, a dye attracted by the bases that compose the lipoproteins of the myelin sheath. The colocalization between the structures labeled by DiD and also by Luxol fast blue demonstrates that these structures are composed of myelin (Fig. 6).

DISCUSSION

Several in vitro and in vivo labeling methods of neural SCs have recently been developed, but they present many limitations or are particularly laborious. For instance, MRI or PET are necessary for the SPIO labeling (Guzman et al., 2007) or the magnetic nanoparticle labeling (Wang et al., 2006). Moreover, BrdU (Lehner et al., 2011) labels only the nucleus and not the whole architecture of cells, although the gene-gun device for biolistic labeling (Zhang et al., 2003) needs sophisticated equipment for its development. In comparison with these methods, DiD labeling has several advantages, including a simple protocol to use (incubation) and to evaluate (fluorescent microscopy), as well as the capacity to label the whole cellular architecture.

As described by Guo et al. (2012), the cells isolated by this protocol are 99.8% positive for nestin and 88.2% positive for Sox. With all the precautions needed for the best in vitro evaluation of the labeling, we found by FACS (Fig. 1 A) and confocal microscopy (Fig. 3G–I) that neurospheres can be 100% labeled by DiD, with no evidence of their alteration (such as microtubule alteration after α-tubulin labeling). Moreover, there is no evidence that DiD labels only some cell subpopulations of the neurosphere. Finally, we showed that DiD can be injected directly in the lateral ventricle of live animals where it keeps it fluorescent properties, is compatible and miscible with the cerebrospinal fluid, and has the capacity to cross the ependymal layer of the SVZ and to diffuse within the cerebral parenchyma (Fig. 4). Overall, these data indicate that DiD is a particularly interesting and suitable dye when planning DiD-based experiments (functionalized nanoparticles, virus, neural SCs and their niche). It is also particularly simple to use and analyze.
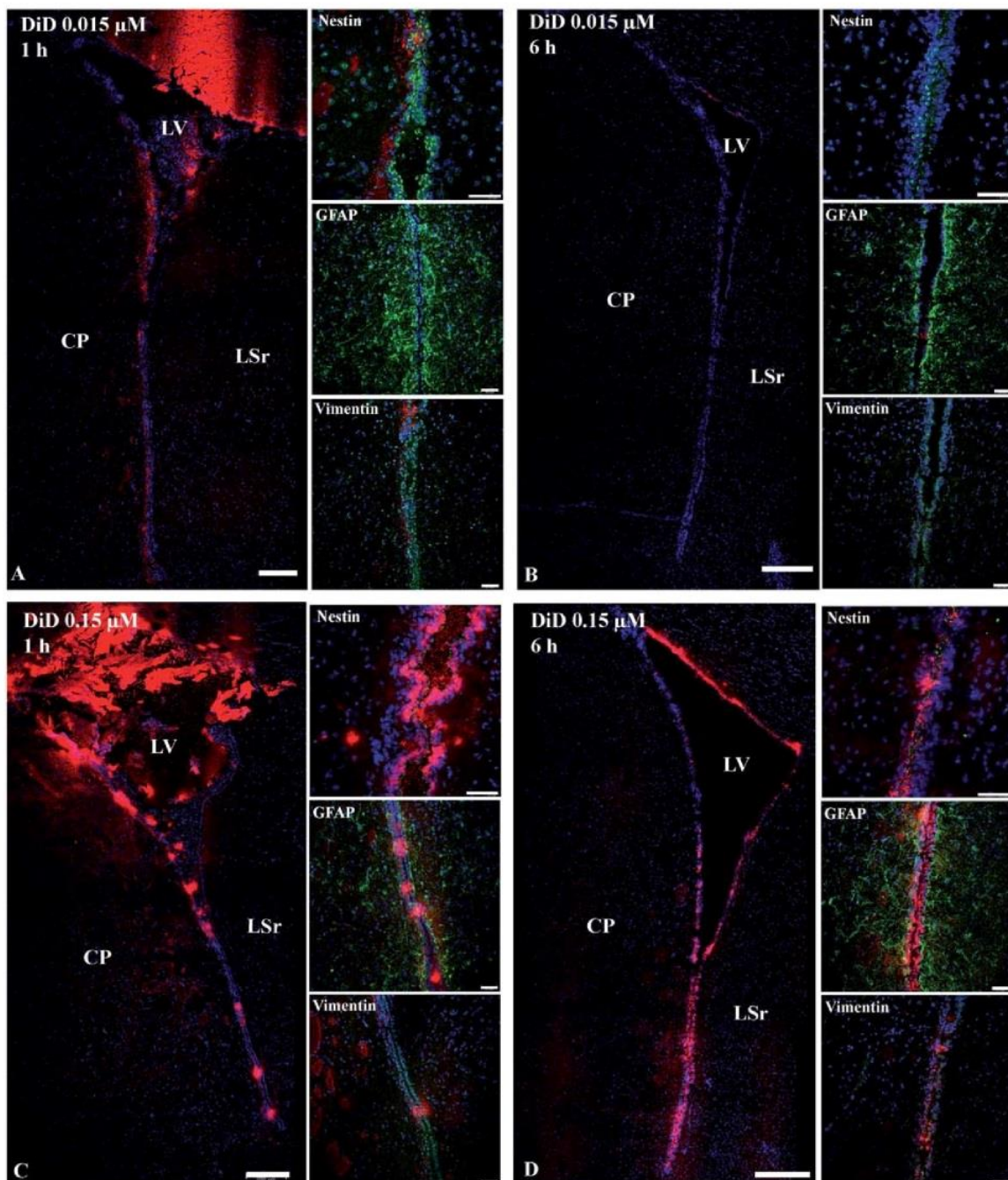
Fig. 4. Brain sections of rats examined at different times after intraven-
tricular injections of different DiD concentration. CP, caudoputamen;
LSr, lateral septal nucleus, rostral; LV, lateral ventricle. DiD 0.015 μM
after 1 hr (**A**) and 6 hr (**B**). DiD 0.15 μM after 1 hr (**C**) and 6 hr (**D**). Blue is DAPI: nucleus. Red is DiD. For each time and concentration,
nestin[+], Vim[+], and GFAP^{+} cells are indicated in green, which is
Alexa Fluo 488. Scale bars = 20 μm. [Color figure can be viewed in
the online issue, which is available at wileyonlinelibrary.com.]

Aside from these advantages, it is important to
control the experimental conditions because they can
influence DiD diffusion and thus its detection and visual-
ization. For instance, low temperature (4 °C) decreases
cellular membrane fluidity, preventing transversal DiD
diffusion within the lipid bilayer when performing in
vitro experiments. Moreover, the use of harsh permeabili-
zation agents (e.g., Triton) during immunochemistry can
partially dissolve cellular membranes, disrupting the lipid
bilayer and allowing DiD to diffuse out of cells. Saponin
and digitonin are cholesterol-specific permeabilizant
agents, but they provide different results. As proposed by
Matsubayashi et al. (2008) for DiI, the reason could be
the differential action of these permeabilizant agents on
cholesterol. Saponin solubilizes cholesterol, allowing DiD
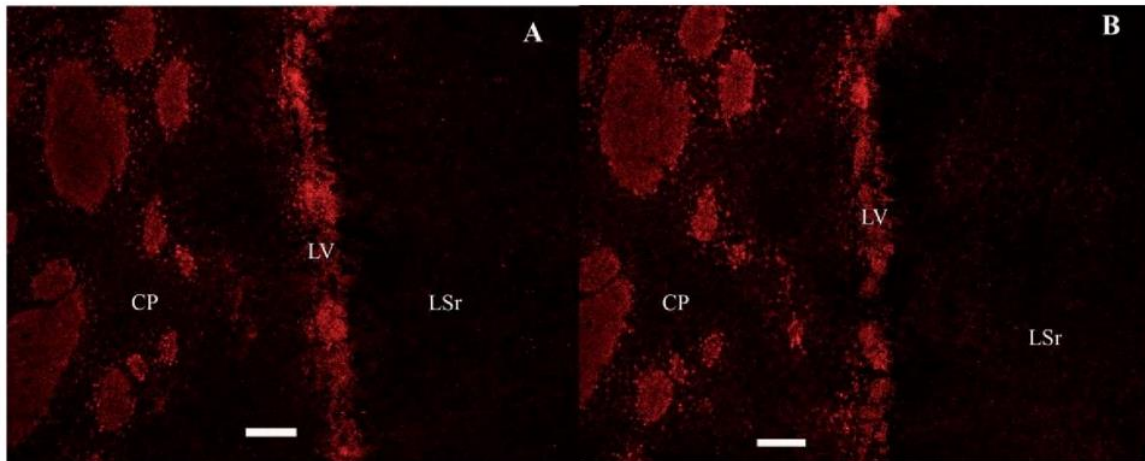to escape from the cellular membrane, whereas digitonin

Fig. 5. **A,B**: Spots of DiD in two consecutive brain sections. Scale bar = 50 μm. [Color figure can be viewed in the online issue, which is available at wileyonlinelibrary.com.]
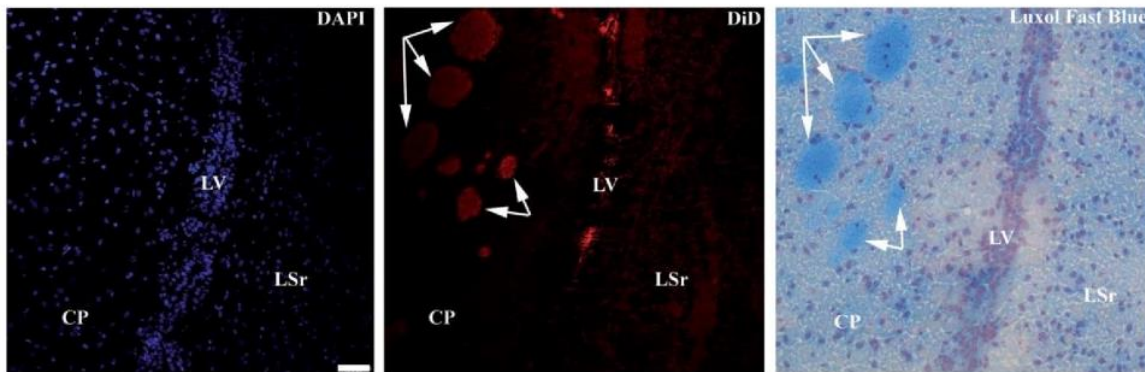

Fig. 6. Different staining of consecutive brain sections: DAPI, DiD, and Luxol fast blue. Scale bar = 50 μm. [Color figure can be viewed in the online issue, which is available at wileyonlineli-brary.com.]

makes a complex with cholesterol, allowing DiD to remain within the membrane. This result also indicates that cholesterol plays a critical role in the diffusion and detection of DiD within the cellular membranes. However, it is possible to avoid the permeabilization step if it does not affect confocal visualization, as evidenced by anti-α-tubulin and DAPI, which are clearly visible without cell permeabilization.

Two different patterns of in vitro DiD labeling were visible on SVZ SCs, punctiform labeling for cells incubated with low concentrations of DiD and uniform labeling for cells incubated with higher concentration of DiD. One possibility is the ratio of ethanol in the final solutions of DiD (1.5/999.5 for 0.015 μM DiD, 15/985 for 0.15 μM DiD, and 150/850 for 1.5 μM DiD). A higher amount of ethanol could also facilitate the diffusion within the cellular membranes by increasing the cellular membrane permeability and by improving DiD dissolution in aqueous solution. Another possible explanation is the accumulation of the fluorescent dye in the cytoplasmic organelles, as previously shown in several studies

concerning carbocyanines (Zorov et al., 2004). The preferential mitochondrial accumulation of DiO for low concentrations was also demonstrated by Terasaki et al. (1984), and the reason is probably the high membrane potential of these organelles (Johnson et al., 1981). Overall, this in vitro investigation shows that, if DiD can easily be used to label SVZ SCs, it is important to control the experimental conditions that could influence the labeling or its visualization significantly.

The in vivo intraventricle injection experiment led us to discover several interesting properties of DiD. First, it is compatible with the cerebrospinal fluid and does not show a major toxic or lethal effect for the animals. Moreover, the fluorescent profile of DiD and its capacity to label cellular membranes are not affected. Cerebrospinal fluid did not affect the diffusion from the lateral ventricle to the SVZ. Also, DiD is able to cross cellular and tissue barriers of the SVZ, and its diffusion in the whole caudo-putamen and lateral septal nucleus occurs rapidly (less than 6 hr). At longer times, the fluorescent signal of DiD decreases, and this is due mainly to dye dilution through

the cerebral parenchyma. In comparison with other dyes used under the same conditions (Doetsch et al., 1999), this behavior is characteristic of DiD. The passage through the ependymal layer makes DiD a suitable tool for central nervous system labeling in many more circumstance than the current dyes, which are spatially limited. It also provides a suitable (positive) tool for a spatially limited labeling of structures in the central nervous system (e.g., functionalized nanovectors). DiD can cross the ependymal barrier of the lateral ventricle and diffuse in the CP and LSr, indicating that the lipid profiles among the components of the SVZ (ependymal cells, stem cells, glial cells, etc.) are not different enough to orientate the diffusion or the accumulation of DiD in a specific compartment of the SVZ. Finally, once in the CP, the fluorescent dye is able to accumulate into myelinated structures. This property could be due to the specific composition of myelin, which is mainly cholesterol based (Gesine et al., 2005). As hypothesized in the case of saponin, which acts on cholesterol, the role of this lipid could be crucial for the diffusion and detection of DiD in cells and tissues.

With regard to the in vivo and ex vivo parts of this article, DiD shows very interesting compatibility with most of the experiments. Its capacity to define myelinated structures in the CP was unexpected but could be particularly useful for other purposes. In the neurodegenerative diseases field, for example, multiple sclerosis or Huntington's disease that are characterized by "demyelination" (Bartzokis et al., 2007), it would be worthwhile to investigate the possible application of DiD for the definition of such myelinated structures and their abnormal patterns.

CONCLUSIONS

Compared with other fluorescent dyes used for the same purpose, the carbocyanine DiD can easily label SVZ SCs in vitro as well as in vivo. Once injected into the cerebrospinal fluid of the lateral ventricle, it labels most of the cellular constituents of the SVZ and also shows the capacity to cross the different barriers and define myelinated structures present in the CP. These interesting properties of DiD allow for its promising application for labeling SVZ SCs during primary culture or for investigating their in vivo biology following injection of the fluorescent probe in the lateral ventricle.

ACKNOWLEDGMENTS

CONFLICT OF INTEREST STATEMENT

ROLE OF AUTHORS

All authors had full access to all the data in the study and take responsibility for the integrity of the data and the accuracy of the data analysis. Study concept and design: JE. Acquisition of data: DC, KB. Analysis and interpretation of data: JE, DC. Drafting of the manuscript: DC. Critical revision of the manuscript for important intellectual content: JE. Statistical analysis: DC. Obtained funding: JE. Administrative, technical, and material support: JE, DC, KB. Study supervision: JE.

REFERENCES

Axelrod D, Wight A, Webb W, Horwitz A. 1978. Influence of membrane lipids on acetylcholine receptor and lipid probe diffusion in cultured myotube membrane. Biochemistry 17:3604–3609.

Bartzokis G, Lu PH, Tishler TA, Fong SM, Oluwadara B, Finn JP, Huang D, Bordelon Y, Mintz J, Perlman S. 2007. Myelin breakdown and iron changes in Huntington's disease: pathogenesis and treatment implications. Neurochem Res 32:1655–1664.

Cave JW, Wang M, Baker H. 2014. Adult subventricular zone neural stem cells as a potential source of dopaminergic replacement neurons. Front Neurosci 8:1–8.

Cheng C, Trzcinski O, Doering LC. 2014. Fluorescent labeling of dendritic spines in cell cultures with the carbocyanine dye DiI. Front Neuroanat 8:1–8.

Doetsch F, Caille I, Lim DA, García-Verdugo JM, Alvarez-Buylla A. 1999. Subventricular zone astrocytes are neural stem cells in the adult mammalian brain. Cell 97:703–716.

Gage FH, Temple S. 2013. Neural stem cells: generating and regenerating the brain. Neuron 80:588–601.

Gan WB, Grutzendler J, Wong WT, Wong RO, Lichtman JW. 2000. Multicolor DiOlistic labeling of the nervous system using lipophilic dye combinations. Neuron 27:219–225.

Gesine S, Brügger B, Lappe-Siefke C, Möbius W, Tozawa R, Wehr MC, Wieland F, Ishibashi S, Nave K. 2005. High cholesterol level is essential for myelin membrane growth. Nat Neurosci 4:468–475.

Godement P, Vanselow J, Thanos S, Bonhoeffer F. 1987. A study in developing visual systems with a new method of staining neurones and their processes in fixed tissue. Development 101:697–713.

Groo AC, Saulnier P, Gimel JC, Gravier J, Ailhas C, Benoit JP, Lagarce F. 2013. Fate of paclitaxel lipid nanocapsules in intestinal mucus in view of their oral delivery. Int J Nanomed 8:4291–4302.

Guerra M. 2014. Neural stem cells: are they the hope of a better life for patients with fetal-onset hydrocephalus? Fluids Barriers CNS 11:1–10.

Guo W, Patzlaff NE, Jobe EM, Zhao X. 2012. Isolation of multipotent neural stem or progenitor cells from both the dentate gyrus and subventricular zone of a single adult mouse. Nat Protoc 7:2005–2012.

Guzman R, Uchida N, Bliss TM, He D, Christopherson KK, Stellwagen D, Steinberg GK. 2007. Long-term monitoring of transplanted human neural stem cells in developmental and pathological contexts with MRI. Proc Natl Acad Sci U S A 104:10211–10216.

Heredia M, Santacana M, Valverde F. 1991. A method using DiI to study the connectivity of cortical transplants. J Neurosci Methods 36:17–25.

148   Carradori et al.

Hoing MG, Hume RI. 1986. Fluorescent carbocyanine dyes allow living neurons of identified origin to be studied in long-term cultures. J Cell Biol 103:171–187.

Holmquist BI, Ostholm T, Ekstrom P. 1992. DiI tracing in combination with immunocytochemistry for analysis of connectivities and chemo-architectonics of specific neural systems in teolost, the Atlantic salmon. J Neurosci Methods 42:45–63.

Johnson LV, Walsh ML, Bockus BJ, Chen LB. 1981. Monitoring of relative mitochondrial membrane potential in living cells by fluorescent microscopy. J Cell Biol 88:526–535.

Klüver H, Barrera E. 1953. A method for the combined staining of cells and fibers in the nervous system. J Neuropathol Exp Neurol 12:400–403.

Ladran I, Tran N, Topol A, Brennand KJ. 2013. Neural stem and progenitor cells in health and disease. Wiley Interdisc Rev Syst Biol Med 5:701–715.

Lehner B, Sandner B, Marschallinger J, Lehner C, Furtner T, Couillard-Despres S, Aigner L. 2011. The dark side of BrdU in neural stem cell biology: detrimental effects on cell cycle, differentiation and survival. Cell Tissue Res 345:313–328.

Mäkinen M, Joki T, Ylä-Outinen L, Skottman H, Narkilahti S, Äänismaa R. 2013. Fluorescent probes as a tool for cell population tracking in spontaneously active neural networks derived from human pluripotent stem cells. J Neurosci Methods 215:88–96.

Matsubayashi Y, Iwai L, Kawasaki H. 2008. Fluorescent double-labeling with carbocyanine neuronal tracing and immunohistochemistry using a cholesterol-specific detergent digitonin. J Neurosci Methods 174:71–81.

Ragnarson B, Bengtsson L, Haegerstrand A. 1992. Labeling with fluorescent carbocyanine dyes of cultured endothelial and smooth muscle cells by growth in dye-containing medium. Histochemistry 97:329–333.

Ramanathan R, Wilkemeyer MF, Mittal B, Perides G, Charness ME. 1996. Alcohol inhibits cell–cell adhesion mediated by human L1. J Cell Biol 133:381–390.

Schwartz M, Agranoff BW. 1981. Outgrowth and maintenance of neurites from cultured goldfish retinal ganglion cells. Brain Res 206:331–343.

Simon GH, Daldrup-Link HE, Kau J, Metz S, Schlegel J, Piontek G, Pichler BJ. 2006. Optical imaging of experimental arthritis using alloge-neic leukocytes labeled with a near-infrared fluorescent probe. Eur J Nucl Med Mol Imag 33:998–1006.

Sims PJ, Waggoner AS, Wang CH, Hoffman JF. 1974. Studies on the mechanism by which cyanine dyes measure membrane potential in red blood cells and phosphatidylcholine vesicles. Biochemistry 13:3315–3329.

Soto CM, Blum AS, Vora GJ, Lebedev N, Meador CE, Won AP, Ratna BR. 2006. Fluorescent signal amplification of carbocyanine dyes using engineered viral nanoparticles. J Am Chem Soc 128:5184–5189.

Spötl L, Sarti A, Dierich MP, Möst J. 1995. Cell membrane labeling with fluorescent dyes for the demonstration of cytokine-induced fusion between monocytes and tumor cells. Cytometry 21:160–169.

Terasaki M, Jaffe LA. 1991. Organization of the sea urchin egg endoplasmatic reticulum and its reorganization at fertilization. J Cell Biol 114:929–940.

Terasaki M, Song J, Wong JR, Weiss MJ, Chen LB. 1984. Localization of endoplasmic reticulum in living and glutaraldehyde-fixed cells with fluorescent dyes. Cell 38:101–108.

The Molecular Probes Handbook. 2010. A guide to fluorescent probes and labeling technologies, 11th ed. Gramd Island, NY: Life Technology. p 575–577.

Wang FH, Lee IH, Holmström N, Yoshitake T, Kim DK, Muhammed M, Kehr J. 2006. Magnetic resonance tracking of nanoparticle labeled neural stem cells in a rat's spinal cord. Nanotechnology 17:1911–1915.

Wolfensohn S, Lloyd M. 2008. Handbook of laboratory animal management and welfare. Hoboken, NJ: John Wiley & Sons.

Yang H, Mao H, Wan Z, Zhu A, Guo M, Li Y, Chen H. 2013. Micelles assembled with carbocyanine dyes for theranostic near-infrared fluorescent cancer imaging and photothermal therapy. Biomaterials 34:9124–9133.

Zhang RL, Zhang L, Zhang ZG, Morris D, Jiang Q, Wang L, Chopp M. 2003. Migration and differentiation of adult rat subventricular zone progenitor cells transplanted into the adult rat striatum. Neuroscience 116:373–382.

Zorov DB, Kobrinsky E, Juhaszova M, Sollott SJ. 2004. Examining intracellular organelle function using fluorescent probes from animalcules to quantum dots. Circ Res 95:239–252.

33 Avenue des Constellations
1200, Bruxelles, Belgium
+32 492933560
Date of birth: 25/06/1986

Citizenship: Italian
dario.carradori@uclouvain.be

DARIO CARRADORI

Pharmacist, PhD Student

EDUCATION/FORMATION

10/2013-present: Double PhD in <u>Life and Health Sciences</u> at **Université d'Angers** (Angers, **France**) and in <u>Biomedical and Pharmaceutical Sciences</u> at l'**Université catholique de Louvain** (Brussels, **Belgium**) funded by the Erasmus Mundus Joint Doctorate in nanomedicine and pharmaceutical innovation- NanoFar (2013-2016)
Research project: "New nanoparticle-based drug delivery systems for neural stem cell targeting and difefrentiation"
Thesis director: Dr. Joel Eyer. Thesis co-director: Dr. Anne des Rieux. Supervisors : Prof. Patrick Saulnier and Prof. Véronique Préat
Research domain: drug delivery, nanomedicine, neural stem cells, neurodegenerative diseases

09/2006-05/2012: Combined Bachelor and Master in <u>Pharmaceutical Chemistry and Technology</u> at **Università degli Studi di Camerino** (Camerino, **Italy**). Results: 107/110, 300 ECTS
Experimental Degree thesis (6 months) with Prof. Piera di Martino and Prof. Karine Andrieux: "*Nanoparticles for brain targeting*"
Research domain: drug delivery, nanomedicine, neurodegenerative diseases

During this period:
Stage (6 months) at Institut Galien Paris-Sud (Chatenay-Malabry, France)
Stage (3 months) at Beijing Institut of Technology (Beijing, China)
Stage (2 months) at Jilin Agricultural University (Changchun, China)

CERTIFICATIONS

2014 Certification of "Design and Realization in animal experimentation" at **Ecole Nationale Vétérinaire de Nantes** (Nantes, **Franc**e)
2012 Habilitation to the profession of Pharmacist in Italy (Camerino, **Italy**)
2012 Master Degree in Pharmaceutical Chemistry and Technology

WORK EXPERIENCES

04/2013-08/2013: Ingénieur d'étude at **Institut Galien Paris-Sud** (Chatenay-Malabry, **France**). *Research domain: drug delivery, Alzheimer's disease, blood-brain barrier, nanomedicine*

09/2012-03/2013: Professional stage at **Institut Galien Paris-Sud** (Chatenay-Malabry, **France**). *Research domain: drug delivery, Alzheimer's disease, blood-brain barrier, nanomedicine*
2015 (6 months): Traineeship at **Camerino Hospital Pharmacy** (Camerino, **Italy**)

RESEACRH FIELDS

Drug delivery, Nanomedicine, Neural stem cells, Neurodegenerative diseases

JOB-RELATED SKILLS

LANGUAGES: Italian *(mother tongue)*, English *(Prof. working proficiency)*, French *(Prof. working proficiency)*, Spanish *(A2 level)*.

INFORMATICS: Office, ImageJ, GraphPad Prism.

LABORATORY: Nanoparticle-based formulations, Drug delivery, Cell cultures (*primary and immortalized*), Biostatistics (*basic*), Polymeric synthesis (*basic*), Fluorescence activated cell sorting, Immunocytochemistry, Immunohistochemistry, Analytical chemistry, qPCR, ELISA, Electrophoresis, Purification methods (*dialysis, gel filtration, ultracentrifugation*), *In vivo* experiments (*biodistribution, pharmacological efficacy, surgery*), Scientific writing (*original research articles, reviews, book chapter*).

OTHERS: Networking, Team worker, Fast learner, Independent, Problem-solver, Efficient, Rigorous, Self-critical.

SCHOLARSHIPS/GRANTS

2016 *1-year scholarship* by **IRP** (1 year)
2013 *Erasmus Mundus Nanofar* by **EACEA** (3 years)
2012 *Professional stage abroad* by **UNICAM** (6 months
2011 *ERASMUS student mobility* by **EACEA** and **UNICAM** (6 months)
2010 *Extra-Europe student mobility* by **UNICAM** (3 months)
2009 *Interlink* by **MIUR** (2 months)

CONGRESS CONTRIBUTION

ORAL PRESENTATIONS

- PhD Day 2017, Bruxelles (**Belgium**): "NFL-lipid nanocapsules target neural stem cells from the brain *in vitro* and *in vivo*".
- SFNano 2016, Paris (**France**): "New drug delivery system to target neural stem cells"
- SFNano 2015, Grenoble (**France**): "Mechanistic study on the interaction between PtX and neural stem cell cellular membranes".

POSTERS

- 14th European Symposium on Controlled Drug Delivery, Egmond aan Zee (**The Netherlands**).2016.
- 4th Nanofar Autumn School, Nantes (**France**). 2015.

- 3rd NanoFar Autumn School, Brussels (**Belgium**). 2014.
- CIMATH2, Nantes (**France**). 2014.
- 2nd NanoFar Autumn School, Santiago de Compostela (**Spain**). 2013.
- Innovation in Drug Delivery: Advances in Local Drug Delivery, Pisa (**Italy**). 2013.
- NPMED13, Milan (**Italy**). 2013.

TEACHING SKILLS

- Ariane Mwema, 6 months (supervision of master student)
- Hanane Choaibi, 2 months (supervision of master student)
- Zahraa El Azabi, 6 months(supervision of master student)

PUBLICATIONS

- Bianco, J., **Carradori**, D., Deumens, R., des Rieux, A. (2017) Rapid serum-free isolation of oligodendrocyte progenitor cells from adult rat spinal cord, **Stem Cell Reviews and Reports**, 1-14, [IF: 3.112]

- **Carradori**, D., Eyer, J., Saulnier, P., Préat, V., and des Rieux, A. (2017). The therapeutic contribution of nanomedicine to treat neurodegenerative diseases via neural stem cell differentiation. **Biomaterials**. 123: 77-91. [IF: 8.557]

- Beloqui, A., Alhouayek, M., **Carradori**, D., Vanvarenberg, K., Muccioli, G.G., Cani,P.D., and Préat, V. (2016). A mechanistic study on nanoparticle-mediated glucagon-like peptide-1 (GLP-1) secretion from enteroendocrine L cells for type 2 diabetes mellitus treatment.. **Molecular Pharmaceutics**. 13.12: 4222-4230. [IF: 4.384]

- **Carradori**, D., Saulnier, P., Préat, V., des Rieux, A., and Eyer, J. (2016). NFL-lipid nanocapsules for brain neural stem cell targeting in vitro and in vivo. **Journal of Controlled Release**, 238, 253-262. [IF: 7.705]

- **Carradori**, D., Gaudin, A., Brambilla, D., and Andrieux, K. (2016). Chapter Three-Application of Nanomedicine to the CNS Diseases. **International Review of Neurobiology**. 130, 73-113 [IF: 2.457]

- **Carradori**, D., Barreau, K., and Eyer, J. (2016). The carbocyanine dye DiD labels in vitro and in vivo neural stem cells of the subventricular zone as well as myelinated structures following in vivo injection in the lateral ventricle. **Journal of neuroscience research**, 94(2), 139-148. [IF: 2.974]

- *Carradori, D., Balducci, C., Brambilla, D., Re, F., Le Droumaguet, B., Flores, O., Alice Gaudin, A., Mura, S., Forloni, G., Wandosell, F., Masserini, M., Nicolas, J., Couvreur, C., and Andrieux, K. A Nanoparticle-Based Therapy Leading to Memory Recovery in Alzheimer's Disease-like Transgenic Mouse Model. To submit*

*- **Carradori**, D., Dos Santos, A.G., Masquelier, J., Paquot, A.,Eyer, J., Saulnier, P., Préat, V., Muccioli, G., Mingeot-Leclercq M.P., des Rieux, A. The lipid composition of neural stem cell plasma membrane could modulate their interaction with NFL-lipid nanocapsules. <u>Manuscript in preparation</u>*

*- **Carradori**, D., Beloqui, A., Saulnier, P., Préat, V., Eyer, J., Miron, V., des Rieux, A. Retinoic acid-loaded NFL-lipid nanocapsules induce neural stem cell differentiation towards the oligodendrocyte lineage. <u>Manuscript in preparation</u>*

*- Xu, Y., **Carradori**, D., Préat, V., Beloqui, A. Size effect on lipid nanocapsules-mediated GLP-1 secretion from enteroendocrine L cells. <u>Manuscritp in prepration</u>*

UNIVERSITE BRETAGNE LOIRE

université angers

UCL
Université catholique de Louvain

Thèse de Doctorat

Dario CARRADORI

Novel nanoparticle-based drug delivery system for neural stem cell targeting and differentiation

Résumé

Les cellules souches neurales (CSNs) se situent dans des régions spécifiques du système nerveux central qui sont appelées niches. Ces cellules sont capables de se répliquer ou se différentier en cellules neurales spécialisées (neurones, astrocytes et oligodendrocytes). C'est grâce à cette propriété de différentiation que les CSNs sont étudiées comme thérapie chez les patients atteints d'une maladie neurodégénérative. En effet, elles pourraient remplacer les cellules neurales altérées et ainsi restaurer les fonctions neurologiques. De nombreuses approches ont été développées afin de stimuler la différentiation des CSNs, dont la plus prometteuse est la différentiation des cellules endogènes directement au sein de leurs niches. Actuellement, il n'existe pas de molécule active ou de système thérapeutique qui cible les CSNs endogènes et qui induit leur différentiation simultanément. Le but de ce travail est de fournir un système de délivrance de molécules bioactives capable de cibler les CSNs endogènes et d'induire leur différenciation in situ. Nous avons développé et caractérisé des nanoparticules lipidiques (LNC), un système de délivrance très versatile. NFL-TBS.40-63, un peptide ciblant les CSNs, a été adsorbé à la surface des LNC afin de les diriger contre les CSNs endogènes. Nous avons observé que ces NFL-LNC ne ciblaient que les CSNs du cerveau et pas de la moelle. Afin d'étudier les interactions spécifiques entre les nanoparticules et les CSNs, nous avons caractérisé et comparé les propriétés de leur membrane plasmique. Enfin, nous avons encapsulé de l'acide rétinoïque, une molécule connue pour stimuler la différentiation des CSNs, dans les LNC-NFL et étudié leur impact sur la différentiation de CSNs in vitro et in vivo. Ce travail contribue au développement de thérapies efficaces et sures pour le traitement de maladies neurodégénératives à travers la différentiation de CSNs endogènes.

Abstract

Neural stem cells (NSCs) are located in specific regions of the central nervous system called niches. Those cells are able to self-renew and to differentiate into specialized neuronal cells (neurons, astrocytes and oligodendrocytes). Due to this differentiation property, NSCs are studied to replace neuronal cells and restore neurological functions in patients affected by neurodegenerative diseases. Several therapeutic approaches have been developed and endogenous NSC stimulation is one of the most promising. Currently, there is no active molecule or therapeutic system targeting endogenous CSNs and inducing their differentiation at the same time. The aim of the work was to provide a drug delivery system able both to target endogenous CSNs and to induce their differentiation in situ. Here, we developed and characterized lipidic nanoparticles (LNC) targeting endogenous NSCs. A peptide called NFL-TBS.40-63, known for its affinity towards NSCs, was adsorbed at the surface of LNC. We observed that NFL-LNC specifically targeted NSC from the brain and not from the spinal cord in vitro and in vivo. To explain this specificity, we characterized and compared NFL-LNC interactions with the plasmatic membrane of both cell types. Finally, we demonstrated that by loading retinoic acid in NFL-LNC we were able to induce brain NSC differentiation in vitro and in vivo. This work contributes to the development of efficient and safe therapies for the treatment of neurodegenerative disease via the differentiation of endogenous NSCs.

Key Words: Neural stem cells, Neurodegenerative diseases, Nanomedicine, Lipid nanocapsules, NFL-TBS.40-63, Subventricular zone, Plasma membrane, Retinoic acid

Mots clés : Cellules souches neurales, Maladies neurodégénératives, Nanomédecine, Nanoparticules lipidiques, NFL-TBS.40-63, Zone subventriculaire, Membrane plasmique, Acide rétinoïque

L'Université Bretagne Loire